Journal which deals with research, Innovation and Originality

Table of Content

CHIEF EDITOR BOARD

Message from Associate Editor In Chief

Let me first of all take this opportunity to wish all our readers a very happy, peaceful and prosperous year ahead.

This is the Fifth Issue of the Forth Volume of International Journal of Engineering Research and General Science. A total of 28 research articles are published and I sincerely hope that each one of these provides some significant stimulation to a reasonable segment of our community of readers.

In this issue, we have focused mainly on the Emerging Scientific tools. We also welcome more research oriented ideas in our upcoming Issues.

Author's response for this issue was really inspiring for us. We received many papers from many countries in this issue but our technical team and editor members accepted very less number of research papers for the publication. We have provided editors feedback for every rejected as well as accepted paper so that authors can work out in the weakness more and we shall accept the paper in near future. We apologize for the inconvenient caused for rejected Authors but I hope our editor's feedback helps you discover more horizons for your research work.

I would like to take this opportunity to thank each and every writer for their contribution and would like to thank entire International Journal of Engineering Research and General Science (IJERGS) technical team and editor member for their hard work for the development of research in the world through IJERGS.

Last, but not the least my special thanks and gratitude needs to go to all our fellow friends and supporters. Your help is greatly appreciated. I hope our reader will find our papers educational and entertaining as well. Our team have done good job however, this issue may possibly have some drawbacks, and therefore, constructive suggestions for further improvement shall be warmly welcomed.

Er. Pragyan Bhattarai,

Associate Editor-in-Chief, P&REC,

International Journal of Engineering Research and General Science

E-mail -Pragyan@ijergs.org

Automated Cooling System

Nayan Girase[1], Mihir Gurjar[2]

[1]UG Student ,Computer Engineering, nayangirase14@hotmail.com, +91-7698180002
[2]UG Student, Computer Engineering, mitbgurjar@gmail.com, +91-9724305394

Abstract— In today's society, advancement in technology has made life easier by providing us with higher level of knowledge through the invention of different devices. However, each technological innovation harbors the potential of hidden threats. One major threat is deteriorating efficiency, main cause behind it is overheating and environment debris. While debris can be filtered but overheating of component causes decrease in life span of components and deterioration in efficiency. This increasing battle with overheating issue has lead to birth of many cooling methods and exhaust system but u cannot know when a coin flip like way all method are not efficient and cost effective and completely reliable so we take it as a challenge to design cost effective and well efficient cooling system .

Keywords— Minimum 7 keywords are mandatory, keyword must reflect the overall highlighting words of research. This must be of Time New Roman Front of size 10.

INTRODUCTION

Definition

Automated Cooling System is device which can be used to maintain temperature of your processor, graphic cards, hard disk, and motherboard by effectively controlling air flow in cabinet whether you need to overclock / video editing / gaming / complex computation process.

It is suitable for Server Racks, Personal Computing and WorkStation where computation process varies accordingly.

Automated Cooling System (ACS) is low budget system which allow user to connect up to 5 fans maximum (may vary) which are guided by software which continuously monitor temperature and controls fans on and off time period.

It has three features:

* Notify user about system overheating and warns user to save work before system trips off.

* Allow user to input temperature, which should be maintained by ACS.

* Allow user to input temperature, when system should start and should turn off after decreasing temperature.

Objective

Objective to design Automated Cooling System is to overcome overheating issues which Detroit efficiency and life span of PC components or causes to permanent break.

Automated Cooling System is designed in such a way that it intelligently controls temperature of component and thus increase efficiency and lifespan of PC component.

Cost is another factor that was taken into account where Water/Oil Cooling cost around 10000 Rs, Automate Cooling System cost 1500 Rs (Excluding fan cost) and 3000 Rs (Including Fan cost).

Scope

Automated Cooling System is scalable design it can be configured in large server to small personal computing system.

Automated Cooling System when configured with Large Server admin does not have to log in to control panel each time to see temperature Automate Cooling System provides on board LCD display which shows temperature relatively.

Automated Cooling System can be configured with Workstation, Large Server, Personal Computers and Office System.

Project Profile

Technology:.Net(VB.net),Bascom,Flash Magic, SinaProg

Front End: Automated Cooling System Software

Back End: Embedded System

Others: USBASP Driver

System Modules/ Modularization of System

User Module

- **Connection**
  1. Connect by Port No and Baud Rate
  2. Disconnect
- **Output Temperature**
  1. Motherboard Temperature
  2. Graphic Card Temperature
  3. Cabinet Temperature
  4. Outside Temperature
- **Input Temperature**
  - ♦ Manual Mode
  - ♦ Automatic Mode

Test Cases

Condition	Without System(Avg temp)	With system(Avg temp)
No processor fan(default)	40 C	37
No processor fan & no system fan	46 C	41
Both system fans	35 C	32
Idle Graphic Card	38 C	35
Graphic Card in use(sort time)	40 C	36
Graphic Card in use(longtime/High use)	48 C	42
Normal Use	38 C	33

Hardware Requirement Analysis

1. PCB
2. ATMega16A Controller
3. 100 uF Capacitor
4. IC 7805
5. LED(red)
6. Push button
7. 11.0592 MHz crystal

8. DC female socket
9. ISP socket
10. LCD 16x2
11. 3 pin female wire
12. Relay 12V
13. LM35 temperature sensor
14. 2 pin green Socket
15. 10 pin male female wire
16. 3 pin male socket
17. 1k resistor
18. 18 pin IC socket
19. 40 pin IC socket
20. 33 pF capacitor
21. 1N4007 diode
22. ULN2803

System Design

- **Block Diagram**
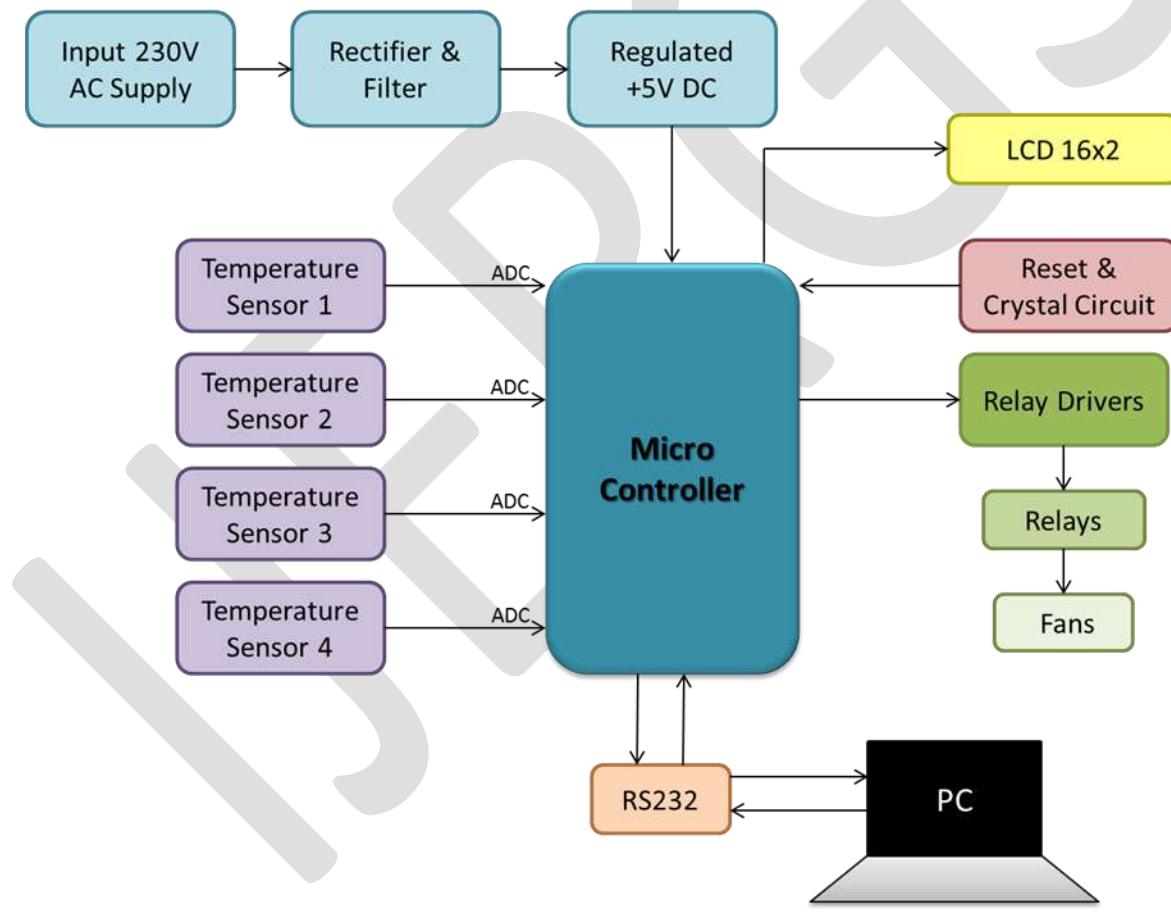
IMPLEMENTATION

- **Hardware and Software Requirement**

Automated Cooling System desktop application is developed only for windows using VB.net which provide intuitive tools and ease core structure to develop software.

Automated Cooling System application can be installed with 3-simple clicks on any windows machine and gets instantly ready for working.

Prolific Usb-To-Serial Driver need to be installed to establish connection of system with device.

- **Screen Layout**
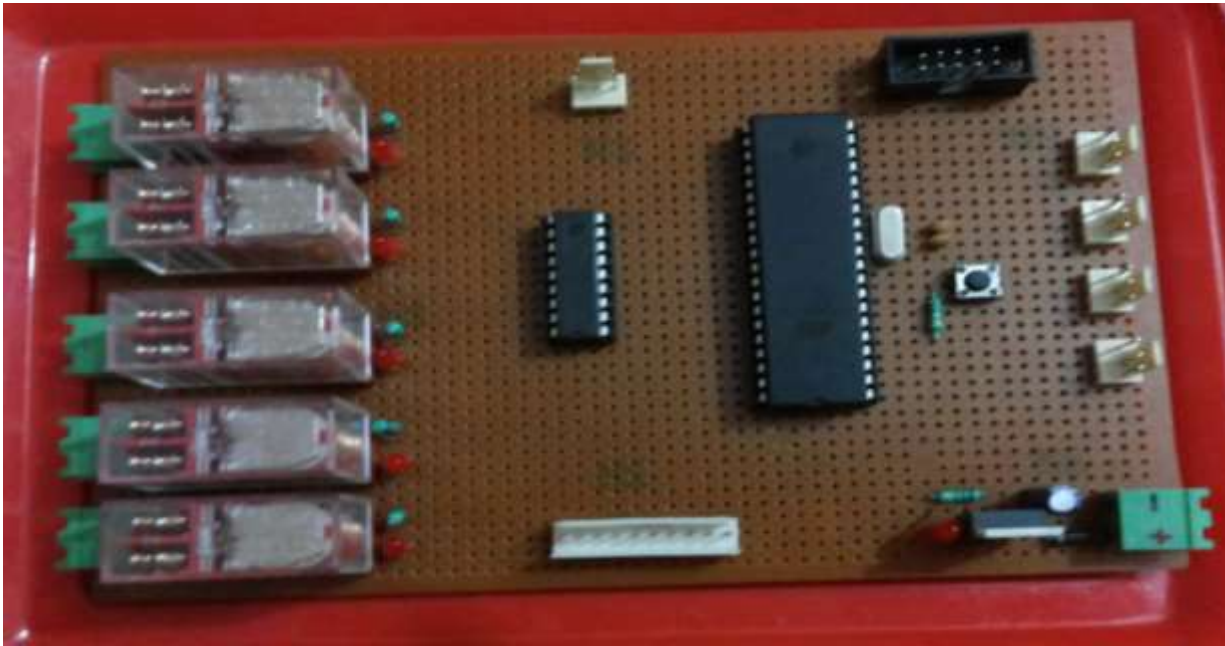
Figure: Circuit Diagram

Start-up Screen
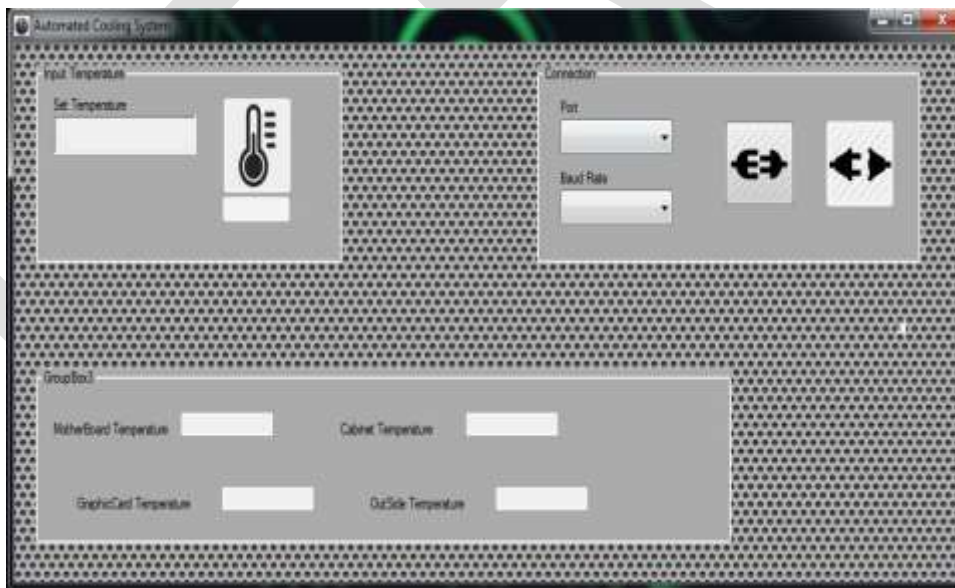
Figure: Automated Cooling System Desktop Application

This is Automated Cooling System desktop application from where user will able to setup connection with device and control automatic and manual mode of device.

Power-Saving Mode

Figure: Power Saving Mode

Initially when system starts device is default loaded to Power Saving Mode in which two fans are kept on 1 Outflow Fan, 1 Inflow Fan to maintain system temperature and save power.

Automatic Mode (Software)
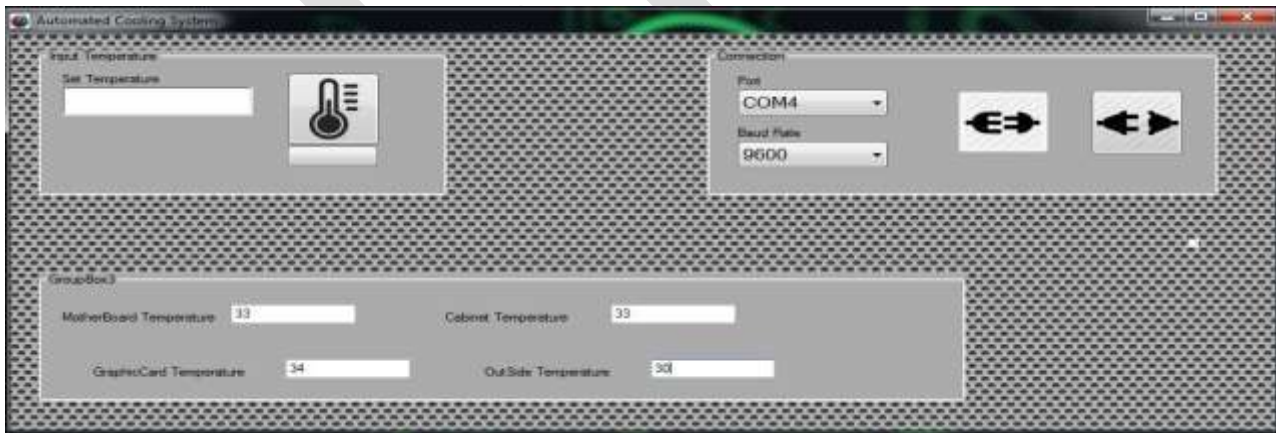
Figure: Automatic Mode (Software)

When software establishes connection it switches device to automatic mode and read temperature from device of respective field.

Automatic Mode (Hardware)

Figure: Automatic Mode (Hardware)

Device has been switched to Automatic Mode when software establishes connection to device. Automatic Mode intelligently calculates difference between temperature and control on/off of each fan respectively.

Manual Mode (Software)

Figure: Manual Mode (Software)

When User give temperature to software and press manual button it reads temperature given by user and compare to temperature of other field if temperature of given field is higher it will turn on/off fans automatically to bring down temperature.

Manual Mode (Hardware)

Figure: Manual Mode (Hardware)

Device has switched to Manual Mode and is controlling on/off of fan on basis of software sending instruction.

CONCLUSION

Limitations of this system are:

1. It cannot reduce temperature below room temperature.

2. User cannot control the rotation speed of fans, he can simply switch on or off.

3. It can only give warning on very high temperature that can harm computer it cannot switch off entire system (If System is on manual mode).

There are so many types of cooing systems in market, with our system we have tried to shown that Air-flow cooling system can be as good as the other type of cooing systems. There are several ways of cooling but in our system we have tried our best to keep it simple, cost efficient and more dependent. Because it switches off the fans when they are not needed it lowers the power consumption, it do not required any maintenance and it also provide control of fans to user we can conclude that our system is a good way of overcome overheating.

REFERENCES:

[1] Steven Holzner, "Visual Basic 6 Programming", Re.2008 India: Dreamtech Press, 2008.
[2] Kevin Le,"Visual Basic Serial COM Port Tutorial (Visual Studio 2010)",[online] 23 Aug 2012, https://www.youtube.com/watch?v=krN6pWm6s6o.
[3] Computer Cooling System Solutionhttp://www.nmbtc.com/nmb-component-applications/server/computer-cooling-system/index.html
[4] AT MEGA 16A Specification http://www.engineersgarage.com/electronic-components/atmega16-microcontroller
[5] USB to RS232 Converter http://www.elecfreaks.com/wiki/index.php?title=USB_to_RS232_Converter
[6] USB to Serial Communication C# Program Example http://codesamplez.com/programming/serial-port-communication-c-sharp
[7] Serial Port Communication Example https://msdn.microsoft.com/en-us/library/system.io.ports.serialport.aspx
[8] How to receive data from serial port RS232 using VB .NET http://www.codeproject.com/Questions/183627/How-to-Receive-data-from-Serial-Port-RS-in-VB-N
[9] How Relays Works? http://electronics.howstuffworks.com/relay.htm
[10] What is Baud Rate? https://en.wikipedia.org/wiki/Baud
[11] Working of ULN2803 http://www.gadgetronicx.com/working-of-uln2803-ic/
[12] ULN2803 driver circuit http://ugpro143.blogspot.in/2011/09/ic-uln-2803-driver-circuit.html

Rheological Behavior of Eco-accommodating Drilling Fluids from Biopolymers

Ragul V[1],Gengadevi.R[*]

[1]DEPARTMENT OF PETROLEUM ENGINEERING, JCT COLLEGE OF ENGINEERING AND TECHNOLOGY, PICHANUR, COIMBATORE
* (ASSISTANT PROFFESOR) DEPARTMENT OF PETROLEUM ENGINEERING, JCT COLLEGE OF ENGINEERING AND TECHNOLOGY, PICHANUR, COIMBATORE

Email id: ragulvenkat111@gmail.com

Abstract: The rheological properties of drilling liquids adjusted with two biopolymers – lignin , and polyanionic cellulose (PAC-R) have been contemplated. The impact of centralization of the biopolymers on the boring liquid was additionally reported. The altered boring liquids were found to obey Herschel Bulkley rheological model. The liquids were additionally observed to be pseudo-plastic with shear diminishing conduct. Polyanionic cellulose demonstrated the most astounding shear rate and shear stress than lignin. This can be ascribed to the straight open long chain structure of PAC-R and its capacity to associate with water, solids and with itself. It likewise went about as a superior viscosifier due to the more negative charge it conveys. Likewise, the plan of biopolymer boring liquid with bentonite has demonstrated to enhance the consistency than that experienced in typical traditional drilling liquids.

Keywords: rheology, biopolymers, drilling fluids, natural polymers, Herschel-Bulkley model

1. Introduction :

Drilling liquids properties are imperative for the achievement of any boring operation. The liquids were initially intended to guarantee that turning boring of underground developments is conceivable and prudent. The drilling liquids accomplish this by (i) moving drill cuttings to the surface, (ii) cooling and cleaning the bore, (iii) decreasing erosion, (iv) keeping up wellbore dependability, and (v) keeping pore liquids from rashly streaming into the wellbore. Also, the boring liquids are basically intended to fabricate a channel cake, which is essentially expected to diminishing filtrate misfortune to the arrangement, be thin and hold the drilling liquid in the wellbore [1]. A standout amongst the most basic elements of boring liquids is to minimize the measure of drilling liquid filtrate entering the hydrocarbon bearing development which can prompt arrangement harm in view of rock wettability changes, fines movement, boring liquid solids stopping and development water science incompatibilities [2]. Rheological conduct of drilling liquids is imperative in their appropriate choice for any well. Rheological properties of boring muds are vital on the grounds that they are utilized to describe properties of the mud, for example, its well purifies, disintegration conservation, cutting material expulsion, water powered count, and pump framework [3]. The rheological standards can be utilized to decide the dynamic execution of a boring liquid conduct in taking care of issues of cleaning gap, suspension of cuttings, water driven counts and mud treatment [4]. The accomplishment of any boring operation depends essentially on the execution and cost viability of the boring liquid utilized [5,6,7]. As indicated by Douglas et al [8,9,10], boring liquids are for the most part ordered into:(i) air or froth based liquids which are utilized where fluid drilling liquid is not the most attractive coursing medium; (ii) oil-based liquid, and (iii) water-based liquid. In light of ecological and cost contemplations, water-based liquids offer properties that are for the most part favored over that of oil-based liquids [11]. Drilling liquids ought to be ecologically amicable and contain the most reduced conceivable measure of contaminations. Subsequently, care ought to be taken in the choice and definition of crude materials [12]. These days, different polymers, which can be as normal (e.g. starch), engineered, and/or adjusted (e.g. carboxymethyl cellulose or) polymers, are utilized as a part of request to control the liquid misfortune and thickness of drilling liquids. In oil-drilling, these polymers decrease filtrate, alter rheological properties, balance out shale and diminish drag, and can be utilized as a part of cutting edge oil recuperation (EOR) forms [13,14]. The deluge of the fluid stage, known as filtrate, in beneficial zones can bring about a noteworthy decrease of porousness and henceforth bring down well profitability [15,16]. The consolidation of normal gums and starch-based materials in boring liquids structures was the essential answer for control this wonder [6]. Various studies on polymers and their utilization in water-based drilling liquids have been done [6,17,18,19]. Dim and Darly, [6] examined the utilization of polymers like guar gum, carboxymethyl cellulose , and hydroxypropylstarch as filtration control operators and as boring liquids. They inferred that filtration parameters like sorptivity and diffusivity of these polymers are subject to temperature. Sorptivity is a measure of the resistance against the liquid coursing through the channel cake, while diffusivity is a measure of the rate of stream of liquid [20]. The impact of polymers on the rheological properties of KC1/polymer-sort boring liquids was concentrated on by Kok and Alikaya, [19]. This study concentrated on the impact of expansion of polymers on consistency file, stream conduct list, and shear stress. The creators watched that consistency record expanded as polymer focus expanded. Consistency list is a measure of the general thickness of a liquid, while stream list is a measure of the level of stream conduct of a liquid [17,21]. The resistance of the liquid to the connected rate of shear or compel is known as the shear stress, which in oil field terms is closely resembling the pump weight [19,22,23]. In the present paper, the impacts of including

different amounts of various biopolymers (Polyanionic cellulose, carboxymethyl cellulose and lignin) to a boring mud test containing bentonite will be accounted for. The rheological properties of the boring liquids will be resolved and examination made. Xanthan gum is an anionic polysaccharide polymer with high sub-atomic weight produced by starch after aging of xanthomonas campestris. Carboxymethyl cellulose is a semi-adaptable anionic cellulose ether polymer [27] that is created by responding antacid cellulose with sodium monochloroacetate under inflexibly controlled conditions. It is a concoction subsidiary of cellulose where a portion of the hydroxyl bunches (- OH) are substituted with carboxymethyl bunches (- CH2COOH) while polyanionic cellulose (PAC) is a sort of anionic cellulose ether of high virtue and high level of substitution, arranged with characteristic cellulose through synthetic adjustment. Its sodium salt is regularly used. The essential distinction amongst the and PAC generation procedures is in the radicalization step and the high level of substitution in PAC. The structures of the biopolymers utilized are shown beneath. As is surely understood for , PAC and other cellulose ethers, the attributes of these materials can be changed by having diverse normal quantities of substituents per glucose unit and distinctive atomic weights [28].

2. Theory:

The ideas of shear stretch and shear rate and their estimation empower the scientific depiction of the stream of drilling muds. The measure of power connected to a liquid decides the shear rate, which in oil field terms is controlled by the stream rate of the liquid through a specific geometric design. Stream models are plots both of stream weight versus stream rate or of shear anxiety versus shear rate.The Power law and Herschel –Bulkley models are portrayed here and utilized forthe portrayal of the boring liquids concentrated on.

2.1. Power Law Model

Power law is a two – parameter model that relates shear stress to shear rate in a nonlinear manner [17,23]. The model does not consider an excess yield stress and states the relation as:

$$\tau = K \gamma^n \qquad (1)$$

where k, and n are consistency and flow indices respectively, is the shear stress, and is the shearrate. Taking the logarithm of the equation, the following term is obtained:

$$\log \tau = \log k + n \log \gamma \qquad (2)$$

Thus, n = slope and k = intercept.

2.2. Herschel-Bulkley Model

Herschel-Bulkley is a three-parameter model that describes the behaviour of yield-pseudoplatics fluids [21].

$$\tau = \tau_o + \log \gamma^{\ n} \qquad (3)$$

where is the shear stress, is the yield stress, k is the consistency index, is the shear rate, and n is the flowindex.

3.Materials

The lignin utilized for this study was gotten from Baker Hughes Houston USA under the exchange name of XAN-PLEX™. Polyanionic cellulose consistent under the exchange name DRISPAC from Yu Long Chemicals China was among the normal polymers utilized as a part of this study. Bentoniteand were acquired from Global Oil Company Nigeria Limited. The hardware/mechanical assembly utilized as a part of this study include: Fan V-G meter 8 speed model viscometer; hamilton shoreline blender; stop watch; electronic measuring parity; spatula, viscometer glass and hamilton shoreline blender container; institutionalized measuring plate and thermometer.

3.1. Experimental Procedure:

The suspension of bentonite tests were set up by submerging 15g of bentoniteclay into 350cm3 of deionized water. The blend was mixed vivaciously for 15 minutes to accomplish homogeneity while discontinuously dislodging any bentonite sticking to the mass of the blending holder. The bentonite suspension was then put away at room temperature in a fixed holder for 24 hours to give space for maturing. Polyanionic cellulose Regular (PAC-R)was added to the Bentonite suspension at different fixations (0.50 g, 0.75g, 1.0g) and the viscometric studies did to decide its rheological conduct on the boring liquid. Reasonable amountsof sodium hydroxide (NaOH) and Potassium chloride (KCl) were added to the examples and blended to alter the pH and for hindrance separately. The technique was then rehashed for and lignin biopolymers separately. The shear-anxiety was resolved utilizing the force law model which accept that all liquids are pseudoplastic.

4. Results and Discussion:

The rheological parameters such as plastic viscosity, yield stress, and apparent viscosity of all of the drilling fluids were calculated and presented in Table 1. Figures 1 – 3 illustrates the relationship between shear stress, and shear rate of the non-Newtonian fluids at different concentration of the biopolymers.

The example of these bends demonstrated an underlying high stretch after which there was a less push with expanding shear. This demonstrates the liquids are pseudoplastics and comply with the Herschel-Bulkley model. As per Hemphill et al. [24], Herschel-Bulkley liquid model requires a specific anxiety to start stream, yet less with expanding shear. The three parameters of Herschel-Bulkley model, i.e., yield stress, liquid consistency, and liquid file were figured by fitting the trial information of shear anxiety as an element of rate of shear to the model in Equation 3. The outcomes demonstrate that the augmentation of the measure of biopolymers, expand the yield anxiety of the last boring liquid as the stream resistance is expanded. This finding is in concurrence with the aftereffects of Khalil and Jan [25]. The expansion in yield stress with focus came about because of an expansion in shear stress required to

Fluid Reference	PAC R			LIGNIN		
	0.50g	0.75g	1.0g	0.5g	0.75	1.0g
Plastic viscosity(P)	1.6	1.9	2.6	1.02	1.02	1.5
Apparent viscosity(P)	9.55	14.35	25.7	8.13	12.09	18.91
Yield Stress(dyn/cm^3)	15.4	24.1	44.3	14.2	17.3	20.3
Flow Index, n	0.419	0.391	0.281	0.327	0.218	0.248
Consistency Index, K	5.813	9.312	19.853	4.813	9.829	9.328

break the gel structure of the mud before stream began. Besides, it could be viewed as that, very still, the mud's chains were trapped and the gel development came about because of the polymer system framed by the physical conglomeration with area of nearby request going about as system intersections The stream file, n, and consistency list, k, of the boring liquids were investigated utilizing Equation 2 andthis relationship is shown graphically in Figure 4 – Figure 6. The n values displayed in Table 1 demonstrates that the stream record, n, is under 1 for every drilling liquid at the different groupings of the biopolymers contemplated showing a shear diminishing conduct. As indicated by Mewis et al. [21], a liquid for which n valueis under 1 (n < 1) is said to have pseudo plastic stream conduct. Further examination of the table uncovers thatthe stream file n, of the drilling liquid diminished with expanding grouping of polyanionic cellulose.
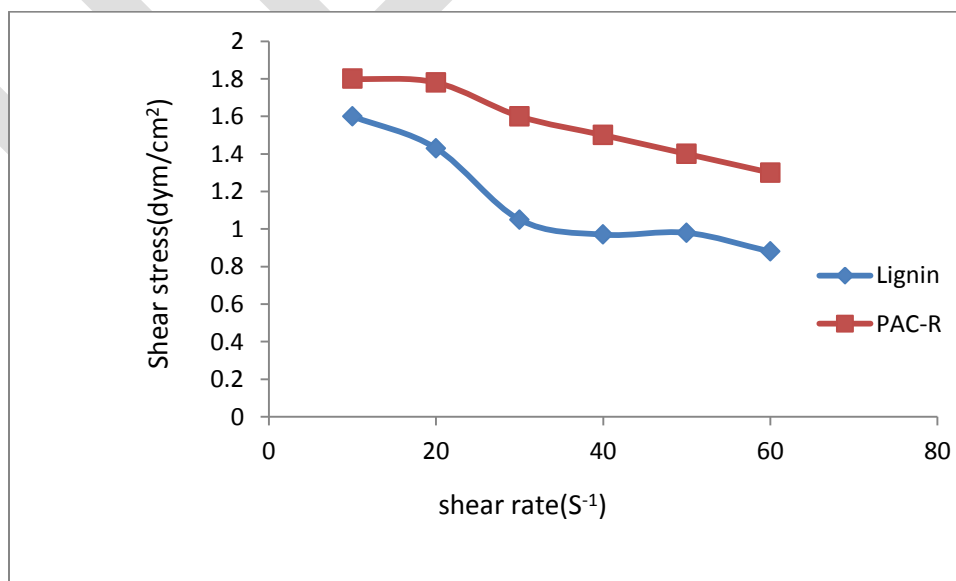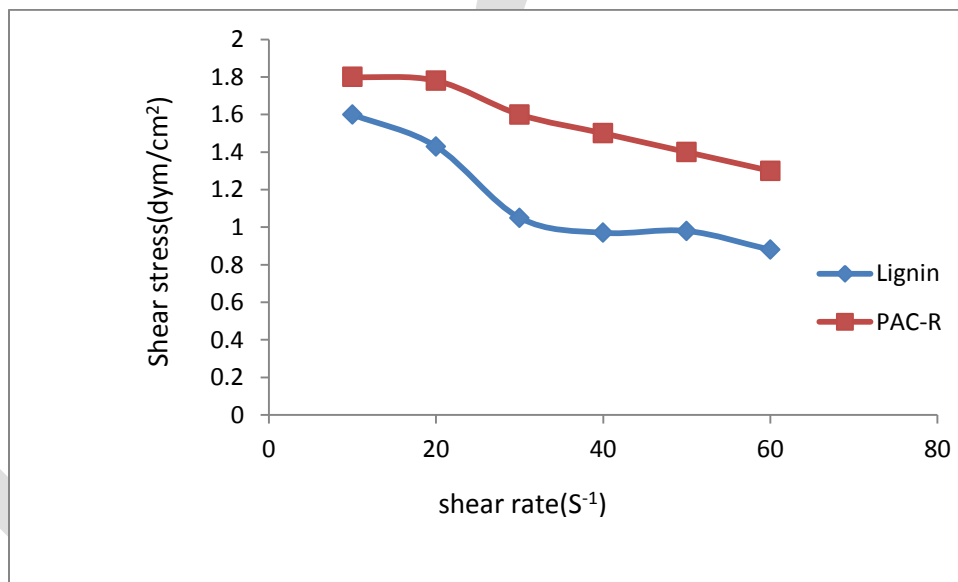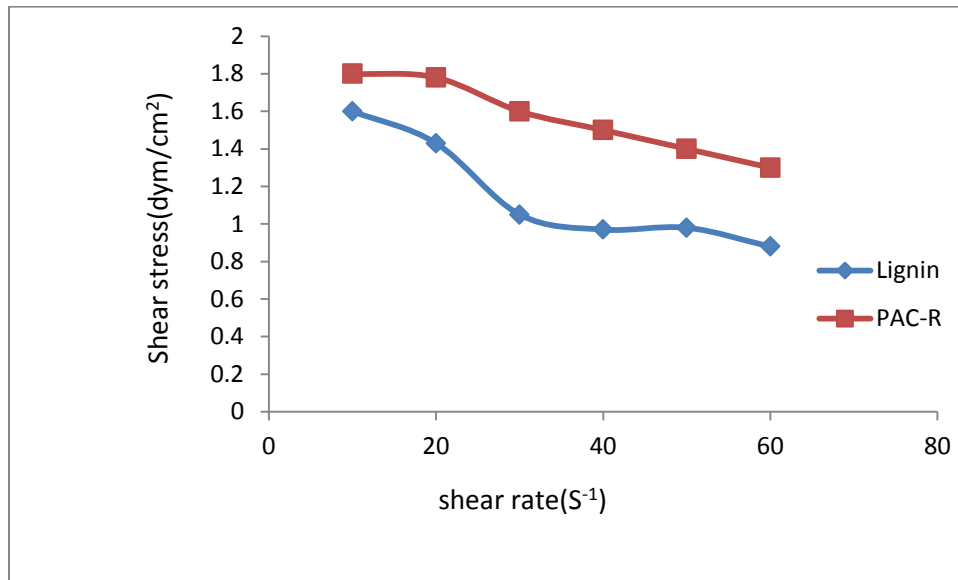
This is as opposed to the discoveries of Chike–Onyegbulaet al [26] who contemplated biodegradable polymer boring mud arranged from Guinea corn starch. The consistency list, k, for the polyanionic cellulose altered boring liquid was found to increment with expansion in the convergence of the polymer in the liquid. The expansion in consistency record, k, with polyanionic cellulose focus came about because of the expansion in the general thickness of the liquid. On account of boring liquids adjusted with lignin and caboxymethyl cellulose, the consistency file, K and stream file, n shows up not to be influenced by the amount of the biopolymer. Oppositely, Khalil and Jan [25], found that the ascertained liquid consistency of their boring liquids gives off an impression of being unequivocally subject to the nearness of glass air pockets, xanthan gum, and mud. Be that as it may, their liquid consistency shows up not to be influenced by the nearness of starch.
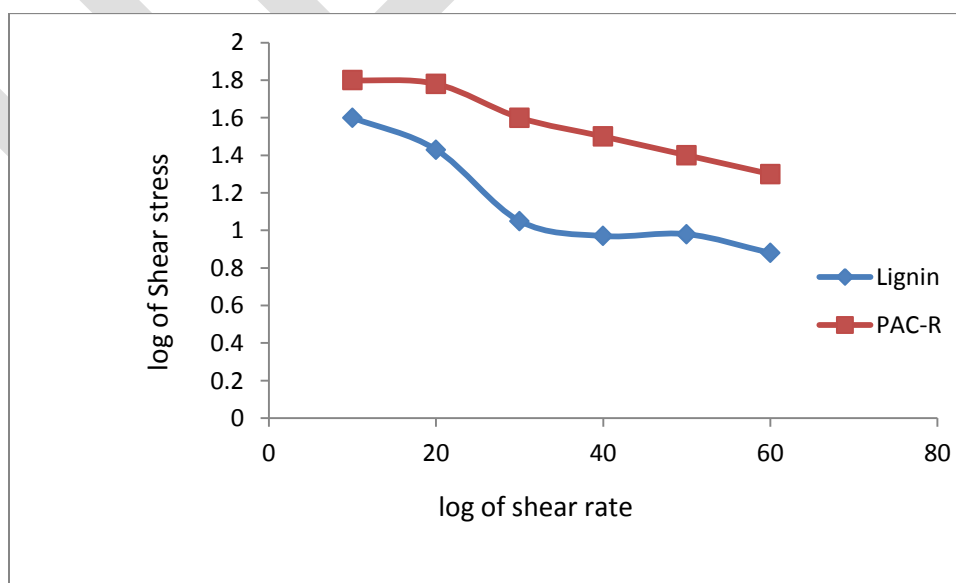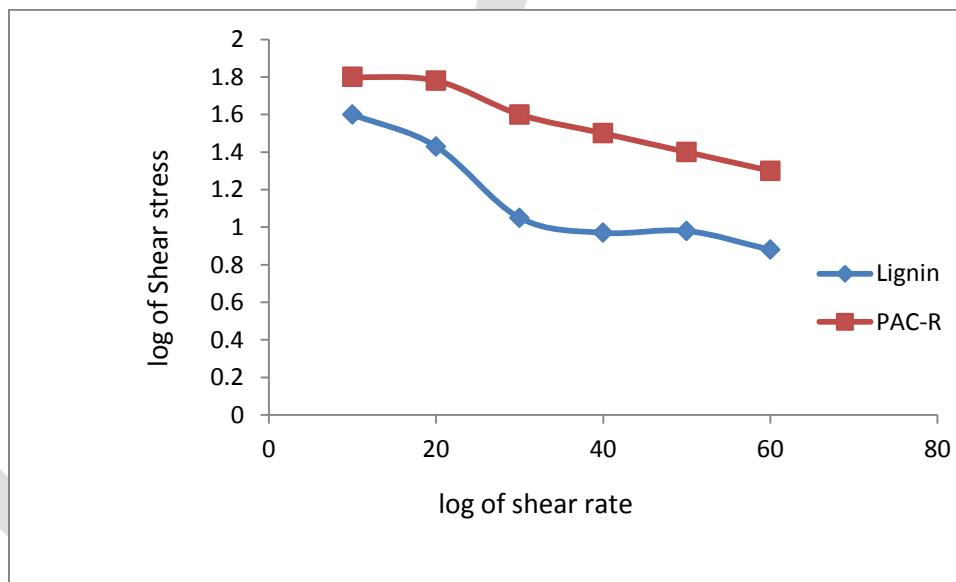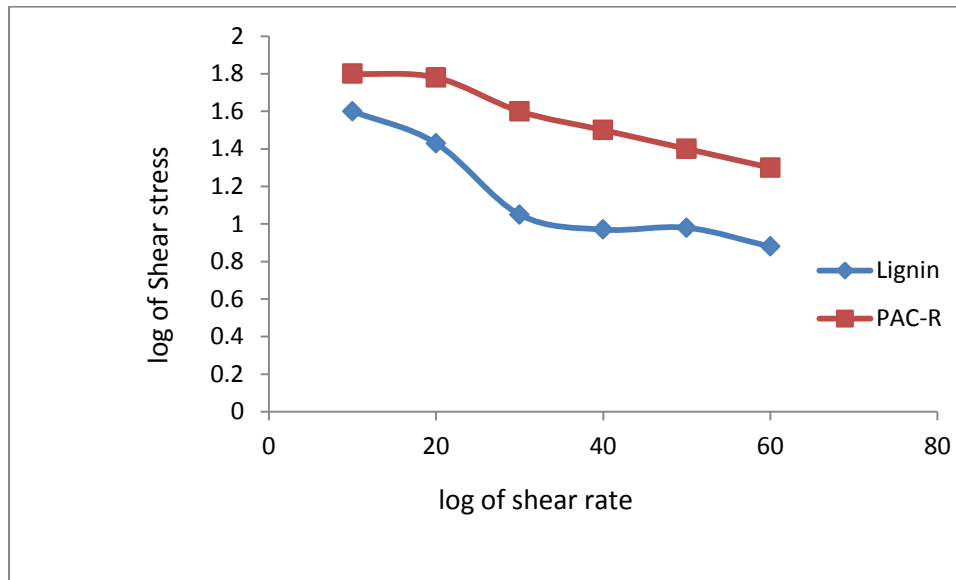
The plot of shear rate as a capacity ofviscosity is appeared in Figure 7 – Figure 9. It is seen from these assumes that the consistency of the boring liquids diminished with expanding shear rate. This came about because of the way that the ensnarement of the liquid's chain at low shear rate blocked shear stream and the thickness was high. The thickness diminished as shear rate was expanded, demonstrating shear diminishing conduct of the drilling liquids. The thickness of a polymer arrangement is identified with the polymer focus, the degree of polymer-dissolvable collaboration, and the polymer structure, for example, atomic weight, shap, sub-atomic adaptability, and sub-atomic compliance [29].
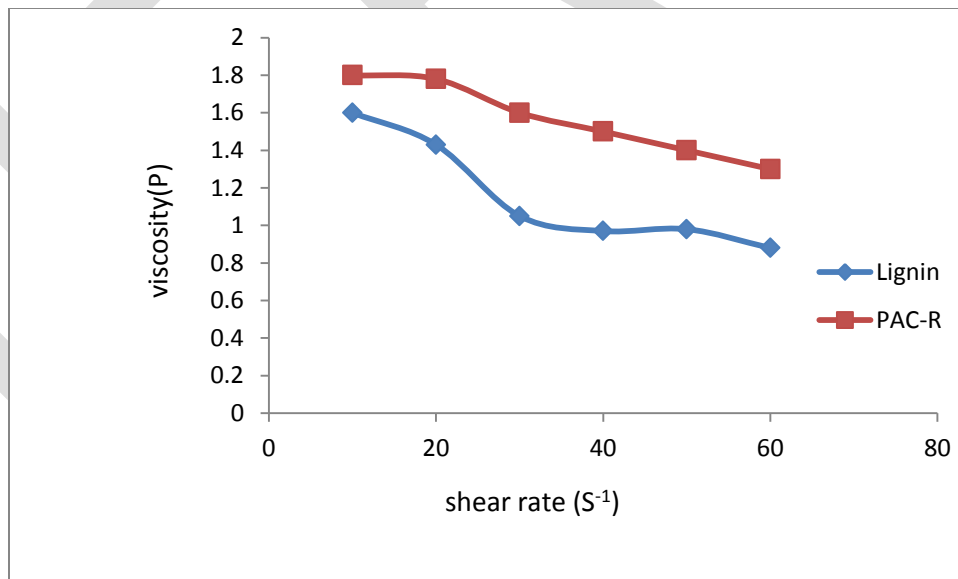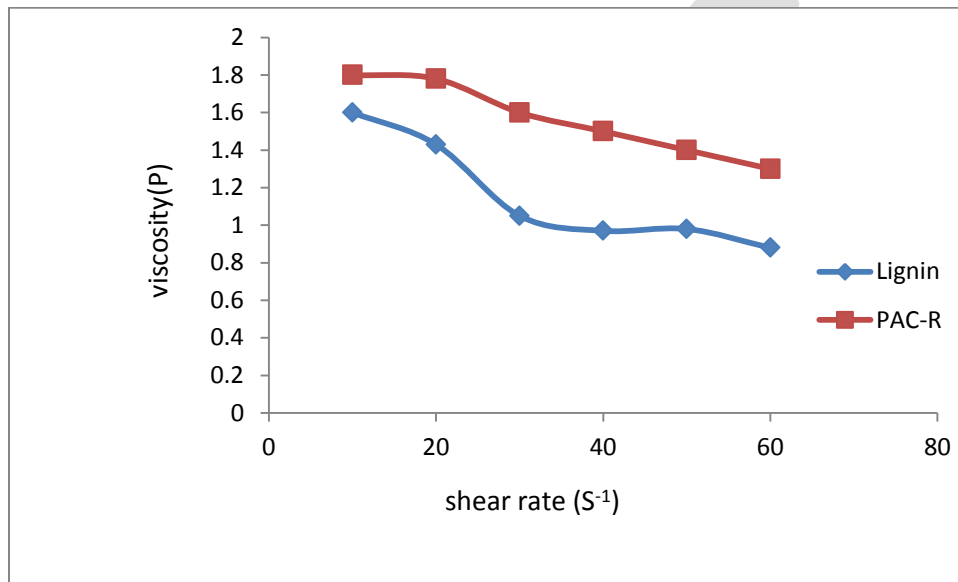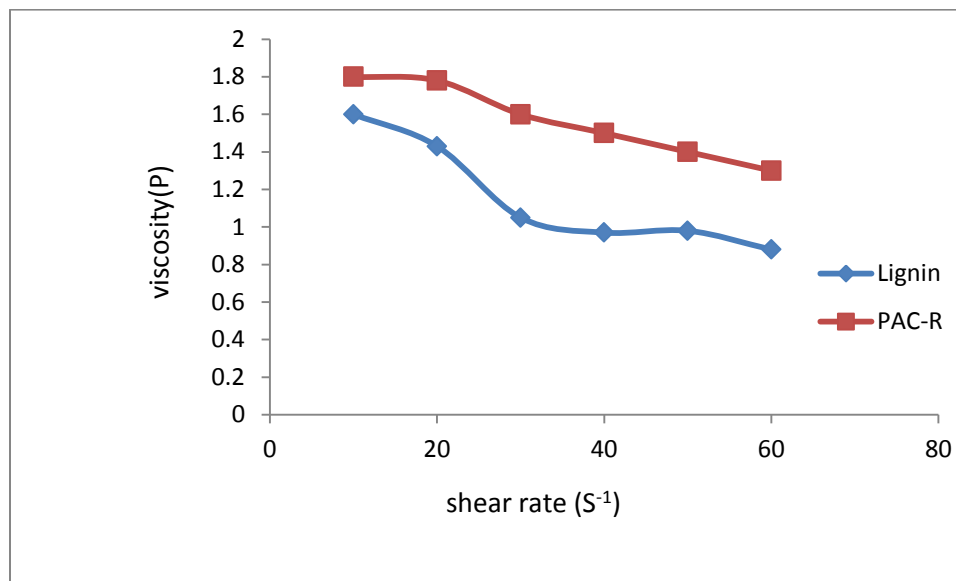
Pseudo-plastics are known not stream with diminishing rate of shear anxiety. It was further watched that the centralization of lignin and caboxymethyl cellulose in the boring liquids did not have any impact on its thickness while; expanding grouping of polyanionic cellulose expanded the consistency of the boring liquid. Hence expanding the grouping of polyanionic cellulose will build its imperviousness to stream under specific levels of connected anxiety.

5. Conclusion :

The Rheological properties of boring liquids can't be overemphasized on account of their conspicuous commitment to the general fruitful boring operations. This study has shown the utilization of earth benevolent biopolymers in the creation of boring liquids. The boring liquids were observed to be non-Newtonian and show pseudo-plastic conduct. The shear stress, yield anxiety, and consistency of the eco-accommodating liquids are subject to focus and have higher qualities indicating higher gel quality and flocculation for the new liquid than for the generally utilized liquids. The consistency of the liquids diminishes with expanding shear rate; accordingly, the new liquids have a shear diminishing conduct. The new biopolymer liquids are along these lines more appropriate for investigation and abuse of oil and gas in naturally delicate zones because of its high effectiveness and immaculateness. Polyanionic cellulose (PAC-R) demonstrated the most noteworthy shear rate and shear stress than carboxyl methyl cellulose and xanplex D. This was a direct result of the straight open long chain structure of PAC-R and its capacity to associate with water, solids and with themselves. It additionally went about as a superior viscosifier as a result of the more negative charge it conveys. Likewise, the plan of polymeric drilling liquid with Bentonite has demonstrated to enhance the consistency than that experienced in typical traditional boring liquids.

REFERENCES:
[1] R. B. Watson, P. Viste, and J. R. Lauritzen, "The influence of fluid loss additives in high temperature reservoirs", Society of Petroleum Engineers Conference Paper, 2012.
[2] B. K. Warren, T. R. Smith, K. M. Ravi, "Static and dynamic fluid-loss characteristics of drilling fluids in a full-scale wellbore", Society of Petroleum Engineers Conference Paper, 1993.
[3] National Iranian Oil Company (NIOC) manual, "Drilling formation", Department of Drilling Chemistry, Ahwaz, Iran, 2002.
[4] S. Z. Kassab, A. S. Ismail, and M. M. Elessawi, "Drilling fluid rheology and hydraulics for oil fields", European Journal of Scientific Research, Vol. 57, Issue 1, p68, 2011.
[5] Deily et al., "New biopolymer low-solids mud speeds drilling operation", The Oil and Gas Journal, vol. 65, No. 26, pp. 62-70, 1967.
[6] H. C. H. Darley, and G. R. Gray, "Composition and properties of drilling and completion fluids", 5th ed. Gulf Professional Publishing, Houston, USA, pp. 66-67, 561-562, 1988.
[7] J. L. Lummus, and J. J. Azar, "Drilling fluids optimization: A practical field approach", PennWell Books, Tulsa-Oklahoma, USA, pp. 3-5, 1986.
[8] J. F. Douglas, J. M. Gas-lorek, and J. A. Swaffield, "Fluid mechanics", 3rd ed. ELBS with Longman, 1995.

[9] American Petroleum Institute, "Drilling fluid testing procedure manual", USA, 2000.

[10] TEAP-ENIAgip Division, "Drilling fluid and waste disposal manual", Nigeria, 2000.

[11] T. Hamida, E. Kuru, and M. Pickard, "Rheological characteristics of aqueous waxy hull-less barley (WHB) solutions", Journal of Petroleum Science and Technology, 69, pp 163-173, 2009.

[12] T. Adam, Jr. Bourgoyne, E. C. Martin, F. S. Keithk, and Jr. Young, "Applied drilling engineering", Society of Petroleum Engineers Text Book Series, Vol. 2, pp. 4082, 1991.

[13] L. M. Zhang, Y. B. Tan, and Z. M. Li, "New water-soluble ampholytic polysaccharides for oilfield drilling treatment: A preliminary study" Carbohydr. Polym.44, pp. 255-260, 2001.

[14] E. Lucas, C. Mansur, and L. Spinelli, Pure and Applied Chemistry, 81, pp. 473, 2009,

[15] A. Przepasniak and P. Clark, Society of Petroleum Engineers, Conference paper SPE-39461, Lafayette, EUA, 1998.

[16] A. Martins, A. Waldman, and D. Ribeiro, Society of Petroleum Engineers, Conference paper SPE-94287, Madrid, Spain, 2005.

[17] N. J. Alderman, D. R. Babu, T. L. Hughes, and G. C. Maitland, "Rheological properties of water-based drilling muds", in 4th International Congress on Rheology, Sydney, 1988.

[18] M. V. Kok, T. Alikaya, "Rheological evaluation of polymers as drilling fluids", Petroleum Science Technology, Vol. 21, Nos. 1-2, pp. 133, 2003.

[19] M. V. Kok, T. Alikaya, "Effect of polymers on the rheological properties of KCl/polymer type drilling fluid", Energy Sources, 27: 405, 2005.

[20] F. H. D Outmans, "Mechanics of static and dynamic filtration", Society of Petroleum Engineer Journal, 63: 210, 1963.

[21] J. Mewis, J. F. Willaim, A. S. Trevor, and W. B. Russel, "Rheology of suspensions containing polymerically stabilized particles", Journal of Chemical Engineering Research Development, 19: 415, 1989.

[22] G. V. Chilingarian, and P. Varabutre, "Drilling and drilling muds" Development in Petroleum Science, 44, Elsevier, Amsterdam, 2000.

[23] M. N. Okafor, and J. F. Evers, "Experimental comparison of rheology models for drilling fluids", SPE Western Regional Meeting, California, Paper ID. SPE-24086-MS, 1992.

[24] T. Hemphill, W. Campos and A. Pilehvari, "Yield-power law model more accurately predicts mud rheology", Oil & Gas Journal, Vol. 91, No. 34, pp. 45-50, 1993.

[25] M. Khalil, and B. M. Jan, "Herschel-Bulkley rheological parameters of a novel environmentally friendly lightweight biopolymer drilling fluid from xanthan gum and starch", Journal of Applied Polymer Science, Vol. 124, Issue 1, pp. 595-606, 2012.

[26] C. O. Chike–Onyegbula, O. Ogbobe, and S. C. Nwanonenyi, "Biodegradable polymer drilling mud prepared from guinea corn", Journal of Brewing and Distilling Vol. 3, No. 1, pp. 6-14, 2012.

[27] C. W. Hoogendam, A. de Keizer, M. A. Cohen Stuart, B. H. Bijsterbosch, J. A. M. Smit, J. A. P. P. Van Dijk, P. M. Vander Horst and J. G. Batelann (1998). "Persistence length of carboxymethyl cellulose as evaluated from size exclusion chromatography and potentiometric titrations." Macromolecules 31, 6297-6309.

[28] J. Kelly and J. John (1983). "Drilling fluid selection, performance and quality control."Petroleum Technology, p889.

[29] B. L. Browning (1967). "Viscosity and molecular weight."In Methods of wood chemistry, Vol. 2. B. L. Browning ed., Interscience Publishers, New York, Ch. 25, 519-557.

Variation in the blue colour intensity and the pH of the PEM of 1.531211SMJ29 Silicon Molybdenum Jeewanu when the PEM is irradiated with clinical mercury lamp and sunlight

Deepa Srivastava

Department of Chemistry, S.S.Khanna Girls' Degree College, Constituent College of Allahabad University, Allahabad, Uttar Pradesh, India

srivastava.deepa@ymail.com

Abstract— The Jeewanu has been prepared in the laboratory in a sunlight exposed sterilized aqueous mixture of some inorganic and organic substances by Bahadur and Ranganayaki. In prebiotic atmosphere possibly energy transducing systems similar to Jeewanu existed which had an ability to convert solar energy into useful forms. Gáinti in 2003 discussed that Jeewanu possesses a promising configuration similar to protocell-like model. Jeewanu is capable of spitting water molecule to hydrogen and oxygen in presence of sunlight and the proton set free, is utilized to fix nitrogen and carbon dioxide.

Effect of variation in the concentration of mineral solution, formaldehyde and ammonium molybdate on pH and colour intensity of the PEM of 1.531211 SMJ38 Jeewanu before and after exposure to sunlight was studied by Srivastava, D.

Keywords— Autopoetic, eukaryote, Jeewanu, PEM, sunlight, mercury lamp, morphology, 1.531211SMJ29, pH

INTRODUCTION

The Jeewanu has been prepared in the laboratory in a sunlight exposed sterilized aqueous mixture of some inorganic and organic substances.[1]

In prebiotic atmosphere possibly energy transducing systems similar to Jeewanu existed which had an ability to convert solar energy into useful forms.

The photochemical, formation of protocell-like microstructures "Jeewanu" in a laboratory simulated prebiotic atmosphere capable of showing multiplication by budding, growth from within by actual synthesis of material and various metabolic activities has been reported[1,2,3,4,5,7,].

Gáinti discussed that Jeewanu possesses a promising configuration similar to protocell-like model. [8]

Jeewanu is capable of spitting water molecule to hydrogen and oxygen in presence of sunlight and the proton set free, is utilized to fix nitrogen and carbon dioxide. [9]

The photochemical reversible oxidation-reduction reaction takes place in the parental mixtures in which Jeewanu are formed. The colourless parental mixture becomes blue when exposed to sunlight because of the reduction of molybdic form of molybdenum of ammonium molybdate to molybdous form, during the Jeewanu formation. In dark, the (ous) molybdenum is again oxidized to (ic) molybdenum turning the parental mixture colourless again. This process makes the mixture blue on exposure to sunlight and colourless in dark. This phenomenon can be observed in the same mixture when shifted from dark to the sunlight and again from

sunlight to dark repeatedly. But for this, the presence of formaldehyde and the contact of the mixture with atmospheric oxygen are essential. This reversible photochemical electron transfer is very interesting in the sense that it resembles the electron transfer of chlorophyll of plants in sunlight during the process of photosynthesis, where organic matter donates the electron.

Jeewanu under certain conditions showed characteristic movements at different periods of exposure. A very characteristic shivering movement, of Jeewanu which were prepared by the mixing of cerous sulphate solution to a mixture of potassium ferrocyanide solution and sucrose along with other constituents, was observed by Verma in 1970. [10]

The movement which is observed in protoplasm is considered to be the movement of locomotion. As this movement of protoplasm is without the aid of external factors, it is considered to be due to some internal causes. Sometimes, certain chemical substances, light and heat act as the external factors inducing the movement of protoplasm. These factors act as stimuli. Light also act as a stimulus as seen in algae which move towards the source of weak light but move away from the source of strong light. Protoplasm also responds to the stimulation of heat. When there are two different temperature areas, protoplasm moves towards the warmer area. However, if the tissue is gently warmed, the protoplasm shows more rapid rotation or circulation motion.

Effect of variation in the concentration of mineral solution, formaldehyde and ammonium molybdate on pH and colour intensity of the PEM of 1.531211 SMJ38 Jeewanu before and after exposure to sunlight was studied by Srivastava, D. [11,12,13]

In this paper, an attempt is made to investigate the effect of irradiation of 1.531211SMJ29 Silicon Molybdenum Jeewanu PEM with mercury lamp and sunlight on the blue colour intensity and the pH of the PEM.

MATERIALS AND METHODS
The following solutions were prepared:
   a) 4% (w/v) ammonium molybdate
   b) 3 % (w/v) diammonium hydrogen phosphate
   c) Mineral solution: It was prepared by mixing various minerals in appropriate proportions.
   d) 36% formaldehyde
   e) 3% (w/v) sodium chloride
   f) 5% (w/v) water soluble sodium silicate

 Procedure:
Two clean, dry, sterilized corning conical flasks of 10 ml capacity were taken and labeled and B. In each flask 15 ml of 4% ammonium molybdate, 30 ml of 3% diammonium hydrogen phosphate, 10 ml of mineral solution, 20 ml of formaldehyde, 10 ml of sodium chloride and 10 ml of soluble sodium silicate were added. The total volume of each flask was 95 ml separately.

Each flask was cotton plugged and shaken well. Flask A was exposed to sunlight and flask B was exposed to mercury lamp keeping the distance of flask B from mercury lamp 32 cms and the mercury bulb used was of 125 W. Both the flasks were exposed simultaneously for same exposure time each day giving half hour exposure daily for first two days, and then 2 hours exposure daily for fourteen days giving a total exposure of 29 hours. The intensity of the blue colour and the pH were noted both before and after each exposure for each flask A and B. the microscopic observations were also done simultaneously both before and after each exposure.

After total 29 hours of exposure, particles of each flask were filtered, dried in a desiccator and weighed. The yields of both flasks were noted.

Table – 1

Effect of irradiation of 1.531211SMJ29 PEM to sunlight and mercury lamp on the pH of the PEM.

Period of exposure in hours	Irradiated to sunlight		Irradiated to mercury lamp	
	Before exposure	After exposure	Before exposure	After exposure
½	3.33	2.72	3.37	2.90
1	2.65	2.60	2.64	2.53
3	2.73	2.70	2.73	2.70
5	2.82	2.80	2.82	2.80
7	2.68	2.60	2.68	2.60
9	2.72	2.60	2.68	2.66
11	2.70	2.65	2.65	2.60
13	2.73	2.62	2.71	2.54
15	2.67	2.61	2.68	2.53
17	2.66	2.62	2.63	2.57
19	2.70	2.65	2.68	2.60
21	2.68	2.65	2.68	2.63
23	2.69	2.59	2.69	2.57
25	2.75	2.70	2.75	2.64
27	2.78	2.66	2.77	2.57
29	2.64	2.63	2.73	2.65

The yields of the two flasks were as follows:

Yield of 1.531211SMJ29 in g

a) Flask A exposed to sunlight   0.2984
b) Flask B exposed to mercury lamp   0.2430

CONCLUSION

The observations indicate that the intensity of the blue colour increased with increase in the exposure time in both the cases i. e. in both the PEM the one exposed to sunlight and the other exposed to the radiation of the clinical mercury lamp light. The difference in the trend of absorbance in both was that the peak of the absorbance in case of the PEM irradiated with clinical mercury lamp light was lower than that of the PEM irradiated with sunlight indicating that some radiations of sunlight other than long ultraviolet is more effective in producing the blue colour in the PEM on exposure. It was further observed that the difference in the blue colour intensity after a night gap and before the next exposure and that after exposure gradually decreased with increase in the exposure time and almost disappeared after 7 hours of exposure. This was found to be true for both the cases of PEM irradiated with sunlight and with clinical mercury lamp light.

In the mixture which was exposed to sunlight the intensity of blue colour was more after the day's exposure. After the mixture stood in shade and in the darkness of the night the next morning the mixture became light in the blue colour intensity. This started after the exposure of half an hour and was observed till 7 hours of exposure. After that the decrease in the colour intensity in dark was not that pronounced.

It has been observed that when 0.2 g of ammonium molybdate in 200 ml distilled water and having 10 ml formaldehyde was exposed to sunlight; the mixture became blue in colour in sunlight. If this mixture was covered with black cloth and kept overnight, the intensity of the blue colour decreased. If the mixture was kept for few days in dark it became completely colourless. When the same mixture was again exposed to sunlight, it turned blue in colour and was bleached on keeping in dark. It has been observed that this process can be repeated again and again for a long time. It has further been observed that it has two limiting factors:

1. There must be oxygen in the overhead space.
2. There must be formaldehyde in the mixture.

In the experiment undertaken above, the reason for not getting significant decrease in the colour intensity of the PEM exposed to sunlight after 7 hours of exposure when kept in dark, might be that all the formaldehyde present in the PEM was used up because the oxygen was always present in the overhead space of the flask in which PEM was kept.

It was interesting to note that the long ultraviolet of clinical mercury lamp produced much less blue colour in the mixture. This shows that the visible part of the solar radiation is more effective in producing blue coloured Mo^{4+} ions from colourless Mo^{6+} ions in presence of chemicals of the PEM.

It has been observed that in shade the pH increased i.e. before exposure after darkness of the night, the pH was more. On exposure the pH decreased in both the cases i.e. in PEM exposed to sunlight and the PEM exposed to radiations of clinical mercury lamp. Another interesting feature observed was that the initial pH was more in both cases and with increase in exposure period, the pH decreased in both the cases.

REFERENCES:

1. BAHADUR, K. AND RANGANAYAKI, S., J. BRIT. INTERPLANETARY SOC., VOL. 23(12), 813-829, 1970.
2. BAHADUR, K., VIJANANA PARISHAD ANUSANDHAN PATRIKA, 6, 94-117, 1963.
3. BAHADUR, K. AND AGARWAL, K.M.L. ZBL. BAKT. 117, (2), 585-602, 1964.
4. BAHADUR, K., (1966), IN "SYNTHESIS OF JEEWANU, THE PROTOCELL", M/S RAM NARAYAN LAL BENI PRASAD, ALLAHABAD, INDIA, 1966.
5. BAHADUR, K., ZBL. BAKT. 121(2), 291-319, 1967.
6. BAHADUR, K. AND RANGANAYAKI, S., SINGH, V.P. AND KUMAR, S., RAVISTA DO. INSTITUTE DE. ANTIBIOTICS RECIFE, VOL. 15(NO) (1/2), 33-36, 1975.
7. BAHADUR K. AND RANGANAYAKI S., "ORIGIN OF LIFE, A FUNCTIONAL APPROACH", M/S RAM NARAIN LAL AND BENI PRASAD, ALLAHABAD, INDIA, 1980.
8. GANTI T. "THE PRINCIPLES OF LIFE", OXFORD UNIVERSITY PRESS, OXFORD, U.K, 2003.
9. BAHADUR K. , RANGANAYAKI S. , SMITH A. AND FOLSOME C. , NATL. ACAD. SCI., INDIA, GOLDEN JUBILEE COMMEMORATION, VOL. 181-198 , 1980.
10. VERMA, M.L., "STUDIES IN ABIOGENESIS OF MOLECULAR ASSOCIATIONS", D.PHIL. THESIS, DEPT. OF CHEMISTRY, UNIV. OF ALLAHABAD, ALLAHABAD, INDIA, 1970.
11. SRIVASTAVA. D., "EFFECT OF VARIATION IN THE CONCENTRATION OF MINERAL SOLUTION ON pH AND COLOUR INTENSITY OF THE PEM OF 1.531211 SMJ38 JEEWANU BEFORE AND AFTER EXPOSURE TO SUNLIGHT", *INTERNATIONAL JOURNAL OF INNOVATIVE RESEARCH IN SCIENCE, ENGINEERING AND TECHNOLOGY (AN ISO 3297: 2007 CERTIFIED ORGANIZATION), (IJIRSET),* VOL. 5, ISSUE 5, MAY 2016, PP 8065 8068. DOI: 10.15680/IJIRSET. 2016. 0505111, 2016.
12. SRIVASTAVA. D., "EFFECT OF INCREASE OF CONCENTRATION OF FORMALDEHYDE IN THE PEM OF 1.531211 SMJ8 ON THE PROTON RELEASE AND DEGREE OF Mo^{6+} REDUCTION TO Mo^{4+} DURING THE EXPOSURE TO SUNLIGHT", *JOURNAL OF NATURAL SCIENCE RESEARCH(IISTE)*, VOL 2, NO.7, 2012, PP 56-59 , 2012.
13. SRIVASTAVA. D., "EFFECT OF VARIATION IN THE CONCENTRATION OF AMMONIUM MOLYBDATE IN THE PARENTAL ENVIRONMENTAL MEDIUM (PEM) ON THE pH AND THE PHOTOCHEMICAL REDUCTION OF Mo 6+ TO Mo 4+ IN THE PEM OF THE SILICON MOLYBDENUM JEEWANU 1.531211 SMJ8 BOTH BEFORE AND AFTER EXPOSURE" , *INTERNATIONAL JOURNAL OF SCIENTIFIC AND ENGINEERING RESEARCH (IJSER)*, VOL 3, ISSUE 6, JUNE-2012,PP750-754. DOI: 10. 14299/000000, 2012.

Development of a Gear Hobbing Fixture to Reduce Ineffective Work and Increase the Productivity using Ergonomics

Mr. Sumeet Shinde*, Mr. Priyanshu Tanna, Mr. AdityaWalunj, Mr. Akshay Ozarde

Department of Mechanical Engineering, Marathwada Mitra Mandal's College of Engineering (Pune University), Pune, India

*Corresponding Author: sumeetshinde109@gmail.com

Abstract--The present work deals with the development of a gear hobbing fixture for manufacturing of gear drive of fuel pump hobbed on Lambert 82 machine. The primary objective is to reduce the time & improve the current working method of manual clamping by using screw clamp. This is achieved by replacing the existing method with a hydraulically actuated clamping and de-clamping mechanism activated by a switch, thus using ergonomic principle of reducing the manual efforts required. In addition to this the other important criteria to be considered are cutting forces and shear experienced, along with total runout, positive location, repeatability, production rate and reliability .

Keywords – fixture, productivity, ineffective work, clamping mechanism, disc springs, hydraulic and pneumatics, switch, ergonomics, BRIEF survey

INTRODUCTION

Gear Hobbing is a widely applied manufacturing process for the construction of any external tooth form developed uniformly about a rotating centre. It is an advance process compared to turning and milling [6]. The fixture used for hobbing process should be designed such that the gear blank is clamped accurately about the machining axis and restrain any undesirable movement throughout the machining. Fixtures consisting of clamps and locators should also ensure a good quality performance beside positioning and holding. Michael Yu Wang [7] stated that fixture layout is the fundamental task of fixture design, to determine the number, type and location of the basic fixturing elements of locators, supports, and clamps, as opposed to the detailed design of the fixture assembly.

Ineffective work can be defined as any efforts put into any process which does not contribute to the productivity, profit or significant returns, and results in wastage of time and energy. Human factors and ergonomics (HF&E), also known as comfort design, functional design, and systems, is the practice of designing products, systems, or processes to take proper account of the interaction between them and the people who use them. In this project we are dealing with the physical ergonomics, which is concerned with human anatomy, and some of the anthropometric, physiological and bio mechanical characteristics as they relate to physical activity.

PROBLEM FORMULATION

Fixtures are very vital parts of conventional as well as modern manufacturing processes since it directly affects the productivity and quality. The total machining time for a workpiece includes work-handling, the methods of locating and clamping and the total machining time should be as minimum as possible. The fixture should also ease the loading and unloading of the workpiece, which will help to reduce the ideal time.

Fig.1 Screw clamping   Fig.2 Workpiece with support
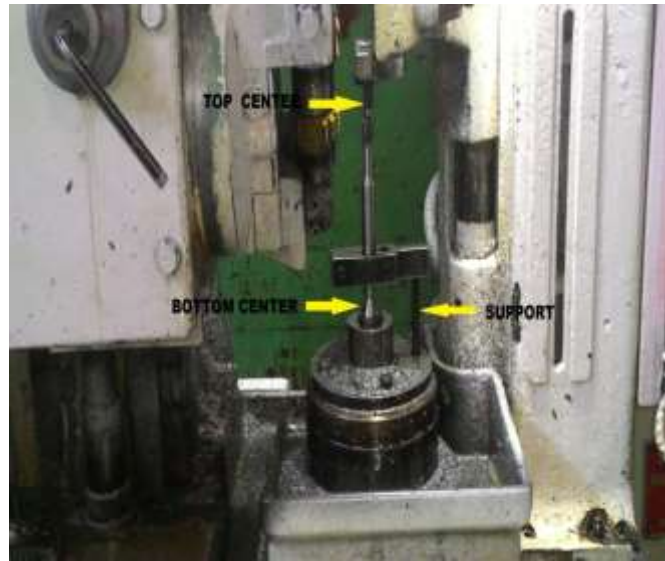
The time taken for setting of the workpiece on the machine was quite high. The above figure explains that the operator first need to hold the workpiece in the clamp and tighten the screw, then hold the workpiece between the centres and wait until the top centre of the machine touches the workpiece. Then as the base table starts rotating, the support shown in the figure which connects the extended portion of the clamp and the base, rotates the workpiece along with the base table. As you can see, this technique of setting the workpiece is not reliable and tedious for the operator when a batch of about 150-200 such gears is to be machined. The chances of job rejection are also very high due to the following reasons-
(A conditional runout tolerance of only **25 microns** is permitted)
• The centres cannot hold the workpiece very firmly due to the high cutting forces.
• Due to the tedious repetitive cycle of setting the workpiece the operator might not properly set the extended part of the clamp on the support.

CONDITIONS TO BE CONSIDERED WHILE DESIGNING THE FIXTURE

• Ergonomics
The existing process is very tedious for the operator and he is subjected to fatigue along with various risk factors and thus a simpler clamping   system   is   to   be   designed.

• Runout tolerance
As the job is used to drive the fuel pump, runout of the job to be maintained is restricted to only **25 microns**. Therefore the fixture should clamp the workpiece uniformly and within the runout limit

• Power operated clamping and de-clamping mechanism
As the primary aim is to reduce the ineffective work introduced due to the manual clamping of the workpiece, we have to use power operated mechanism. Various options were considered like using electric motor, vacuum pump and hydraulic-pneumatic power to actuate the clamps.
Due to lack of space, high operating cost and difficulties in effectively implementing the mechanism, the options like electric motor and vacuum pump were obviated. The most viable solution was to use Hydraulic and Pneumatic power. The implementation of the mechanism using the hydraulic-pneumatic source is explained later in the coming section.

• Tool travel
The upper and lower limit of tool travel from the base is 8.1" and 2.95" respectively. Therefore we have to maintain the portion of the job to be machined within these limits.

DEVELOPMENT OF MECHANISM AND ITS IMPLEMENTATION
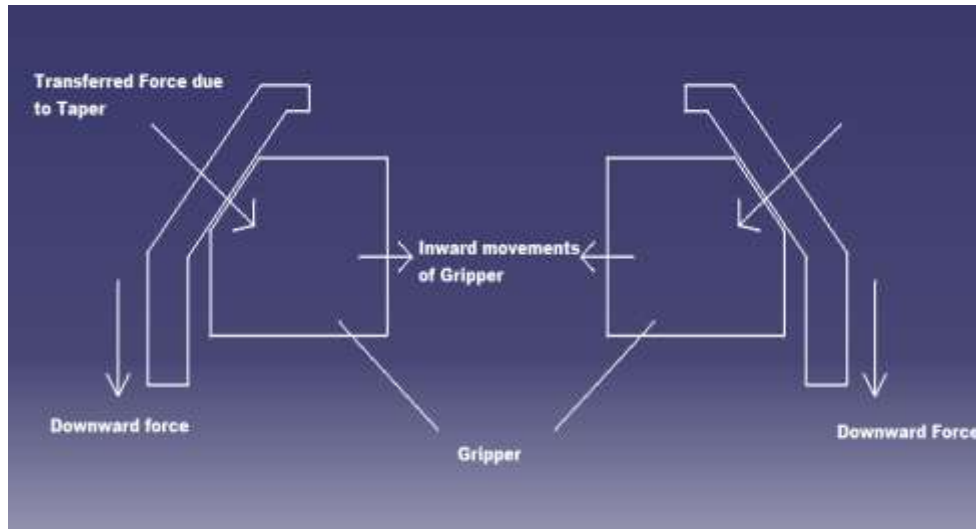
Fig.3 Block Diagram of Basic Mechanism

A simple clamping mechanism is used as shown in figure consisting of grippers and a taper part having linear vertical motion. The taper portion of the outer part is in contact with the taper edge of the gripper. As the outer part moves downwards, the gripper starts moving inwards. This simple principle is used to develop the clamping mechanism of the fixture.
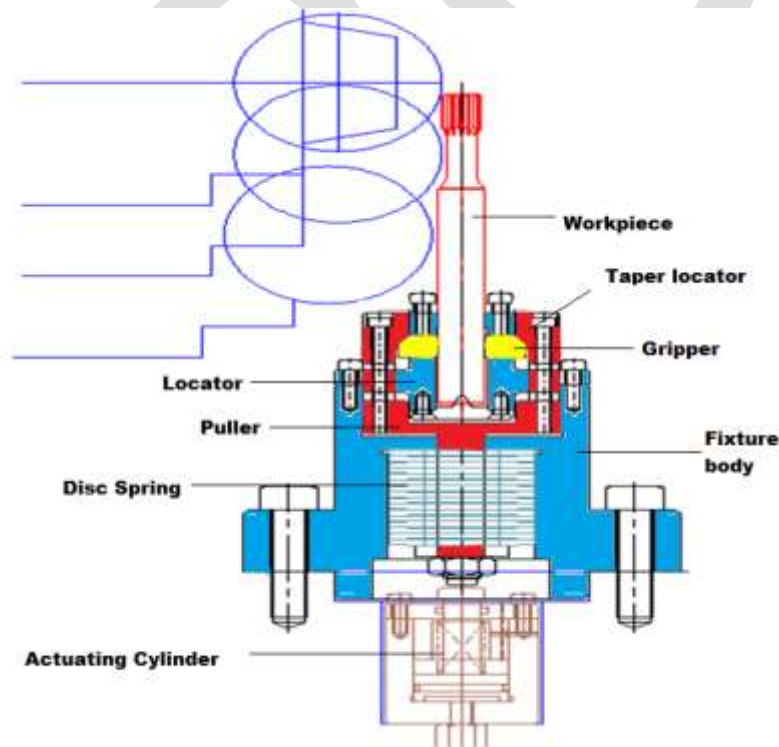
Fig.4 Sectional View of the fixture

Challenges
The challenge while implementing the above described mechanism was that there are two motions to be considered

- Linear Motion of taper locator, puller and gripper during clamping (shown in Red colour)
- Rotation of the total fixture, as it has to be attached to the base plate. (achieved with the help of blue coloured parts)

The Taper Locator and Puller are used to clamp the workpiece in position and have linear vertical motion. The puller by default is pulled downward due to the spring action of disc spring. Due to this downward motion of taper locator, the grippers move inwards and thus clamp the workpiece.

To de-clamp the workpiece an actuating cylinder, attached below the base table, which has a very small clearance between the piston and the puller end, is used. This cylinder is hydraulically powered and pushes the puller upwards which moves the taper locator upwards and thus generates a clearance between the gripper and taper locator. Thus the grippers become free slides in guides provided and they can move outwards and job can be removed.
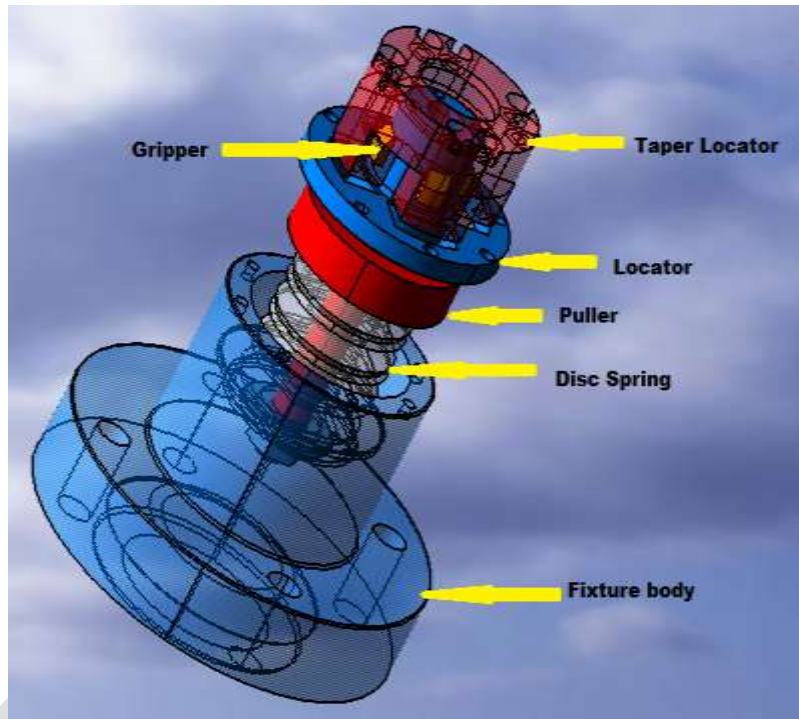
Fig.5 3-D Exploded view of the Fixture

In order to make the fixture rotate with the base table, the Taper Locator is interlocked with the Locator. From the figure, we can see that the taper locator has projected ends which fit into the slots in the locator. The locator is attached to the fixture body which is attached to the base. This arrangement rotates the fixture (hence the workpiece) with the same RPM as that of the table.

DISC SPRINGS

As mentioned in the above condition of Tool Travel, the combined height of the fixture and workpiece should not cross the upper limit of the tool travel. By using conventional helical spring there is a possibility of exceeding this limit, therefore we will be using Disc spring which exerts the same force as that of a helical spring but with lesser space requirement and deflection.

Advantages of Disc Spring are-
- High load capacity with small deflection
- High load to size ratio
- Consistent performance under design loads
- Longer fatigue life
- Flexibility in stack arrangement to meet the desired load requirement

HYDRAULIC & PNEUMATIC CIRCUIT
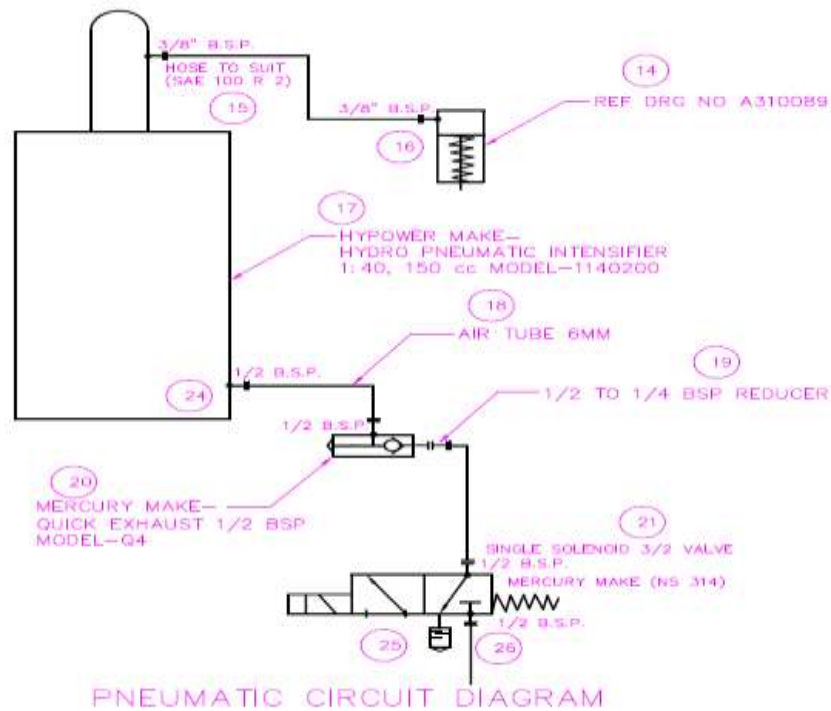
Fig.6 Pneumatic circuit Diagram

The available power supply in the company was Pneumatic supply of 3.5bar which is used for the cleaning of the burr by compressed air gun, this same supply is to be used to actuate the cylinder which in turns de-clamps the job. This pressure isn't enough to de-clamp and also this line is common to all the machines in the plant, there is a possibility of pressure drop as there might be another operator using it. Hence to compensate for this loss and to avoid any interruption in the operation of the fixture mechanism we have used an intensifier in the circuit of ratio 1:40. The line after the intensifier is hydraulic using oil of grade SAE100R2.

RESULTS AND DISCUSSIONS

1. TIME-SAVING
The time measured for setting and handling of the job without fixture was about
11sec and with fixture it is 5sec.

2. ERGONOMICS
BRIEF Survey (Baseline Risk Identification of Ergonomics Factors).The BRIEF Survey is intended to find any ergonomic risk factors that may cause any musculoskeletal symptoms to the employee operating the machine. Lower the score of the survey, greater will be the safety and better ergonomics. The BRIEF Survey of the process shows a very significant improvement from 30 to 8 points.

Fig.7
(Before Improvement)

Fig.8
(Before Improvement)

Fig.9
(After Improvement)

Fig.10
(After Improvement)

3. PRODUCTIVITY

Number of jobs rejected per 100 jobs manufactured without fixture = 2
Number of jobs rejected per 100 jobs manufactured with fixture = 0
Therefore, Material Productivity without fixture = 98%
Material productivity with fixture = 100%

ACKNOWLEDGEMENT

CONCLUSION

With the ever increasing demand and pace of production it is necessary to improve the process of production. The proposed clamping mechanism has successfully reduced the ineffective work and the risk factors and eventually results in an over-all increase in the productivity. The mechanism introduced here can be used to develop similar fixtures which demand clamping of any circular workpiece.

REFERENCES:

[1] Patang Vidyut Chandra "An effort to apply work and time study techniques in a manufacturing unit for enhancing productivity" International Journal of Innovative Research in Science, Engineering and Technology, ISSN: 2319-8753, Vol. 2, Issue 8, August 2013

[2] Dusko Pavletic, Mirko Sokovic "Quality Improvement Model At The Manufacturing Process Preparation Level" International Journal for Quality research, UDK- 658.5, Vol.3, No. 4, 2009

[3] Jennifer N. Schumann "An Analysis of Ergonomic Risk Factors Relating to Strains at Company XYZ" A Research Paper Submitted in Partial Fulfillment of the Requirements for the Master of Science Degree in Risk Control, The Graduate College University of Wisconsin-Stout May, 2007

[4] Shailesh S. Pachbhai, Laukik P. Raut "A Review on Design of Fixtures" International Journal Of Engineering Research and General Science, ISSN 2091-2730, Feb-Mar 2014

[5] Amar Raj Singh Suri, A.P.S. Sethi "Development of Gear Hobbing Fixture Design for Reduction in Machine Setting Time" International Journal of Scientific and Research Publications, ISSN 2250-3153, Volume 2, Issue 10, October 2012

[6] Mihir K. Shah, Vivek A. Deshpande, Ramchandra M. Patil "A Review on Lean Tools & Techniques: Continuous Improvement in Industry" International Journal of Advance Industrial Engineering, E-ISSN 2320 –5539, 16 Dec 2015, Vol.3, No.4 (Dec 2015)

[7] M. Y. Wang "Optimum 3D Fixture Layout Design" Intelligent Control and Automation, Proceedings of the 3rd World Congress, 26 June-2 July 2000

[8] K.V.S. Seshendra Kumar "Design of Gear Cutting Fixture for CNC Gear Hobbing Machine" International Journal of Scientific and Research Publications, ISSN 2250-3153, Volume 2, Issue 9, September 2012

[9] Mutombozana Tapiwa, Mugwindiri Kumbirayi, Chikuku Tauyanashe "The use of Work Study Techniques in Optimizing Manufacturing Plant Maintenance Processes: an Investigation into a Fertilizer Manufacturing Company in Zimbabwe" International Journal of Science and Research (IJSR), ISSN: 2319-7064, Volume 2 Issue 2, February 2013

[10] Sandeep Soni, Ravindra Mane "Design and Modeling of Fixture for Cylinder Liner Honing Operation" Global Journal of Researches in Engineering Mechanical and Mechanics, ISSN: 2249-4596, Volume 13 Issue 7 Version 1.0, 2013

[11] Abdul Talib Bon, Daiyanni Daim "Time Motion Study in Determination of Time Standard in Manpower Process" Proceedings of EnCon2010 3rd Engineering Conference on Advancement in Mechanical and Manufacturing for Sustainable Environment, Kuching, Sarawak, Malaysia, April 14-16, 2010

[12] W. Patrick Neumann "Identifying and Managing Risk in the Design of High Performance Work Systems" Doctoral Thesis, Department of Design Sciences Lund University, Sweden, 2004

Implementation of a Parallel Multiplier for FFT Application

Saniya Paulson

M.tech Student,SSET Karukutty, spsans62@gmail.com, 9496715586

Abstract— Multipliers will play an important role in today's digital signal processing and various other applications. The multiplication operation consists of producing partial products and then adding these partial products the final product is obtained. Thus the speed of the multiplier depends on the number of partial products and the speed of the adder. In parallel multipliers number of partial products to be added is the main parameter that determines the performance of the multiplier. The main aim in VLSI field is to make a multiplier which increases the speed and reduces the area and power. This paper focuses on the implementation of a 8-point and 16-point FFT using a parallel multiplier designed using Advanced Modified Booth Encoding Algorithm(AMBE) for 8-bit signed-unsigned number multiplication. This paper describes comparison of various multipliers based on area and delay. Simulations are done using Xilinx 14.2ISE and implemented on SPARTAN-6 FPGA board.

Keywords— AMBE,FFT, Parallel multiplier, Signed, Unsigned, Partial products, Adder, Multiplier

INTRODUCTION

Enhancing the processing performance and reducing the power dissipation of the systems are the most important design challenges for multimedia and digital signal processing (DSP) applications, in which multipliers frequently dominate the system's performance and power dissipation. Most digital signal processing methods use nonlinear functions such as discrete cosine transform (DCT) or discrete wavelet transform (DWT). Because they are basically accomplished by repetitive application of multiplication and addition, the speed of the multiplication and addition determines the execution speed and performance of the entire calculation. As the multiplier requires the longest delay among the basic operational blocks in digital system, the critical path is determined by the multiplier, in general. Multiplication is most commonly used in every step of the world. It is nothing but the addition by the multiplicand adds multiplier no. of times. But, it takes very large hardware resources and simulation takes very large time for the final output. The multiplication mainly consists of two steps:

i) To generate Partial products and

ii) To add all these partial products until the final output.

The main aim in VLSI field is to make a multiplier which increases the speed and reduces the area and power. Earlier multipliers were used either for signed or unsigned numbers like Baugh-Wooley multiplier[1][2] for signed numbers,array multiplier[3] for unsigned numbers, Braun array multiplier[4] for unsigned numbers etc. In this paper earlier multipliers are compared and a parallel multiplier[5][6] using Advanced Modified Booth Encoding Algorithm for both signed and unsigned number is being implemented. This multiplier reduces the total chip area as well as the power. Hence it is used to obtain a 8-point FFT and a 16-point FFT .

RESULTS FROM THE LITERATURE SURVEY

TABLE1: COMPARISON OF MULTIPLIERS

Parameter	Array Multipier	Baugh-Wooley Multiplier	Combined Multiplier	MBE Multiplier[7][8][9]	AMBE Multiplier[10][11]
Multiplier Type	Unsigned	Signed	Either signed or unsigned	Signed	Both signed&unsigned
No.of slice LUTS	105	146	247	153	137
No.of bonded IOBs	32	32	33	35	33
Delay(ns)	17.668	21.371	20.245	13.842	11.924

The evaluation results show that the AMBE has better performance, reduced delay and area. Hence it is used to implement 8-point and 16-point FFTs.

PROPOSED ADVANCED MODIFIED BOOTH ENCODING MULTIPLIER (AMBE)
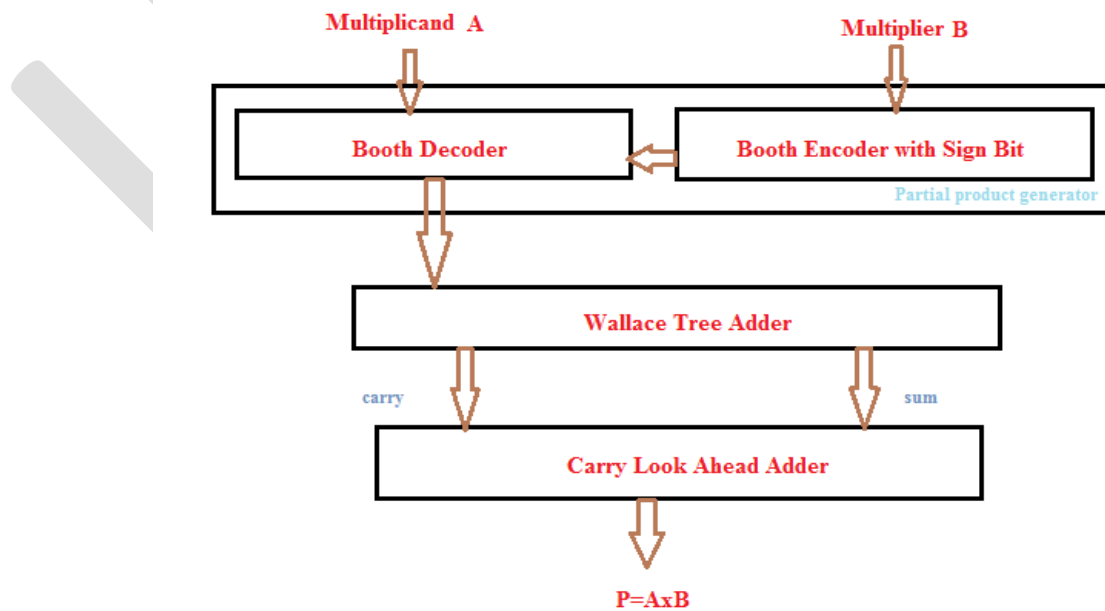
Fig 1: Block diagram of proposed AMBE multiplier

The proposed AMBE follows the same architecture diagram as that of modified booth encoding multiplier.The difference is that the encoder is extended with 2 sign bits. There are Booth Encoder, Booth Decoder, Wallace Tree adder and Carry Look Ahead adder blocks .

The Booth Encoder encodes the multiplier bits and generates the encoded signals {-2, -1, 0, 1, 2}. The logic diagram for Booth Encoder is shown in fig 2. The Booth encoder encodes the signals X1_a, X2_a, and Z.
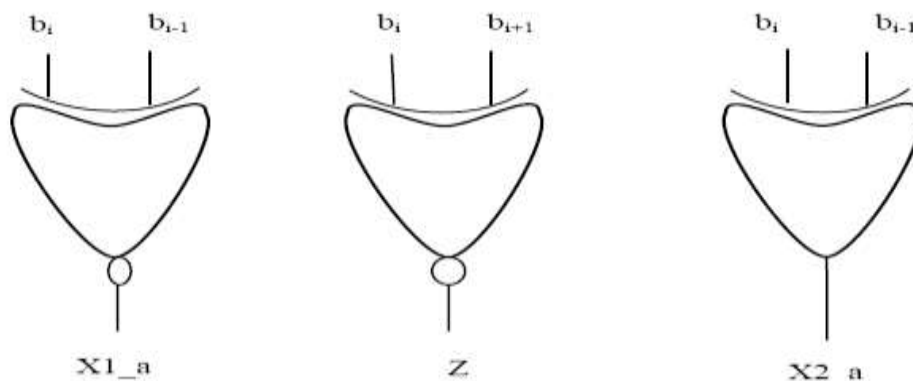
Fig 2: Logic Diagram of Booth Encoder

Using MBE logic, Booth decoder generates the partial product bit, which is given by Equation (1).

$$pij = \overline{\overline{(a_i \oplus b_{i+1} + b_{i-1} \oplus b_i)} \ \overline{(a_{i-1} \oplus b_{i+1} + b_i \oplus b_{i+1} + b_{i-1} \oplus b_i)}} \qquad (1)$$

Equation(1) is implemented as shown in Fig 3. The proposed AMBE multiplier does not separately consider the encoder and the decoder logic, but instead implemented as a single unit called a partial product generator.
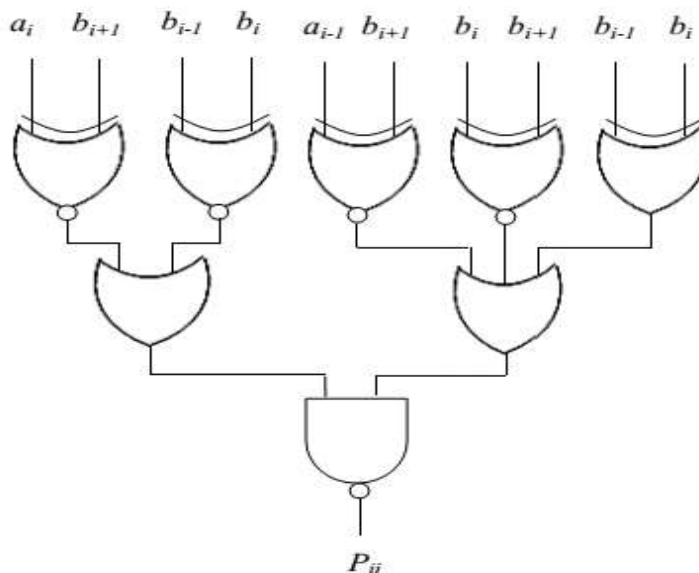
Fig 3: Logic Diagram of 1-bit Partial Product Generator Circuit

The negative partial products are converted into 2's complement by adding a negate (N_i) bit. The Negative bit is represented by Equation(2).

$$N_i = b_{i+1} \overline{(b_{i-1} \, b_i \,)} \qquad (2)$$

The Equation (2) is implemented as shown in Fig 4.
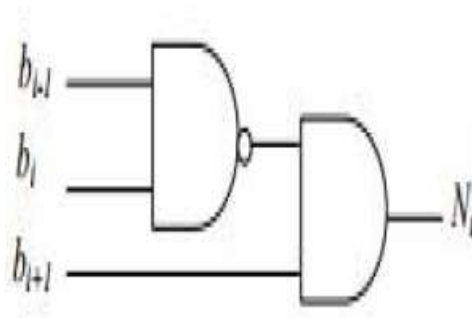
Fig 4: Logic Diagram of Negative bit Generator Circuit

Table 2: Truth table of proposed AMBE

b_{i+1}	b_i	b_{i-1}	Value	X1_a	X2_a	Z	Neg
0	0	0	0	1	0	1	0
0	0	1	1	0	1	1	0
0	1	0	1	0	1	0	0
0	1	1	2	1	0	0	0
1	0	0	-2	1	0	0	1
1	0	1	-1	0	1	0	1
1	1	0	-1	0	1	1	1
1	1	1	0	1	0	1	0

The sign extension bit is converted to signed-unsigned number by Equations (3) and (4).

$$a8 = s\_u * a7 \qquad (3)$$
$$b8 = s\_u * b7 \qquad (4)$$

The logic Diagram of Equation (3) and Equation (4) are implemented as shown in Fig 5.
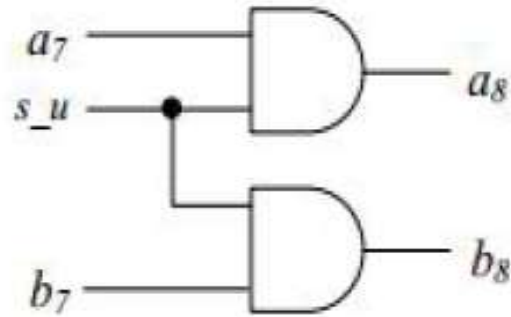
Fig 5: Logic Diagram of Sign Extension bits

One bit control signal called signed-unsigned (s_u) bit is used to indicate whether the multiplication operation is signed number or unsigned number. When Sign-unsign s_u = 0, it indicates unsigned number multiplication, and when s_u = 1, it indicates signed number multiplication.

It is required that when the operation is unsigned multiplication the sign extended bit of both multiplicand and multiplier should be extended with 0, that is a8= a9= b8= b9= 0. It is required that when the operation is signed multiplication the sign extended bit depends on whether the multiplicand is negative or the multiplier is negative or both the operands are negative.

For this when the multiplicand operand is negative and multiplier operand is positive the sign extended bits should be generated are s_u = 1, a7=1,b7= 0, a8= a9 =1, and b8= b9=0. And when the multiplicand operand is positive and multiplier operand is negative the sign extended bits should be generated are s_u =1, a7=0, b7=1, a8=a9=0, and b8= b9=1.

Table 3: s_u bit operation

SIGNED-UNSIGNED BIT (s_u)	TYPE OF OPERATION
0	Unsigned
1	Signed

Fig 6 represents the partial products generated from fig 5. There are 5 partial products and Negative bit generator. These partial products are X1, X2, X3, X4 and X5. These partial products are added by Wallace tree Adder which uses Carry Save Adder circuit. It adds partial products until final two outputs are left.

$$a_7\ a_6\ a_5\ a_4\ a_3\ a_2\ a_1\ a_0$$

$$b_7\ b_6\ b_5\ b_4\ b_3\ b_2\ b_1\ b_0$$

$\overline{p_{08}}$ $\overline{p_{08}}$ p_{08} p_{07} p_{06} p_{05} p_{04} p_{03} p_{02} p_{01} p_{00}		X1
$1\ \overline{p_{18}}$ p_{17} p_{16} p_{15} p_{14} p_{13} p_{12} p_{11} p_{10}	N_0	X2
1 -------------------------------p_{20}	N_1	X3
1 ----------------------------p_{30}	N_2	X4
p_{47} p_{46} p_{45} p_{44} p_{43} p_{42} p_{41} p_{40}	N_3	X5

$$P_{15}\ P_{14}\ P_{13}\ P_{12}\ P_{11}\ P_{10}\ P_9\ P_8\ P_7\ P_6\ P_5\ P_4\ P_3\ P_2\ P_1\ P_0$$
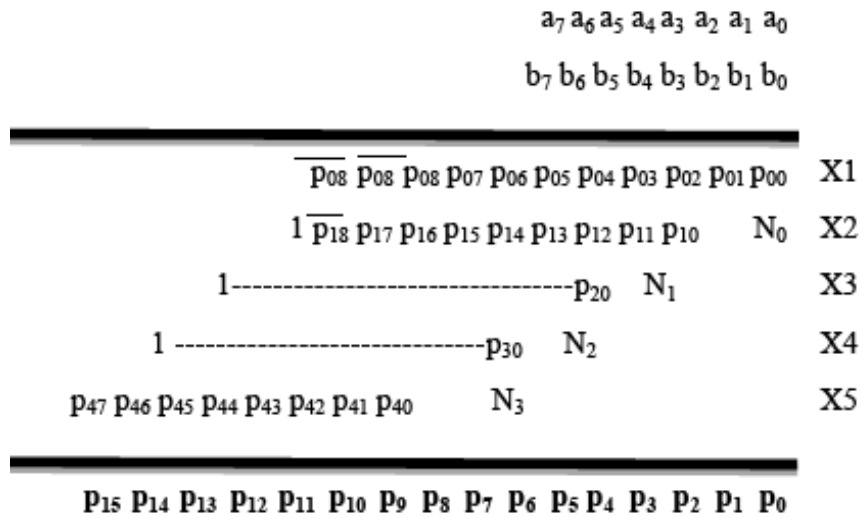
Fig 6: 8x8 signed unsigned generated Partial Product bits

Carry Save Adder (CSA) tree diagram is shown in fig 7 below. When there are only two outputs are left, Carry Look Ahead (CLA) Adder[12] is used to do the final addition and give the Final product.

P=AxB
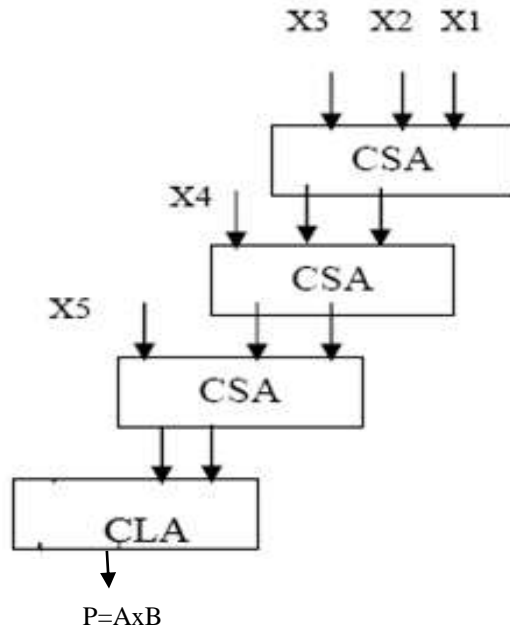
Fig 7: Wallace Tree Adder

The 8-point and 16-point FFTS shown below are implemented using this proposed AMBE multiplier.
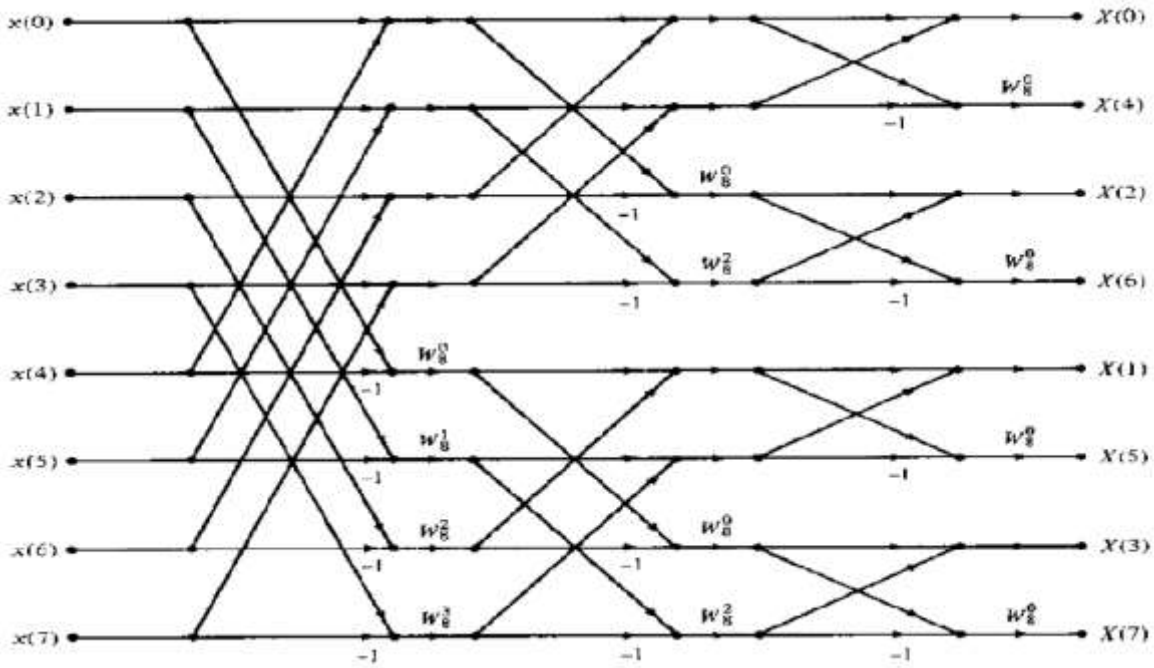
Fig 8: 8-point FFT diagram
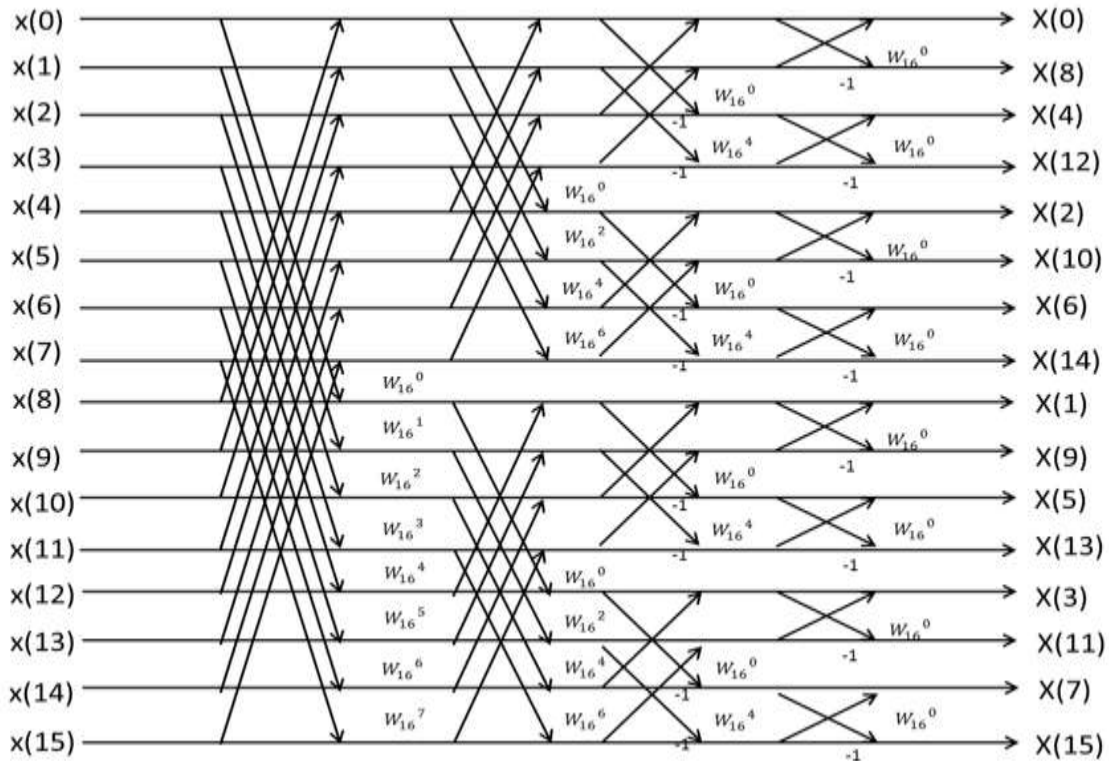
Fig 9: 16-point FFT diagram

SIMULATION RESULTS
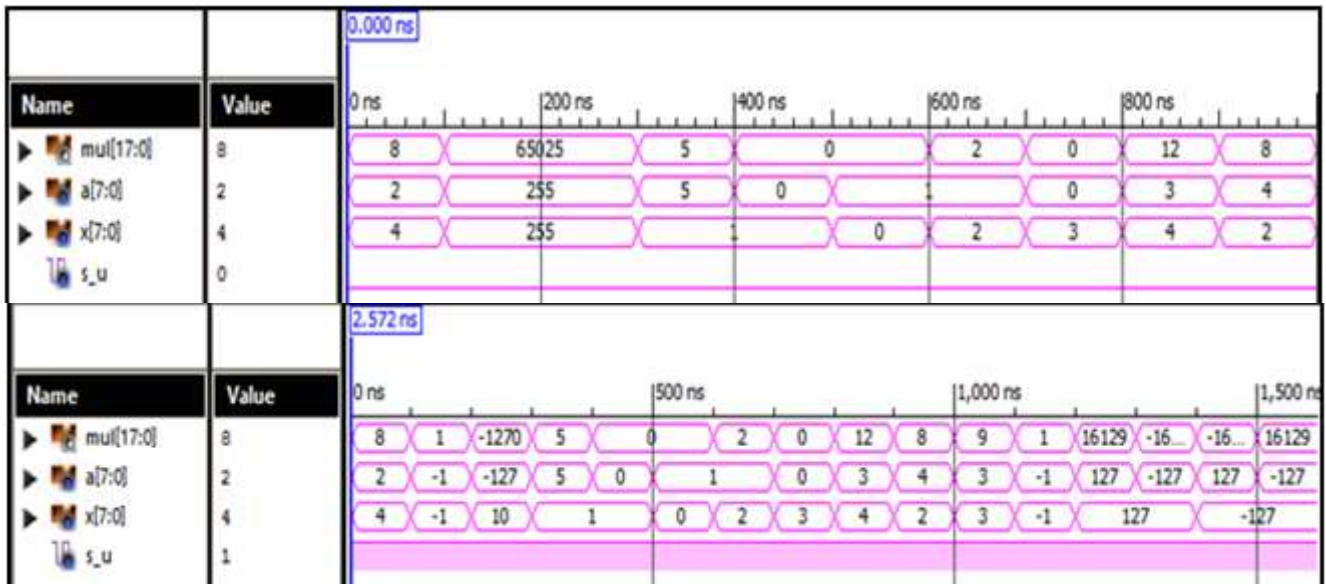
Fig 10: Simulation waveform of 8x8 AMBE
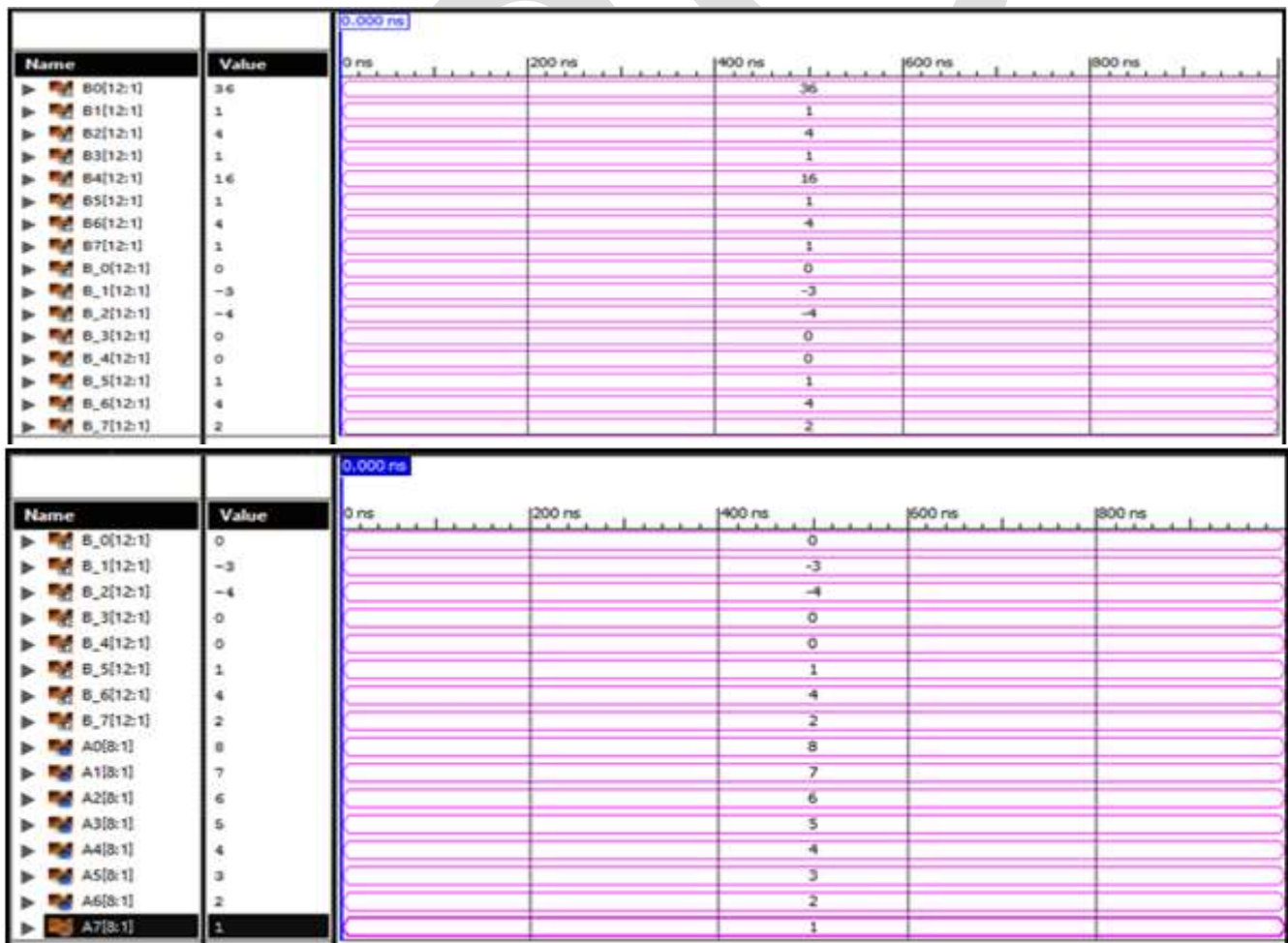
Fig 11: Simulation waveform of 8-POINT DIF FFT

Name	Value
A0[8:1]	15
A1[8:1]	14
A2[8:1]	13
A3[8:1]	12
A4[8:1]	11
A5[8:1]	10
A6[8:1]	9
A7[8:1]	8
A8[8:1]	7
A9[8:1]	6
A10[8:1]	5
A11[8:1]	4
A12[8:1]	3
A13[8:1]	2
A14[8:1]	1
A15[8:1]	0

Name	Value
Y_0[8:1]	0
Y_1[8:1]	0
Y_2[8:1]	-8
Y_3[8:1]	8
Y_4[8:1]	-20
Y_5[8:1]	4
Y_6[8:1]	-3
Y_7[8:1]	19
Y_8[8:1]	-41
Y_9[8:1]	3
Y_10[8:1]	-5
Y_11[8:1]	11
Y_12[8:1]	-3
Y_13[8:1]	-1
Y_14[8:1]	16
Y_15[8:1]	20

Name	Value
Y0[8:1]	120
Y1[8:1]	8
Y2[8:1]	8
Y3[8:1]	8
Y4[8:1]	7
Y5[8:1]	9
Y6[8:1]	8
Y7[8:1]	8
Y8[8:1]	5
Y9[8:1]	9
Y10[8:1]	9
Y11[8:1]	9
Y12[8:1]	26
Y13[8:1]	-10
Y14[8:1]	1
Y15[8:1]	15

Fig 12: Simulation waveform of 16-POINT DIF FFT

CONCLUSION

Multiplication is most commonly used in every step of the world. The main aim in VLSI field is to make a multiplier which increases the speed and reduces the area and power. The proposed 8-bit Advanced Modified Booth Encoding Parallel Multiplier has so far obtained the less area and delay than all other multipliers. It performs both signed and unsigned operations in parallel. AMBE uses the same architecture as that of a Modified Booth Encoding Multiplier, but the difference is that the encoder has been extended with a sign bit. The evaluation results show that the proposed design has better performance, reduced delay and area. Hence it is used to implement 8-point and 16-point FFTs. The simulations have been done on Xilinx 14.2ISE and implemented on SPARTAN-6 FPGA board.

REFERENCES:

[1] Indrayani Patle, Akansha Bhargav, Prashant Wanjari, "Implementation of Baugh-Wooley Multiplier Based on Soft-Core Processor," IOSR Journal of Engineering (IOSRJEN) e-ISSN: 2250-3021, p-ISSN: 2278-8719 Vol. 3, Issue 10 (October. 2013), ||V3|| PP 01-07 .

[2] Pramodini Mohanty,VLSI Design,2011-2012: "An Efficient Baugh-Wooley Architecture for Both Signed & Unsigned Multiplication", PramodiniMohanty et al./ International Journal of Computer Science & Engineering Technology (IJCSET).

[3] N. Ravi, A.Satish, Dr.T.Jayachandra Prasad and Dr.T.Subba Rao,"A New Design for Array Multiplier with Trade off in Power and Area," IJCSI International Journal of Computer Science Issues, Vol. 8, Issue 3, May 2011 ISSN (Online): 1694-0814 www.IJCSI.org.

[4] Ms. Madhu Thakur ,Prof. Javed Ashraf , " Design of Braun Multiplier with Kogge Stone Adder & it's Implementation on FPGA", International Journal of Scientific & Engineering Research, Volume 3, Issue 10, October-2012 ISSN 2229-5518 .

[5] W.-C. Yeh and C.-W. Jen, "High-Speed Booth Encoded Parallel Multiplier Design," IEEE Transactions on Computers, vol. 49, no. 7, pp. 692–701, July 2000.

[6] T.V.Subbi Reddy and J.Nirmala Bai, "16-Bit High Speed Modified Booth Multiplier for Signed and Unsigned Numbers", International Journal of New Trends in Electronics and Communication (IJNTEC) Vol.1, Issue.3, Oct. 2013.

[7] Kavita,Jasbir kaur, "Design and Implementation of an Efficient Modified Booth Multiplier using VHDL" , Special Issue: Proceedings of 2nd International Conference on Emerging Trends in Engineering and Management, ICETEM 2013.

[8] Shiann-RongKuang, Jiun-Ping Wang, and Cang-Yuan Guo, "Modified Booth multipliers with a Regular Partial Product Array," IEEE Transactions on circuits and systems-II, vol 56, No 5, May 2009.

[9] Ravindra p rajput, M.N Shanmukha swamy, "High Speed Modified Booth Encoder Multiplier for Signed and Unsigned Numbers",2012, 14th international conference on modelling and simulation, doi 10.1109/uksim.2012.99.

[10] Shaikh Kailash Baba& D. Rajaramesh, "Design & Implementation of Advanced Modified Booth Encoding Multiplier", International Journal of Engineering Science Invention ISSN (Online): 2319 – 6734, ISSN (Print): 2319 – 6726, Volume 2 Issue 8 August. 2013 PP.60-68.

[11] K. Tsoumanis, N. Axelos, N. Moschopoulos, G. Zervakis, and K. Pekmestzi, "Pre-Encoded Multipliers Based on Non-Redundant Radix-4 Signed-Digit Encoding", IEEE TRANSACTIONS ON COMPUTERS, VOL. 65, NO. 2, FEBRUARY 2016.

[12] C. Padma ,Y. Mahesh, "Design of High Speed Modified Booth Encoded Parallel Multiplier using Carry Look Ahead Adder", i-manager's Journal o ,Vol. No. 1 Embedded Systems 2 February - April 2013.

PERFORMANCE EVALUATION OF ASYNCHRONOUS TRANSFER MODE (ATM) AS A VEHICLE FOR WIDE BANDWIDTH INTERNET CARRIAGE

D. E. Bassey., B. E. Okon., E. E. Eyime

Department of Physics,

University of Calabar, Calabar,

Cross River State, Nigeria.

benokon16@yahoo.com, **basseyde1@yahoo.com**

Abstract- The convergence of telecommunications and computer communication technologies heralded by innovations in Internet services requires the development of interworking units to convert different data formats and control procedures into a single unique protocol. Therefore, creating an information transfer protocol such as Asynchronous Transfer Mode (ATM), as a transport and switching model will enhance quality of service delivery. ATM is a standard for carriage of a complete range of user traffic through a single network. It is designed to unify telecommunications and computer networks. The study embarked on a simulation project where different LANs were modeled and configured to convey cells or packets under high speed, with the aid of ATM switching and transport nodes. Through "pinging", the network was examined in terms of carriage of converged signal with respect to time. In addition, wire-shark packet analyzer was activated to access the transferred time of each packet and converts these packets for assessment using window protocol. The study noted that like other Internet transport protocols, ATM also suffered different forms of threats. Recommendations were made from the study.

Keywords: ATM, ISDN, Ethernet, LAN, Interworking unit.

1. INTRODUCTION

Digital communication environment is generally characterized by two main support technologies: on one hand is computer oriented communications and Local Area Networks (LAN), supported by Ethernet or Token ring specifications [2,9]. This technique is based on data packets, using locally or remotely interconnected computers and terminals. On the other hand is the Public Switched Networks (PSN), based on data circuits such as the Integrated Services Digital Networks (ISDN) with capabilities to interconnect a large variety of terminal equipment and also interconnect several LANs remotely through switch or constant rate links [5,12].

In recognition of the main objective of ATM, Interworking units (IWU) were built in for the purpose of converting ISDN and Ethernet traffic to the ATM formats. These conversion procedures located on the lower layers of the OSI protocol reference model (the Physical Layer and the Medium Access Control Layer) [1,6], were briefly discussed.

2. LITERATURE REVIEW

The proposed Interworking device has two data buses: the Utopia Bus, which sustains the cell transfer between line interface modules and the processor bus, which allows ATM cells, ISDN channels and Ethernet packets, to be transferred between line interfaces, the processor, and the memory [3,18].

The Interworking unit has two ISDN interfaces for the basic and the primary access, respectively. The Basic Access Interface is specified at the reference point by several ITU recommendations. With a transmission rate of 144 Kbit/s, S bus is able to inter-connect at least 8 terminals, by sharing one or two 64 Kbit/s time slots for data information transfer (B channel), while the signaling information is transported out of band on a 16 Kbit/s D Channel [7,16].The Basic Access Interface can be used to interconnect ISDN terminals to Local Area Networks (LANs) over a Public Switched Network (PSN), through one or more of the other interfaces of the IWU [13].

Since many computer terminals communicate through an Ethernet interface, according to IEEE 802.3 standards, namely: 10 Base T and 100 Base T specifications, the proposed IWU have to handle these interfaces at physical and logical levels in order to convert the Ethernet environment to ATM specifications [14].

The Interworking unit has two ATM physical interfaces operating at 156 Mbit/s. On the ATM interface, the cells were mapped according to ITU-T recommendation (G. 804) [17], on the frame described by G. 703 [15]. This interface is appropriate for the interconnection of ATM environments over the interconnect LANs [4].

The introduction of the Asynchronous Transfer Mode(ATM), which is neither circuit nor packet oriented transmission protocol, but a conjunction of the best of both techniques, permits the convergence of routing and switching technologies and the specification of new communication platforms, supported by different interfaces and transfer protocols. The integration of this technology, within

telecommunications and computer networks, requires the development of special adaptation units with interworking functionalities [10]. Also, the compatibility between different types of services requires the development of adaptable protocols for data presentation, at the application level. On the other end, the compatibility between distinct systems forces the specification of common physical and logical interfaces and the development of Interworking units (IWU), to adapt different transmission, switch and flow control protocols [8,11].This paper, therefore, presents a simple model that interrogates Asynchronous Transfer Mode (ATM), as a vehicle for high speed bandwidth applications and discusses the integration of such device into different network scenarios.

3.   METHODOLOGY
3.1   Modeling
A model is a demonstration of a system in a very simple way with the intention of advancing the idea of the real system. A simulator on the other hand is the process of manipulating a model in a way that its function with respect to space and time the proto-type of the model. Modeling as a means of representation has a long history. Man has tried all possible means of modeling creation, with a view to improving his living condition. Motivated by this fact, ATM transmission protocol was simulated and configured as a high speed carrier for a unified, converged network. This configuration served as a model to the real practice of ATM protocol.

3.2   ATM Networks Configuration
The ATM network was configured by using a set of ATM switches interconnected by point-to-point ATM links. Two types of interfaces were configured within the simulated network to support the switches. They were the user to network interface (UNI) and the network to network interface (NNI).The UNI was used to connect ATM end devices like routers and host to an ATM switch. While the network-to-network interfaces (NNI) was used to connect two ATM switches within the network. Table 1 is a comparative review of different protocols and network speed.

Table 1: Comparison between protocols and network speed

Protocol	Cable	Speed	Topology
Ethernet	Twisted Pair, Coaxial, Fiber	10 Mbps	Linear Bus, Star, Tree
Fast Ethernet	Twisted Pair, Fiber	100 Mbps	Star
LocalTalk	Twisted Pair	.23 Mbps	Linear Bus or Star
Token Ring	Twisted Pair	4 Mbps - 16 Mbps	Star-Wired Ring
FDDI	Fiber	100 Mbps	Dual ring
ATM	Twisted Pair, Fiber	155-2488 Mbps	Linear Bus, Star, Tree

SOURCE: http/www.atmforum.com

3.3 Materials

From Table 1, different network protocols were analyzed with a view to selecting the most effective transport protocol that can converge telecommunications signal and computer networking. From these analyses, ATM was selected as the choice protocol for the needed convergence. The following materials used for the study are hereby briefly explained:

i. ATM switch: ATM switches are electronic devices with high speed networking capacity used to transfer data from one end to the other. ATM switches support voice, video and data services and are designed to switch fixed-size data units called cells. Cells are used in ATM communications. The simulated ATM switch received the input cells or information from another ATM device, read and updated the cell header information in order to switch the information cell towards its end-points.

ii. GNS3: Graphical Network Simulation tool was used to design the ATM network.

iii. ATM end points: The end points used for the study were personal computers, IP phones, printers, work-stations and routers.

iv. Networking Cables: The cables employed here were straight-through cables, cross over cables and serial DCE cables.

3.4   System Configuration
The configuration of the unifying network carriage was carried out through a set of wireless switches configured on user network to network interface (UNI). Through the UNI, routers were configured as host to an ATM-configured switch. Another interface was configured through NNI to connect two ATM switches into the simulated network.

The simulator used was a software package called the GNS3 (Graphical Network Simulator).This is an open source graphical network simulation tool used to design flexible network. This package was selected after examining several other packages. They were flexible with ATM, Ethernet and frame relays. GNS3 guarantees a true network setting to carry out the configurations. It can run in all popular window versions. Its graphical user-interface was made in a way that no further customization was needed. GNS3 main program window enabled the researcher to drag network devices like routers, switches, firewalls, work stations, IP phones, etc., into the working interface. Through this medium, different connections were created and the focal features of the study were achieved: design

of high quality complex network topology, simulation of simple Ethernet, ATM and frame relay switches, connection of the simulated network to the real wall and packet-capture using wire shark.

Further to the above, the following end points were aiding tools:

1) Personal Computers: personal computers were linked to the Local Area Network (LAN) via cables connection. The personal computer used was a laptop. It was used to send data and video services to the ATM network.

2) IP phone: IP phones were used to deliver voice communication through the ATM network. The model used was a software based phone.

3) Routers: routers were employed to make decisions on the directions of IP packets and route them correctly. A router can be set-up between the Internet service providers (ISP) and the customer network to direct information to either way. The function of a router was to forward packets to other networks until the packet reaches its destination. The router interfaced the two Local Area Network (LANs) used for the study. The routers used were CISCO IOS 7200 routers.

4) Networking cables: Networking cables were used to connect one network device to another network to form a LAN. Further to this accessories, were other shared components such as printers and scanners. The project was wired using the following networking cables.

5) Straight-through cables: Straight-through cables were used to link dissimilar networking devices like switch to pc, switch to router, router to switch, etc. Straight-through cables were used when each end of the communication linkages transmitted and received packets from different pairs. Similarly cross over cables were used to connect similar network devices like pc to pc, router to router, switch to switch, hub to hub, etc. Serial DCE cables were also used to provide the clock signals in order to communicate through bus topology and to connect one router to the other in the network.

3.5 Configuration-commands used to activate the ATM switch

The simulator used to model the ATM network was the GNS3.The above highlighted components of the network was configured using the following man-machine language commands:

Set the VCI to VPI ratio. The switching process of the ATM network was based entirely on the VCI to CPI ratio. The VCI to VPI values control the memory distribution in the network. It specifies the maximum value of the VCIs to support the VPI. Fig. 1 is a plate showing ATM switch port numbers configured during the project.

To set the VCI to VPI ratio, the under listed procedures present samples of man-machine language commands initiated.

The numbers used were as follows:

1:1:100=10:1:200

Where

Port = 1
VCI = 100   } Source network
VPI = 0

Port = 2
VCI = 200   } Destination network
VPI= 0
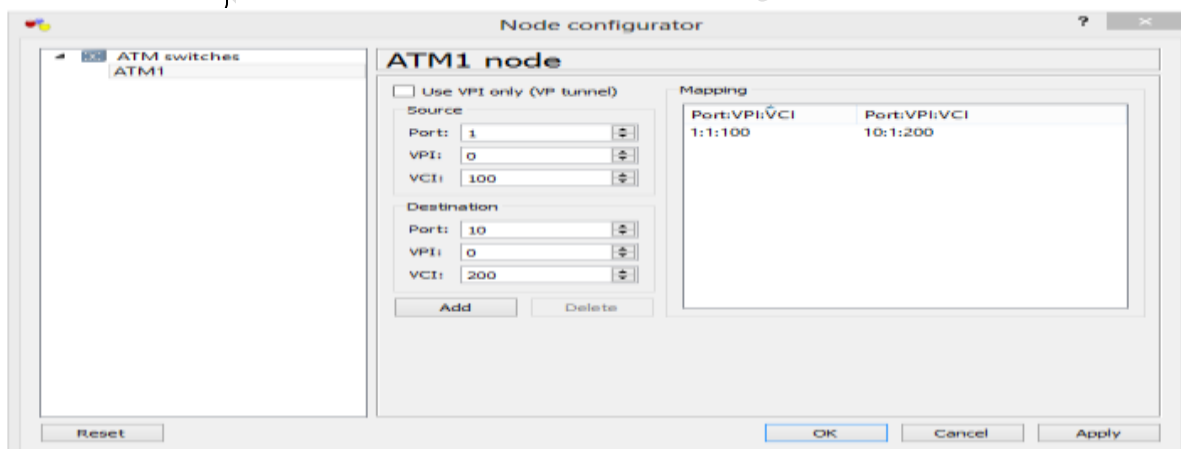
FIG. 1: ATM switch port numbers

3.6 Configuration of the routers

The routers used for this work were the CISCO IOS 7200 model. The router was chosen because of the in-built ATM configuration in it. The following procedures present summarized system configuration used.

Router 1

R1> enable

R1# configured terminal
R1 (config) # interface ATM1/0
R1 (config-if)# IP address 192.162.1.1 255.255.255.252
R1 (config-if)# map-group atm-cir-123
R1 (config-if)# no shut down
R1 (config-if)#atmpvc 1 1 100 aa/5 snap
R1 (config-if)# no atmilmi-keepalive
R1 (config-if)# exit
R1 (config)# map-list atm-cir-123
R1 (config)# IP 192.168.1.2 atm-VCI broadcast
R1 (config)# interface Ethernet 2/0
R1 (config-if)# IP address 192.168.2.1 255.255.255.0
R1 (config-if)# no shut down.

Configuration for router II
R2> enable
R2# configured terminal
R2 (config) # interface ATM1/0
R2 (config-if)# no shut down
R2 (config-if)# IP address 192.168.1.2 255.255.255.252
R2 (config-if)# map-group atm-cir-123
R2 (config-if)#atmpvc 1 1 200 aa/5snap
R2 (config-if)# no atmilmi-keepalive
R2 (config-if)# exit
R2 (config)# map-list atm-cir-123
R2 (config)# IP 192.168.1.1 atm-VCI broadcast
R2 (config)# interface Ethernet 2/0
R2 (config-if)# IP address 192.168.3.1 255.255.255.0
R2 (config-if)# no shut down.

Switch 1 (sw-1) and switch 2 (sw-2): (sw-1) and (sw-2) in the ATM Network were activated to function as manageable switches. They do not have special configuration in the GNS3 simulator. They simply acted as plug and play switches.

  Pinging is a computer-based administrative utility used to test the connectivity of end devices in the network. It can also be used to calculate the transmission time used by a message sent from the source-end device to the destination-end devices.

At the end of the ATM network configuration processes, pinging commands were used to test the ability of the device to terminate the packets in real-time. The pinging commands used for the personal computer, the IP phone and the work-station are presented below: The Pinging commands activated during the transceiver processes are respectively presented as follows: Personal computer (Fig, 2), IP phone (Fig.3) and Work-station (Fig.4).
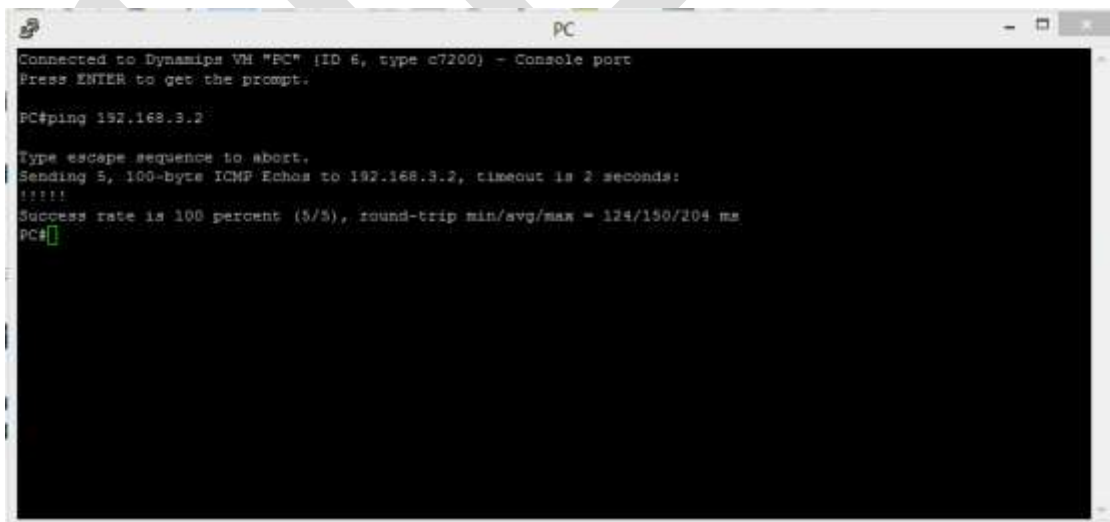
FIG. 2: Pinging command for the personal computer
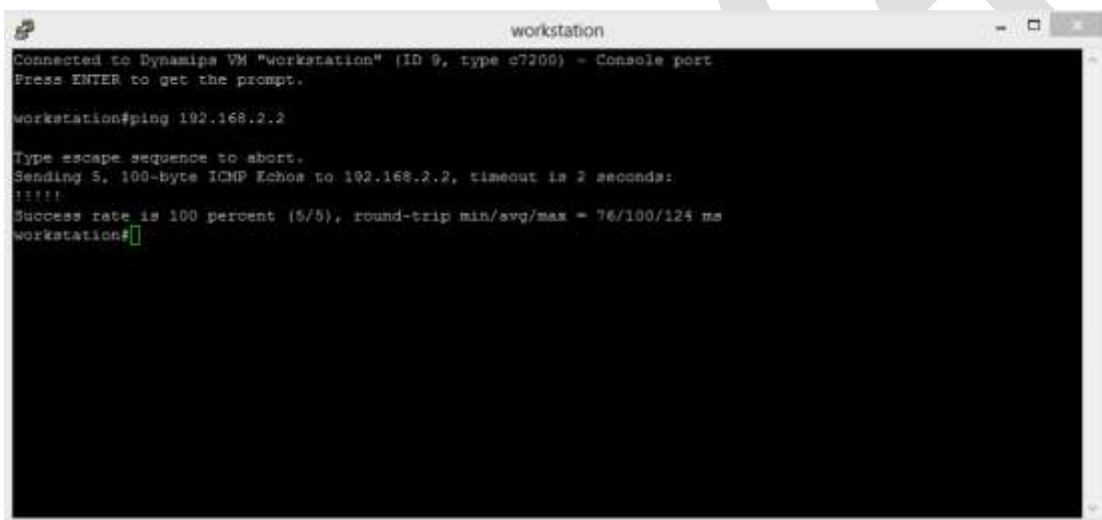
FIG. 3: Pinging command for the IP phone

FIG. 4: Pinging command for the work-station

4.   RESULTS AND DISCUSSIONS

4.1 Interpretation of Results

Fig. 5 below shows results obtained after the simulation process. Here, an ATM network was simulated and configured to send information at a speed of 155Mbps.The figure shows two LAN networks: the remote network and the headquarters' network. All the network devices and their IP addresses are also shown. The ATM switch with an IP address 192.168.1.0 connects the two LANs; thereby making the ATM network a WAN. End devices such as personal computers, IP phones, servers and workstations with their various IP addresses were also connected. The switches serve as a link between the end devices and the routers. The routers job is to forward packets from the remote network to the headquarters' network. At the end of the configuration, pinging commands were used to test the connectivity of the devices in the network. Packets were sent successfully from the remote network to the headquarters' network. Table 2 is the presentation made on samples of IP addresses used in configuring the ATM network.

TABLE 2

Samples of IP addresses used in configuring the ATM network

S/N	IP Address	Sample	Remark
1	network address	192.168.1.0	WAN
		192.168.2.0	Remote Network (LAN)
		192.168.3.0	headquarter Network (LAN)
2	Host Address	192.168.1.1	Router 1
		192.168.2.2	Router 2
		192.168.2.1	PC
		192.168.2.2	IP Phone
		192.168.3.1	Server
		192.168.3.2	Work Station
		192.168.3.3	
3	Subnet Mask	255.255.255.0	- LAN
		255.255.255.252	- WAN
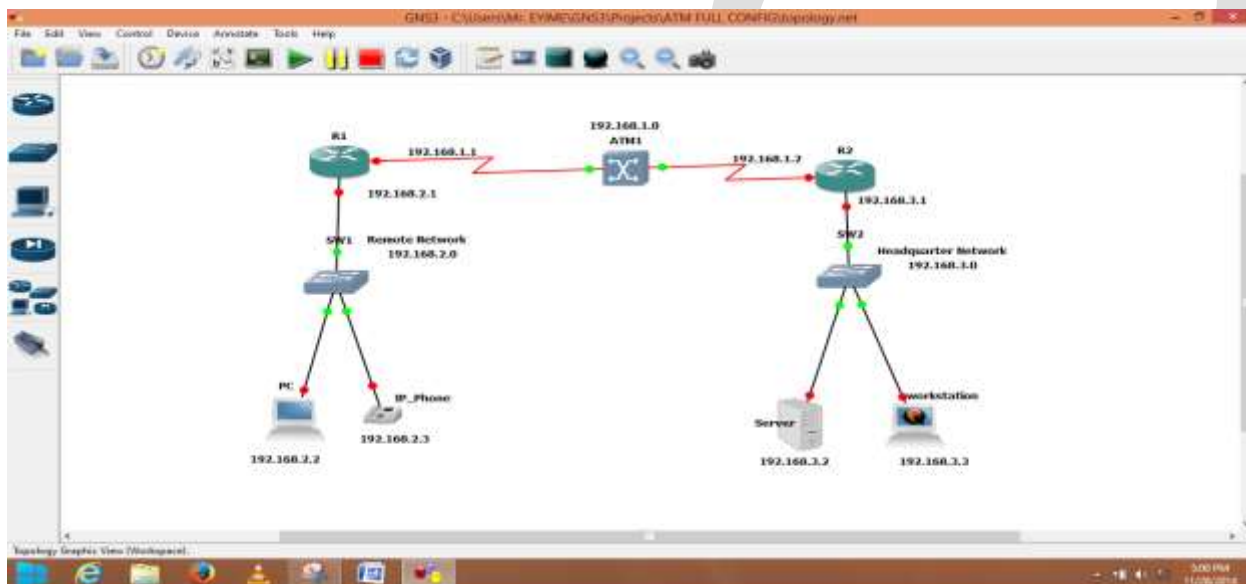
FIG. 5: The ATM network model

4.2   Analysis of Results using Wire Shark

Wire shark is a network packet analyzer. A network packet analyzer is capable of capturing network packets and showing its details as much as possible. Wire shark application helps users to know exactly what is happening inside the network. Wire shark is the best open source packet analyzer used today.

After configuring the simulated network, the packet analyzer (wire shark) was activated to examine the functionality of the network. Key issues were examined through wire-shark application (network administrator) to troubleshoot issues arising from the simulated network, check security issues, debug protocol performance and access the networking protocols. Through activating the wire-shark, the simulated network progressively accessed all the captured line packets, examined and displayed details of these packets, save the captured packets and converted these packets to be accessible through windows. Fig. 6 shows Wire-shark configuration captured at the remote network and Fig. 7 is the configuration of Wire-shark captured at the headquarters' network
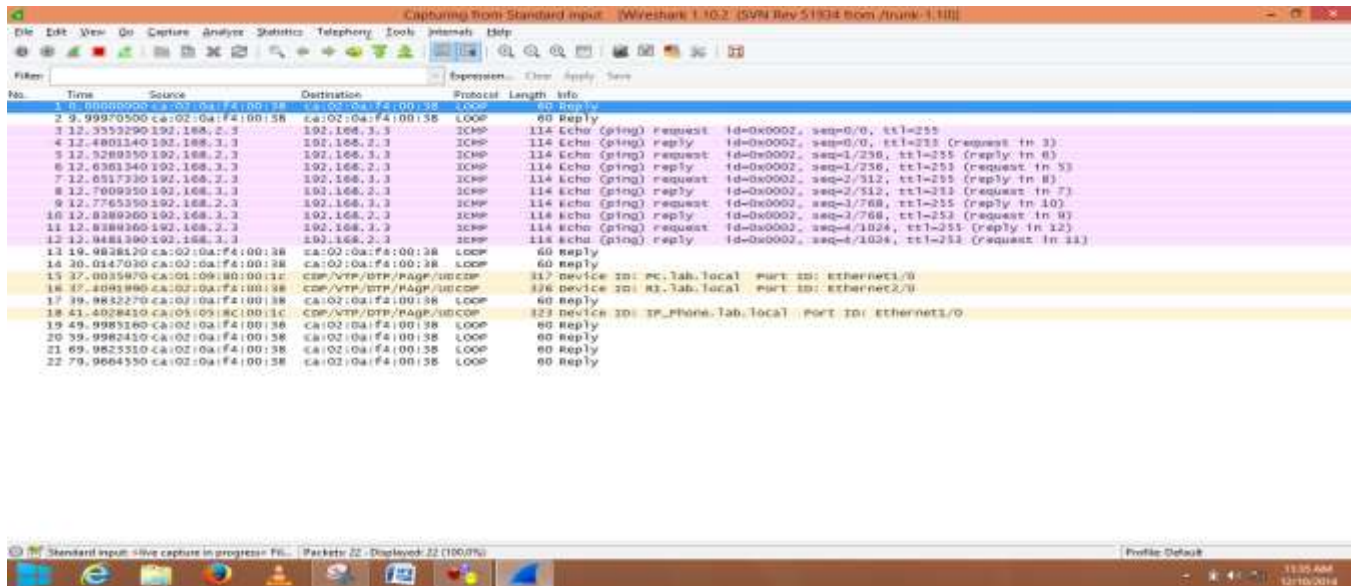
FIG. 6: Wire shark captured at the remote network
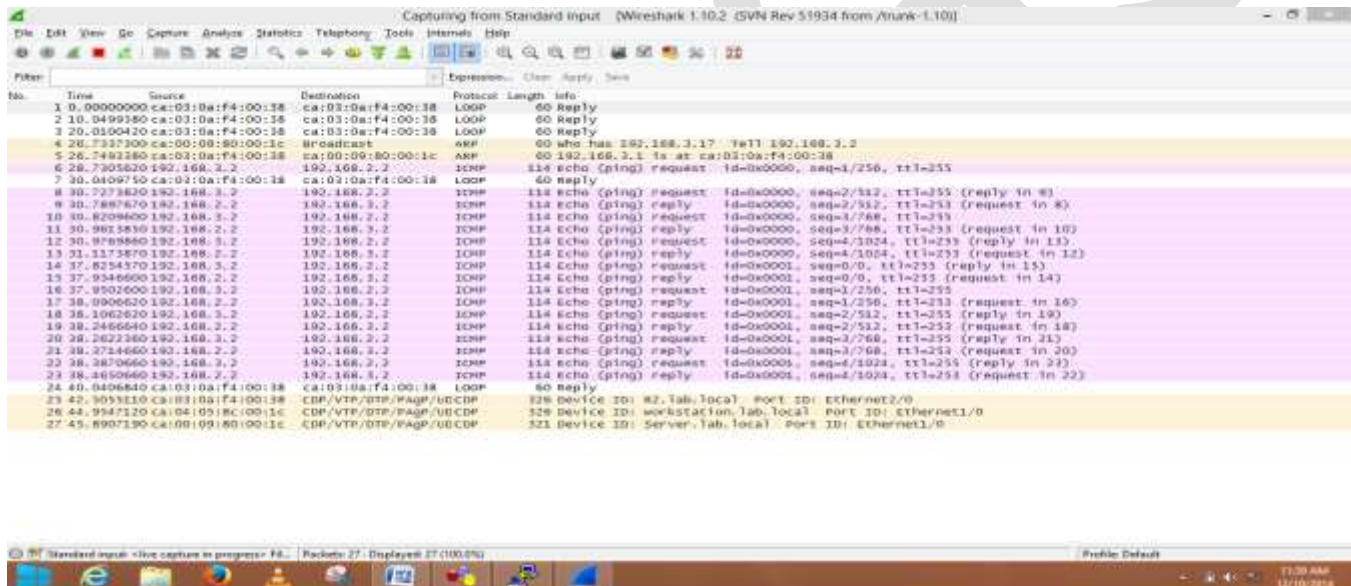
FIG. 7: Wire-shark captured at the headquarters' network

4.3 Analysis of transfer time using Wire-shark

Many analyses were carried out from the results obtained. However, an example of the analyses carried out is hereby described:

Let the remote network be IP address = 192.168.2.0. Let the headquarter network be IP address = 192.168.3.0. To analyze the time the packet left the remote network, IP address = 192.168.2.0 (click enter)

Press CTRL + ALT + 0 to show the time the packet left the remote network (2014-12-22   12:30:00).

To analyze the time the packet reached the headquarters network, IP address = 192.168.3.0 (click enter)

Press CTRL + ALT + 0 to show the time the packet reached the headquarter network (2014-12-22   12:30:01).

4.4 Threats in ATM network

From the study, it was noted that the ATM networks suffered many threats. Examples of some of these threats and their brief descriptions are as follows:

(a) Eavesdropping threat: Here, the attacker linked up to the transmission medium and gained illegal contact to the information. Eavesdropping is a common threat in networks and has been discovered by this study to also occur under ATM network configuration, in spite of the speed of the network.

(b) Spoofing threat: in this case, the attacker pretended to be another user (third party) in order to access the information of the victim with the intention to destroy them. Spoofing attack has some special ways of manipulating information. It might be that the attacker needed special permission to access the unique environment. The study confirmed that ATM operating under a public

network environment is subject to spoofing threat. This was observed when a third network was introduced to serve as the intruding network. In the same vein, since a network is often connected to another network using the Internet, it was not possible to stop the attackers from having access. However, this theory was further put to test by configuring the attacker with a special code not recognized by the network. In the light of this, the attacker, which can be viewed as a virus, was blocked and prevented from having access to other legitimate packages. By so doing, the destructive effect of the virus was reduced, if not eliminated.

(c) Service denial: Since ATM network employs connection-oriented services, a connection, called Virtual circuit (VC) was established and controlled by a set of signals. Virtual circuit was connected by set-up signals and disconnected by drop-party signals. It was observed that the virtual circuit and the network were disconnected when an attacker sent drop party signals to any transitional switch between the Virtual circuit and the network. By regularly sending these signals, the attacker was able to destabilize the links between the users, thereby reducing the Quality of Service (QOS) rendered by the ATM network.

(d) Virtual circuits stealing: When two ATM switches in a network are manipulated, the virtual circuit may be stolen by another customer. For instance, if Virtual circuit-1 and Virtual circuit-2 are two channels activated to pass through switch A and switch B, when user-1 and user-2 were configured to use Virtual circuit-1 and Virtual circuit-2 respectively; if switch A and switch B are synchronized, switch A can switch Virtual circuit-1's cells from switch A to switch B along Virtual circuit-2, while switch B shall switch back this cells to Virtual circuits-1. However, if switch-A and switch-B failed to recognize these changes, then, the status-quo remains and stealing occurs.

(e) Threat to traffic analysis: under this scenario, the illegal user accessed the message, analyzed and interpreted the message of the communicating parties of the Virtual circuits. This was accomplished through illegal entry into the volume and timing of information processed. This threat was possible because the source and destination points were taken from the cell-header and the routing table.

4.5   Security framework for ATM network

Security is one of the major hurdles of network administrators. In system designing, the services' security is usually considered after the network has been designed. This method has consequently proven unsatisfactory. The study made conscious efforts to avoid such traps by making security one major part in the process of designing the ATM network. This was done in order to ensure confidentiality, data integrity, accountability and network availability.

Maintaining confidentiality and data integrity are very important in ATM network security. Under accountability, all the ATM network management activities are accounted for. Each network administrator is expected to be liable for any action taken. Being accountable means validation and non-repudiation. It is also necessary for network operators to manage the network and also account for the services rendered. Availability means that all valid users should be able to get access to the ATM services. No service denial should occur. This is necessary so that the quality of service operation can be guaranteed. In view of the above reasons, the following functions were activated to test the ATM security services:

i. Verifying identities: ATM security services were able to create and authenticate the identity of any performer in the ATM network.

ii. Controlling access and permission: The performers in the ATM network were not able to have access to resources they were not permitted to access.

iii. Protecting the confidentiality: Reserved information was transmitted confidentially.

iv. Protecting the information integrity: The integrity of the reserved packets was guaranteed by the security services introduced.

v. Accountability: The ATM security services were observed to be accountable for every action executed.

vi. Functionalities logging: The ATM security services were able to retrieve data configured for security activities in the network facility with the ability to trace this data to their entry points.

vii. Reporting of alarm: The ATM security service was able to produce alarm information relating to threatening variables and selective security situations. This is a relevant tool to aid maintenance officers.

viii. Auditing: In a situation where there was a bridge in security, the ATM security service was able to evaluate the logged information appropriately.

ix. Recovering Security: When there was a breach in data security, the ATM security service was able to identify the threat and recover the network.

5.   CONCLUSION

This study confirmed that ATM is a blend of hardware and software packages that offer high speed networking backbone to end-to-end users with improved quality of service delivery, when compared to other network protocols. It further established Asynchronous Transfer Mode to be more than the basic structure of the Broadband Integrated Services Digital Network (B-ISDN). Rather, it is a shared platform for the transmission and switching of circuit or packet oriented networks. ATM, as Interworking unit presented in this study, has a flexible architecture based on a central processor unit that controls the information flux between the modular interfaces, broads through two independent data buses, and is able to process in real time, the protocol conversion between the involved data formats. This electronic device can be integrated on a wide variety of communication infrastructures and traffic environments: such as interconnection of ATM, ISDN or LAN terminals, locally or remotely, over a public telecommunications network.

REFERENCES:

[1]. Bassey, D. E., Okon, B. E. & FaithPraise, F. O. (2016). Design and Construction of a GSM-Based Multipurpose Measuring Device for UHF Signal Strength Levels. International Journal of Science, Engineering and Technology Research, Vol. 5, Issue 3, pp. 841-846.

[2] Coppo,P., D'Ambrosio,M. & Melen,R (2003):Optimal cost/performance design of ATM switches. IEEE/ACM Transactions on Networking Vol: 1 Iss: 5 p. 566-575,

[3] Bassey, D. E., R. C. Okoro., J. C. Ogbulezie. (2016). Design Considerations of Different Segments of UHF Wireless Network in Cross River State, Nigeria. International Journal of Science, Engineering and Technology Research, Vol. 5, Issue 3, pp. 835-840.

[4] Bassey, D. E., Okon, B. E. & Effiom, E. O. (2016). Pilot Case Study of GSM - Network Load Measurement in Ikeja - Nigeria. International Journal of Science, Engineering and Technology Research, Vol. 5, Issue 3, pp. 824-829.

[5] Bassey, D. E., Ogbulezie, J. C. & Okon, B. E. (2016). Modeling a Low Latency IP Network in Nigeria. International Journal of Science, Engineering and Technology Research, Vol. 5, Issue 3, pp. 830-834.

[6] Bassey, D. E., Okoro, R. C., Okon, B. E. (2016). Modeling of Radio Waves Transmission of Building Located around Niger Delta Urban Microcell Environment Using "Ray Tracing Techniques". International Journal of Science and Research, Vol.5, Issue 2, pp. 337-346.

[7] Bassey, D. E., Okoro, R. C., Okon, B. E. (2016). Issues of Variance of Extreme Values in a Heterogenous Teletraffic Environment. International Journal of Science and Research, Vol. 5, Issue 2, pp. 164-169.

[8] Bassey, D. E., Okoro, R. C. & Okon, B. E. (2016). Issues Associated with Decimeter Waves Propagation at 0.6, 1.0 and 2.0 Peak Fresnel Zone Levels. International Journal of Science and Research, Vol. 5, Issue 2, pp. 159-163.

[9] Bassey, D. E., Okoro, R. C., Okon, B. E., & Eyime, E. E. (2016). Broadband – Infrastructural Deficit and ICT Growth Potentials in Cross River State, Nigeria. International Journal of Innovative Research in Computer and Communication Engineering (IJIRCCE), Vol. 4, Issue 5, pages 8465-8476.

[10] Bassey, D. E & Okon, B. E (2015). Comparative Studies between Reduction of Discrete Frequency Ranges and Radiated Sound Levels (A Case Study of 50 kVA Diesel Engine Cooling Fan). International Journal of Technology and Research (IJTNR), Vol. 3, Issue 4, pages 85-92.

[11] Bassey, D. E., Okon, B. E., Faith-Praise, F. O., & Eyime, E. E. (2016). Characterization of Traffic Flow Consumption Pattern and Subscribers' Behaviour. International Journal of Innovative Research in Computer and Communication Engineering (IJIRCCE), Vol. 4, Issue 5, pages 8484-8493.

[12] Bassey, D. E., Okon, B. E. & Effiom, E. O. (2016). 'Broadband Network Penetration and Growth Pattern in North Eastern Part of Nigeria'. International Journal of Scientific & Engineering Research (IJSER), Volume 7, Issue 3, pages 1156-1170.

[13] Bassey, D. E., Okon, B. E. & Umunnah, R. (2016). 'The Security Implications of Virtual Local Area Network (VLAN), Niger Mills, Calabar, Nigeria'. International Journal of Scientific & Engineering Research (IJSER), Volume 7, Issue 3, pages 1187-1194.

[14] Bassey, D. E., Ogbulezie, J. C. & R. Umunnah (2016). Empirical Review of Basic Concepts of Teletraffic Postulates. International Journal of Scientific & Engineering Research, Volume 7, Issue 3, pages 1171-1186.

[15] Bassey, D. E., Akpan, Aniefiok. O. & Udoeno, E. (2016). UHF Wave Propagation Losses Beyond 40 Percent Fresnel Zone Radius in South-South Nigeria. International Journal of Science and Research, Volume 5, Issue 2, pp. 740-745.

[16] Bassey, D. E., Ogbulezie, J. C. & Effiom, E. O. (2016). Local Area Network (LAN) Mock-up and Prevention of Cybernetics Related Crimes in Nigermills Company Using Firewall Security Device. International Journal of Scientific & Engineering Research, Volume 7, Issue 3, pages 1124-1130.

[17] Okon, B. E & Bassey, D. E. (2016). Discrete Frequency Noise Reduction of 100 kVA Diesel Engine Cooling Fan International Journal of Engineering Research and General Science, Volume 4, Issue 4, pages 414-422.

[18] Sexton, M. and Reid, A. (1997): Broadband Networking: ATM, SDH and SONET, Artech HouseInc., Boston, London, ISBN 0-89006-578-0.

INVESTIGATION OF THE EFFECT OF MOBILE NUMBER PORTABILITY ON NETWORK SWITCHING CAPACITY IN NIGERIA

D. E. Bassey., A. P. Orim., and S. Ekwe.

Department of Physics,

University of Calabar, Calabar,

Cross River State, Nigeria.

basseyde1@yahoo.com

Abstract- Mobile Number Portability is the aptitude of a subscriber to change his / her Network Provider (NP), without losing his / her original Mobile Station Integrated Services Digital Network (MSISDN) number. This laudable process was recently introduced into the Nigerian Telecommunications environment, in view of its impact on competition and quality of service among various Network Providers (NPs). Ironically, the initial excitement it generated gradually faded. More than four years after its introduction, the statutory agency, the Nigerian Communication Commission has not made any statement on the success or failure of the exercise. In view of this, this study resorted to modeling a similar environment to investigate the switching capability of mobile network operators transacting this porting regime. The assumption made was that all calls (seeds) were successfully originated and routed using SS7 protocol. The model was framed after taking cognizance of how the signaling traffic was routed for real-time services under a certain bandwidth switching capacity. Among other key performance indicators, the exercise indicated congested switching nodes: an indication that porting activities will introduce traffic congestion if the operational channels are not expanded to accommodate high traffic generated through porting activities. The study collaborates the reasons for the unimpressive performance witnessed on the Number Portability programme in Nigeria.

Keywords: Donor network, Mobile network operators, Number portability, Originating network, Switching capacity.

3. INTRODUCTION

1.1 Mobile Number Portability in Nigeria.

The introduction of Mobile Network Portability (MNP) in Nigeria was welcomed with great expectations; arguably, to bring in the needed competition among the various Network Providers (NPs), and above all, form the needed catalyst to commit operators on Quality of Service (QoS) delivery. Ironically, more than four years after its introduction, the Nigerian Communication Commission has not made any policy statement on the success or failure of the exercise. Besides, the initial excitement it generated has gradually faded. MNP is the ability of a subscriber to change his / her Network Provider (NP), without losing his / her original Mobile Station Integrated Services Digital Network (MSISDN) number [14]. Prior to the introduction of MNP, if a subscriber is dissatisfied with the Quality of Service (QoS) of his/her NP, the individual is left with the option of continuing with that NP in order not to lose contact with friends and associates who are familiar with that MSISDN number, or acquire a new MSISDN number from another NP [7]. The ported MISISDN belongs to a set of static assigned number block, which was earlier assigned to the donor NP [19]. When ported successfully, the ported MSISDN shall be served by the recipient NP [1].There are three types of Number Portability. They are:

(i)   Service Portability: This is a situation where a subscriber can change from Fixed to Mobile Line or verse versa, and from Public Switched Telephone Network   (PSTN) to Integrated Services Digital Network (ISDN) [11].
(ii) Service Provider Portability: This can be referred to as the changing of a subscriber from one NP to another (i.e. Mobile to Mobile or Fixed to Fixed) [5].
(iii) Location Portability. This happens when a subscribe changes his geographical location.

A significant amount of work is required technically to implement number portability due to the restructuring of the telecommunications infrastructure [13]. This restructuring may involve creating a new database and selecting or implementing different routing methods for various types of calls and messaging services [9].

This work focuses on the second model of Number Portability and therefore limits the study to the effect of MNP on network switching capacity in Nigeria.

1.2   MNP Routing Schemes

MNP means moving from one NP to another without losing your MSISDN number. This transaction involves three parties such as [2]:
   (a) Donor Network: The NP who initially assigned the MSISDN number to the subscriber.

(b)   Originating Network: The NP which originates a call to a ported MSISDN number.
(c)   Recipient Network: The new NP which is the new host of the ported MSISDN number.

For the purpose of simulating the Nigerian model, consideration was given to the donor network, originating network and recipient network; which are usually from different NPs [3].

From the definitions above, one can see that the Donor network of a subscriber does not change, and the Recipient network does not need to allocate another MSISDN number to the ported SIM. Also, the MSISDN number does not depend on the network hosting the ported number. The role of the mentioned parties varies and a particular NP can play more than one role at a time [12].

4.   LITERATURE REVIEW

The importance of MNP on the deregulation wave sweeping the telecommunications sector cannot be overemphasized. [4] while researching on the effect of mobile number portability on consumers in South Africa, observed that strengthening the regulatory environment is required in order to ensure fair competition and consumer protection. He noted that there were gaps in respect of the MNP regulation due to weak regulatory frame-work. According to him, the regulatory body lacked the capacity to enforce and monitor compliance. [6] conclusion was based on analyses from 38 countries (1999 to 2004), that: when the quality of service was put together with ported lines, it had an impact on the switching capacity and average prices. In some countries, MNP was associated with increased switching cost, congestion and lower prices; especially for countries with porting times lower than five days. Countries with less stringent porting times have not experienced churn or revenue effects [8]. The routing scheme and the porting times affect the success of MNP in any country. Other examples are as follows: the telecommunications' regulator in Chile, introduced Mobile Number Portability (MNP) in January 2012, and by June 2013, it recorded 616,686 pre-paid subscribers and 480,571 post-paid customers who successfully ported their numbers to their choice carriers[15].Ghana's National Communication Authority (NCA) introduced MNP on 6 July 2013, one year after the introduction of MNP, about 370,107 mobile numbers ported successfully, representing 1.6 per cent of the total active mobile numbers in the market [17]. Following the introduction of MNP in Colombia, by August 2011, a total of 441,163 customers have switched providers. The greatest concentration of ports was in the first quarter of 2012, when 167,914 people moved operators, while the number dropped to 132,344, the next quarter [22] .India unveiled MNP in November 2010, and two months later in January 2011, 1.7 million of over 200 million subscribers had ported [18].When MNP was introduced in UK in 1999, it took 25 days to port. Before April 2011, porting time reduced to two days [20]. Efforts have been made to reduce it to 24 hours, while in Ecuador, a total of 29,029 requests by subscribers to port their numbers had been received by January 25, 2010, and exactly one year after MNP was introduced in the country[21].The number in Brazil was even higher, with 3.48 million of 210 million subscribers seeking to port, just six months after MNP was unveiled; while Romania, which introduced MNP in October 2008, recorded over 31,000 subscribers porting by February of the following year. Presently [23]. Nigeria's regulator has not made any official statement on the number of ported lines and the success rate recorded so far. In view of this, this study resorted to modeling a similar environment to investigate the switching capability of mobile network operators transacting this porting regime.

3.   CONCEPTUAL FRAMEWORK

3.1   Modelling

Different seeds of subscribers seeking MNP services were simulated and the time taken to access different switching nodes of the Donor NP through to the Recipient NP was recorded using the simulation's tool-kit. The assumption made was that all calls (seeds) were successfully originated and routed using SS7 protocol [4]. The model was framed after taking cognizance of how the signaling traffic was rooted for real services under a certain bandwidth switching capacity [8]. Also consideration was given for multiple network-provider environment; noting that the donor NP and recipient NP belonged to different operators. This scenario was chosen in line with the Nigerian Telecommunications environment. The simulation task was accomplished using Packet tracer software to simulate the porting processes and in some cases one or more components were substituted with a component in the stimulating software to give a general scenario of the integrated network. The software used and the routing model employed are discussed briefly.

3.1.1   Routing models

The SS7 network scenario was used from the interconnection of the various components on the network. The switching protocol considered in this case was to ease possible traffic congestion that may be experienced during porting processes [16]. Two NPs were considered in designing the model; since they were the minimum subscribers' interface required for an MSISDN number to be ported. This made the SS7 architecture scaled down to have the same signaling points and links. The SS7 used the signaling protocols known as the Transaction Capabilities Application Part (TCAP) routing protocol [6].

3.1.2   Simulation software

Going by the aim of this research work: to find out the performance impact of MNP on the switching capacity of the Donor or Receptor network in Nigeria, the study relied on estimation since the NCC refused to supply empirical data even after conscientious efforts were made [21].The software used for simulation is the Packet Tracer software. Packet Tracer provided the convenient environment to construct and stimulate traffic flow scenario using variable inputs similar to what is obtained during real-time signal

flow [17]. The TCP IP protocol was used in the Packet Tracer simulation. The design model focused on the SS7 protocol used by GSM networks [10].

3.2   Method

The method employed by this study was first designing the signal flow diagram and there after the process flow was developed. This was followed by the creation of the design scenario.

3.2.1   MNP signaling process flow.

In view of the inability to get traffic process flow data from MCH due to non-authorization from NCC, the study relied on the following key assumptions:

(i)   The recipient NP sent a porting request to the MCH after the subscriber has filled the porting request form.

(ii)   The recipient NP advised the subscriber to send an SMS to the MCH through his Donor NP to the MCH.

(iv)   The MCH sent a request for the subscriber's profile to the Donor NP.

(v)   The Donor NP released details of the subscriber's profile and confirmed that porting activity commenced.

(v)   The MCH wrote the details of the subscriber in her NPDB.

(vi)   The MCH sent a porting response to the recipient NP permitting the subscriber to activate the Subscriber.

(vii)   The MCH informed the subscriber through the Donor NP to switch of his phone and there after started using his new NP.

    (viii)   The MCH controlled and administered the porting process as illustrated in Figure 1 in the MNP Signal Process Flow Diagram modelled after the simulation activities.
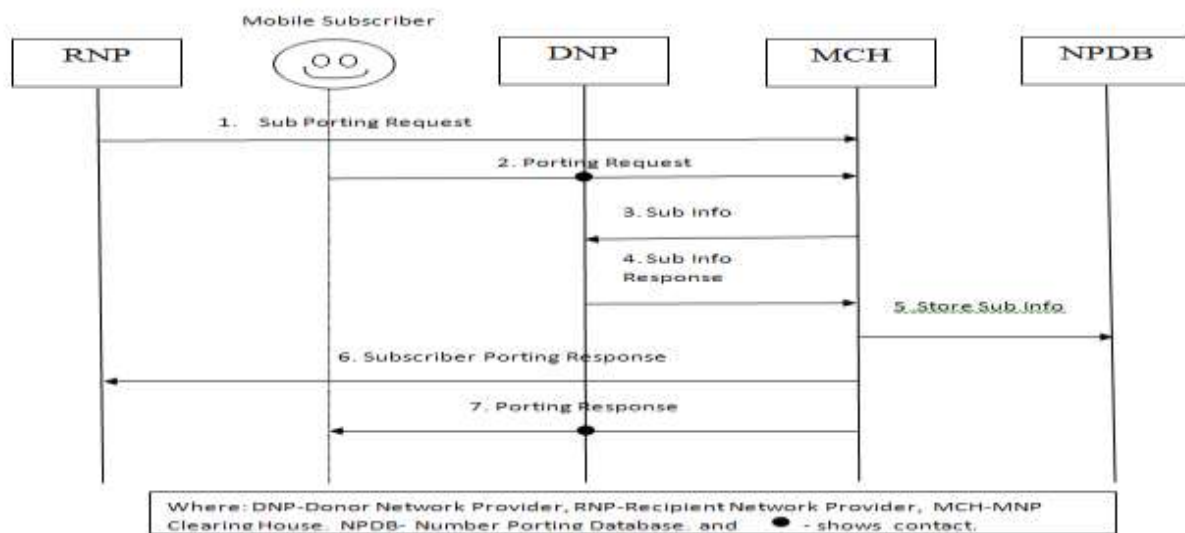
Fig.1:   MNP signal process flow diagram

3.2.2   MCH process flow.

The MCH process flow tabulated in Fig. 1 and fig.2were through the format explained below:

    When signal arrive the MCH, it decides what action to take next; depending on its operating state. If it is idle, it goes straight to execute the signal. And if it is in the process of writing on the NPDB,it sends the signal to the hold-process. Finally, if it is in the process of executing the last signal, it sends the signal to the wait process. Figure 2 is the flow diagram of MCH.
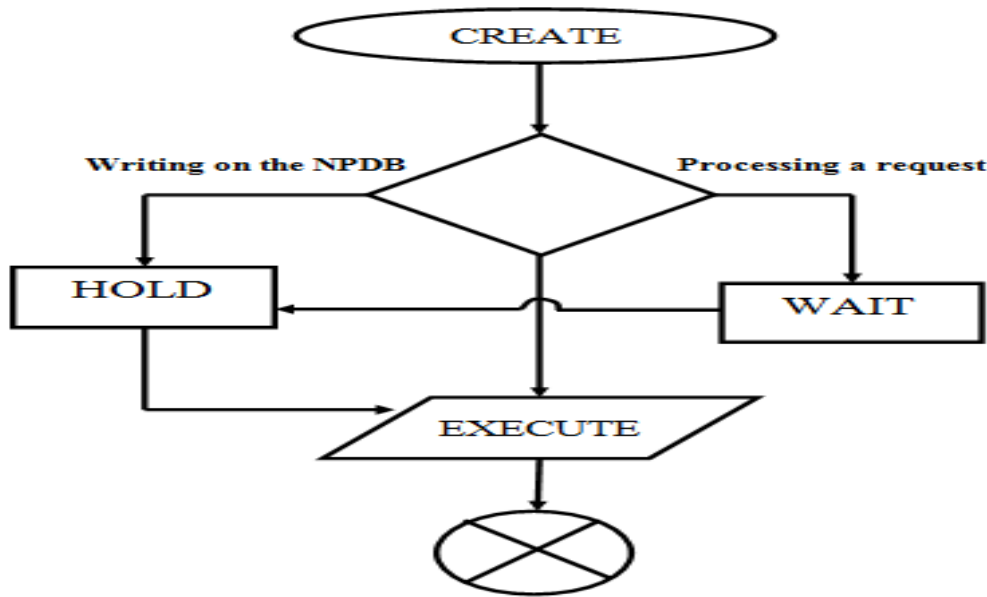
Fig.2:   MCH Flow Diagram

3.2.3   Simulation design

The simulations were processed by using the tool-kit for traffic modelling in Computer and Telecommunication networks. MNP message exchanges from the subscribers and their routing functionalities to the end point were simulated in order to compare the impact of performance of each routing scheme under SS7 signaling mode [3]. Consideration was given to the fact that Number Portability occurs using the facilities of two network operators (RNP and DNP). The message goes through these switching nodes to reach the Donor NP. Then, the Donor NP will first check whether the called party directory number is in the directory. With the updated routing information, the call is forwarded to the recipient network.

This therefore brings to fore the primary task of this model: to study the routing of MNP transaction through the host network to the recipient, and finally to the subscriber. All these signaling and switching nodes were considered during the simulation processes [11]. The components chosen on the Packet tracer environment were as close to the real scenario as possible; though assumptions were made in order to trace the signal flow. The diagram in Figure 3shows the MNP signal processes. The figure illustrates the signaling processes and inter-partner relationship.
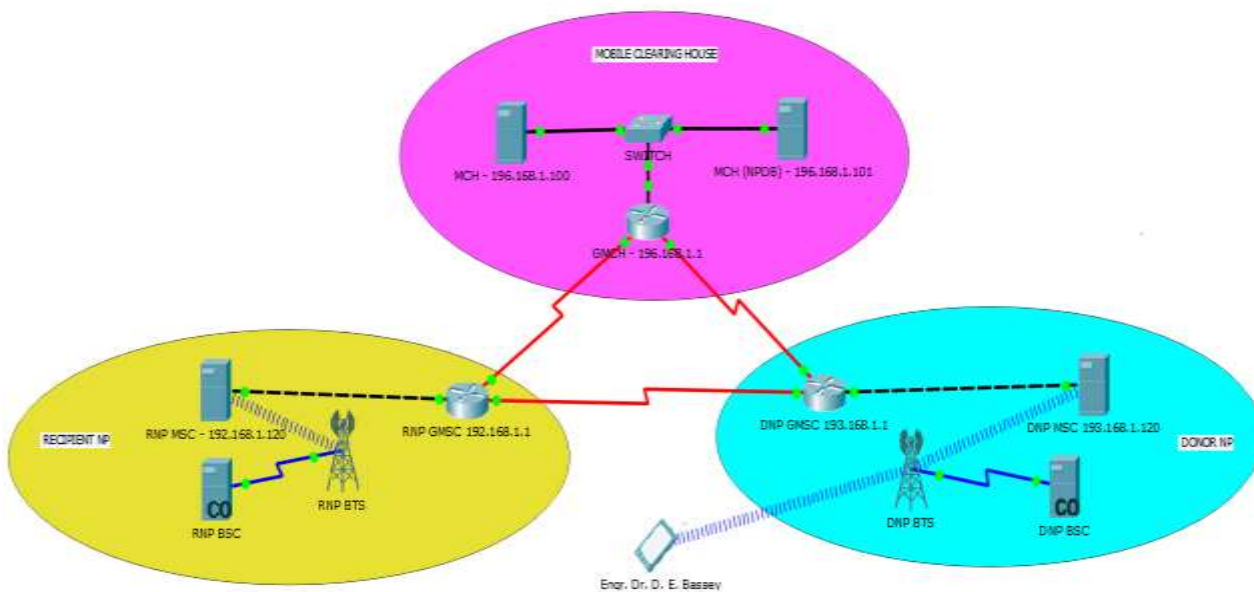
Fig. 3: Interworking reference model

3.2.4   Design Scenario

The design was tested from point to point to check for connectivity of all components on the Packet Tracer environment. The design was simulated following the MNP signaling process flow with the assumptions that signals were transmitted from the MSC. The processes followed are as follows:

The signal packet leaves the Recipient NP to the MCH. The MCH waits for the request from the Subscriber, which comes through the Donor NP. The MCH on receiving the request from the subscriber conducts confirmation that the subscriber is still in the Donor NP network, and further request for the profile of the subscriber. The Donor NP sends both the confirmation and the subscriber's profile to the MCH. The MCH writes the subscriber's profile on NPDB and there-after sends an authorization to the Recipient NP to activate the subscriber on the network. The MCH sends another message to the subscriber to initiate a hard reset in order to activate it on the Recipient NP. This MNP signaling process flow was design to monitor some parameters in some components like the MSC, GMS, NPDB.

3.3   Parameters

Five distinct parameters were employed during the simulation process. They are presented as follows:

• Average arrival rate of in-coming transactions (λ_{calls}):

$$\lambda_{calls} = 1/t_{calls}, \tag{1}$$

where t_{calls} is the average inter-arrival time of incoming signal.

• Average service rate of the network operator:

$$(\mu_{netServ}): \mu_{netServ} = 1/t_{netServ}, \tag{2}$$

where $t_{netServ}$ is the average service time from the links to the network operator.

• Average processing rate at the NPDB (μ_{dbServ}): $\mu_{dbServ} = 1/t_{dbServ}$,   (3)

where t_{dbServ} is the average processing time from the links to NPDB.

• External link delay (τ_{exLink}): This simply refers to the delay experienced on the out-door links of the operator's network. That is from the donor network to the recipient network or from the originating network to the centralized NPDB (which in the case of this research work was induced). The scenario presented in this study is based on analyses carried out in terms of seeds. Seeds in this case refers to a group of subscribers modeled after real traffic scenario.

4.0 RESULTS AND DISCUSSION

The Figures presented below show the forward routing scheme in the simple model adopted for this study. The following results were obtained from the simulation of one to hundred subscribers under different switching conditions. When a request for MNP was originated, a message was generated to the Donor NP to set up a call segment carrying information which includes the called party number and the routing label. In addition, different routing nodes that passed through the traffic were examined. Figure.4 presents the models for MNP routing schemes for one subscriber. The transaction was analyzed by measuring the arrival time for each transaction and the number of switching nodes the MNP traffic accessed. Fig. 4 to Fig. 8 show results obtained after simulating a traffic scenario carrying one, ten, fifty, and hundred porting requests. These seeds (subscribers) were varied and analyzed based on the time taken for the MNP request to access a switching node of each network and the total number of nodes accessed after completion of the porting process.

4.1   Simulation for One Subscriber

The following results were obtained for the simulation of one subscriber. Figure 4 shows that more switching activities took place on the Donor network compared to the Recipient network. The resources of the MCH were more utilized due to its control and administrative role on the transaction. The graph also shows the arrival time for one subscriber; indicating the point to point arrival time for the various switching nodes accessed during the porting process.
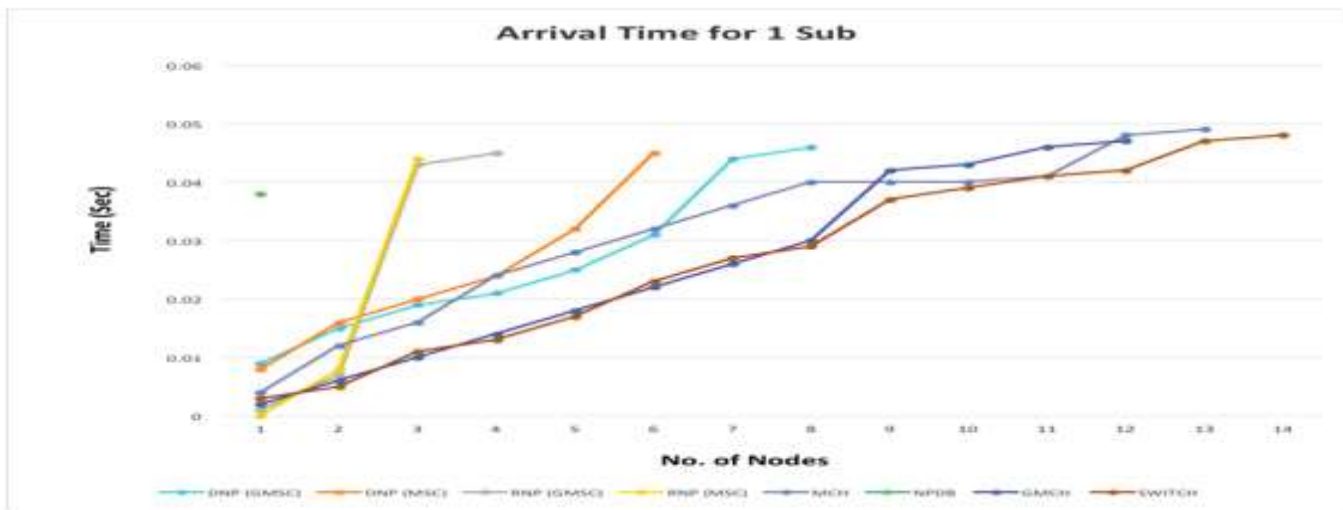
Fig. 4:   Graph of arrival time for one subscriber

Fig. 5:   Graph of activity rate for one subscriber

As shown in Fig. 5, more activities took place in the Donor NP than the Recipient NP during the porting process. The MCH has the highest number of activities as it serves as the control and administrative centre for the process

4.2   Simulation for Ten Subscribers

The graph in Fig. 6 shows the arrival time for seeds of ten subscribers (summary). It indicates a different dimension from the last report.   Traffic usage time was shorter; an indication that the transaction was allotted more time than when they were fewer subscribers. This further shows the capacity of the switching facility to efficiently accommodate fewer subscribers than when they are many.
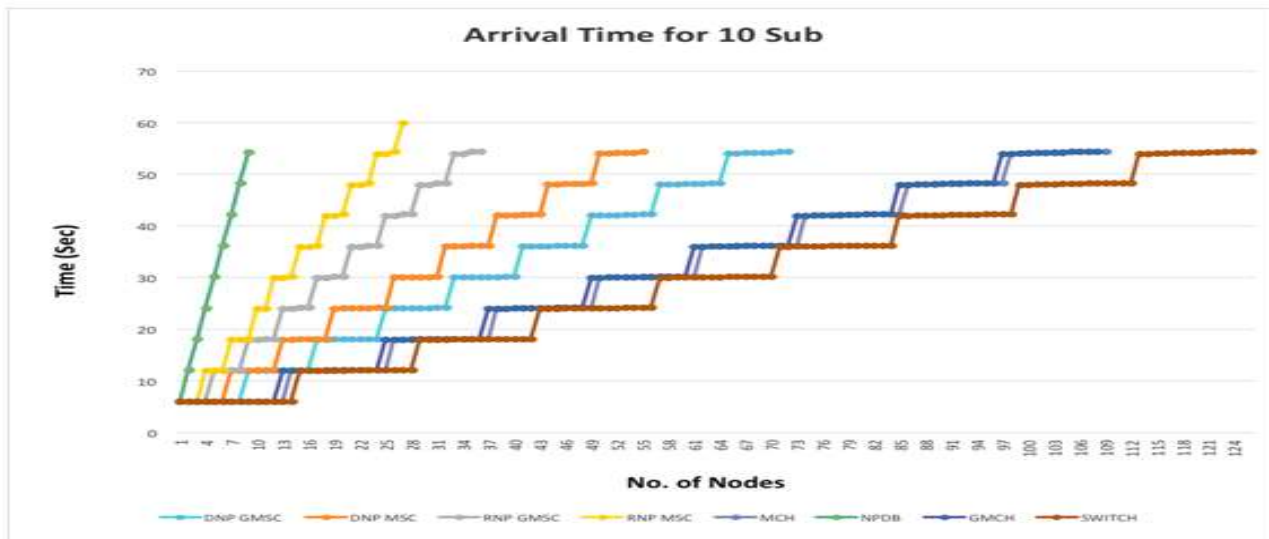
Fig. 6

4.3   Simulation for Fifty Subscribers

The graph in Fig. 7 shows a different dimension in the arrival time for a seed of fifty subscribers. This phase of traffic transactions reduced gradually with time due to the increase in the number of processes that took place at various nodes. The number of seeds selected were a summary of the total seeds (50) used for this class of simulation.
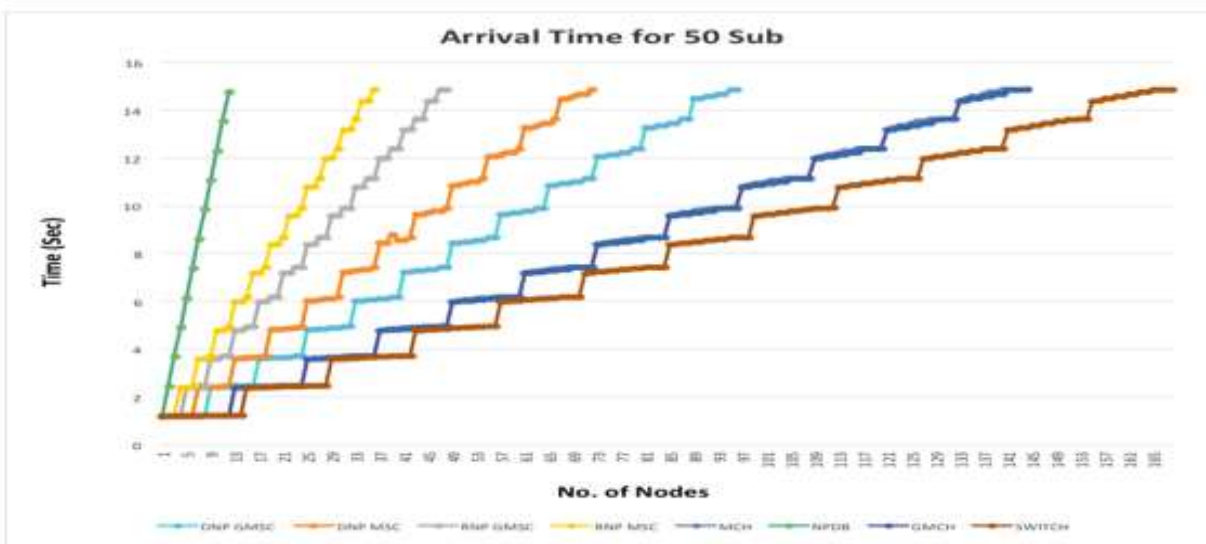
Fig. 7:   Summary of graph of arrival time for fifty subscribers.

4.4   Simulation for Hundred Subscribers

The graph in Fig. 8 shows the summary of arrival time for a seed of hundred subscribers. The graph shows a gradual linear shape: an indication that the time taken for the switching modules to process one hundred subscribers correspondingly increased as the number of subscribers seeking porting services increased.
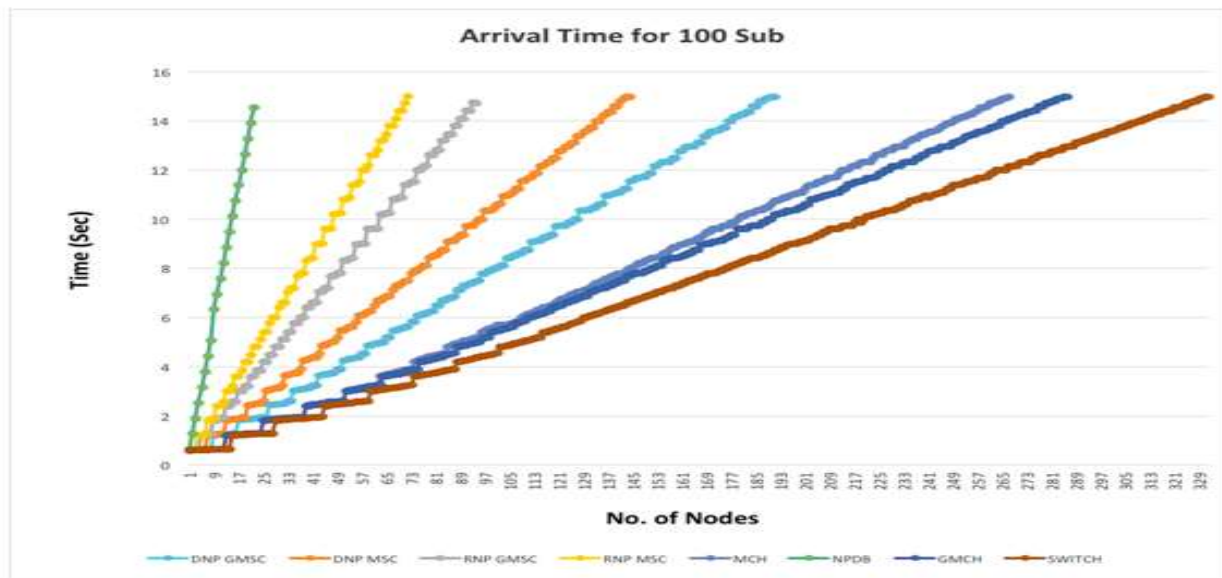
Fig. 8:   Graph of arrival time for hundred subscriber (summar)

4.5   Simulation Analysis

The data obtained during the porting process of each seed of subscribers within a 60- second simulation time was very large. In view of this, a different time frame was used. A 15-second simulation window was therefore used and the summary of the analyses are presented graphically. Further to this, simulation parameters showing average arrival time for various seeds are presented in the Tables (Table 3 – Table 7).

Table 3: Processing time for one subscriber

NODE	TIME (SEC)
RNP	0.024
DNP	0.048
MCH	0.084
MCH (NPDB)	0.012

Table 4: Processing time for ten subscribers

NODE	TIME (SEC)
RNP	0.24
DNP	0.48
MCH	0.84
MCH (NPDB)	0.12

Table 5: Processing time for fifty subscribers.

NODE	TIME (SEC)
RNP	1.2
DNP	2.4
MCH	4.2
MCH(NPDB)	0.6

Table 6: Processing time for hundred subscribers.

NODE	TIME (SEC)
RNP	2.4
DNP	4.8
MCH	8.4
NCC (NPDB)	1.2

Figure 9 shows a comparison between the average arrival rates and the average service rate for each seed. Also they show processing rate at the **NPDB** for each seed. This graphical presentation takes a closer look at the effect of the porting process when a seed of ten, fifty and hundred subscribers were ported within a time frame of 15 seconds. This figure also supports the signaling scheme shown in Figure 5; indicating that increase in the average arrival rate of a network is based on the increase in the number of MNP requests made by subscribers.

Fig. 9:   Comparison of the average arrival rate.
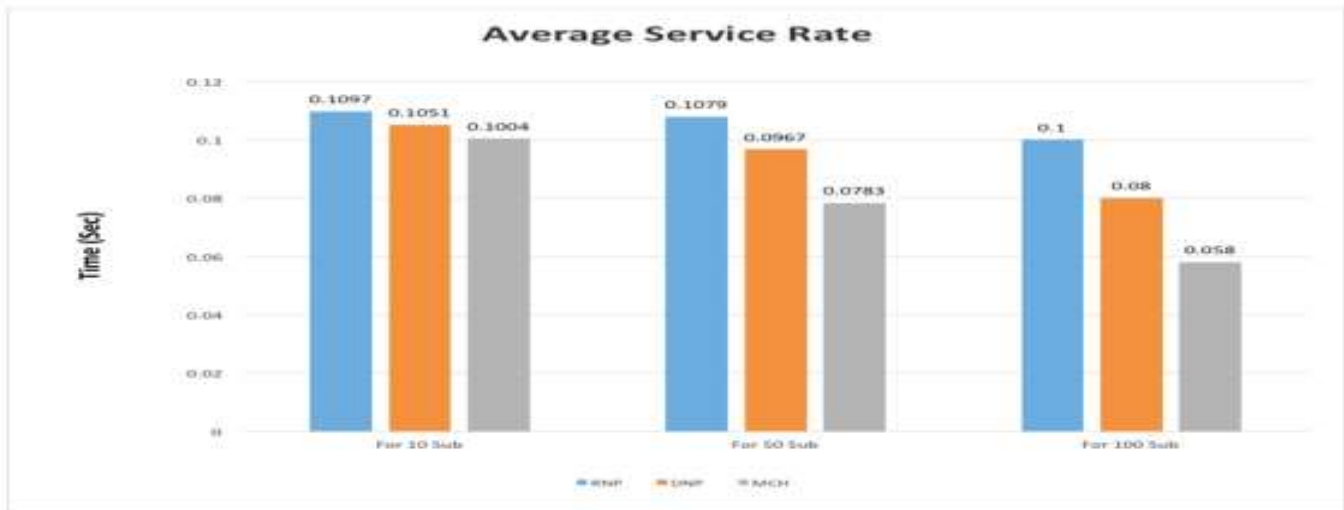
Fig. 10: Comparison of the average service rate.

The service rate is the time allocated by the network to service its subscribers. Figure 10 shows that increase in the number of subscriber per time (that requested for porting service) has a lesser service rate thanwhen there were fewer subscribers. This is an indication that service time allocated can deliberately be reduced in order to reduce pressure on the bandwidth configured for real-time income generating traffic.
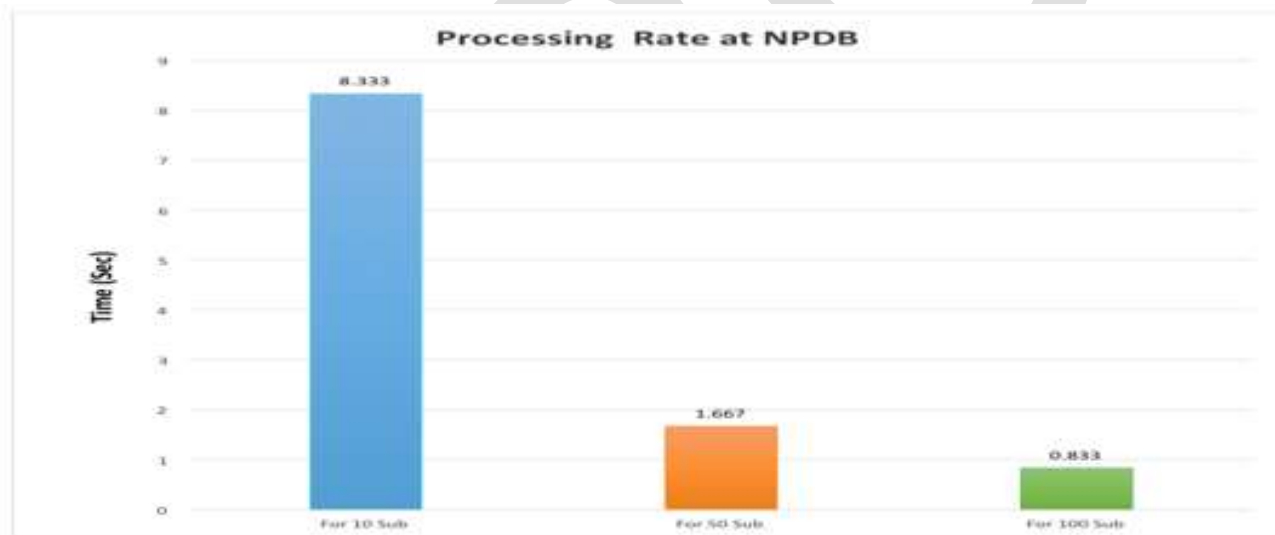
Fig. 11: Comparison of the processing rate at NPDB for different seeds

5.   CONCLUSION AND RECOMMENDATIONS

5.1   Conclusion
Number portability allows a subscriber to change service provider, geographical location or service type without changing his phone number. This unique technology has become a mandatory service in many countries in view of its numerous advantages. The aim of the study is to find out the rate at which traditional services (voice, data, and video) carried out by these network providers shall be affected if the rate of port number- requests become very high. This is so because of the assumption that all service arrivals are Poissonian and the service time is exponentially distributed.   The performance of the network was therefore measured with respect to the percentage of the numbers ported as against the average arrival rate, service rate and the processing rate. These variables account for the switching capacity of a network.

The simulating model was deployed using Packet Tracer tool-kit. The study noted that initiating an MNP request up to completion, requires the signal passing through many switching nodes, which traditionally are routing nodes for normal services (call, SMS, data, video). Besides, the study also indicated that MNP request set-up is more complex and has a longer duration than the normal services. The study revealed that the ported subscribers in Nigeria are still a far cry of what is expected, considering the high subscriber-base in the country. The study further inferred that since not less than two networks are usually involved in the porting processes and administration, different signaling protocols, bandwidth capacity and technologies can be involved. Traffic interconnects agreement between these different operators, existing load levels and deliberate propagation delays created through software configuration are hindrances to the porting process. The study also noted that since the MNP transactions occupy the same switching ports with the traditional services, MNP services encounter delay traffic terminations.

This is in view of different routing platforms; which may invariably cause deliberate frustrations from operators with limited switching capacity; through extension of the processing time, or reduced time allotted for porting services. Besides, the Donor NP can deliberately create bottle necks in view of the infrastructure involved, losing their subscriber base and depleting their operational income. The study also noted that congestion becomes the order of the day, as termination of traffic simulated during porting transaction becomes very slow as the number of seeds increased.

The essence of this exercise is to monitor real-time traffic under a combination of porting numbers and traditional traffic flow. The exercise indicated congested switching nodes, which is an indication that porting activities will introduce traffic congestion if the operational channels are not expanded to accommodate high traffic that may be generated through porting regime. Furthermore, results obtained after the simulation shows that the NPDB is the least used resource in the porting process and has a processing rate of $833msec^{-1}$ for 100 subscribers, $1667msec^{-1}$ for 50 subscribers and $333msec^{-1}$ for 10 subscribers. The service rate of each network was monitored in a 15sec simulation window. The result also shows that the service rate for 10 subscribers is given as $105.1msec^{-1}$ for the Recipient NP, and $107.9msec^{-1}$ for the Donor network; while for 50 subscribers, it is $96.7msec^{-1}$ for the Recipient NP and $109.7msec^{-1}$ for the Donor NP. Similarly, for 100 subscribers it is $100msec^{-1}$ for Recipient NP and $80msec^{-1}$ for Donor NP. The Recipient NP has average arrival rate of $130msec^{-1}$, while the Donor NP is $131msec^{-1}$ for 100 subscribers. The Recipient NP average arrival rate of $125.9msec^{-1}$ and the Donor NP is $126.3msec^{-1}$ for 50 subscribers. Finally, the Recipient NP has average arrival rate of $110.8msec^{-1}$ and the Donor NP is $110.7msec^{-1}$ for 10 subscribers. The study collaborates the reasons for the unimpressive performance of the Nigerian Communications Commission on Number Portability programme in Nigeria.

5.2 RECOMMENDATION

This research work was accomplished with minimum details of the switching nodes involved in traffic carriers for Mobile Network Portability. This was due to limited data from network operators and NCC; thereby restricting our sources of knowledge to simulation packages to model a similar traffic scenario. However, further effort should be made to access relevant data from statutory bodies in view of the importance of the study.
.

REFERENCES:

[1] Fife, E. & Pereira, F. (2002) *Socio-economic and cultural factors affecting adoption of broadband access: A cross-country analysis*. Retrieved November 18, 2012 from http://www.marshal.usc.edu/ctm/publications/FITCE2002.pdf.

[2] Bassey, D. E., Okon, B. E. & FaithPraise, F. O. (2016). Design and Construction of a GSM-Based Multipurpose Measuring Device for UHF Signal Strength Levels. International Journal of Science, Engineering and Technology Research, Vol. 5, Issue 3, pp. 841-846.

[3] Bassey, D. E., R. C. Okoro., J. C. Ogbulezie. (2016). Design Considerations of Different Segments of UHF Wireless Network in Cross River State, Nigeria. International Journal of Science, Engineering and Technology Research, Vol. 5, Issue 3, pp. 835-840.

[4] Bassey, D. E., Okon, B. E. & Effiom, E. O. (2016). Pilot Case Study of GSM - Network Load Measurement in Ikeja - Nigeria. International Journal of Science, Engineering and Technology Research, Vol. 5, Issue 3, pp. 824-829.

[5] Bassey, D. E., Ogbulezie, J. C. & Okon, B. E. (2016). Modeling a Low Latency IP Network in Nigeria. International Journal of Science, Engineering and Technology Research, Vol. 5, Issue 3, pp. 830-834.

[6] Bassey, D. E., Okoro, R. C., Okon, B. E. (2016). Modeling of Radio Waves Transmission of Building Located around Niger Delta Urban Microcell Environment Using "Ray Tracing Techniques". International Journal of Science and Research, *Vol.5, Issue 2,* pp. 337-346.

[7] Bassey, D. E., Okoro, R. C., Okon, B. E. (2016). Issues of Variance of Extreme Values in a Heterogenous Teletraffic Environment. International Journal of Science and Research, Vol. 5, Issue 2, pp. 164-169.

[8] Hart, J., Reed, R., & Bar, F. (1992). The building of the internet: Implications for the future of broadband networks. *A journal of Telecommunications Policy, 16*, 666–689.

[9] Bassey, D. E., Okoro, R. C. & Okon, B. E. (2016). Issues Associated with Decimeter Waves Propagation at 0.6, 1.0 and 2.0 Peak Fresnel Zone Levels. International Journal of Science and Research, Vol. 5, Issue 2, pages 159-163.

[10] Bassey, D. E., Okoro, R. C., Okon, B. E., & Eyime, E. E. (2016). Broadband – Infrastructural Deficit and ICT Growth Potentials in Cross River State, Nigeria. International Journal of Innovative Research in Computer and Communication Engineering (IJIRCCE), Vol. 4, Issue 5, pages 8465-8476.

[11] Bassey, D. E & Okon, B. E (2015). Comparative Studies between Reduction of Discrete Frequency Ranges and Radiated Sound Levels (A Case Study of 50 kVA Diesel Engine Cooling Fan). International Journal of Technology and Research (IJTNR), Vol. 3, Issue 4, pages 85-92.

[13] Bassey, D. E., Okon, B. E., Faith-Praise, F. O., & Eyime, E. E. (2016). Characterization of Traffic Flow Consumption Pattern and Subscribers' Behaviour. International Journal of Innovative Research in Computer and Communication Engineering (IJIRCCE), Vol. 4, Issue 5, pages 8484-8493.

[14] Bassey, D. E., Okon, B. E. & Effiom, E. O. (2016). 'Broadband Network Penetration and Growth Pattern in North Eastern Part of Nigeria'. Retrieved September 5, 2016 from http://www.ijser.org/onlineResearchPaperViewer.aspx?Broadband-Network-Penetration-and-Growth-Pattern-in-North-Eastern-Part-of-Nigeria.pdf

[15] Bassey, D. E., Okon, B. E. & Umunnah, R. (2016). 'The Security Implications of Virtual Local Area Network (VLAN), Niger Mills, Calabar, Nigeria'. Retrieved September 5, 2016 from http://www.ijser.org/onlineResearchPaperViewer.aspx?The-Security-Implications-of-Virtual-Local-Area-Network--VLAN--Niger-Mills--Calabar--Nigeria.pdf

[16] Mason, A. (2011). *Assessment of economic impact of wireless broadband in Nigeria*. Retrieved January 5, 2013 from http://serving.webgen.gsm.org/5926DA9A-2DD6-48E7-BAD4-50D4CD3AF30A/projects/Spectrum/DigitalDividend/DDtoolkit/uploads/assets/downloads/07/wireless-broadband-in-nigeria.pdf.

[17] Bassey, D. E., Ogbulezie, J. C. & R. Umunnah (2016). Empirical Review of Basic Concepts of Teletraffic Postulates. International Journal of Scientific & Engineering Research, Volume 7, Issue 3, pages 1171-1186.

[18] Bassey, D. E., Akpan, Aniefiok. O. & Udoeno, E. (2016). UHF Wave Propagation Losses Beyond 40 Percent Fresnel Zone Radius in South-South Nigeria. International Journal of Science and Research, Volume 5, Issue 2, pages 740-745.

[19] Bassey, D. E., Ogbulezie, J. C. & Effiom, E. O. (2016). Local Area Network (LAN) Mock-up and Prevention of Cybernetics Related Crimes in Nigermills Company Using Firewall Security Device. International Journal of Scientific & Engineering Research, Volume 7, Issue 3, pages 1124-1130.

[20] Okon, B. E & Bassey, D. E. (2016). Discrete Frequency Noise Reduction of 100 kVA Diesel Engine Cooling Fan International Journal of Engineering Research and General Science, Volume 4, Issue 4, pages 414-422.

[21] Ogbulezie, J., Onuu, M., Bassey, D. & Etienam-umoh, S. (2013). Site specific measurements and propagation models for GSM in three cities in Northern Nigeria. *American Journal of Scientific and Industrial Research, vol. 4, Issue 2*, pages 238-245.

[22] Okon, B. E., & Umunnah, R. A (2015). Identification of Threats to Communication Security, Effects and Ways of Mitigation the Threats. International Journal of Scientific & Engineering Research (IJSER), Vol.6, Issue 5 pages. 1219-1235.

[23] Atiya, F. K. (2010). Mobile Number Portability: Challenges and Solutions. *Journal Of Emerging Trends In Computing and Information Sciences.4 (6)2079-8407*

Design and Fabrication of Hybrid Automatic Transfer Switch Using Programmable Logic Controller

Adeel Khan, Mian Rizwan, Muhammad Ramzan

Electrical Engineering Department, University of Gujrat, HHC, Pakistan

Adeeltn@gmail.com; rizwan.nazeer26@uog.edu.pk

Abstract: Most of the large scale industrial critical loads agonize from voltage intermissions and sags which can source a weighty economic loss. The thyristor-based solid state transfer switch and mechanical based automatic transfer switch used to protect loads against these power quality problems. However, the static transfer switch has a significant amount of losses the reason of forward voltage drop of the thyristor and automatic transfer switch cannot efficiently meets the requirements for the load which are sensitive to voltage and will trip due to delayed transfer time. This research proposes a 3-phase system 400V hybrid Automatic transfer Switch. Hybrid ATS is combination of thyristor switch in parallel with mechanical switch. HATS realizes low power intake in normal operating conditions and transfers efficiently when needed. The HATS has four transfer strategies proposed in this paper which are totally dependent on the type of application. On the basis of different fault locations it takes the decision whether to transfer or not when it realizes the overlapping transfer of neutral wire. Transfer on the source end and not transfer on the load.

Keywords— Power supply reliability, Power quality, transfer switch, Hybrid Transfer Switch

1. INTRODUCTION:

POWER quality problems have been always troubling the large scale industries, for example we can say that iron as well as steel industry. In many cases voltage interruption and sags become the source to show the way to pool quality products and it also make the production line paralysis. Such kind of process can also become reason to cost momentous financial loss for the customers of any industry. The unbroken power supply and changeable voltage restorer are developed to get rid of such kind of issues, but due to high cost they may not be suited to large scale of industries.[1]-[3] Usually, there are two or more power feeds in the enterprise. One's performance as go in far and other is alternative. The thyristor based on solid state transfer switch (STS) and mechanical based on automatic transfer switch (ATS), It can be the most cost effective solution of the power quality issues.
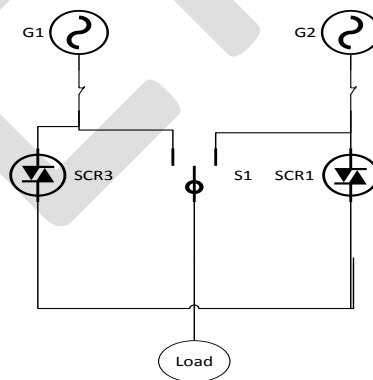
Fig. 1. Main Diagram Structure of HATS

The transfer time of the STS is precise and transfer process has a smaller impact to critical loads. So the power of STS is very patent and plain. When thyristor are undergoing in conduction state. So that, STS requires a huge and cooling system of very high quality. Production or invention of Hybrid ATS is very useful to reduce the loss of consumption. Hybrid switch device contains a pair of antiparallel thyristors and a designed mechanical parallel switch, in this way circuit within 1ms. However structure and motivating circuit are simplified or to become less complex [4]. Structure's perspective four transfer strategies are projected to follow different applications. Projected HATS also realizes the overlapping transfer of the neutral wire and it can easily justify the fault location and decides a correct way to transfer or not first, operation principles contains operation rule transfer strategy. Voltage sag detection method, fault location identification (justification) method. Overlapping transfer of the neutral wire is discussed [5]-[7]. Design details

containing hardware and software are presented then laboratory tests are carried out to verify the rules at last, field experiments are carried out, and the results show the prototypes is functional.

2. OPERATION PRINCIPLES:

The structure of the HATS has been mentioned above in Figure 1. TS1 and TS2 are the antiparallel thyristor switches which are connected to the projected (preferred) source and alternative source. Without any hurdle and the moving contact is connected to the load. QS1, QS3, QS5 are solitude switch or isolating switch. QS2 and QS4 are bypass switches. In order to justify maximum flexibility of power supply to load, all the operation rules are necessary for the HATS which are following:

1. In normal state only One Source will be connected the load.
2. When the alternate source voltage is within the normal situation and contains the same phase order with the projected or preferred source it allows transfer operation.
3. The device must be reliably connected the load to the alternate source after cutting off preferred source. If any error happens which was not expected and alternate source cannot be closed any way, then device will be able to reconnect the load the preferred source.
4. To expand the fault range we have to attach or inherit a transfer to HATS when faults happen.
5. Transfer should be stopped during overlapping. For example, during the starting point of motor the load bus voltage may be pulled low. In such kind of case the transfer operation is hindered because the load voltage will difficult to recover even if the HATS transferred to the alternate source.

3. CRITICAL LOAD:

Critical load do not accept any interruption in the power supply. Critical loads such as electronic protection equipment and control. Hence they are always should be online fed from the UPS. The UPS convert the AC voltages which are coming from the main source or preferred source, to DC voltage and store in batteries bank and providing the power supply by converting through DC to AC invertors. But due to high power losses during the converging process and feeding in AC type.

It should be noted that all loads are categorized according to the requirement hence determining the equipment size and the overall cost.

4. HARDWARE CONNECTIONS
4.1. Power Circuit:

Connections of power circuit are shown in fig. 2.

Where the three phase load is fed either from Main Source or the Alternative source through the connectors which are parallel with thyristor [8]-[10].
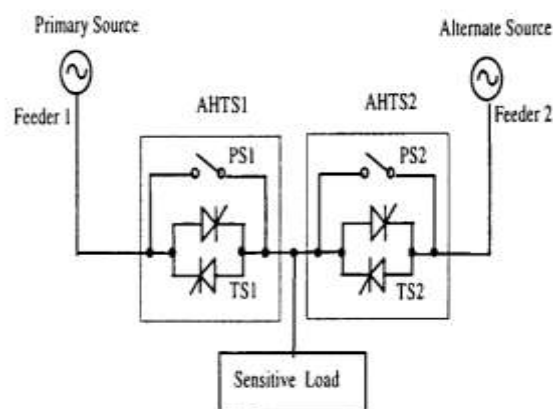
Fig. 2. Power Circuit Diagram

4.2. Control circuit:

The hardware is consist of a DC power supply which'll be use for the control circuit of PLC, sample circuits of alternative source supply and preferred source power supply two SCR driver units [11], ATS1-2 Drivers unit ,etc. A Programmable logic controller PLC is use to control the system to fulfil the requirements of our proposed research. Connections are shown in fig. 3.
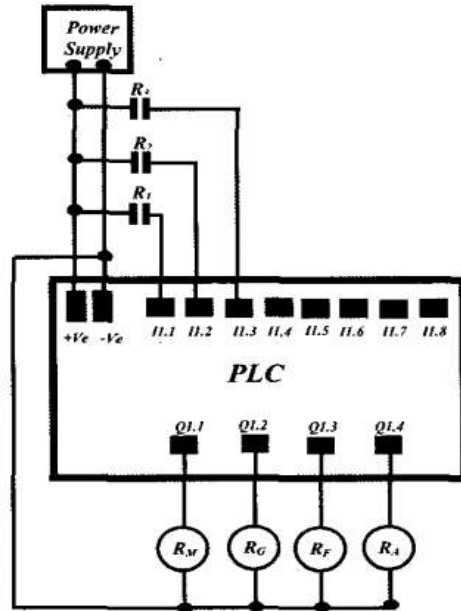
Fig. 3. Connections of Control Circuit of PLC

5. SOFTWARE PROGRAMMING:

The structure of operations for the planned setup can be shortened as

5.1. Fault Condition:

If any phase of main Supply is out of order (R1 or R2 is OFF)

1. Instantaneously disconnect the MAIN Source through its contactor (Rm is OFF)
2. After this Load will be connected through thyristor with minimum (delay Rf is ON)
3. After time delay (T2) ,built up voltage from the alternative Source
4. Check for the alternative Source output voltages (R3 is ON)
5. If not required voltage than disconnect the alternative Source and again connect to Main Source (Rg is ON)

5.2. Normal Condition:

If no one of MAIN source phase is our (R1 & R2 is ON)

1. Load will be disconnected the alternative Source and connect through (RG is OFF) the thyristor with are parallel with Connectors for period (T4)
2. After time delay (T5), Connect the MAIN source through its contactor (Rm is ON)
3. After time Delay (T6), disconnect the thyristors (Rf & Ra are OFF)

6. PROCEDURE DESIGN:

The decision logic module check and deicide to transfer a signal to other source and check the transfer signal is valid or not. If valid then transfer logic module will start the transfer and control the transfer procedure. After the transfer, a verified signal which will be

generated on conformation of transfer signal was valid will be sent to the decision logic module and procedure will organize for next transfer signal. [13]

The flowchart of program of decision logic module and the transfer logic module is shown in fig. 4 ATS1 and ATS2 have 3 (Three) position.

1. Load is connect to primary source (which is our preferred source)
2. At this Position load is connect to secondary (alternative source)
3. Load is not connect to no source (zero position)

This flowchart fallows the procedure of BBM (Make Before Brake) strategy. During the transfer procedure, if any fault happened in preferred source then logic module will transfer the load to alternative source. After the recovery of preferred source, transfer logic module will return the load to preferred source for the maximum power reliability. During the transfer procedure, neutral wire will not be cut off [1],[11],[12]
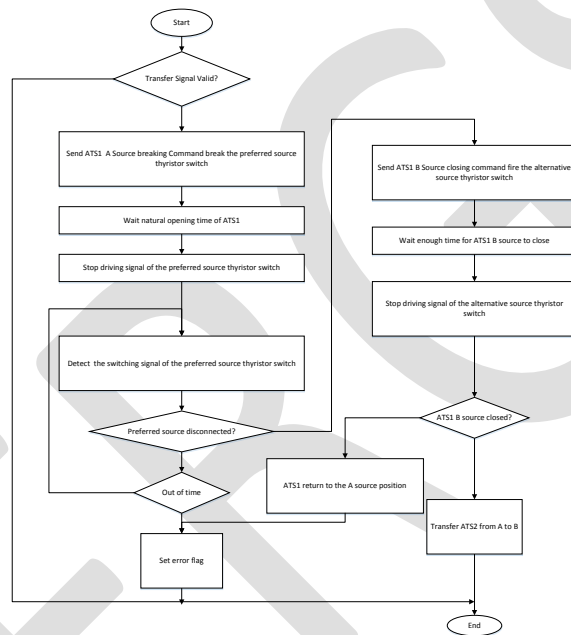
Fig. 4. Transfer logic Flowchart

TABLE 1.

Parameters of Prototype

Rated Voltage	400V
Rated Current	200A /400A
Interrupting Current	450A / 900A
Cooling Method	Natural
Applications	Three phase four wire system
Operation Mode	Auto or manual
Load type	AC-22iA
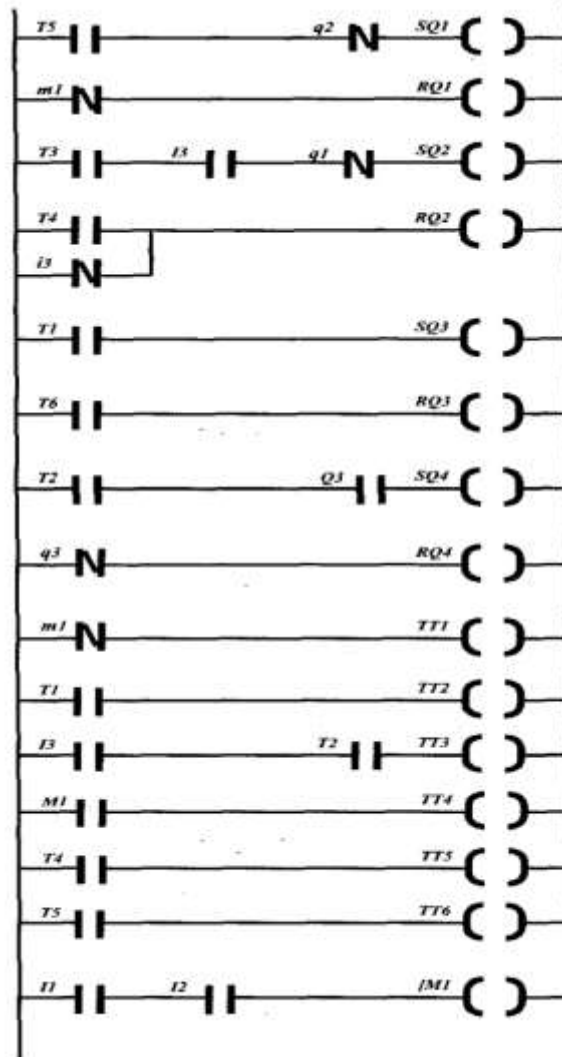
Fig. 5. Ladder Diagram of PLC program

The ladder program, shown in fig. 5. Has been developed using PC software provided with the PLC. Program symbols are listed in Table 1. The program has been simulation than download to the PLC using the PC program which is provided. It should be noted that timer values could be individually set according to system requirements and limitations.

Symbol	Type	Comment
11	Input	Main voltage Vm
13	Input	Alternative Source voltage
Q1	Output	Main Contactor
Q2	Output	Alternative Source Contactor
Q4	Output	Alternative Source voltage buildup
M1	Marker	Fault/ Normal Condition
T1	Timer	To disconnect the main and connect with Alternative Source
T3	Timer	To Connect with Alternative Source
T4	Timer	To disconnect Alternative Source

T5	Timer	To connect the Main Source

Table 1 List of Program Symbols

7. INDUSTRIAL PROTOTYPE:

The HATS and control circuit which designed this paper is shown in fig 6.

HATS can work in both mode

1. Automatic Mode   2. Manual Mode
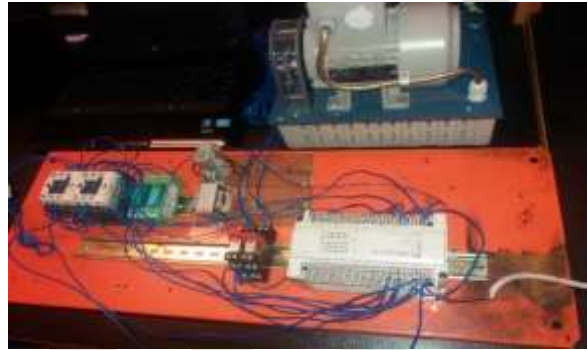
Fig. 6. Control Circuit and Prototype of project

These mode are selected by user through a selector on the front of panel board. In automatic mode, the HATS will work according to the transfer logic module or program which is burn in programmable logic controller. In other mode or manual mode the transfer will take place according to the user requirement.[14] Even when the PLC operate unusually, the HATS can still be worked manually. The characteristics of the HATS are displayed in TABLE 1

8. RESULTS:

The transfer strategy has been implemented on the prototype and tested in lab. The experiments setup is shown in fig 6 and parameters are

I. Source 400V three phase, frequency 50Hz
II. Load Motor R=35ohm and L=4.7mH;
III. Resistance in Series R_f=30 ohm

Rf and a Switch in parallel are used take voltage sag application on primary source. The switch S operate manually. The experiments results of break before make (BBM) transfer strategy are shown in fig 7.
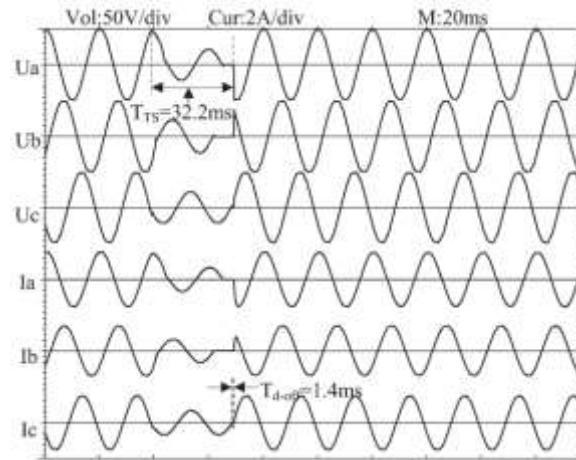
Fig. 7. Load voltages and load currents curves. From top to bottom A,B,C phases of voltages and currents.
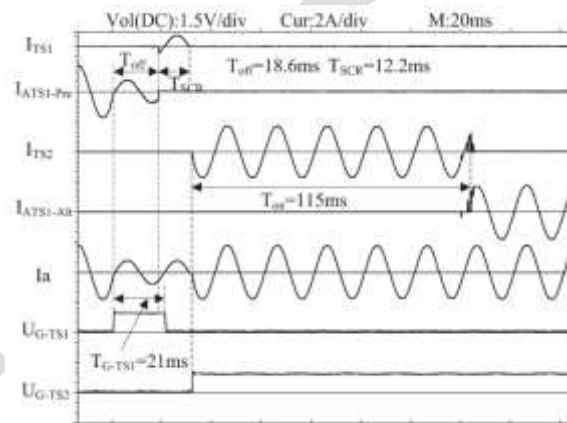
Fig. 8. Commutation Curves of phase A, currents of TS1, ATS1, alternative source for TS2 and ATS1

According to the results, load is not connected to any one of two available sources and their short time is T_{d-off}, 1.4ms at this time, no current is flowing between the sources. The total transfer time T_{TS} is almost equal to 32.2ms. Shown in fig. 8. In figure, a phase commutation graphs during the transfer process.ATS1's characteristic opening time T_{off} is 18.6 ms , and thyristor conducting time is 21 ms to preferred source.

Therefore when ATS1's start to opening, the primary thyristor start conducting instantaneously and thyristor conducting time is almost 12.3 ms as shown in figure mention above.

9. CONCLUSIONS

Automatic transfer switch is most cost operational solution of power quality problems as we seen in industry. As we suggested a Hybrid automatic transfer switch, which will has features and benefits as mentioned below:

- In large scale industries, for power quality enhancement during disturbance.
- In different small scale institute/ industry having their own generation for uninterrupted supply without breakeven not for one second
- For experiments and research work in research organizations

10. ACKNOWLEDGEMENTS

REFERENCES:

[1] Bing Tian, Chengxiong Mao, Jiming Lu, Dan Wang, Yu He, Yuping Duan, and Jun Qiu "400 V/1000 kVA Hybrid Automatic Transfer Switch" *IEEE TRANSACTIONS ON INDUSTRIAL ELECTRONICS, VOL. 60, NO. 12, DECEMBER 2013*

[2] H. Mokhtari, S. B. Dewan, and M. Reza Iravani, "Analysis of a static transfer switch with respect to transfer time," *Power Del.*, vol. 17, no. 1, pp. 190–199, Jan. 2002.

[3] M. Takami, T. Ise, and K. Tsuji, "Studies toward a faster, stabler and lower losses transfer switch," in *Proc. IEEE Power Eng. Soc. Winter Meeting*,Jan. 2000, vol. 4, pp. 2729–2734.

[4] J. W. Schwartzenberg and R. W. De Doncker, "15 kV medium voltage static transfer switch," in *Conf. Rec. 30th IEEE IAS Annu. Meet.*,Oct. 1995, pp. 2515–2520.

[5] D. L. Ransom, "Choosing the correct transfer switch,, Jun. 2012, pp. 170–175.

[6] M. A. P. De Azpeitia, A. Fernandez, D. G. Lamar, M. Rodriguez, and M. M. Hernando, "Simplified voltage-sag filler for line-interactive uninterruptible power supplies," *Ind. Electron.*, vol. 55, no. 8,pp. 3005–3011, Aug. 2008.]

[7] J. D. Barros and J. F. Silva, "Multilevel optimal predictive dynamic voltage restorer," *Ind. Electron.*, vol. 57, no. 8, pp. 2747–2760, Aug. 2010.

[8] H. Mokhtari, S. B. Dewan, and M. Reza Iravani, "Analysis of a static transfer switch with respect to transfer time," *Power Del.*, vol. 17, no. 1, pp. 190–199, Jan. 2002.

[9] H. Yasaman and H. Mokhtari, "Performance evaluation of hybrid transfer switches in grounded and ungrounded medium-voltage electrical systems," in *Proc. CIGRE/IEEE PES Int. Symp. Qual. Secur. Elect. Power Del. Syst.*, Oct. 2003, pp. 91–96.

[10] F. Gonzalez-Espin, E. Figueres, and G. Garcera, "An adaptive synchronous-reference-frame phase-locked loop for power quality improvement in a polluted utility grid," *Ind. Electron.*, vol. 59, no. 6, pp. 2718–2731, Jun. 2012.

[11] M. Takeda, H. Yamamoto, T. Aritsuka, I. Kamiyama, and G. F. Reed, "Development of a novel hybrid switch device and application to a solidstate transfer switch," in *Proc. IEEE Power Eng. Soc. Winter Meeting*, Feb. 1999, vol. 2, pp. 1151–1156.

[12] M. Takami, T. Ise, and K. Tsuji, "Studies toward a faster, stabler and lower losses transfer switch," in *Proc. IEEE Power Eng. Soc. Winter Meeting*, Jan. 2000, vol. 4, pp. 2729–2734.

[13] M. J. Sullivan, T. Vardell, and M. Johnson, "Power interruption costs to industrial and commercial consumers of electricity," vol. 33, no. 6, pp. 1448–1458 Nov./Dec. 1997.

[14] F. Gonzalez-Espin, E. Figueres, and G. Garcera, "An adaptive synchronous-reference-frame phase-locked loop for power quality improvement in a polluted utility grid," *Ind. Electron.*, vol. 59, no. 6, pp. 2718–2731, Jun. 2012

Application of GIS & CFD for design of Pump Intake

D. Ram Mohan Rao[1], Zameer Ahmed[2], Dr. K.Ram Mohan Reddy[3], Dr. Y. Ellam Raj[4]

1.Prof., Dept of Civil Engg., MJCET, Hyderabad, e-mail: dharwadarmr@gmail.com,
2. Director (Tech), NCPE IIPL, Hyd,
3. Professor and Head, Water Resources Division, JNTU Hyd,
4. Dean, AVN institute of Engineering and Technology, Hyd

Abstract— Hydraulic structures used to withdraw water from a river or reservoir. As the high levels of circulation in the flow upstream of the pump sump region leads to asymmetry in the approach flow, this influences considerably the quality of intake design. The vortices originating at the lateral walls, floor or at the free surface can form in the vicinity of the pump intake area can be classified as either free-surface vortices or sub-surfaces vortices according where they originate. [1] All the vortices formed like this induce high levels of unsteady swirl inside the pump column, which results to uneven loading on impeller, and reduce the efficiency of the pumps. One of the major problems in water intake flows is a swirling-flow problem in the pump sump. If this problem is not solved, the effectiveness of the intake is reduced which directly influences the efficiency of the pump. Significant cost savings could be realized if the designs for pump intakes and other structures could be developed using computational fluid dynamics (CFD) models. CFD code can successfully predict vortices, and these models can be used extensively in design of basins with pump intakes.

Keywords— Pump Intake, CFD, Raster GIS, Vortices, Submergence, Sink, Superimposition, k-e model

Introduction

The function of proper intake structure of pumps is to supply uniformly distributed flow of water to the suction bell of pump. Uneven distribution, higher discharges favor formation of vortices, and cause low submergence. The intake of air into suction pipe reduce the capacity accompanied by noise and vibration. All possible streamlining efforts should be incorporated in the design to reduce formation of wakes. The amount of submergence mainly depends upon approach design and pump capacity. Good intake design also eliminates hydraulic phenomena and other conditions, such as sedimentation and accumulation of floating debris that can have a negative impact on pump performance. In addition, the sump should be kept compact and straightforward to reduce the installation footprint and minimize construction costs. The complete analysis is highly mathematical and complicated Navier Stokes equations can be seldom solved to provide viable engineering solutions. The other alternatives available are simulation using CFD software, model analysis and similitude. Raster GIS can simulate various velocity potential functions like uniform flow, vortex flow and has capability of superimposing the above functions in order to estimate possible velocities and depth of submergence.

Circular intakes offer more compact layout on account of smaller circumference and hence minimizes the sump volume and constructional costs. This cost enhancement is significant if the river bed is rock formation. However, circular geometries are recommended for lesser velocities and discharges. In the present study the adoptability of circular geometry is studied for a lift irrigation pump well having wet well diameter 7.0m with two pumps. The diameter of each suction pipe is 1.0 m and discharge of each pump is 1.31m3 /s

Literature Review

Tanweer S. Desmukh & V.K Gahlotuses studied the commercial CFD package ANSYS CFX-10 to predict the three dimensional flow and vortices in a pump sump model. The CFD model predicts the flow pattern in detail and the location, and nature of the vortices. However, considerable post-processing of the basic data is needed to fully comprehend the details of the flow. Thus CFD model can be used to study the effect of various parameters and hence can become an important tool for optimization of pump sump geometry. Kadam Pratap M. and D. S. Chavan studied the flow characteristic in a pump sump of physical model by using Computational Fluid Dynamics (CFD) code FLUENT.

The experimental procedures include the data collection using a flow meter and swirl meter (Rotometer /Vortimeter). Two types of measurements were conducted which are flow, and swirl angle. A visual test that involves the dye tracing technique was also carried out to characterize the flow. The CFD analysis is done at critical cases, Grid generation is done in ICEM-CFD and numerical analysis

are carried out in FLUENT , and flow is analyzed with the help of velocity stream lines and vector plot and velocity contour at the entrance of pump chamber, in CFD-POST software and concluded on experimental and cfd results.

A C Bayeul-Lainé, G Bois and A Issare produced the flow pattern and confirm the geometrical parameter influences of the flow behavior in such a pump. The numerical model used solves the Reynolds averaged Navier-Stokes (RANS) equations and VOF multiphase model for two cases. In the validation of this numerical model, emphasis was placed on the prediction of the number, location, size and strength of the various types of vortices. Previous studies, without simulation of air entrainment, have shown the influence on a single type of mesh with different cell numbers, different intake pipe depths and different water levels, for two turbulence models closure.

Cecilia Lucino, Sergio Liscia Y Gonzalo Duró verified the ability of a commercial computational fluid dynamic (CFD) code to predict the formation of vortices in a pump sump. It was intended to identify vortices of diverse origin and intensity in a geometrically simple pump sump of which experimental results under the same operating conditions are known.

Intake Structures and Pumps:

The basic function of the intake structure is to help in safely withdrawing water from the source over predetermined pool levels and then to discharge this water into the withdrawal conduit. Intake wells are widely used to draw water and pump to various applications. They can be classified as dry, wet well intakes. Wet well intakes provide sufficient storage to allow fluctuations in water levels. These intakes are used in stormwater, waste water pumping, lift irrigation schemes, water supply schemes, cooling applications in power plants. Efficiency of pumps depends pump bays, dimple vortex, air entraining vortex, submergence vortex, Swirling flow and placing of the pumps where as economy depends on proper sizing of intake structure.

A. FREE SURFACE VORTICES

The static pressure (head) of the delivered water significantly changes while passing through the pump from the inlet to the outlet. The minimum overpressure is around the entrance of the impeller. Steam bubbles arise here, if the pressure of the delivered water decreases below the pressure value of saturated steam with the same temperature. In the course of energy conversion in the pump, the pressure increases again along the stream when the water is passing through the pump and when it exceeds the pressure of the steam the bubbles are crushed (cavitation) thus starting to destruct the impeller mechanically. To prevent cavitation at the inlet of the pump the minimum inflow pressure should be maintained.

Each pump has a minimum suction head value, at which it can still work. This value is always smaller than the atmospheric pressure value expressed in pressure head of the liquid to be delivered. This value is known in the Anglo-American literature as the necessary "net positive suction head" - that is the NPSH of a pump.

This value can be considered as a loss factor and must be always subtracted from the theoretical suction head. Manufacturing companies always indicate these values for different deliveries and revolutions, since along with the increase of delivery these values increase as well. To apply properly these values, the $NPSH_a$ value of the pump under the actual conditions should be calculated.

Simulation of Pump Intake Flow

In the present investigation to study the influence of submergence depth required above suction pipe to avoid influence of vortices, the 'Basala Doddi Pump' Located in Kurnool district is considered. The following are the technical specifications of the pump considered in the present simulation: 'Basala Doddi' pump intake has wet diameter 7.0m with two pumps. The diameter of each suction pipe is 1.0m m and discharge is 1.31m3 /s. The MWL in the well is 318.5m and the floor level of the well is 308.436m The LWL is312.0m.The level of suction bell-bottom is 309.5m
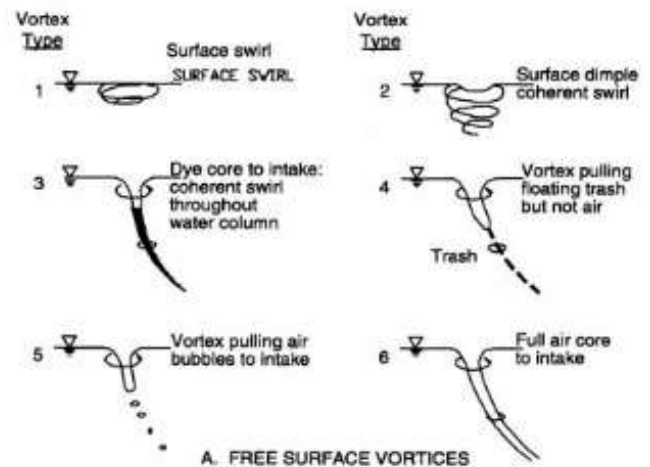
The level of water above the floor is 3.564m for low water level. The clearance between floor level and suction pipe bottom is G=C=1.064m. The submergence depth above of suction bell-bottom is 3.564-1.064=2.5m,for low water level of 312.5m.The minimum submergence depth required is 1.8m as per code.

As per FSI ,

$$S = D(1 + 2.3 F_D) \qquad (1)$$

$$F_D \text{ is Froude number} = V/\sqrt{(gD)} \qquad (2)$$

Where   V=velocity of suction inlet .

D=bell diameter.

$$V = Q/A = [(1.31 \times 4)/(\pi \times 1.0892)] = 1.406 \text{ m/s.}$$

$$FD = 1.406/\sqrt{(9.81 \times 1.089)} = 0.43.$$

$$S = 1.089(1 + 2.3 \times 0.43) = 2.17\text{m. (FSI sump design guidance)}$$

The minimum submergence required to prevent strong air core vortices is 2.17m for Basala Doddi pump intake. The actual submergence of 2.5m is greater than minimum required and possibility of air core vortices is almost negligible.

The 2d flow is simulated from the concept of potential flow theory. Each suction pipe is assumed as a sink. The equation for potential lines is given by [2]

$$\Phi = m \times \ln(r) \qquad (3)$$

Where Φ = velocity potential function

m = strength of sink.

r = radial distance from sink.

$$m = Q/(2\pi b) \qquad (4)$$

Where   Q = 1.31 m3/s.

 b = height of bell invert above floor level.

b = 1.064m as per the design drawings.

m = 1.31/(2π*1.064).

m = 0.196m2/s

On account of two suction pipes placed symmetrically along the center line of horizontal axis, two sinks are placed with constant strength m 0.196m2/s. In potential flow theory two valid stream functions or velocity potential functions can be superimposed to obtain a valid combination of velocity potential functions. The velocity potential valid for a sink is simulated using SAGA GIS and the functions and their combinations are given in the following figures. Figure 1 shows the Velocity potential function from SAGA GIS showing potential values for single sink. Similarly Figure 2 and Figure 3 represents the velocity potential function from SAGA GIS showing potential function from SAGA GIS showing potential values for second sink and the potential function from
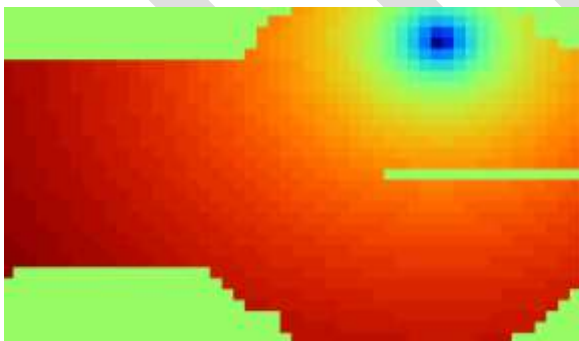
Figure 1: Velocity potential function from SAGA GIS showing potential values for single sink.
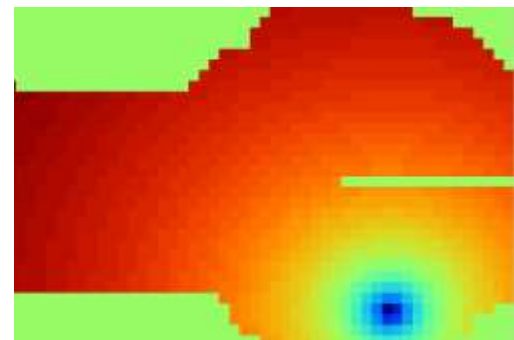
Figure 2: Velocity potential function from SAGA GIS showing potential values for second sink

the combination of two sinks respectively.
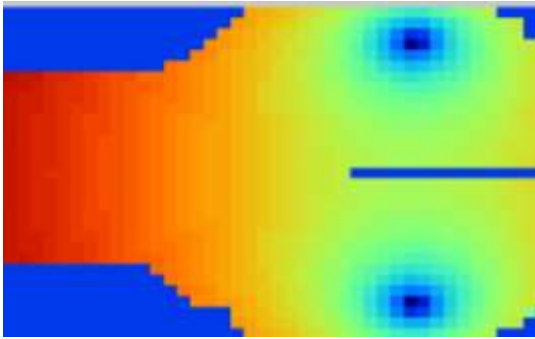
Figure 3: The potential function from the combination of two sinks
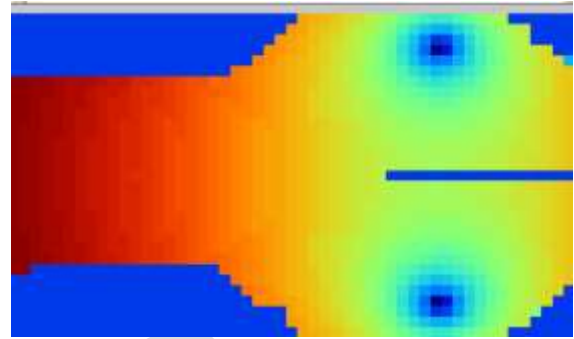
Figure 4; The constant head is superimposed for the given boundary conditions

Velocity potential for a The water surface profile on account of the superimposed Sinks is also presented and the minimum head above pump suction bowl is 5.5m which is much higher than minimum submergence depth, avoiding the possibility of vortex formation.

The resulting potential heads on account of two sinks and minimum water level of 2.5 m above the suction pipe inlet.

From the above analysis it is verified the possibility of strong vertex core and cavitation is almost negligible.

3D Analysis

The pump intake flow of Basala Doddi irrigation scheme is also simulated by using Fluent software (Which uses finite volume approach to solve continuity and Navier stokes equation.).The geometry of approach duct and pump intake well is generated using Gambit software. The pressure distribution along the bottom wall, inlet and outlets are provided in the following results.

Water is used as fluid material with a constant density of $998.2 kg/m^3$ with hydrostatic pressure variation. Standard $k - e$ model is used for turbulent flow. This model is used as Reynolds number is much higher to simulate turbulent kinetic energy dissipation. One thousand iterations are used for the convergence criteria and appropriate boundary conditions are imposed. The converged solution results are provided in the following figures.
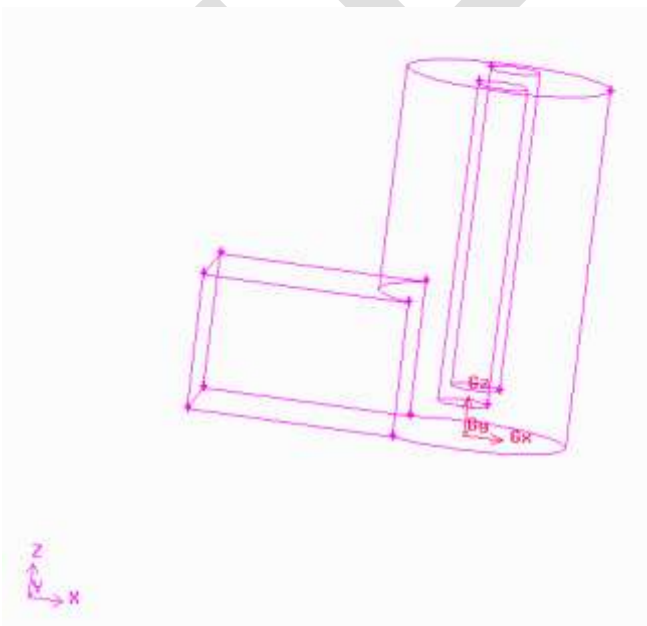
Figure 5: 3D pipe intake model generated with Gambit software
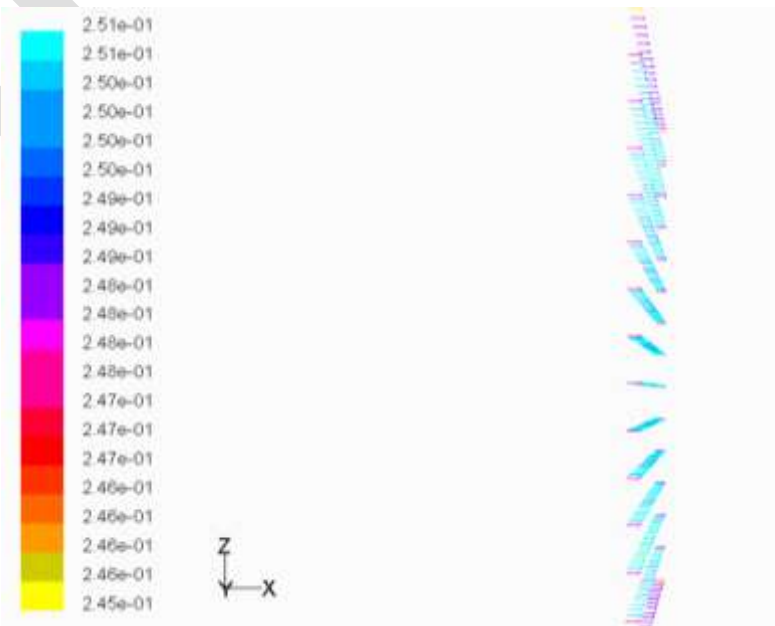
Figure 6: Velocity profile at duct inlet of area 10.5m^2 with almost constant magnitude of
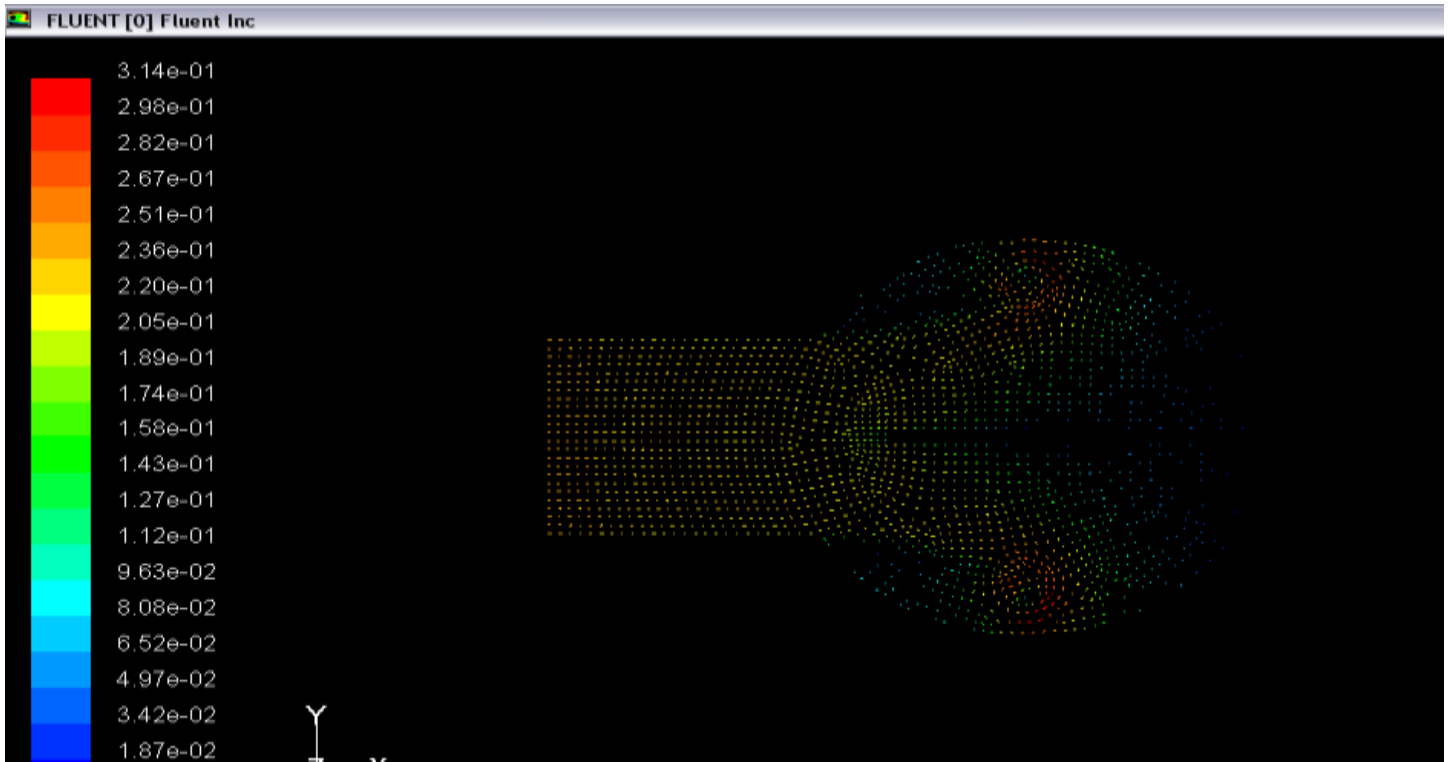
Figure 7: Velocity profile and stream flow pattern along the bottom wall of the well with maximum velocity of 0.32m/s
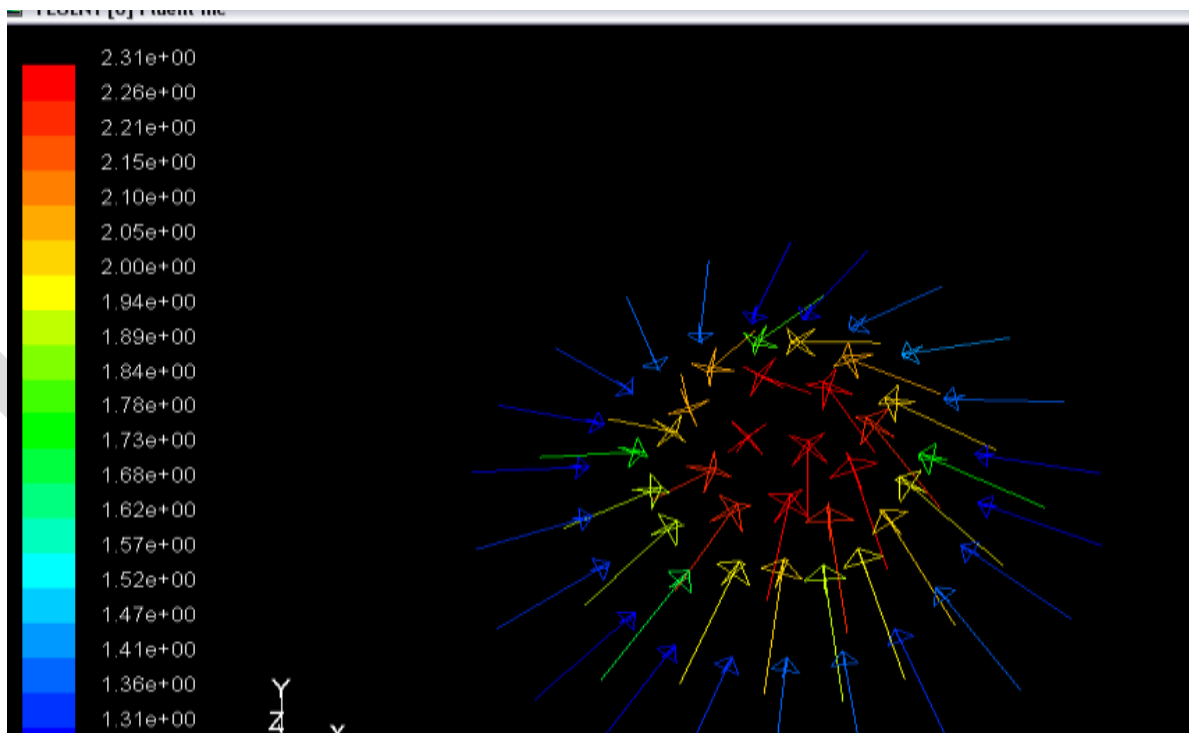
Figure 8: The velocity vector profile through one of the pipe suction pipe (The max & mini velocities are 2.28m/s and 1.25m/s
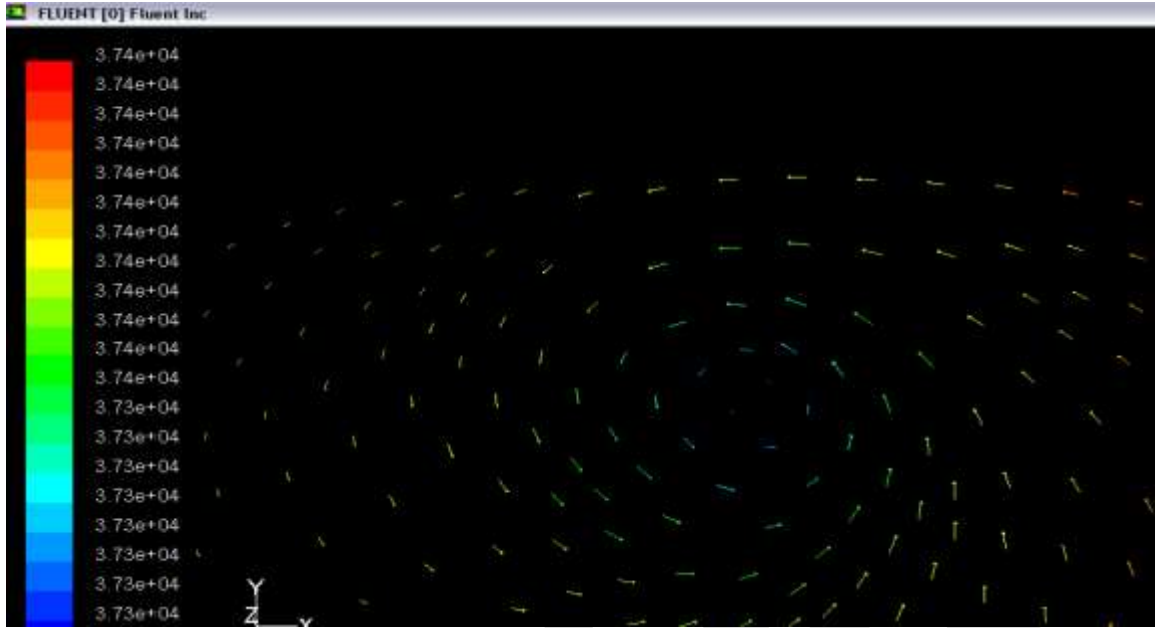
Fig 9: The pressure profile on the bottom wall of the well with the minm and maxm values of 37.3KPa to 37.4Kpa.
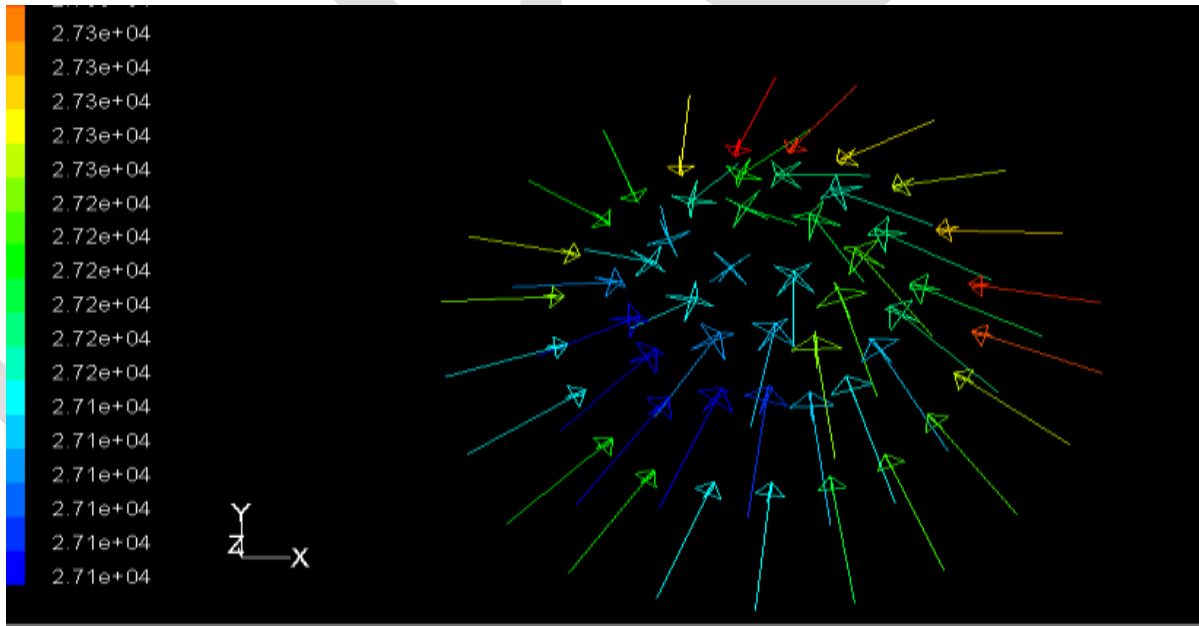
Fig 10: Pressure profile through one of the pump intakes suction intakes. (min and max pressures are 27.1 and 27.4 Kpa guage)

The above mentioned gauge pressures are much higher in order to avoid vortex formation.
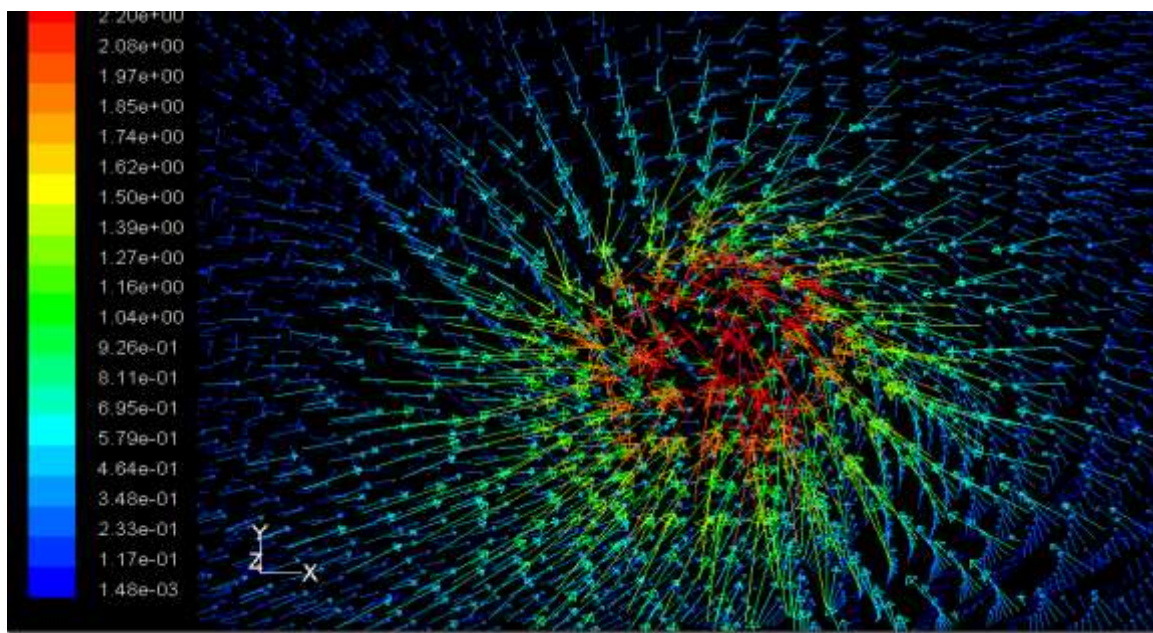
Fig 10: **Flow pattern inside the intake**

Conclusion

1. The minimum submergence depth required above suction pipe bowl is 2.17m, to avoid strong air core vortices. The depth of submergence is 2.5 m from Two D analysis and 2.76m from Three D analysis.
2. The maximum velocities are .39m/s and 1.1m/s respectively, inside pipe intake well , which are less than permissible values.
3. Splitters are provided in order to avoid swirl velocities. The required criteria for all clauses are met during normal operating conditions.
4. Raster GIS can be used for in fluid flow simulations

REFERENCES:

1. Melville, B.W., Ettema, R. and Nakato, T., 1994, "Review of flow problems at water intake pump sumps." EPRI Research Project RP3456-01 Final Report, Electric Power Research Institute, Palo Alto, CA.
2. "Principles of fluid mechanics and fluid machines", Narayana Pillaii, C.R.Ramakrishnan, University press
3. Fluid mechanics by Frank White, McGraw-Hill Series in Mechanical Engineering
4. A Gentle Introduction to SAGA GIS, Victor Olaya, Edition 1.1 — Rev. December 9, 2004
5. ANSI 9.8 – 2008, Pump Intake design, Hydraulic Institute standards, New Jersy
6. Rane et al., International Journal of Advanced Engineering Research and Studies E Int. J. Adv. Engg. Res. Studies/III/II/Jan.-March.,2014/ ASSESSMENT FOR ALTERNATIVES OF GEOMETRY FOR THE INTAKE SIDE OF THE SUMP TO ENHANCE PERFORMANCE 1 Jagruti Dilip Rane, 1M E- Mechanical Design, appearing, 2Department of Mechanical Engineering, 3Director-Ethika Engineering Solutions India Pvt. Ltd., Pune

Optimization of foam concrete masonry blocks

Geethu Kallunkal 1, Dr. Elson John2

[1]Mtech Scholar, Civil Engineering,, Mar Athanasius College of Engineering, Email:kallukalgeethu@gmail.com,

[2]Assistant Professor, Civil Engineering,, Mar Athanasius College of Engineering.

Abstract— Foamed concrete is a versatile material which consists primarily of a cement based mortar mixed with at least 20-25% of volume air. It is non-load bearing structural element which has lower strength than conventional concrete. Foam concrete is widely used in construction field and quite popular for some application because of its light weight such as reduction of dead load, non-structural partitions and thermal insulating materials. Strength of foam concrete depends upon the foam added. Stable foam production depends upon the type of foaming agent, concentration of foam, method of preparation of foam. In this study the compressive strength of foam concrete was conducted for the specimens. Specimens were made to find out the Suitable foam concentration, by adding 2g, 5g, 8g, 10g of sodium lauryl sulphate in 100ml, 500ml, 1000ml respectively. Volume of foam by weight of cement added to the concrete is estimated at 5%, 10%, 15%, and 20%. In order to increase the strength of foam concrete, test were conducted on specimens with Flyash as the partial replacement of cement and quarry dust as the partial replacement of sand at varied percentages. Based on the experimental investigations optimization the foam concrete masonry blocks with an appreciable strength and density is carried out.

Keywords— foam concrete, lightweight concrete, mortar, foam, flyash, quarry dust, interlocking masonry blocks, sodium lauryl sulphate, compressive strength.

1.INTRODUCTION

1.1 FOAM CONCRETE

Concrete is the second most widely consumed substance on earth, after water. In concrete construction, self-weight represents a very large proportion of the total load on the structure, hence there are clearly considerable advantages in reducing the density of concrete by using Light Weight Concrete(LWC). The chief of these are the use of smaller sections and the corresponding reduction in the size. Furthermore, with lighter concrete the form work needs to withstand a lower pressure than would be the case with ordinary concrete , and also the total weight of materials to be handled is reduced with a consequent increase in productivity. LWC also gives better thermal insulation than ordinary concrete. The practical range of densities of lightweight concrete is between 3.00 and 18.50 kN/m^3, the weight reduction of concrete structure would results in less structural steel reinforcement. One such LWC is foamed concrete.

Foam concrete is a very fluid, lightweight cellular concrete fill material, produced by blending a cement paste (the slurry or mortar), with a separately manufactured, pre-formed foam. The density of foam concrete is determined by the ratio of foam to slurry and densities range typically between 300 and 1800 kg/m^3.

Foam concrete also known as foamed concrete, foamcrete, cellular lightweight concrete or reduced density concrete, is defined as a <u>cement</u> based slurry, with minimum of 20% (per volume) <u>foam</u> entrained into the plastic <u>mortar</u>, this differentiates foam concrete from (a)Gas or aerated concrete, where bubbles are chemically formed through reaction of aluminum powder with calcium hydroxide and other alkalis released by cement hydration and (b) Air entrained concrete, which has much lower volume of entrained air. Mostly no <u>coarse aggregate</u> is used for production of foam concrete. The correct term would be called as mortar instead of concrete. Sometimes it may be called as "Foamed Cement" or "Foam Cement" because of mixture of only cement and foam without any fine aggregate.

Fig.1.1 Foam Concrete

Foamed concrete possesses characteristics such as high strength-to-weight ratio. Using foamed concrete reduces dead loads on the structure and foundation, contributes to energy conservation, and lowers the labor cost during construction. It also reduces the cost of production and transportation of building components compared to normal concrete and has the potential of being used as a structural material.

Foam concrete contains unique characteristics that can be exploited in civil engineering works. It requires no compaction but will flow readily from an outlet to fill restricted and irregular cavities, and it can be pumped over significant distances and heights, thus it could be thought of as a free flowing self setting material.

The foamed concrete is considered as an economical solution in fabrication of large scale lightweight construction materials and components such as structural members, partitions, filling grades, and road embankment infill's due to easy production process from manufacturing plants to final position of the applications. In practice, foamed concrete has been commonly used in construction applications in different countries such as Germany, UK, Philippines, Turkey, and Thailand.

Historically, the Romans first realized that by adding animal blood into a mix of small gravel and coarse sand with hot lime and water and agitating it, small air bubbles were formed making the mix more workable and durable. However, the first Portland cement based foamed concrete was patented in 1923 by Axel Eriksson[1] . Further, the initial comprehensive review was conducted by Valore [2] on cellular concrete. Over the past 20 years, substantial improvements in production equipment and better super plasticizers, foam agents have permitted the use of foamed concrete in a larger scale and many efforts have been made to study the characteristics and behavior of foamed concrete comprehensively in order to simplify its usage in structural applications. So far, some researchers reported that the foamed concrete possesses superior properties such as low density which helps to reduce structural dead loads, foundation size, labor, transportation and operating costs. Besides, it enhances the fire resistance, thermal conductivity and sound absorbance due to its textural surface and micro-structural cells.

1.2 CONSTITUENT MATERIALS

Foamed concrete consists of basic and supplementary components. The basic components are cement, sand, and water for mortar, plus aggregates to produce concrete, while the supplementary materials are fly ash and silica fume.

1.2.1   Binder

Cement is the most dominant binder in foamed concrete. The types of cement used in the foamed concrete are ordinary Portland cement, rapid hardening Portland cement, calcium sulpho aluminates cement, and high alumina cement, which can be used in ranges between 25% and 100% of the binder content. However, other supplementary materials such as silica fume, fly ash, lime, and incinerator bottom ash can also be replaced with a percentage of cement ranging between 10% and 75%.The supplementary materials are used to improve mix design consistency, long term strength and to reduce costs. Each supplementary material may contribute to properties of foamed concrete in different fashions. For instance, the purpose of using silica fume is to strengthen the foamed concrete in a short time due to their filler characteristics and pozzolanic behavior, while fly ash needs a longer time to reach the maximum strength comparing to cement. Therefore, the supplementary materials should be used as partial replacements according to desirable foamed concrete properties.

Concrete with densities between 800 and 1200 kg/m3 have been produced using lightweight coarse aggregate in foamed cement matrix

1.2.2 Foam Agent

Foaming agents required for producing aqueous stable foam can be either natural based like resin soap and glue, hydrolyzed protein such as keratin, cattle hooves and fish scales, blood, saponin and casein or synthetic based like detergents (sodium lauryl sulfate, alkalyaryl sulphonate.1 Synthetic foaming agents are preferred for the following advantages; (i) allows a greater control over density of material than protein based foams2 (ii) possess permanent properties (since they are produced in accordance with technical requirements) and (iii) longer working life. Proper selection of foaming agent is essential as the type of foaming agent used influences the final strength of foamed materials.Foam agents control the concrete density through a rate of air bubbles created in the cement paste mixture. Foam bubbles are defined as enclosed air-voids formed due to the addition of foam agent. The foam agents are commonly synthetic, protein-based, detergents, glue resins, hydrolyzed protein, resin soap, and saponin.The most common foam agents are synthetic and protein based. The protein based foam agents result in a stronger and a more closed-cell bubble structure which permits the inclusion of greater amounts of air and also provides a more stable air void network while the synthetic ones yield greater expansion and thus lower density. The content of the foam agent has a considerable effect on properties of both fresh and the hardened concrete. It is reported that the excessive foam volume results in a drop in flow. However, the flow is significantly affected by mixing time. Greater the mixing time, the more the entrained air, though, prolonged mixing may cause the loss of entrained air by dropping the air content. Moreover, water-reducing chemical admixtures are likely to cause instability in the foam and subsequently are not usually used. The air voids range between 6% and 35% of the total volume of final mix in most foamed concrete applications. The foam is produced by blending the foam agent, water and compressed air (generated by an air-compressor) in pre-calculated proportion ratios in a foam generator calibrated for a discharge rate.

1.2.2   Water and Plasticizers

A water requirement in foamed concrete depends upon the constituents and the use of admixtures. Water content is also governed by the uniformity, consistency and stability of the desired mix. Low water content caused the mix to be too stiff and bubbles broke during mixing which resulted in an increased density. Similarly, at high water content, the slurry was too thin to hold the bubbles which caused segregation of the foam from the mix and consequently the final density was increased. In general, the water to cement ratio range was suggested to be from 6.5% to 14% of the target density. Furthermore, the quality of used water counts in the production of foamed concrete. Water used for the foamed concrete mix design should be clean, fresh and absolutely drinkable. However, undrinkable water could also be used when foamed concrete gains 90% of strength at 7−28 days similar or equal to samples made with water from a municipal supply.

The plasticizers are significantly utilized to improve workability and to stabilize the compatibility of foamed concrete. They are practically defined as water reducers used to increase the performance of fresh concrete by easing its mobility and plasticity; however, no significant effects on concrete segregation were observed. One of the most popular plasticizers in the foamed concrete production is FluorosSurfactant (FS1). The FS1 is generally used to reduce the amount of mixing water and also marginally accelerates the strength gain of the produced foamed concrete. The plasticizers content is approximately between 0.45% and 5% of foam agent volume.

2. LITERATURE REVIEW

Sathya Narayanan.al[1] Studies deals with the identification of suitable set accelerator for foam concrete made using sodium lauryl sulphate as foaming agent, that is facilitating demoulding time within 2 h. As conventional accelerators, calcium chloride, calcium nitrate, triethanol amine were not-effective in foam concrete, alum and Class-C fly ash were tried. Demoulding test was performed to the mixes having optimum density (1200–1300 kg/m3).from the studies it showed Class-C fly ash has been identified as the most appropriate accelerator for foam concrete mix with SLS. Use of Class-C fly ash as (i) complete replacement of sand and (ii) combination mixes provide flexibility in its adoption as an accelerator. Class-C fly ash was observed as a potential set-accelerator, facilitating demoulding at 90 min.

Y.H. Mugahed Amran et.al[2] The paper dealt with the studies of properties and applications of foamed concrete, which included a review of foamed concrete constituents, fabrication techniques, and properties of foamed concrete. Foamed concrete consists of basic and supplementary

components. This paper provided a review of foamed concrete constituents, fabrication techniques, and properties of foamed concrete. It also aimed in providing a comprehensive insight into possible applications of foamed concrete in the construction industry today.

The compressive strength is considered as the primary function of the desirable density design, as a main consideration for this lightweight concrete, which can finally be used to fabricate structural, non or semi-structural components. Meanwhile, durability is another property of foamed concrete that needs to be at a level which can effectively allow it to resist the aggressive environments. This can be achieved by selecting the most suitable type of foam agent added. Foam agents produce a uniformed distribution of pores, where they decrease the segregation problem in an early state, prevent the ingression of chloride, prohibit sulphate attack and increase the time range during fire while enhancing its fire resistance. Stable foamed concrete production depends on many factors such as type of foaming agent, method of preparation of foaming agent to initiate a uniform or homogeneous distribution of air voids (bubbles), design calculation accuracy of the mixture, and foamed concrete production, hence the enhancement of performance in fresh and hardened states are significantly elaborated. In order to produce foamed concrete with high consistency and stability, it is recommended to reduce the volume of foaming agent, using partial replacement of cement by either fly ash or silica fume which reduces the process of heat of hydration.

Ma Cong.al [3] Ordinary Portland cement, soil and foaming agent are the raw materials used to make soil-based foamed concrete. The effects of foam content and silica fume on the physical properties of soil-based foamed concrete, such as the dry density, 28-day compressive strength, thermal conductivity, water resistance and pore structure, were studied. The experimental results indicate that the foam and silica fume contents have a large impact on the physical properties of soil-based foamed concrete. The thermal conductivity, density, water resistance and compressive strength decrease with increasing volume fractions of foam. The compressive strength, the thermal insulation and water resistance are all improved by increasing the content of silica fume. Soil-based foamed concrete consisting of 20% silica fume with a density of 800 kg/m3, compressive strength of 7.5 MPa and thermal conductivity of 0.16 W/m K can be used as water-resistant lightweight concrete. The hygroscopic tests were performed and the results indicate that

the addition of silica fume has some effect on the hygroscopic property of soil-based foamed concrete. Several fitting curves have been obtained, the fitted functions developed by the Kumaran model and Cubic function have better fitting parameters.

Kanagalakshmi et.al[4] A study on the effect of quarry dust as sand replacement material on compressive strength of foam concrete was conducted because of its low strength, some material is used in order to increase the foam concrete strength. This project was carried out to determine the compressive strength of foam concrete by using quarry dust as partial sand replacement material. This report presents the feasibility of the usage of quarry dust as 10 %, 20 %, 30 %, 40% and 50% for sand in foam concrete. Mix design was formulated and developed for four different proportion of quarry dust in foam concrete. Tests were conducted on cubes to study the compressive strength of concrete made of quarry dust and results were compared with the control foam concrete. It is found that the compressive strength of foam concrete made of quarry dust is nearly 43% more than the control foam concrete. Based on the results of the experimental investigation, it is proposed that burnt clay bricks can be effectively replaced with the foam concrete blocks. Finally cost benefit assessment was done to prove the economy of the foam concrete bricks.

Hilal et.al [5] studied on void structure and strength of foamed concrete made without/with additives. Study has been undertaken to investigate the effect of different additives on the strength foamed concrete by characterizing air-void size and shape parameters and identifying the influence of these parameters and changes to cement paste microstructure on strength. Nine different mixes, made using a preformed foam, were investigated with varying density (nominally 1300, 1600 and 1900 kg/m^3) without/ with additives (silica fume, fly ash and super plasticizer) used either individually or together. Optical microscopy and scanning electron microscopy were used in this investigation. Compared to the conventional mixes, inclusion of additives (individually or in combination) helped to improve both the cement paste microstructure and air-void structure of foamed concrete. For a given density, although the additives in combination led to increased void numbers, higher strength was achieved due to reduced void size and connectivity, by preventing their merging and producing a narrow void size distribution. Furthermore, super plasticizer has the most beneficial influence on voids when used alone and it further improves void structure (smaller and number voids) when used in combination with other additives. Not only enhancement of void structure but also improved cement paste microstructure both contribute to the strength of the foamed concrete.

Zhaoming Huang et.al [6] Studied on proportioning and characterization of Portland cement-based ultra-lightweight foam concretes. Due to desirable thermal insulation properties, superior fire-resistant and higher durability, ultra-lightweight foam concretes are recommended to achieve energy efficiency in buildings. Generally, aluminate cement, sulphoaluminate cement and other quick hardening cementations materials are used to

control the stability of air-voids in foam concretes. These special cementations materials are relatively expensive and not universally available, retarding the application and popularization of foam concretes. In the present study, the proportioning and properties of Portland cement based ultra-lightweight foam concrete were investigated. The results show that ultra-lightweight foam concretes with apparent density of100–300 kg/m^3 can be prepared using Portland cement, fly ash, hydrogen peroxide and chemical admixtures. Collapse and air-voids escape can be avoided by adding thickening agent and foam stabilizing emulsion into foam concretes. Most of pores in ultra-lightweight foam concretes were non-connected pores with size of 2.0–4.0 mm, resulting in a lower thermal conductivity, desirable compressive and tensile strengths

.**Hwang and Tran[7]** investigated Foamed Light Weight Aggregate (FLWA) manufactured with Hydrogen Peroxide (HP) as a foaming agent and using cold-bonded agglomeration process, a relatively low-polluting, energy efficient method of FLWA production. Foamed lightweight aggregate for self-consolidating concrete were surface treated to improve the performance of the aggregates. Moreover, 8 types of FLWA were used as coarse aggregate to produce Self Consolidating Concrete (SCC). A variety of tests were conducted to evaluate the effects of the foaming agent and the surface treatments on the properties of the cold-bonded lightweight aggregate. The workability, unit weight, and strength of the SCC specimens were determined in accordance with established standards. The FLWA type with the lowest specific gravity was binary mixture of 80% Fly Ash (FA) and 20% Ground Blast Furnace Slag (GBFS) at an HP concentration of 7%, with a specific gravity of 1.27. The cold-bonded lightweight fly ash aggregate manufactured for this study used hydrogen peroxide as the foaming agent in order to produce a porous microstructure inward aggregate that reduced the specific gravity of light weight aggregate. The self-consolidating FLWA concrete designed achieved uniform mixtures with fresh densities ranging from 21.06kN/m^3 to 18.89 kN/m^3. Additionally, all mixtures of SCC made with the 8 types of aggregates showed excellent workability: (1) slump flow: 660–750 mm; (2) V-funnel time: 18–31 s; (3) Passing Ability(PA): 0.8; (4) the rounded shape and smooth surface of LWA with surface modification enhanced the flowability, viscosity, and passing ability of SCC. Specific gravities of FLWA were 13% less than unfoamed LWA.Moreover, the foaming agent negatively affected water absorption and strength of LWA, which were later improved by surface treatment. The 28-day compressive strength of all SCC specimens ranged from 38.3 to 47.8 MPa, which exceeds the minimum strength required. Furthermore, the compressive strength of SCC related strongly to the strength and water absorption of FLWA. The stronger strength of FLWA resulted in stronger SCC, while the increase in water absorption of FLWA reduced compressive strength of SCC.

Kozłowskia et.al [8] studied fracture energy of foamed concrete based on three-point bending test on notched beams. A series of static loading tests was performed to determine the fracture properties of foamed concrete of varying density. Beams with dimensions of 100×100×840 mm with a central notch were tested in three-point bending. Then, remaining halves of the specimens were tested again as un-notched beams in the same set-up with reduced distance between supports. The tests were performed in a hydraulic displacement controlled testing machine with a load capacity of 5kN. Apart from measuring the loading and mid-span displacement, a Crack Mouth Opening Displacement (CMOD) was monitored. Based on the load − displacement curves of notched beams the values of fracture energy and tensile stress at failure were calculated. Subsequently, the flexural tensile strength was obtained on un-notched beams with dimensions of 100×100×420 mm. Moreover, cube specimens 150×150×150 mm were tested in compression to determine the compressive strength. An increase of the density of foamed concrete results in an increase of Fracture Energy (G_F) and maximal tensile stress (σ_t). For the notched beams of density of 488 to 1024 kg/m^3 the mean values (based on five specimens per mix) of $G_{F\mu}$(based on the load-deflection relationship) and σ_t obtained were of 1.39-12.54 N/m and 0.112-0.555MPa respectively. The $G_{F(CMOD)}$to $G_{F(u)}$ratio for all tested beams was constant and equals 0.37±0.01; The mean value of flexural tensile strength (based on ten specimens per mix) obtained for the un-notched beams of density of 488-1024 kg/m^3 was 0.163-0.585MPa.

Zhihua et.al [9] Studied on the preparation and characterization of super low density foamed concrete from Portland cement and admixtures. Foamed concrete with its super low density of between 150kg/m^3 and 300kg/m^{3}was prepared by means of chemically foaming and so called mixing and foaming process in laboratory. Conventional Portland cement was selected as the main binding material instead of rapid hardening special cement such as sulfo aluminate cement. Chemical and physical admixtures were properly introduced for the regulation of the rheological property and hardening speed of the fresh cement mixture slurry as well as the physical properties of the hardened foamed concrete. Ultrafine Ground Granulated Blast Furnace Slag Powder(UGGBFSP) with its Blaine specific surface area 800 m^2/kg, was used in experiment to regulate the rate and amount of hydration heat evolution and to control the temperature raise of the freshly placed foamed concrete in order to prevent it from uneven volume deforming or cracking. Hydrogen peroxide (H_2O_2) is selected as a chemical foaming agent to avoid the side effect such as retarded setting and delayed hardening of the cement paste caused by the introduction of some organic physical foaming agent which is believed to be one of the reasons causing the collapse or sinking of the freshly placed foamed concrete. Polycarboxylate Super plasticizer (SP) is used to reduce the w/c ratio

of the cement mixture slurry as far as possible. Alkali free Setting Accelerator (SA) synthesized in laboratory with alumina sulfate as its main constituent and with its solid content 40% was selected for regulating the setting time of the cement in order for the mixture slurry to set and harden quickly as possible immediately after foaming and placing, meanwhile to keep the mixture slurry with a good flowability before and during foaming. Besides, Polypropylene Fiber(PF) and Styrene Arylate Emulsion(SAE) and Organic Silicone waterproofing agent(OS), and Foam Stabilizer(FS) with sodium dodecyl benzene sulfonate as its main constituent were also introduced into the fresh mixture slurry of Super low density Foamed Concrete(SFC) in order to improve the volume integrity and toughness and water resistance of the hardened foamed concrete. Thus he concluded that SFC with its dry density between 150 kg/m^3 and 300kg/m^3 can be prepared with Portland cement as binding material and with the proper addition of ultrafine blast furnace slag powder and with the aid of some physical and chemical admixtures by means of the so called mixing and foaming process.

2.1. OBJECTIVES

From the literature review, it was identified that many studies have been carried out on light weight concrete considering the future possibilities. It was noted that very few studies have been conducted on Lightweight Foamed Concrete(LFC) which has a great potential in future. Based on the review conducted, it was observed that the majority of investigations were limited to evaluating the foam concrete properties, rather than focusing on characteristics of foam itself.

The objectives of the work may be summarized as:

- To determine the optimum concentration of foam in foam concrete.
- To investigate the optimum percentage of foam to be added to mortar so as to reduce density with desired strength.
- To find out the optimum replacement of cement with fly ash and sand with quarry dust to the optimized foam concrete to make it more light weight with desired strength.
- Study the performance of optimized foam concrete masonry blocks of 300mm x 200mm x 150mm.

2.2. SCOPE

- This study is limited to optimization of light weight foam concrete in laboratory without coarse aggregate.
- To find the optimum foam concentration by adding Foaming agent sodium lauryl sulphate at 2g, 5g, 8g, 10g at 100ml, 500ml, 1000ml of water respectively.
- To investigate and compare the different dosages of foam to be added to mortar (variations adopted are 0%, 5%, 10%, 15%, and 20%) to make it light weight and to use it in foamed concrete studies.
- To investigate the effect of replacement of cement with freely available fly ash and sand with quarry dust(Various percentages) to the optimized foam concrete to obtain maximum strength.
- Further optimization of foam concrete in interlocking masonry blocks.

2.3. METHODOLOGY

1. Cement sand proportion taken is 1:1,1:2,1:3
2. Finding the optimum amount sodium lauryl sulphate in water as category I.
3. Finding the optimum amount of foam percentage by weight of cement to be added

to mortar for foamed concrete which is designated as category II.

4. Finding the optimum amount of cement replacement by fly ash and sand replacement by quarry dust in LFC (category III).
5. Comparison of optimized foamed concrete blocks from category III to commercially available solid blocks available in the market.
6. Studying the performance of foam concrete masonry blocks by constructing a wall of 1m x 1m

3. MATERIALS AND METHODS

3.1 GENERAL

The common ingredients of foam concrete are cement, fine aggregate, foaming agent and water. The physical and chemical properties of each ingredient has considerable role in the desirable properties of concrete like strength and workability.

3.1.1 Portland Cement

Portland cement is the most common type of cement in general use around the world, used as a basic ingredient of concrete. Portland cement is also

used in mortars(with sand and water only) for plasters and screeds, and in grouts (cement/water mixes squeezed into gaps to consolidate foundations, road-beds, etc.). When water is mixed with Portland cement, the product sets in a few hours and hardens over a period of weeks. In principle, the strength continues to rise slowly as long as water is available for continued hydration, but concrete is usually allowed to dry out after a few weeks and this causes strength growth to stop.For any given set of materials, there is an optimum cement content beyond which little or no additional increase in strength is achieved from increasing the cement content. Ordinary Portland cement of 53 grade (Deccan cement) conforming to IS:12269 is being used in the investigation. The cement was tested for various physical properties according to relevant Indian Standards.

3.1.1.1 Specific gravity of cement

The specific gravity of cement was determined using Le Chatelier apparatus and the specific gravity test of cement as per IS specifications. Kerosene which does not react with cement is used in the test.

3.1.1.2 Standard consistency of cement

The percentage of water required to produce a cement paste of standard consistency is that particular percentage of water which allows the Vicat plunger to penetrate for a depth of 5mm to 7mm from the bottom of the Vicat mould. Standard consistency of cement is found using an apparatus called Vicat Apparatus and the test was conducted according to IS specifications.

3.1.1.3 Initial setting time of cement

Initial setting time was found by using the Vicat Apparatus and the test was conducted as per IS specifications. [11]

The results obtained in the tests on cement are tabulated in Table 3.1.

Table 3.1 Physical properties of Cement

Sl.No	Properties	Values
1	Specific Gravity	3.125
2	Standard consistency	30%
3	Initial setting time(in minutes)	65

3.1.2 Fine Aggregate

Fine aggregate is the inert or chemically inactive material, most of which pass through a 4.75mm sieve and contains not more than 5% coarser material. The fine aggregates serve the purpose of filling all the open spaces in between the coarse particles. Thus, it reduces the porosity of the final mass and considerably increases its strength. The fine aggregate to be used in this study is manufactured sand. Aggregate which is passing through 1.7mm sieve is being used as they are much fine otherwise bubbles of foam will get break up making the concrete more stiffer and denser.

3.1.2.1 Specific gravity of fine aggregate

Specific gravity of fine aggregate was determined as per the procedure described in IS specifications [12] and is tabulated in Table 3.2.

Table 3.2 Specific Gravity of Fine Aggregate

Weight of the sample (W_1 kg)	0.5
Weight of the pyconometer + water (W_2 kg)	1.534

Weight of pyconometer + water + sample (W_3 kg)	1.846
Specific gravity	2.66

3.1.2.2 Sieve analysis of fine aggregate

Sieve analysis of fine aggregate was done as per the test procedure specified in the IS code.

Fineness modulus = 3.553

According to Table 4 of IS 383:1970, the fine aggregate is from Zone II

3.1.2.3 Water absorption of fine aggregate

The water absorption of fine aggregate was determined as per the procedure laid down in the IS code [18] and is given in Table 3.3

Table 3.3 Properties of Fine Aggregate

Sl no.	Properties	values
1	Specific gravity	2.66
2	Fineness modulus	3.553
3	zone	II
4	water absorption	10.2%

3.1.3 Water

The common specifications regarding quality of mixing water is water should be fit for drinking. Such water should have inorganic solid less than 1000 ppm. This content lead to a solid quantity 0.05% of mass of cement when w/c ratio is provided 0.5 resulting small effect on strength. Water used in the study was potable water. The water used for concreting should have a pH value lying in between 6 and 8 and it should be free from organic matter.

3.1.4 Fly Ash

Fly ash, the most widely used supplementary cementations material in concrete, is a by-product of the combustion of pulverized coal in electric power generating plants. The particle sizes in fly ash vary from less than 1μm (micrometer) to more than 100μm with the typical particle size measuring under 20μm. Fly ash is primarily silicate glass containing silica, alumina, iron, and calcium. Minor constituents are magnesium, sulphur, sodium, potassium, and carbon. The relative density (specific gravity) of fly ash generally ranges between 1.9 and 2.8 and the colour is generally grey or tan.

Fly ash used in this study was low calcium (ASTM Class F) Fly ash and it is use as filler by replacing it with sand The specific gravity of Fly ash as provided by the supplier is 2.5. The major influence on the fly ash chemical composition comes from the type of coal. The physical and chemical characteristics depend on the combustion methods, coal source and particle shape.

Fig.3.1 Fly Ash

3.1.5 Quarry dust

Quarry dust, a by-product from the crushing process during quarrying activities is one of those materials being studied, especially as substitute material to sand as fine aggregates. Quarry dust have been used for different activities in the construction industry such as for road construction and manufacture of building materials such as lightweight aggregates, bricks, tiles and autoclave blocks. Researchers have also been conducted to study the effects of partial replacement of sand with quarry dust in the properties of freshly mixed and hardened concrete applications. It was deduced from those studies that partial replacement of sand with quarry dust without the inclusion of other admixtures resulted in enhanced workability in the concrete mixes. The basic tests on quarry dust were conducted as per IS-383-1987 and its specific gravity was around 1.95. Wet sieving of quarry dust through a 90 micron sieve was found to be 78% and the corresponding bulking value of quarry dust was 34.13. Quarry dust has been used for different activities in the construction industry such as road construction and manufacture of building materials. As the properties are good as sand, the quarry dust is used as fine aggregate in replacement with sand in cement concrete. The advantages of quarry dust are cost effective, easily available, consumption reduces the pollution in environment and effectively used as a replacement material for river sand. Further, Hundreds of stone crushing plants in our country generate several thousand tons of quarry dust every day. This quarry dust is considered to be solid waste material. If it is possible to use this in making mortar/concrete by replacement of river sand, then it will solve the problem of its disposal. Moreover, the utilization of quarry dust, which can be called as manufactured sand after removal of micro fines below 150 micron size by sieving, has been accepted in the industrially advanced countries of the West as the river sand, which is one of the constituents used in preparation of cement mortar/concrete, has become highly expensive and scarce. Usage of quarry dust as partial replacement to river sand/natural sand further modified by partial replacement of pozzolanic materials like fly ash is receiving more attention these days as their use generally improves the properties of cement/concrete.

Fig 3.2 Quarry Dust

3.1.6 Sodium Lauryl Sulphate

Sodium lauryl sulphate (SLS) is a synthetic detergent (cleaning agent) and surfactant (which means it makes bubbles). It has a high pH as it is an alkali substance and has the appearance of a white powder. Sodium lauryl sulphate is sometimes referred to as the coconut surfactant because it can be manufactured from coconut oil. Being derived from inexpensive coconut and palm oils, Sodium coco-sulphate is essentially the same compound, but made from less purified coconut oil. Sodium lauryl sulphate (SLS) is a cheap, very effective cleansing and foaming agent (foams quickly). It is probably the most commonly used anionic surfactant in the personal-care business. It's an ingredient in a wide range of personal care products such as soap, shampoo and conditioners, bubble bath, moisturisers, cleansers, facial scrubs and shaving cream and toothpaste but in lower concentrations. Sodium lauryl sulphate is used to remove oily stains because it has a thickening effect that helps form lather. It is used in dishwashing liquids and laundry detergent. It's also used, in much higher concentrations, in industrial products such as car wash soap, engine degreasers, and floor (carpet) cleaners. SLS is an excellent foaming agent, and this is one of the reasons it's included in many personal care products, such as toothpaste. Sodium lauryl sulphate gives thick, rich foam . Properties of SLS is tabulated in Table 3.4.

Fig. 3.3 Sodium lauryl sulphate

Table 3.4: Properties of Sodium Lauryl Sulphate

Formula	$NaC_{12}H_{25}SO_4$
Molar mass	288.372 g/mol
IUPAC ID	Sodium lauryl sulphate
Melting point:	206 °C

3.2. PROPORTIONING AND PREPARATION OF FOAM CONCRETE

Often trial and error process is adopted to achieve foam concrete with desired properties Even though the strength of foam concrete depends on its density, for a given density, the strength can be increased by changing the constituent materials. Also, for a given density, the foam volume requirement depends on the constituent materials Hence for a given strength and density requirement, the mix design strategy should be able to determine the batch quantities. There are mainly two foaming techniques adopted (a)Pre-foaming (b)Mix foaming technique.

Pre-formed foaming is preferred to mix-forming technique due to the following advantages:

(i)   lower foaming agent requirement.

(ii)   A close relationship between amount of foaming agent used and air content of mix.

Most common types of mixers (tilt drum or pan mixer used for concrete or mortar) are suitable for foam concrete. The type of mixer and batching and mixing sequences of foam concrete depends upon pre-formed foam method or mix-foaming method.

4. EXPERIMENTAL PROGRAMME

The experimental investigation starts with the preparation of control mix of cement sand proportion of 1:1, 1:2, 1:3.

The first stage dealt with optimizing cement sand ratio of 1:1.The optimum amount of sodium lauryl sulphate in water is determined by adding 2g, 5g, 8g and 10g of foaming agent in 100ml, 500ml and 1000ml of water respectively. The mix was optimized with the compressive strength of foamed concrete in varying foam concentration.

Further optimum percentage of foam by weight to be added to the mix is determined. Foamed concrete mixes were prepared with 5%, 10%, 15%, 20% of foam by weight of cement. The control mix was optimized with the compressive strength of foamed concrete in different percentages of foam.

The third stage dealt with the replacement of cement with fly ash as its specific gravity is less than that of cement and sand filler with quarry dust is carried out which can bring down the self weight and to achieve the targeted compressive strength. Different percentages of replacement with flyash and quarry dust is carried out at the ratios 10-0, 20-0, 30-0, 40-0, 50-0 and 30-0, 30-10, 30-30, 30-40, 30-60, 30-80, 30-100 respectively.

The fourth stage dealt with the study of performance of foam concrete interlocking masonry blocks by constructing a wall of 1m X 1m.

4.1 TEST TO BE CONDUCTED ON CONCRETE

4.1.1 Fresh Concrete

 Concrete workability is the relative ease with which a fresh mix can be handled, placed, compacted, and finished without segregation or separation of the individual ingredients. Good workability is required to produce concrete that is both economical and high in quality. Fresh concrete has good workability if it can be formed, compacted, and finished to its final shape and texture with minimal effort and without segregation of the ingredients.

4.1.1.1 Spread test of mortar

The spread test gives the quick assessment of the fluidity of high-slump concrete mixes. Equipment for the spread test comprises of a suitable base, a standard slump cone, metal scoop and a metric rule.

The base should be clean, flat, smooth-surfaced, and rigid and non-absorbent with a lateral dimension of not less than 600mm. It should be level and free from vibration during the test. Here a levelled glass plate is used as a base surface. Standard slump apparatus, a mini slump cone mould was used. The steps involved in spread tests are:

Place the moistened cone, narrow end downwards, on the centre of the base plate.

a) Remix the concrete sample thoroughly and then fill the slump cone taking care to avoid segregation.

b) Subject the cone to a quick vertical lift. Hold the upper end of the cone until the flow of concrete ceases.

c) Remove the slump cone and measure the spread of the concrete orthogonally.

d) Average of two measurements is reported as the spread of the mix.

Fig 4.1 spread test on mortar   Fig 4.2 slump cone

4.1.2 Hardened Concrete

The following moulds were used to cast the concrete specimens for various studies as per IS : 516-1959.

1)   70.8mm x 70.8mm x 70.8mm moulds were used to cast mortar cubes to determine the compressive strength of concrete.

2)   300mm x 200 mm x 150mm moulds were used to cast concrete blocks to determine the compressive strength of concrete.

Fig 4.3. 70.7mm x 70.7mm x 70.7mm cubes

Fig 4.4. 300mm x 200 mm x 150mm blocks

The specimens in the mould were covered and kept at room temperature for 24 hours. These were then kept submerged in water for curing.

For determining the hardened properties the test specimens were removed from the water bath and the surface was removed using a dry cloth, immediately before testing. Testing of hardened concrete plays an important role in controlling and conforming the quality of cement concrete works. The main purpose of testing hardened concrete is to conform that the concrete used has developed the required strength.

4.1.2.1 Compressive strength

Out of many test applied to the concrete, this is the most important test, which gives an idea about all the characteristics of concrete. By this single test one judge that whether concreting has been done properly or not. The test is conducting according to IS 516:1959.

Compressive strength of concrete depends on many factors such as water-cement ratio, cement strength, quality of concrete material, and quality control during production of concrete etc.

Clean the bearing surface of the testing machine. Place the specimen in the machine in such a manner that the load shall be applied to the opposite sides of the cube cast. Align the specimen centrally on the base plate of the machine. Rotate the movable portion gently by hand so that it touches the top surface of the specimen. Apply the load gradually without shock and continuously at the specified rate till the specimen fails. Record the maximum load as denoted by equation 4.1 and note any unusual features in the type of failure.

$$Compressive\ strength = \frac{Load\ applied\ in\ Newtons}{Cross\ sectional\ area\ in\ mm^2} (4.1)$$

4.1.2.2 Density of the mix

After preparing the mix, wet densities and dry densities of each mix containing different proportions of foam volume was found out and compared .The wet density is found out by weighing each mould filled with the mortar mix and dividing the value by the volume of mould. The cube specimens shall be dried to constant mass and then cured for 3 days, 7 days and 28 days. The overall volume is computed in cubic meters. The blocks shall then be weighted in kilograms to the nearest 10gm.Thus dry densities is found out by using equation 4.2 weighing the dried cube specimens and the same is repeated at 3, 7 and 28 days of curing of mortar cubes.

$$Density = \frac{Weight}{Volume} \quad (4.2)$$

5. RESULTS AND DISCUSSIONS

5.1 MECHANICAL PROPERTIES OF FOAMED CONCRETE

5.1.1 Spread Test on Foamed Concrete

After raising the slump cone, the spread flow of the mortar is measured using tape. Average of the measurement is taken in 2 opposite directions. Mix which is both stiffer and heavily flowing one is avoided. Mix with average flow of 100mm is obtained as optimum without any stiffness and segregation.

5.1.2 Density of the control mix

The wet and dry densities of the specimens with trial mixes 1:1, 1:2, 1:3 calculated at 3, 7 and 28 days and are tabulated in Table 5.2.

Table 5.1: Wet and Dry Densities of control mixes with 1:1, 1:2, 1:3 mix

Control mix ratio	Wet density(kg/m^3)	Dry Density (kg/m^3)		
		3days	7days	28days
1:1	1897	1891	1886	1882
1:2	1830	1824	1817	1812
1:3	1792	1796	1791	1782
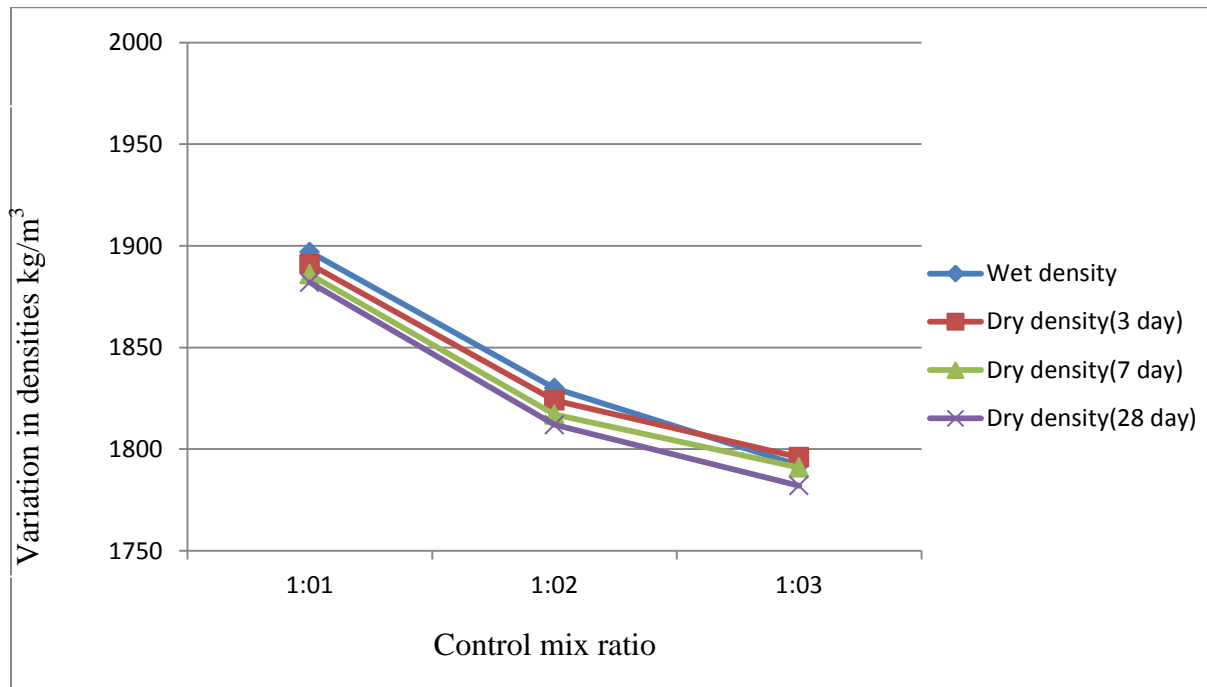
Fig 5.1 Wet densities and dry density of control mixes

5.1.2 Compressive strength of the control mix

The compressive strength of the specimens with trial mixes 1:1, 1:2, 1:3 calculated at 3, 7 and 28 days and are tabulated in Table 5.3

Table 5.2 : Comparison in Compressive strength of control mixes with 1:1, 1:2, 1:3 mix

Control mix ratio	Compressive Strength (N/mm^2)		
	3 days	7 days	28 days
1:1	22.5	32.5	57
1:2	21.15	27.6	44.12
1:3	19.84	25.84	41.15
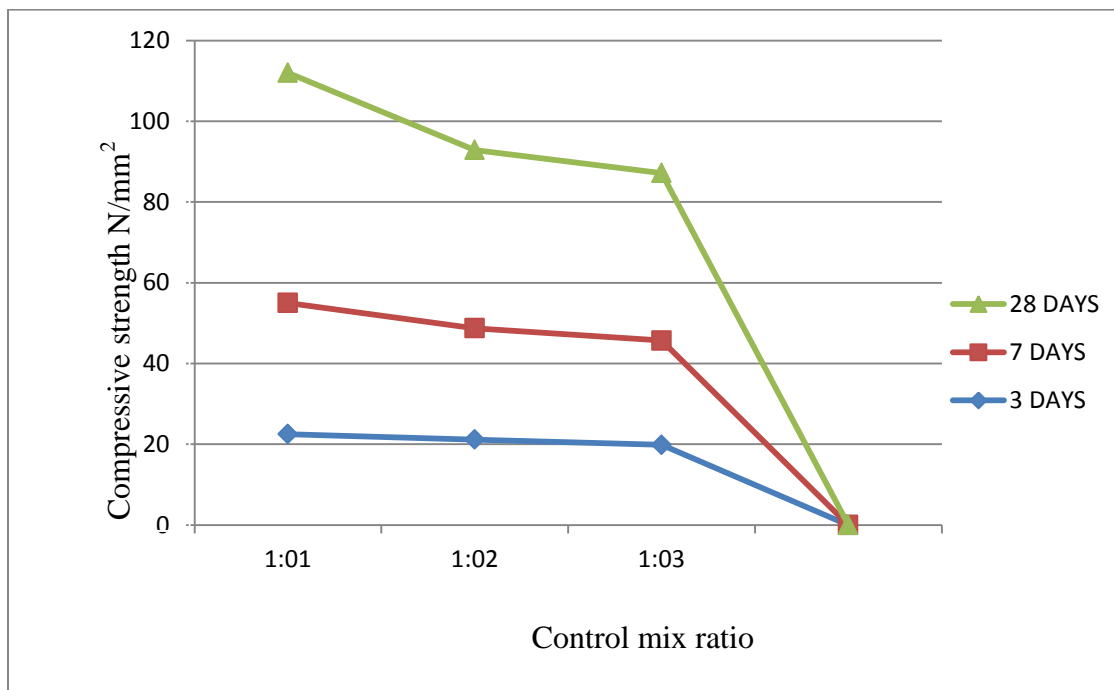
Fig 5.2 Compressive strength of control mixes

From the above observations the compressive strength showed a higher value when the mix proportion is taken as 1:1. i.e. 1 part of cement and 1 part of sand. Fixing the control mix of 1:1 the further experiments with foam concrete is carried out.

5.2 OPTIMIZATION OF CONCENTRATION OF FOAM

The concentration of foam is optimized by adding 2g, 5g, 8g, 10g of foaming agent(Sodium lauryl sulphate) in 100ml, 500ml ,1000ml of water. Corresponding values are found out.

5.2.1 Density of foam concentrations

The wet and dry densities of foamed concrete with different percentages of foam are calculated at 3, 7 and 28 days and are tabulated in Table 5.4 to 5.7

Table 5.3: Wet and Dry Densities of Foamed Concrete with 2g sodium lauryl sulphate concentration

Water (ml)	Wet density(kg/m^3)	Dry Density (kg/m^3)		
		3days	7days	28days
100	1708	1701	1695	1688
500	1730	1724	1717	1712
1000	1742	1736	1731	1722

Table 5.4: Wet and Dry Densities of Foamed Concrete with 5g sodium lauryl sulphate concentration

Water (ml)	Wet density(kg/m^3)	Dry Density (kg/m^3)		
		3days	7days	28days
100	1669	1652	1657	1658
500	1680	1677	1667	1662

1000	1691	1686	1681	1678

Table 55: Wet and Dry Densities of Foamed Concrete with 8g sodium lauryl sulphate concentration

Water (ml)	Wet density(kg/m^3)	Dry Density (kg/m^3)		
		3days	7days	28days
100	1625	1619	1616	1611
500	1638	1631	1626	1621
1000	1658	1651	1643	1639

Table 5.6: Wet and Dry Densities of Foamed Concrete with 10g sodium lauryl sulphate concentration

Water (ml)	Wet density(kg/m^3)	Dry Density (kg/m^3)		
		3days	7days	28days
100	1586	1581	1578	1574
500	1594	1589	1585	1579
1000	1612	1609	1605	1602

From the observations of Tables 5.4 to 5.7, it can be noticed that, with the different concentrations of foam, there is reduction in density compared to conventional concrete. As the foam concentration goes on increasing the weight of foam concrete also get decreased which makes it more lightweight.

5.2.2 Compressive strength of concentration of foam

The specimens with varying dosages of foam concentration were tested for compressive strength at the 3rd, 7th and 28th day of curing and the results are tabulated in Table 5.8 to 5.11

Compressive strength is calculated for 2g sodium lauryl sulphate in 100ml, 500ml, 1000ml respectively and corresponding values are tabulated.

Table 5.8 Compressive strengths with 2g sodium lauryl sulphate

Water (ml)	Compressive Strength (N/mm^2)		
	3 days	7 days	28 days
100	7.1	10.09	14.96
500	7.9	11.05	15.31
1000	8.52	12.24	16.18
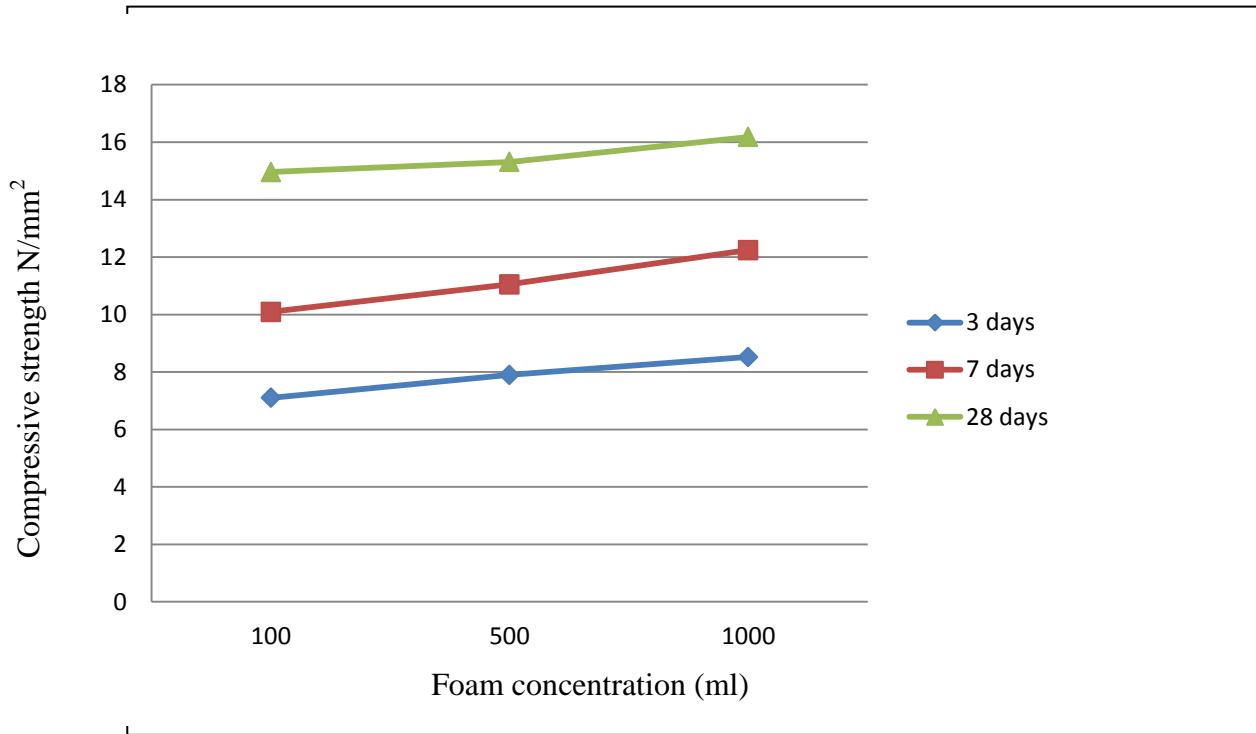
Fig 5.3 Compressive strengths with 2g sodium lauryl sulphate

Compressive strength is calculated for 5g sodium lauryl sulphate in 100ml, 500ml, 1000ml respectively and corresponding values are tabulated.

Table 5.9 Compressive strengths of 5g sodium lauryl sulphate

Water (ml)	Compressive Strength (N/mm^2)		
	3 days	7 days	28 days
100	6.1	9.5	13.85
500	6.8	10.75	14.75
1000	7.25	11.50	15.6
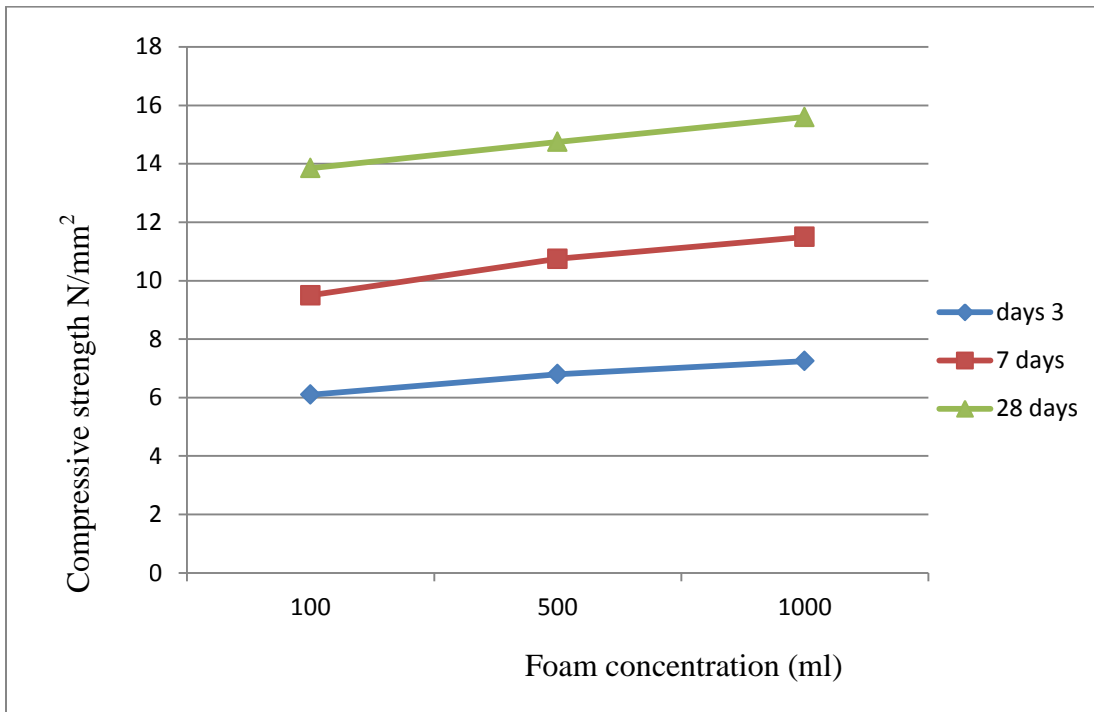
Fig 5.4. Compressive strengths with 5g sodium lauryl sulphate

Compressive strength is calculated for 8g sodium lauryl sulphate in 100ml, 500ml, 1000ml respectively and corresponding values are tabulated.

Table 5.10 Compressive strengths of 8g sodium lauryl sulphate

Water (ml)	Compressive Strength (N/mm^2)		
	3 days	7 days	28 days
100	5.8	8.09	11.80
500	6.2	9. 5	12.25
1000	6.5	10.5	14
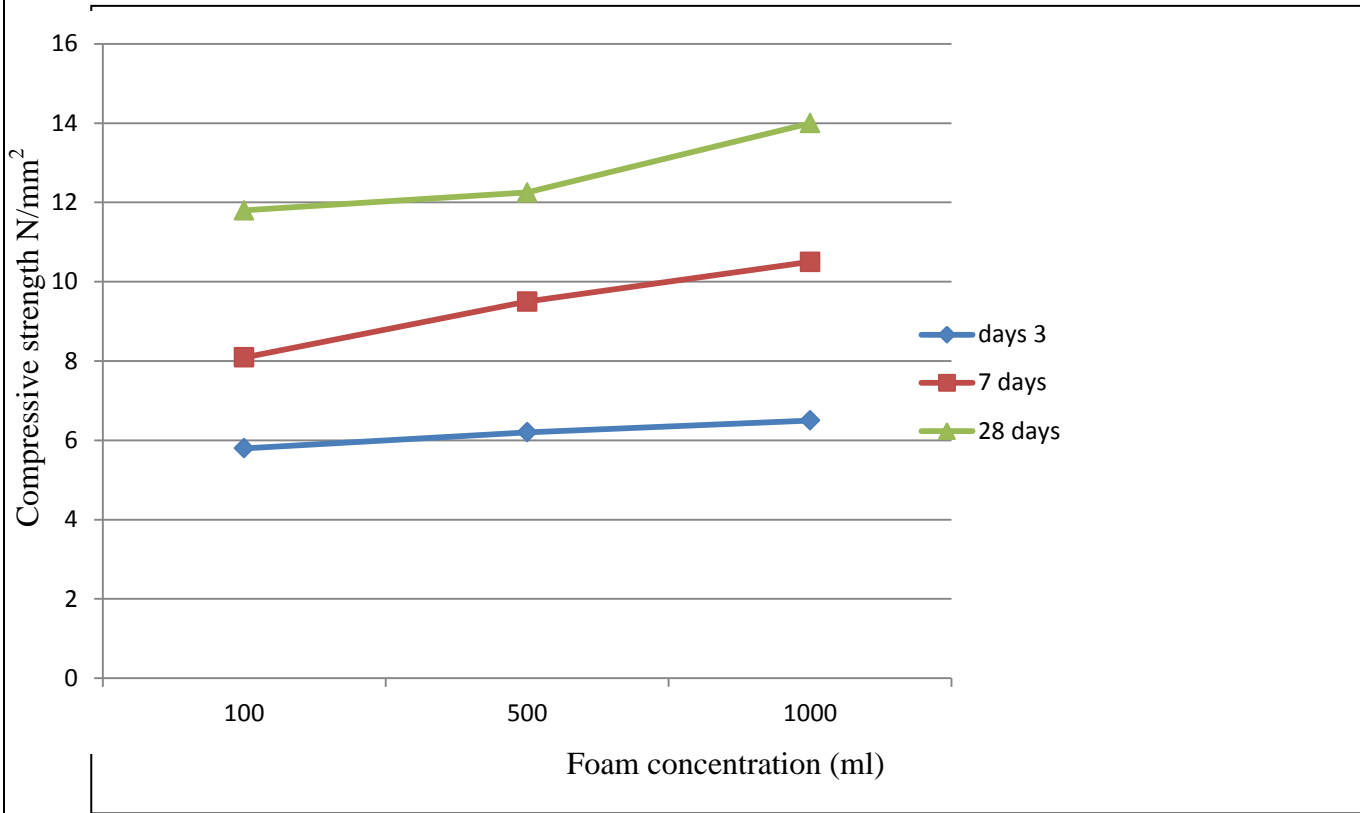
Fig 5.5 Compressive strengths with 8g sodium lauryl sulphate

Compressive strength is calculated for 10g sodium lauryl sulphate in 100ml, 500ml, 1000ml respectively and corresponding values are tabulated.

Table 5.11 Compressive strengths of 10g sodium lauryl sulphate

Water (ml)	Compressive Strength (N/mm^2)		
	3 days	7 days	28 days
100	3.40	5.8	9.5
500	4.5	7.25	10.36
1000	5.5	9.30	12.5
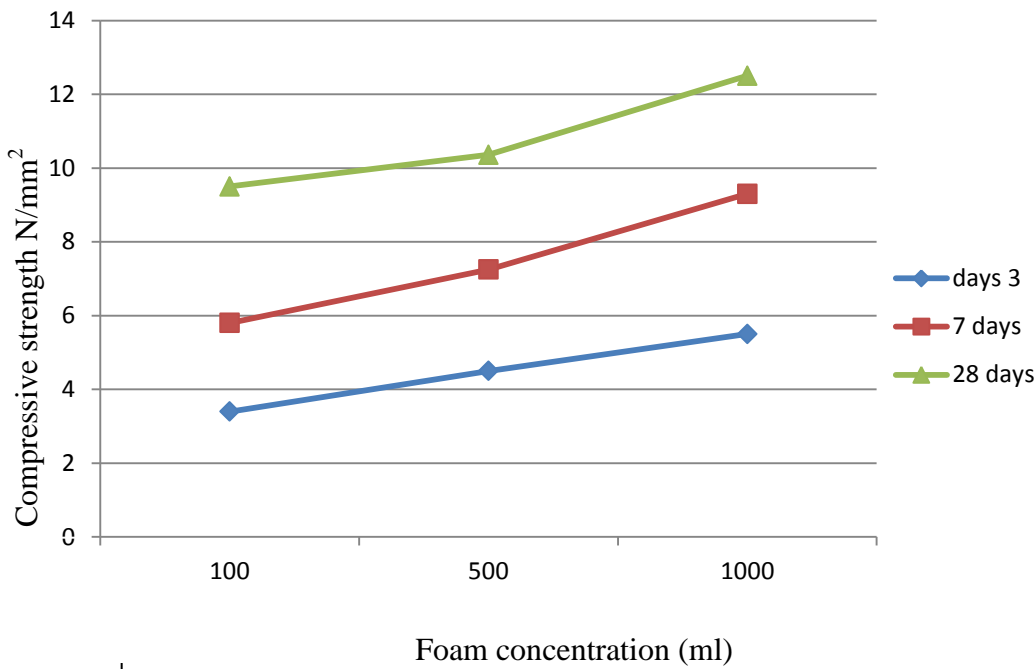
Fig 5.6 Compressive strengths with 10g sodium lauryl sulphate

From the observations of Table 5.8 to 5.11, it can be noticed that, the foam concentration of 5g shows the higher compressive strength, with desired density compared to other concentration, and it is noticed that the strength decreases when it comes to higher concentration of foaming agent. Optimizing the foam concentration of 5g in 100ml of water the Percentage Variation of Foam is calculated.

5.3 OPTIMIZATION OF FOAM VOLUME IN CONCRETE

The amount of foam that should be added to concrete is optimized by making 3 specimens each with 5%, 15%, 20%, 25% foam volume. The results are valued and tabulated.

5.3.1 Density of foam volume

The wet and dry densities of foamed concrete with different percentages of foam are calculated at 3, 7 and 28 days. Wet and dry densities of specimens at 3, 7 and 28 days are tabulated in Table 5.12.

Table 5.12: Wet and Dry Densities of Foamed Concrete with Percentage Variation of Foam

Foam % by weight of cement	Wet density(kg/m^3)	Dry Density (kg/m^3)		
		3days	7days	28days
0%	1897	1891	1886	1882
5%	1669	1652	1657	1658
10%	1582	1578	1573	1564
15%	1549	1544	1537	1532
20%	1512	1508	1502	1497

From the observations of Table 5.12, it can be noticed that, with the addition of foam by weight, there is reduction in density compared to conventional concrete. As the percentage of foam goes on increasing the weight of foam concrete also get decreased which makes it more lightweight.

5.3.2 Compressive strength of foam volume

The specimens with varying dosages of foam with were tested for compressive strength at the 3rd, 7th and 28th day of curing and the results are tabulated in Table 5.13

Table 5.13. Comparison of compressive strength with various percentages of foam

foam (% by wt of cement)	Compressive Strength (N/mm^2)		
	3 days	7 days	28 days
0%	22.5	32.5	57
5%	6.7	12.5	15.5
10%	5.4	7.6	12.57
15%	3.10	8.4	9.06
20%	2.9	3.8	6.5
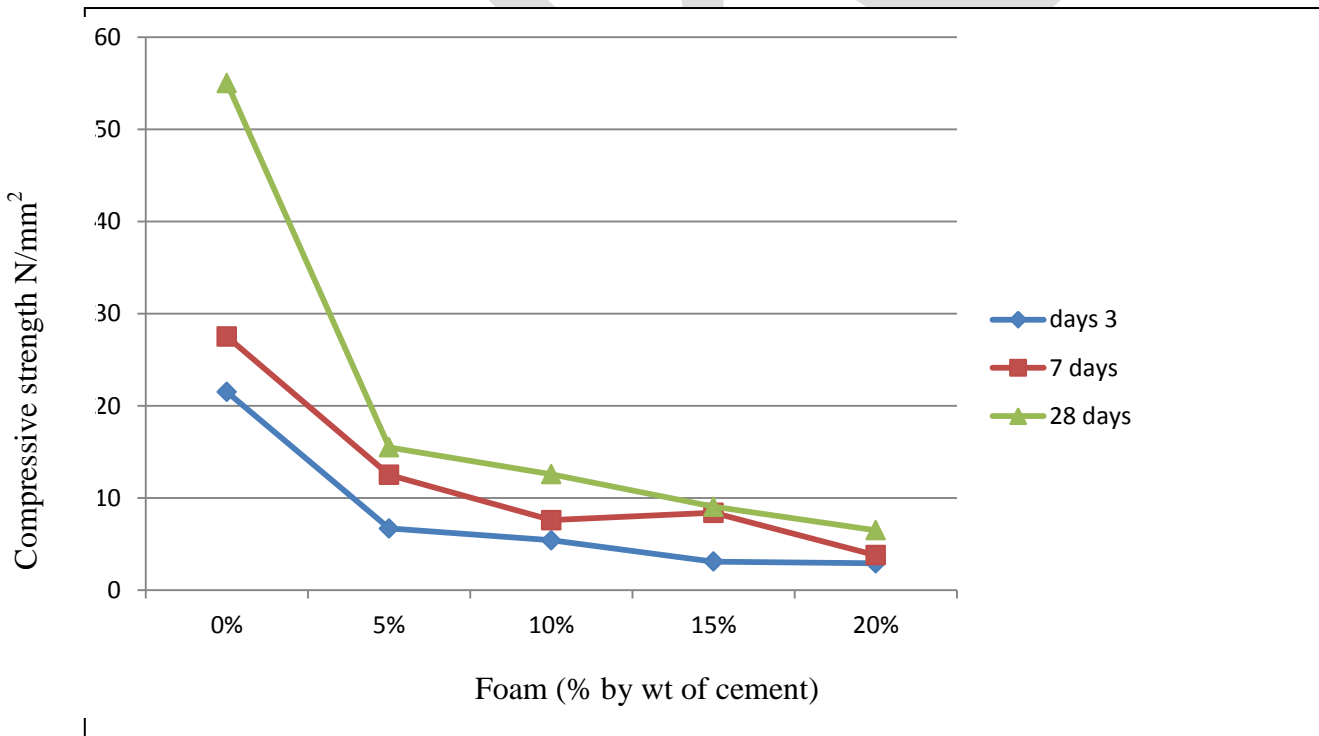
Fig 5.7 Compressive strength with various percentages of foam

From the observations of Table 5.13, it can be noticed that, with the addition of foam by weight, the foamed concrete specimens shows significant reduction in compressive strength. Thus reduction increases with increasing percentage of foam and the compressive strength is very low when the percentage of foam reaches about 20% by weight of cement. Thus, the optimum percentage of foam by weight of cement is fixed as 5%.

5.4 REPLACEMENT OF CEMENT BY FLYASH

5.4.1 Density of replacement of cement by flyash

The wet and dry densities of foamed concrete with replacement of cement by flyash is calculated at 10-0,20-0,30-0,40-0,50-0. Wet and dry densities

of specimens at 3, 7 and 28 days are tabulated in Table 5.14

Table 5.14. Wet and Dry Densities of Foamed Concrete Variation in percentages of Cement by Flyash

Replacement (%)	Wet density(kg/m^3)	Dry Density (kg/m^3)		
		3days	7days	28days
10-0	1649	1642	1637	1634
20-0	1632	1628	1623	1620
30-0	1624	1619	1614	1597
40-0	1595	1591	1586	1583
50-0	1583	1579	1576	1572

Fig 5.9 Wet and Dry Densities of Foamed Concrete Variation in percentages of Cement by Flyash

5.4.2 Compressive strength of replacement of cement by flyash

Compressive strength of foamed concrete with replacement of cement by flyash is calculated at 10%-0, 20%-0,30%-0,40%-0,50%-0 at 3rd, 7th and

28th day of curing and the results are tabulated in Table 5.15

Table 5.15. Comparison of compressive strength of Variation in percentages of Cement by Flyash

Replacement (%)	Compressive Strength (N/mm^2)		
	3 days	7 days	28 days
10-0	8.2	9.5	15.5
20-0	7.5	8.8	18.2
30-0	6.8	8.1	23.8
40-0	5.6	7.5	23.5
50-0	5.1	6.2	22.5
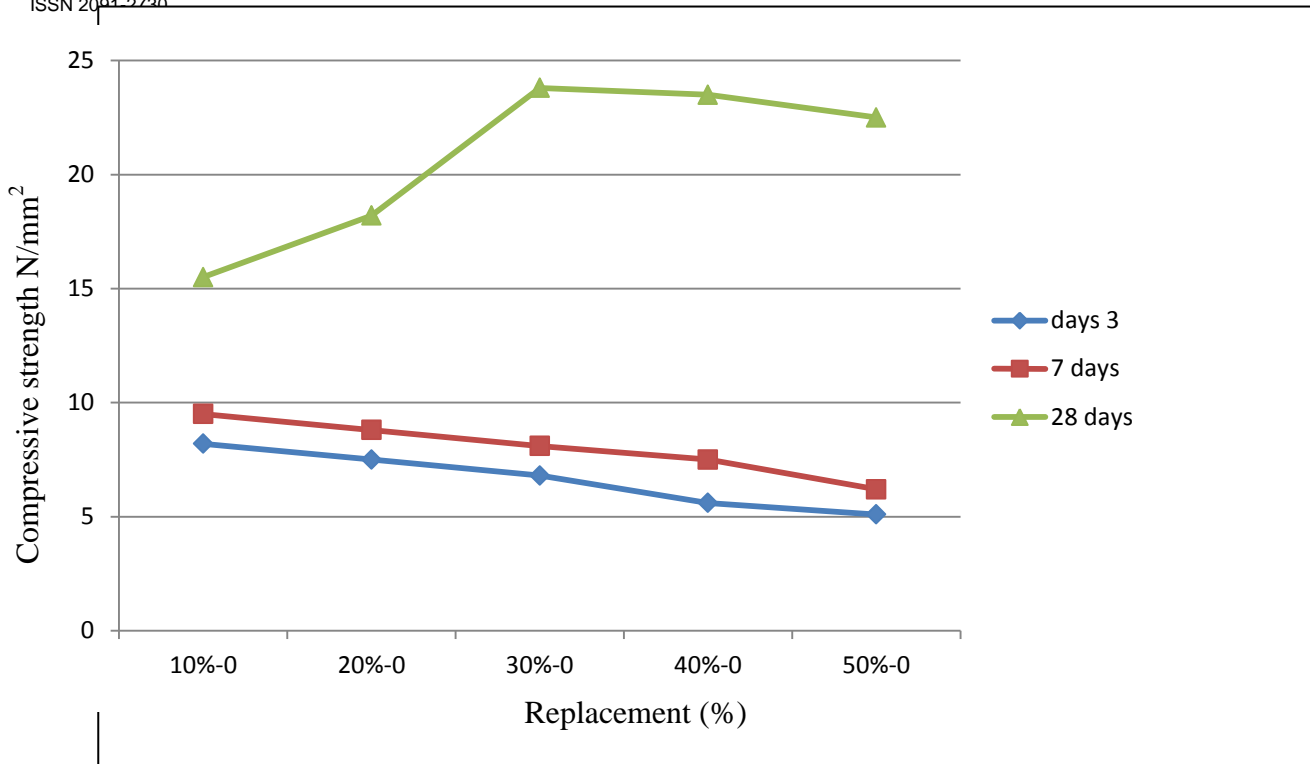
Fig 5.8 Compressive strength of Variation in percentages of Cement by Flyash

From the observations of Table 5.15, it can be noticed that, As the level of flyash replacement increases the early-age strength decreases. However, long-term strength development is improved when fly ash is used. The percentage replacement is found optimum when 30% cement is replaced by flyash. The compressive strength shows a decrease in value when the replacement percentage increases

5.5 REPLACEMENT OF CEMENT BY 30% FLYASH AND PERCENTAGE VARIATION IN SAND BY QUARRY DUST

5.5.1 Density of replacement of cement by 30% flyash and percentage variation in sand by quarry dust

The wet and dry densities of foamed concrete with replacement of cement by flyash and sand by quarry dust are calculated .Wet and dry densities of specimens at 3, 7 and 28 days are tabulated in Table 5.16

Table 5.16. Wet and Dry Densities of Foamed Concrete Replacement in Cement by 30% Flyash and Variation in percentages of Sand by Quarry dust

Replacement (%)	Wet density(kg/m^3)	Dry Density (kg/m^3)		
		3days	7days	28days
30-0	1628	1622	1620	1618
30-20	1620	1616	1613	1610
30-30	1613	1608	1594	1591
30-40	1589	1584	1582	1589
30-60	1581	1578	1572	1578
30-80	1574	1571	1579	1576
30-100	1568	1566	1563	1561

5.5.2 Compressive strength replacement of cement by 30% flyash and percentage variation in sand by quarry dust

Compressive strength of foamed concrete with replacement of cement by 30% flyash and sand by quarry dust are calculated at 30-0, 30-20, 30-30, 30-40, 30-60, 30-80, 30-100 at 3rd, 7th and 28th day of curing and the results are tabulated in Table 5.17

Table 5.17. Comparison of Compressive strength of Foamed Concrete Replacement in Cement by 30% Flyash and Variation in percentages of Sand by Quarry dust

Replacement (%)	Compressive Strength (N/mm^2)		
	3 days	7 days	28 days
30-0	7.6	9.2	18.3
30-20	8.33	10.16	21.4
30-30	6.6	8.3	23.5
30-40	8.4	10.5	22.25
30-60	8.2	9.53	21.8
30-80	7.83	8.62	20.5
30-100	6.60	9.5	19.6
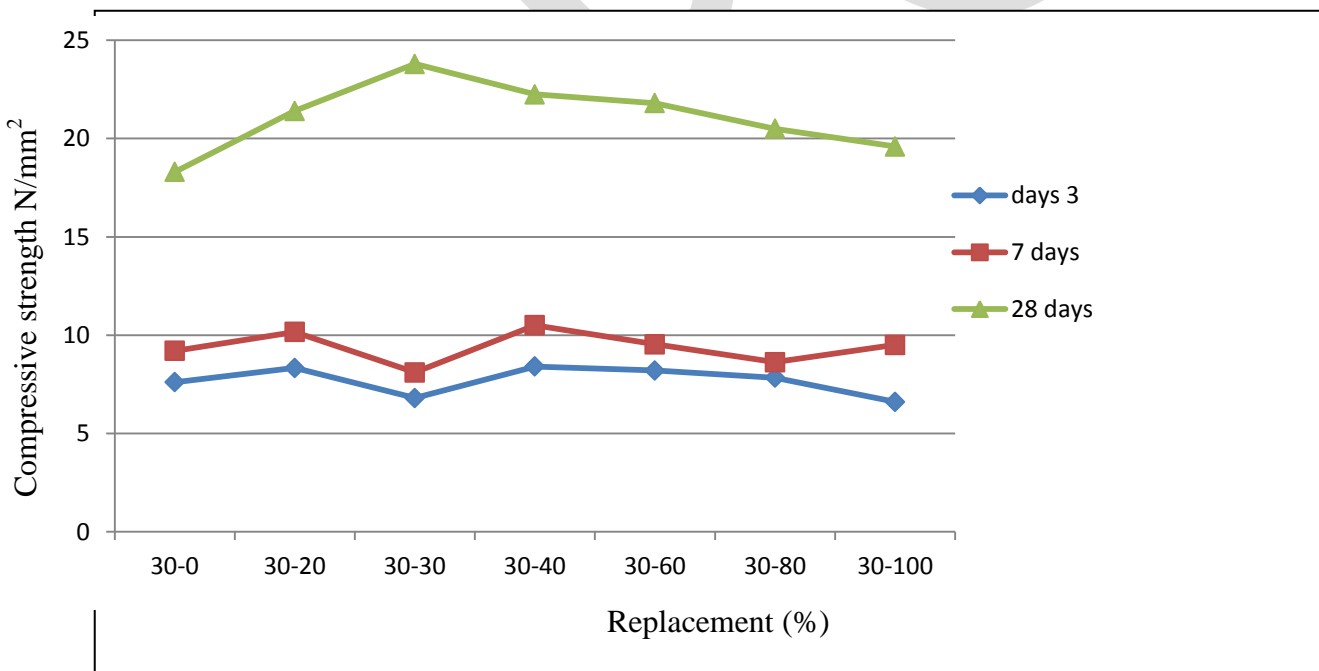
Fig 5.9. Compressive strength of Foamed Concrete Replacement in Cement by 30% Flyash and Variation in percentages of Sand by Quarry dust

From the observations of Table 5.17., it can be noticed that, the Replacement of the sand with quarry dust shows an improvement in compressive strength of the concrete in the presence of fly ash. Quarry dust can be a suitable partial replacement material to sand to produce concretes with fair ranges of compressive strength. It shows an increase in compressive strength up to 30% replacement. As the level of replacement increases the compressive strength decreases.

5.6 OPTIMIZATION OF FOAM CONCRETE INTERLOCKING MASONARY BLOCKS

5.6.1 Density of foam concrete interlocking masonry blocks

Foam concrete masonry block of 300mm*200mm*150mm is made and Wet, Dry densities of the specimens at 3, 7 and 28 days are tabulated in Table 5.18

Table 5.18.Wet and dry density of foam concrete interlocking masonry blocks

Foam Volume	Replacement Ratio(Flyash-Quarry dust)	Wet Density(kg/m^3)	Dry Density (kg/m^3)		
			3days	7days	28days
5%	30-30	1688	1684	1679	1675

5.6.2 Compressive strength of foam concrete interlocking masonry blocks

The compressive strength of foam concrete masonry block with dimension 300mm*20mm*15mm are calculated at 3rd,7th and 28th day of curing and tabulated in table 5.19

Table 5.19 Compressive strength of foam concrete interlocking masonry blocks

Replacement (%)	Compressive Strength (N/mm^2)		
	3 days	7 days	28 days
30-30	1.98	2.96	10.82

Thus, foam concrete interlocking masonry blocks with optimized quantities showed a desirable 28 day strength as per the codal specifications.

CONCLUSIONS

From the study of foamed lightweight concrete it is found fly ash and quarry dust which is a waste products have sufficient potential as the replacement of cement and sand for making much lesser denser and stronger bricks. Following are the conclusions derived from the experimental results:

- Foam concentration as optimized at 5g of sodium lauryl Suphate when added to 100ml of water.

- Strength was maximum attained when 5% of foam by weight of cement were added to the concrete.
- Fly ash which is a waste product from coal industry replaces cement which makes the foamed concrete much less denser and stronger 30% replacement showed better strength.
- The use fly ash which is freely and readily available can make foamed concrete cost effective.
- Replacement of quarry dust which is again a waste product , makes the concrete less denser and enhances the strength.. It showed the maximum strength when 30% of sand is replaced by quarry dust.
- Foamed light weight blocks can be used for wall panels, insulating panels over the wall to make it more thermal insulating.
- Fly ash and quarry dust used enables the large utilization of waste product which brings down the exploitation of natural resources; reduce the emission of green house gases.

REFERENCES:

[1]   Y.H. Mugahed Amran, Nima Farzadnia, A.A. Abang Ali "*Properties and Applications of Foamed Concrete" a review* a Journal of Construction and Building Materials ELSEVIER, Vol. 101, pp. 990-1005, 2015.

[2]   Yuanyuan Zhang, Yin Chi and Lihua X "*Study on the Preparation and Properties of High-porosity Foamed Concretes Based on Ordinary Portland Cement"* journal of material design ELSEVIER Vol.100, 2015.

[3]   Ameer A. Hilal, Nicholas Howard Thoma, Andrew Robert Dawson*, "Void Structure and Strength of Foamed Concrete Made without/with Additives"* Construction and Building Materials Vol.85, pp. 157–164, 2015.

[4]   Zhaoming Huang, Tongsheng Zhang, Ziyun Wen "*Proportioning and Characterization of Portland Cement-based Ultra-lightweight Foam Concretes"* Construction and Building Materials Vol.79, pp. 390–396, 2015.

[5]   DR.A.S.Kanagalakshmi, K.Sasikumar, E.Britto Pravin "*An Investigation on Foam Concrete With Quarry Dust Replacement For Filler In Mix Design"* Journal of Emerging Technology in Computer Science and Electronics Vol.13, pp.0976-1353, 2015.

[6]   Ma Cong, Chen Bing "*Properties of a foamed Concrete With Soil As a Filler"* Construction and Building Materials Vol.76, .pp.61-69, 2015.

[7]   Pan Zhihua, Li Hengzhi, Liu Weiqing "*Preparation and Characterization of Super Low Density Foamed Concrete from Portland Cement and Admixtures*" Construction and Building Materials Vol. 72, pp.256–261,2014.

[8]   Norlia Mohamad Ibrahim, Shamshinar Salehuddin, Roshazita Che Amat, Nur Liza Rahim and Tengku Nuraiti TengkuIzhar "*Performance of Lightweight Foamed Concrete with Waste Clay Brick as Coarse Aggregate*" Journal of APCBEE Procedia 5, pp. 497 – 50,.2013.

[9]   G.Indu Siva Ranjani b, K.Ramamurthy "*Behaviour of Foam Concrete under Sulphate Environments*" Journal of Cement & Concrete Composites,vol.34, pp. 825–834, 2012.

[10]   Prakash T.M, Naresh kumar B.G, Karisiddappa, Raghunath S " *Properties of Aerated(foamed) Concrete Blocks"* Journal of scientific and research Vol.4, pp.2229-5518, 2013.

[11]   J.Sathya Narayan, K.Ramamurthy " *identification as set-accelerator for Enhancing the productivity of Foam Concrete Block Manufacture"*Construction and Building Materials Vol.37, pp.144-152, 2012.

[12]   K.Ramamurthy, E.K. Kunhanandan Nambiar, G.Indu Siva Ranjani " *A Classification of Studies on Properties of Foam Concrete"* Cement and Concrete Composites Vol.31, pp.388-396, 2009.

Design & Implementation of Cost Effective Automatic Transfer Switch

Adeel Arshad[1], Mian Rizwan[2], Adil Maqsood[1]

1. Department of Electrical Engineering, University Of Gujrat, Pakistan
2. Lab Engineer, Department of Electrical Engineering, University Of Gujrat, Pakistan
* **Corresponding Author:** E-mail: adeelarshad048@gmail.com ,rizwan.nazeer26@uog.edu.pk

Abstract— In many developing countries, electric power generated by utility supply authority is inadequate to meet the demands of their customers. This Power variability has necessitated the need for alternative source of power supply i.e. Generator to back up the utility power supply. Changing between the main supply line and the alternative supply poses yet another problem. Various attempts have been made to advance automatic power changeover switch but there are some limitations with them. Our proposed scheme presents the design and construction of microcontroller based automatic transfer switch and a better and cost effective approach that makes use of digital integrated circuits and microcontroller which reduces the number of components as well as increase the speed of the system. The ATS also contains an alarm system for indicating generator failure or fuel outage.

Keywords— ATS; Backup Generator; Power Supply; Cost Effective; Microcontroller; Home Automation;

1. INTRODUCTION

Today, electric power plays very important role in lifeline of any country and its continuous availability at minimum cost certifies the country's growth. That marks it very important factor in developing the economy and the standard of living of a country. [5] [11][12] The role of electric power in everyday requirement of individuals and nations cannot be exaggerated, specifically in this era of the proliferation of consumer electronics and electrical appliances for both home and industrial use. The need is quite evidently on an ever increasing demand. The global economy hang on largely on constant supply of electric power for growth, so countries with deprived supply of electricity may not advance in this 21st century. While the period of inconsistency of supply electricity is long forgotten in many technologically advanced nations of the world, many developing countries still writhe holdups arising from persistent power disasters. The provision of alternative power source i.e. generator has no doubt brought assistance but not without an assistant challenge linked with manual operation of the changeover. [1][6] Therefore, poor state of power supply in developing countries, demands for alternatives sources of power generation and automation of electrical power generation to back up the electric utility supply. Over time, automation of electrical power supply has become vital as the rate of power outage is predominantly high. As a result of this power outage, developing countries experience slow development processes in both the public and private sectors of their economy. Investors from foreign places don't feel secure to come and set up business in the face of the large market made accessible in such populated countries, because of common power failures practiced. [2][7][8][9][10]

Therefore, it is for these reasons that transfer switches were developed. Initially, these switches were designed for manual operations, but with an increase in the technological advancement of electrical power control, Automatic transfer switches (ATS) were created. It eliminates the element of user contact in starting a generator and changing power supply from one source to another. Some of the approaches which have been engaged to implement change over system include manual change over switch box, automatic change over system with electromechanical relays and change over system with automatic transfer switch. Each of these methods have some drawbacks that make it undesirable. These contribute to the high cost of these methods. [4]

The proposed approach makes use of digital integrated circuits and microcontroller which reduce the component count as well as improve the speed of the system. The ATS is connected to both power supply sources and supplies the load with power from only one of the sources at any particular instant in time.

2. DESIGN METHODOLOGY

2.1 SENSING THE MAIN SUPPLY VOLTAGE

The main supply voltage can be sensed by down converting the 220V AC to 5V DC using 15k ohm resistor, bridge rectifier and filter. When the main supply is active, the voltage sensing circuit provides 5V DC and when the main supply fails, the voltage sensing circuit gives 0V at its output.

2.2 CONTROLLING THE GENERATOR ON/OFF SWITCH AUTOMATICALLY

The generator ON/OFF switch open or short the two wires connected to it when the generator needs to be started or when the generator needs to be turned off. Relays can be used to open or short these two wires to start or stop the generator. The relay coil is energized by 5V DC main supply voltage coming from the microcontroller due to sensing circuit. When the voltage is available, the relay coil will be energized. Since when the voltage is available, generator remains off so microcontroller will send signal to relays to keep the wires connected to the generator ON/OFF switch open circuited. When the power failure occurs, the voltage sensing circuit sends 0v at its output and the microcontroller will send 5v signal to relay. Relay makes the ON/ OFF switch short circuited allowing the generator to be started by the generator start circuit.

2.3 STARTING THE GENERATOR AUTOMATICALLY

The generator is started automatically when the main power fails and the voltage sensing circuit provides the 0V at its output. Starting the generator requires short the wires connected to Generator ON/OFF switch which is done by sending signal from microcontroller to relay, short circuiting the wires connected to self-start switch momentarily. This circuit needs to be placed in parallel with the self-start switch which is normally open circuited. The circuit also provides a path which is normally open in the presence of grid voltage. The path has to be short circuited for a short period of time to engage the self momentarily. This is implemented by using relays. The whole circuit is controlled by the microcontroller. When the voltage from main supply is present, the path in series with the self-start switch is open circuit. When the main power fails the path is short circuited for a couple of seconds. When the main power fails, the coil of Relay is de-energized and the path is short circuited engaging the self-start mechanism of generator. The self-start mechanism is engaged only for the time duration set in the program dumped in the microcontroller and is disengaged when the timer expires. The generator will take 7 self (number of self are set by user), in case if generator does not start in first self or even after 7 self, then ATS will turn on the buzzer to indicate that generator fails to start.

2.4 AUTOMATICALLY TRANSFERRING THE LOAD

The time delay is required to allow the generator output to stabilize and is set to about 30 seconds. The circuit connects the generator output voltage to the load after this time delay. Before the generator turned off, the main power is connected to the load.

Automatic transfer switches for generators consist of three parts namely (as shown in Figure (2.0))

- A transfer mechanism to move the contacts from one source to another
- Contactor to connect and disconnect the load to source of power
- A logic control unit to constantly monitor the condition of the power sources.

The ATS monitors the supply of voltage from a single phase line and a generator supply that base its control operation on the availability or unavailability of electric power supply from either source. It consists of a series of relays contactors and protective devices that help form the control circuit of the ATS. [2]
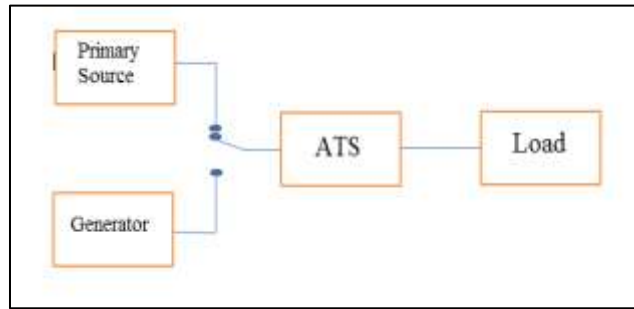
Fig. 2.0: Physical understanding of ATS operation

There are five cases that defines how ATS works; (PS is Primary supply)

1. PS on, Generator off
2. PS off, generator starts & load shifting
3. PS resumes, while generator on self
4. Generator fails to start & buzzer on
5. PS resumes, load shifting & Generator off

The algorithm for ATS is shown in Figure (2.1)
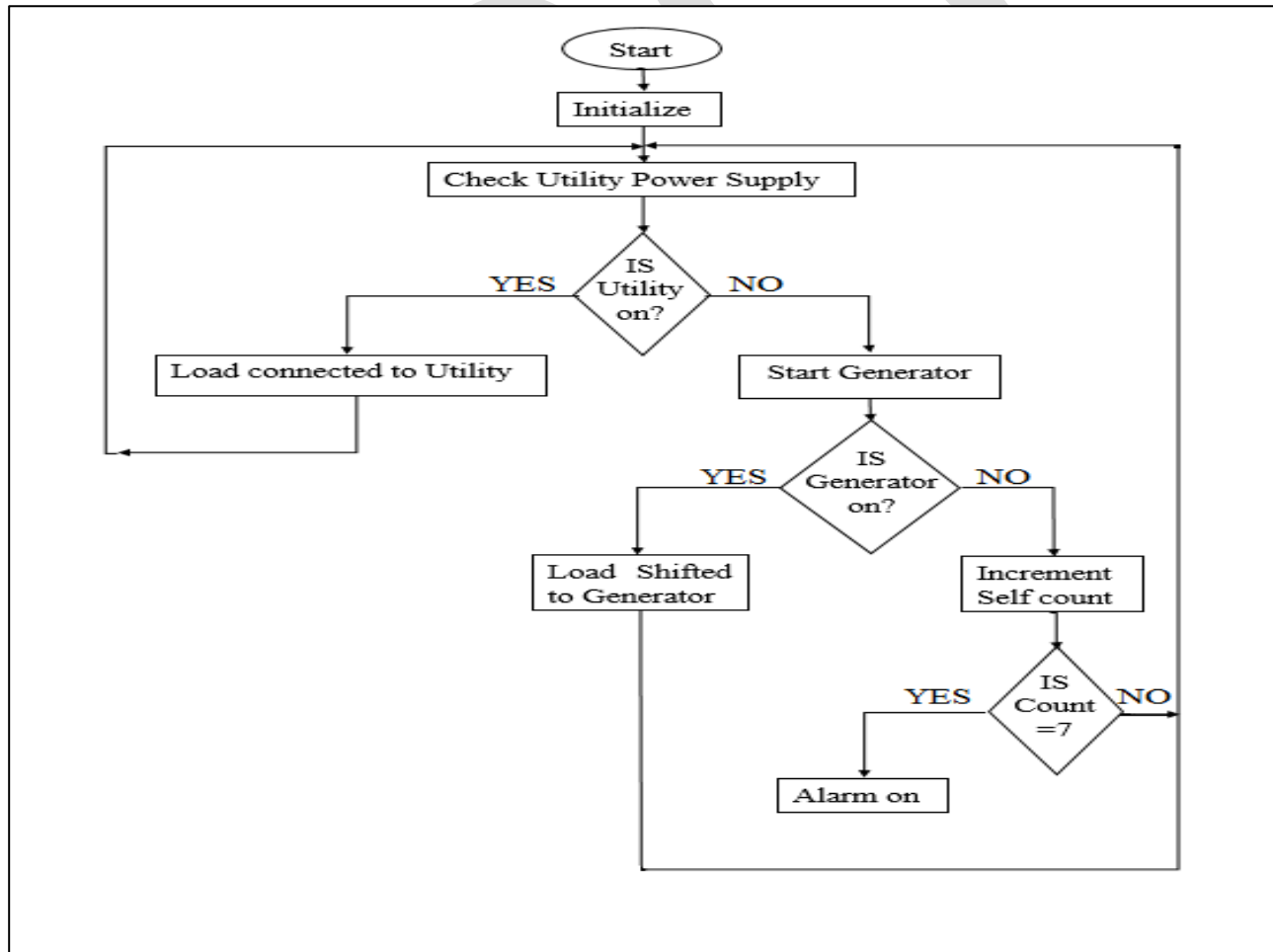
Fig. 2.1: Algorithm for purposed control scheme
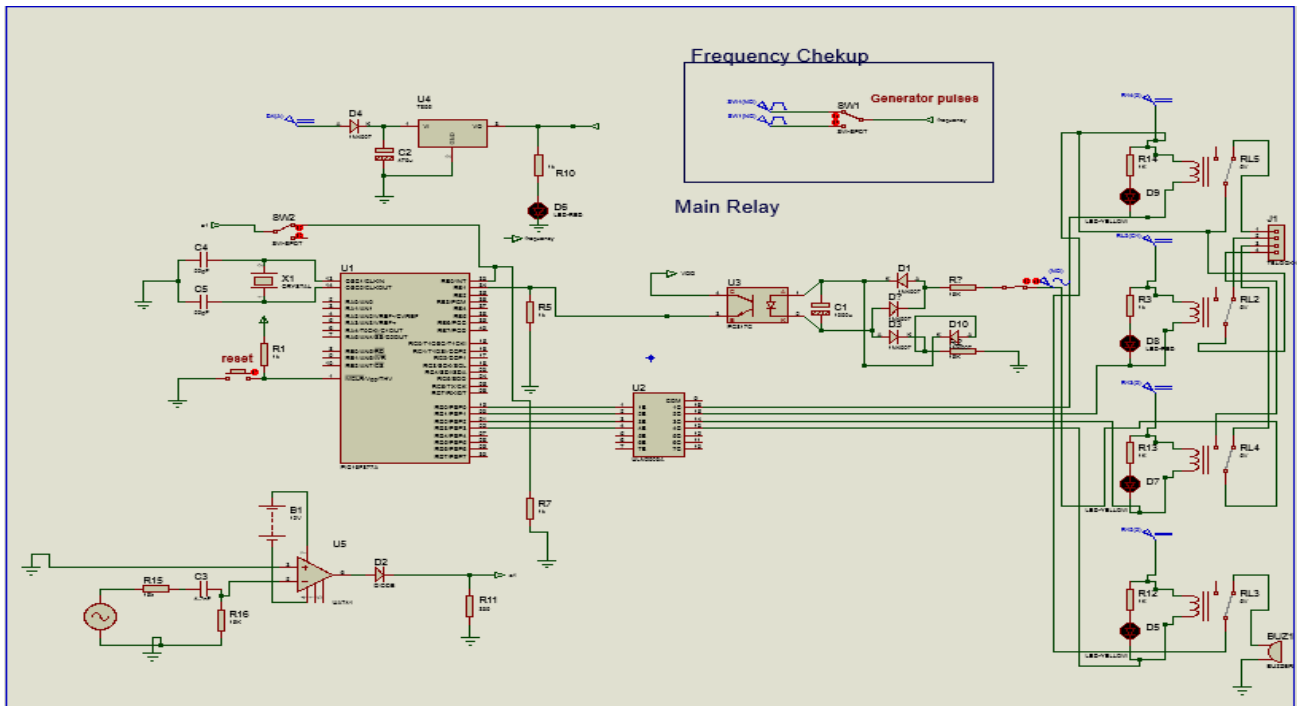
Fig. 3.0: Simulation results proteus

3 SIMULATION RESULTS

Simulation diagram of ATS is shown in Figure (3.0)

3.1 PS ON, GENERATOR OFF

Initially system is in normal condition i.e. PS is available and generator is at standby mode. Throughout this condition load is being served from primary source of power. At that moment GS is off, while ATS continuously checking the state of system. As PS shut down ATS proceeds to further steps and eventually shift the load from PS to generator. Figure (3.1)
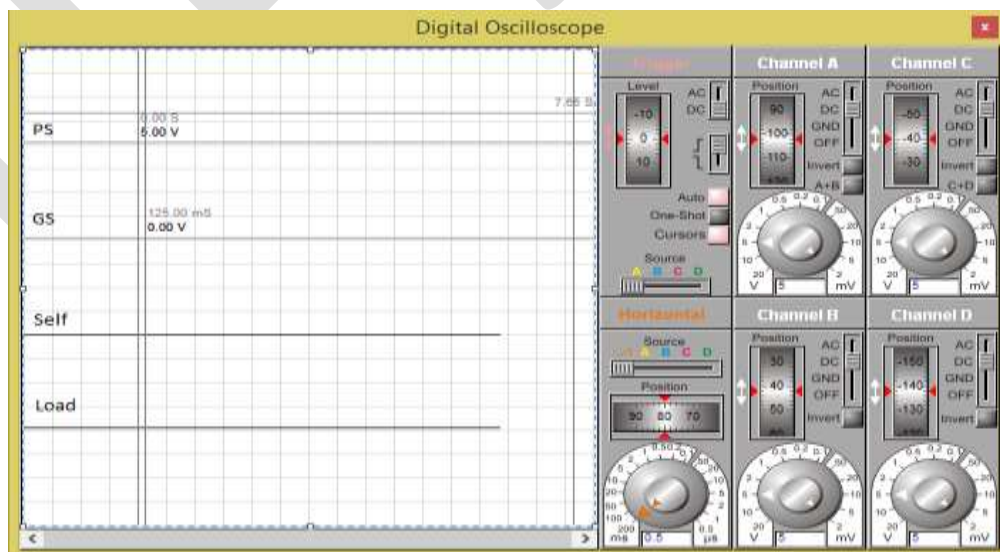
Fig. 3.1: System conditions when load is fed by power source
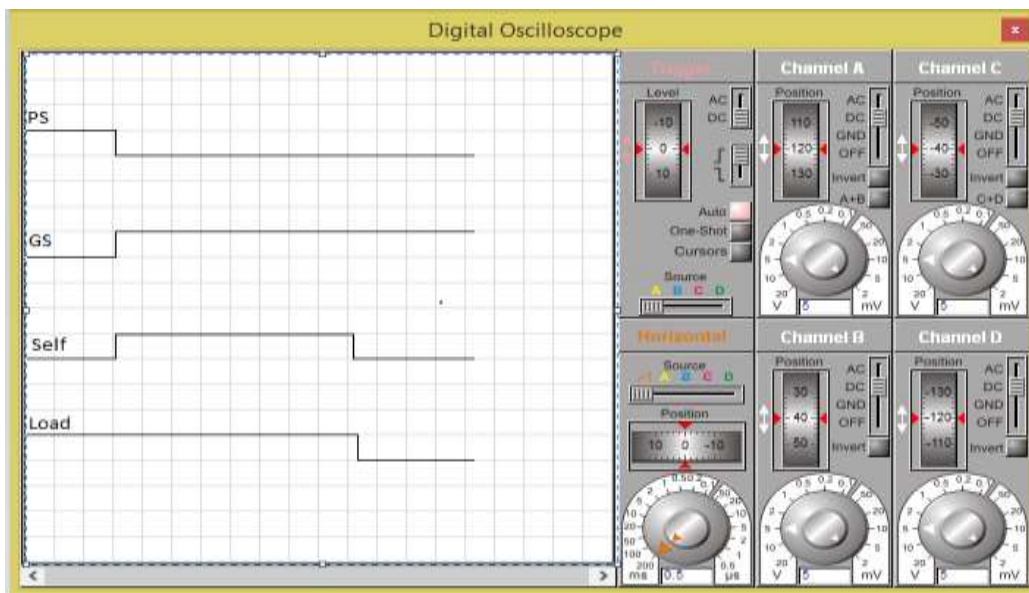
Fig. 3.2: System conditions when power failure from main source occurs

3.2 PS OFF, GENERATOR STARTS & LOAD SHIFTING

ATS working starts, when PS no longer available. Simulation result is attached which showing that when PS shut down, GS instantaneously turns ON and also at the same time generator starts to take self. Self-duration is set to some extent 400ms. A frequency checking circuit is installed. If generator starts within prescribed self-time, next progression is load shifting within 30ms. Figure (3.2)

3.3 PS RESUMES, WHILE GENERATOR ON SELF

When PS is not available ATS starts working which is to start generator and load shifting from PS to Alternative source i.e. generator. In case PS returns when ATS in self mode then normal operation is interrupted and immediately load shifted to PS while GS switched off after 30ms. Figure (3.3)
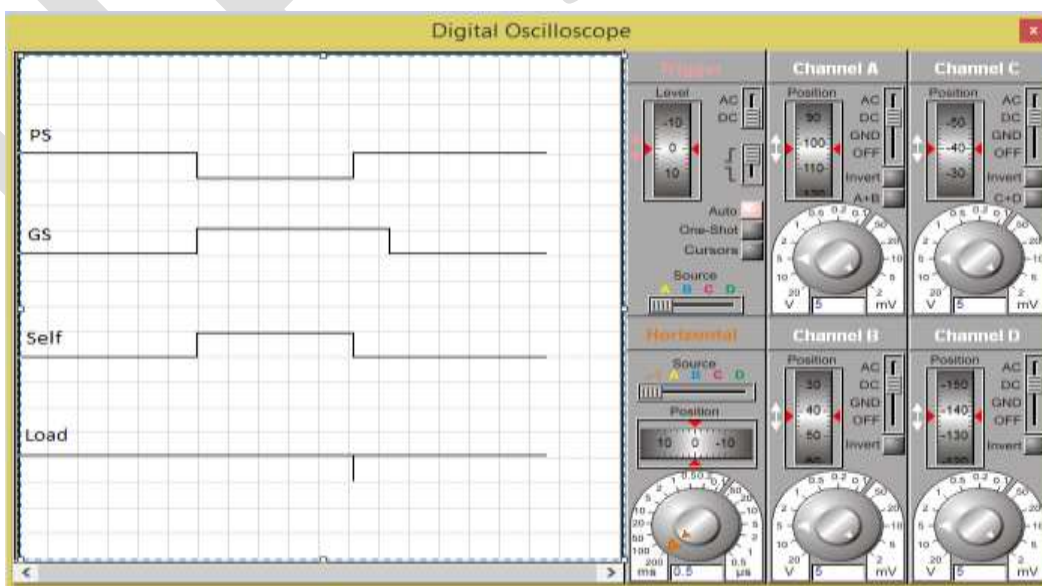
Fig. 3.3: Case when power take up again while generator on self
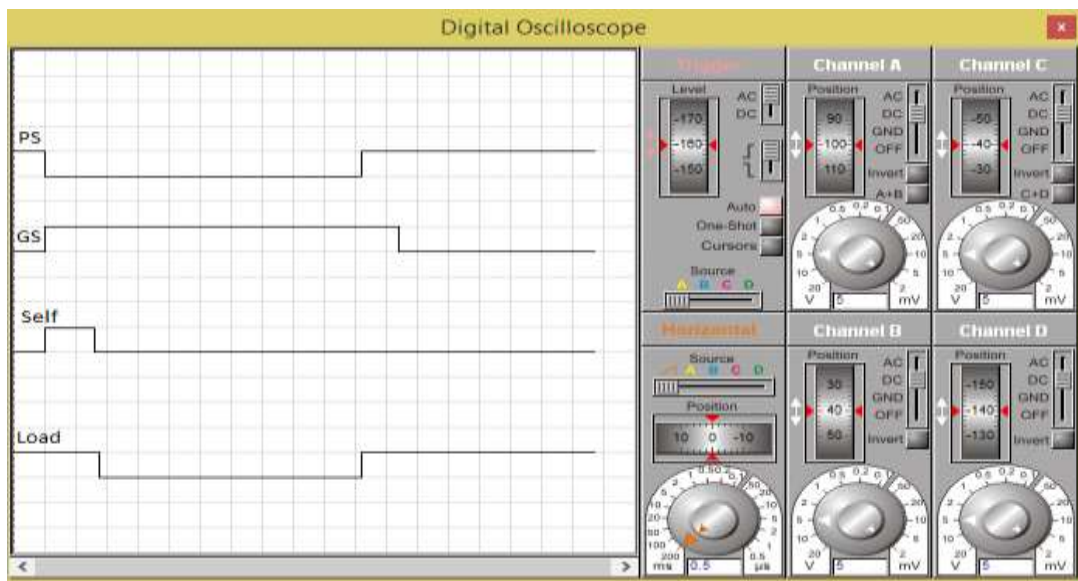
Fig. 3.4: Load shifting from generator when power from main source take up again

3.4 PS RESUMES, LOAD SHIFTING & GENERATOR OFF

When generator is in operational condition and load is being attended from generator, ATS constantly sense the PS. When PS resumes, ATS shifts the load immediately to PS and turns off the generator after delay of 30sec. Figure (3.4)

3.5 GENERATOR FAILS TO START & BUZZER ON

In case of power failure GS turns on and generator drives on self-mode. If generator fails to starts after seven self's due to fuel shortage or any fault in generator which are some hurdles that intrude the normal operation of ATS. In this case ATS conduct yourself like user friendly and indicate the interruption by alarming, turns off the GS and stop to take self. After initiating alarm ATS must be reset manually by user later on clearing the fault i.e. fuel check/hardware check. Figure (3.5)
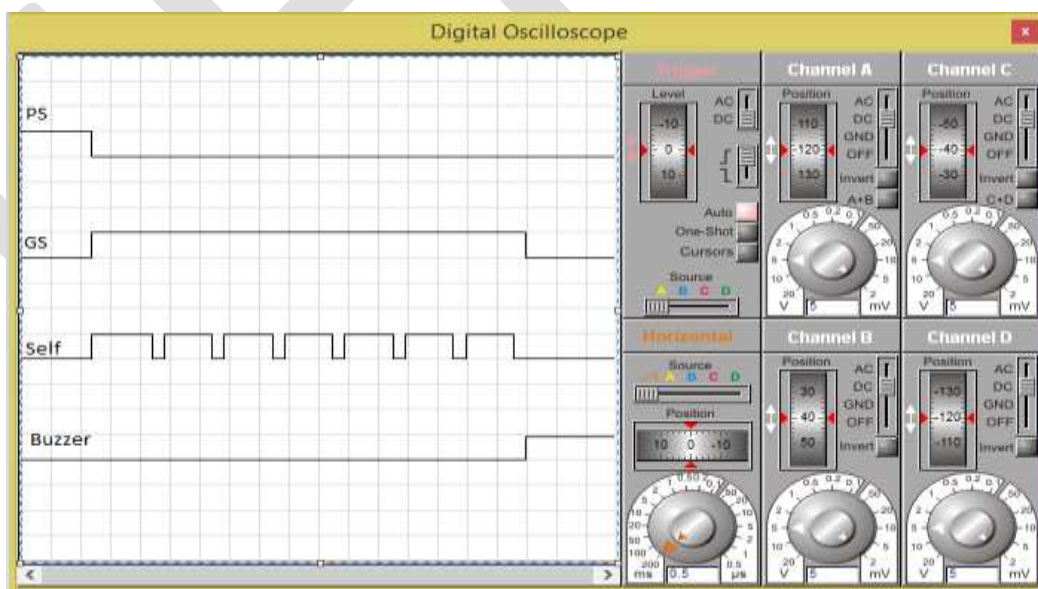
Fig. 3.5: Situation when generator fails to start

4 HARDWARE RESULTS

The automatic Transfer switch was successfully implemented and tested. The photograph of the implemented system is shown in Figure (4.0)

Fig. 4.0: Hardware implementation

4.1 HARDWARE OUTCOMES

The switching mechanism of the generator is done with a 12V dc supply battery and auxiliary contacts of the timer relays and the contactor.

4.1 PS ON, GENERATOR OFF

According to simulation results in fig3.1 hardware results are also same i.e. when power is available from utility generator in it's off condition.Fig4.1

Fig. 4.1: System conditions when load is fed by power source

4.2 PS OFF, GENERATOR STARTS & LOAD SHIFTING

In case of power failure switching take place between power source and generator as shown in Fig4.2
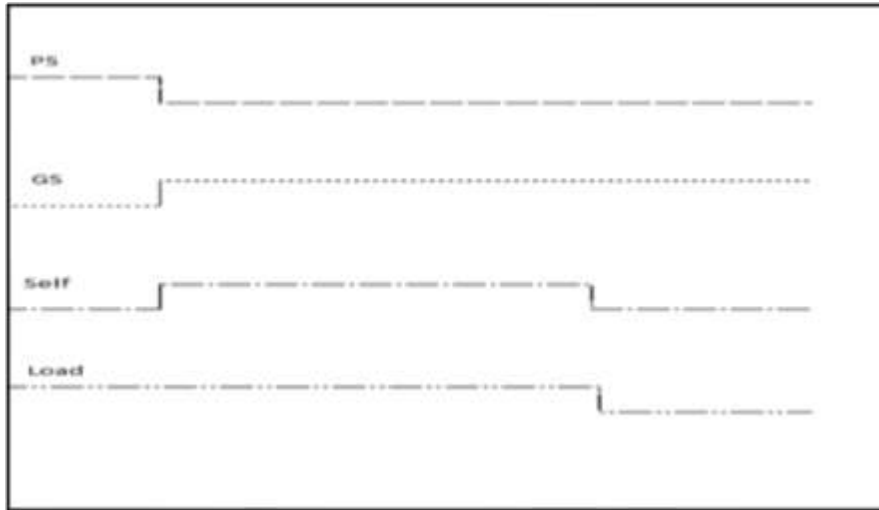
Fig. 4.2: System conditions when power failure from main source occur

4.4 PS RESUMES, LOAD SHIFTING & GENERATOR OFF

Fig4.4 is an explanation of a case when utility power take up again major switching take place i.e. load shifting & after some while (about 30S), generator choke signal activate and turned off the generator.
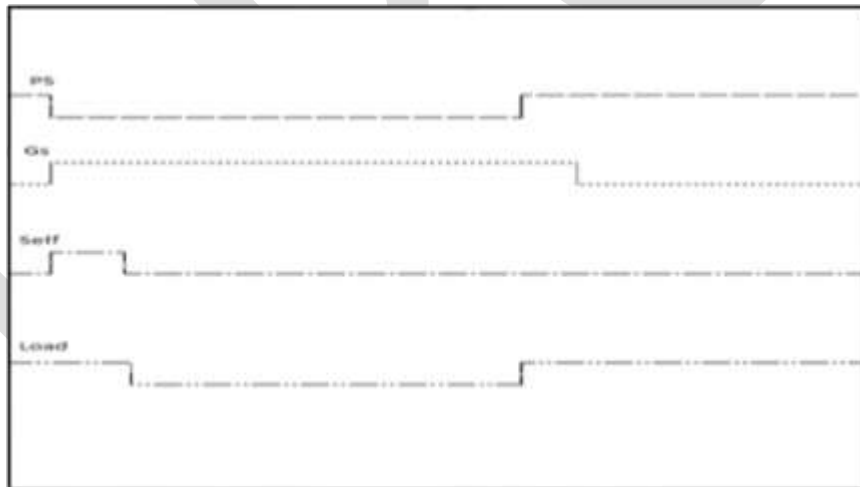
Fig. 4.4: Load shifting from generator when power from main source take up again

4.3 PS RESUMES, WHILE GENERATOR ON SELF

In case power supply take up again when generator on self immediately load shift to main power source and generator stop to start. Fig4.3 is an evident.
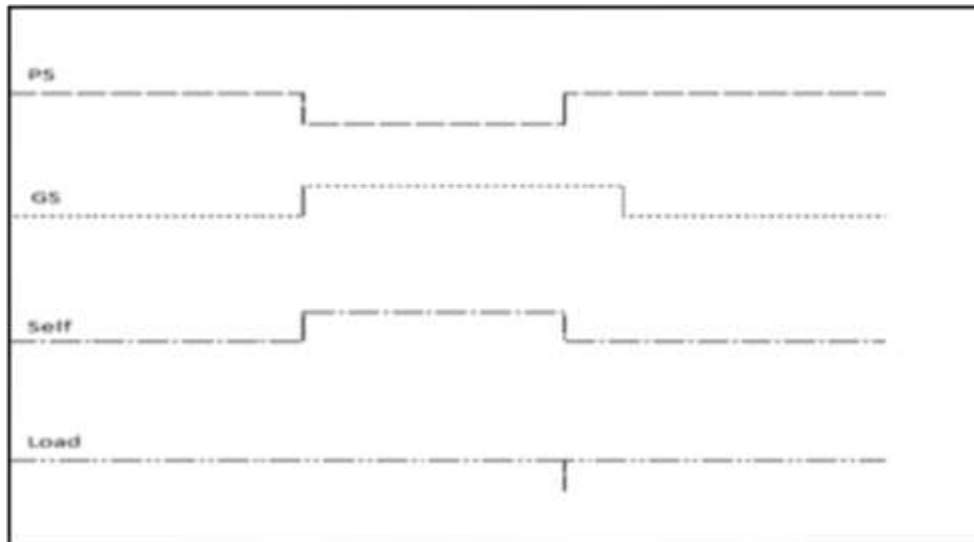
Fig 4.3: When power take up again while generator on self

4.5 GENERATOR FAILS TO START & BUZZER ON

In case generator fails to start predetermined attempt according to fig4.5 (about 7 attempts), buzzer will on showing that there are something wrong like fuel shortage or any kind of hardware failure.
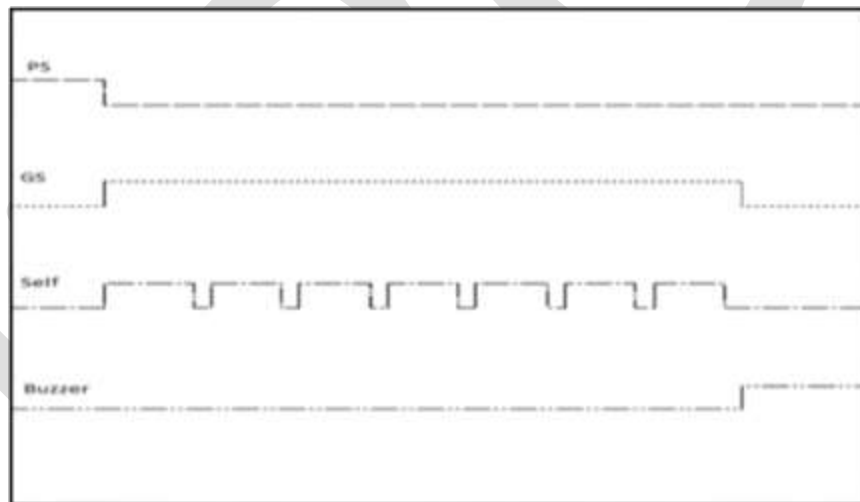
Fig. 4.5: Situation when generator fails to start

CONCLUSION

The manual start/stop and load transfer panel on the generator can still be used after the addition of the automatic controller. There is also a feedback in the circuit to sense whether the generator has started. It engages the self-start motor once at the start of the power failure and retry if the generator does not start in the first try. The total cost of the ATS is very low. Many aspects of automatic transfer systems for the critical power environment have been examined. ATS has the ability to monitor, control and switch between power sources in few seconds. It also provides the comfort of starting a standby generator when there is power failure from the mains without the need of human intervention. The system worked satisfactorily with respect to designed specification. The reliability of the controller is also very high due to the small number of components used in the circuit. The controller also takes very small time to put together and install on a household generator. The circuit is ideal for the countries with high rate of grid power failures.

REFERENCES:

[1]   C. Chukwuemeka, O. Babajide, O. John, J. Agidani, and V. Onyedikachi, "Design and Implementation of Microcontroller Based Programmable Power Changeover," vol. 6, no. 12, pp. 51–56, 2015.

[2]   P. P. Autade, "AN EMBEDDED 1 / 3 PHASE AUTOMATIC TRANSFER SWITCH," vol. IX, no. V, pp. 9–14, 2015.

[3]   A. F. Agbetuyi, A. A. Adewale, J. O. Ogunluyi, and D. S. Ogunleye, "DESIGN AND CONSTRUCTION OF AN AUTOMATIC TRANSFER SWITCH FOR A SINGLE PHASE POWER GENERATOR ."

[4]   N. C. M, M. E. S, and U. Godwin, "A COST EFFECTIVE APPROACH TO IMPLEMENTING CHANGE OVER," vol. 2, no. 2, pp. 62–72, 2012.

[5]   A. K. Gupta, C. Singh, G. Singh, and A. Kumar, "Automatic Cost Effective Phase Selector," pp. 3919–3925, 2015.

[6]   A. A. Roy, F. Newton, and I. Solomon, "Design and Implementation of a 3-Phase Automatic Power Change-over Switch," no. 9, pp. 7–14, 2014.

[7]   M. S. Ahmed, A. S. Mohammed, and O. B. Agusiobo, "Development of a Single Phase Automatic Change-Over Switch," vol. 10, no. 1, pp. 68–74, 2006.

[8]   J. A. Oladosu, R. O. Amuge, and A. A. Baruwa, "ANNALS of Faculty Engineering Hunedoara – International Journal of Engineering DEVELOPMENT OF AN INTELLIGENT AUTOMATIC TRANSFER SWITCH FOR SINGLE PHASE ELECTRICAL," 2016.

[9]   L. Nashelsky, "E LECTRONIC D EVICES AND C IRCUIT T HEORY."

[10]   B. Brown, J. Guditis, S. D. Critical, and P. Competency, "Critical-Power Automatic Transfer Systems – Design and Application," pp. 1–18.

[11]   "Design and Implementation of Automatic Three Phase Changer Using LM324 Quad Integrated Circuit," vol. 2, no. 4, pp. 1–15, 2014.

[12]   M. Christian, "Smart Phase Change-over system with AT89C52 Microcontroller," vol. 1, no. 3, pp. 31–34, 2012.

[13]   A. Afram, A. Afram, and A. A. Farooq, "A Low Cost Generator Auto Transfer Switch (ATS) Controller for 2-3 KVA Household Generators A Low Cost Generator Auto Transfer Switch (ATS) Controller for 2-3 KVA Household Generators," no. March, 2016.

Linking Student Interest and Engagement to Inquiry-Based Teaching in Engineering Classes

Bibi Rawiyah Mulung

BEng Electrical and Electronics Engineering, Faculty of Engineering

Universiti Teknologi Brunei, Brunei Darussalam

Abstract- Although several aspects of teaching have changed over time, traditional teaching is still deeply rooted into many institutions worldwide. Contrary to passive traditional teaching, inquiry-based teaching is a constructive way of teaching and learning which involves some forms of student participation. In this paper, I am presenting an analysis of the results from a study I have conducted on engineering students from three different engineering departments. My main method of data collection was questionnaires. My research was mainly focused on student interest and engagement as measures of the success of inquiry-based teaching in their classes. It was found that inquiry-based teaching can indeed raise student interest and engagement and can go as far as encourage engineering students to attend classes more regularly.

Keywords: inquiry-based teaching; engineering education; student engagement; educational research

Introduction

In many engineering classes, the lecturer uses presentation slides and tools such as a projector and screen to explain conceptual relationships to students. These students merely listen passively and are expected to memorize and reproduce this knowledge during the examinations. In this case, the lecturer and the presentation slides are the source of authority and the students are passive receivers of information. An inquiry-based teaching method works in a very different way from the traditional teaching method. When educators resort to inquiry-based teaching, they are no longer the only source of authority in the classroom. The students are made to participate actively as well. In inquiry-based teaching, students may be made to identify issues to the concepts being taught and asked to provide logical solutions to these. The students' contribution to the teaching-learning process ensures that they are made to develop analytical skills such as researching, questioning and communicating.

The reason for choosing engineering students for this study is that a rapidly expanding knowledge base in the field of engineering makes it difficult for educational curricula to keep up with the changes. The least that engineering institutions can do is to ensure that their graduates have a strong foundation of engineering concepts and skills. Unfortunately, this is often not the case. I believe that inquiry-based teaching could be the solution to eradicate the passiveness in teaching engineering.

In order to successfully reach a conclusion in this research, it was first important to determine the level of student interest and student engagement in a traditional classroom. This acts as a measure. The primary goal of this study was finding out whether engineering students show more interest and become more responsive when inquiry-based teaching is implemented. The changes that can be brought about through inquiry-based teaching have also been discussed. The factors leading to the differences in student response when being taught using the traditional teaching method compared to when they are being taught using an inquiry-based teaching method have been identified through this research.

My target group consists of engineering students. It is further divided into electrical engineering students, civil engineering students and mechanical engineering students. The results I have collected through questionnaires have allowed me to make both a quantitative and a qualitative analysis of student interest and engagement in class when inquiry-based teaching is adopted.

Literature Review

Many studies have previously been published on inquiry-based teaching. Researchers have been trying to investigate its effectiveness and feasibility across many disciplines and across many levels ranging from elementary school to universities. They have also been trying to further break down inquiry-based teaching into different categories such that studies on inquiry-based teaching can be narrowed down to specific types of inquiry-based teaching.

The authors in [1] deduced that inquiry-based teaching can generally be divided into three categories, each of which can be tackled using two types of inquiry-based teaching approaches:

1. Experience-centered lessons; through Free and Illustrated approaches.
2. Problem-centered lessons; through Solution and Method approaches.
3. Question-centered lessons; through Topic and Chaperoned approaches.

It was concluded that the Free Approach is the type of inquiry-based teaching which sustains student interest and causes students to be engaged most in the class. However, the authors of this particular study were elementary school teachers who carried out the experiment using a group consisting of elementary school children only.

In [2], two main research questions regarding inquiry-based teaching are addressed. The first one is about the main factors that determine the inquiry-based methods which the instructors adopt considering the teaching systems in place. The second question is relevant to the main features on which the teachers base their thinking on to adopt these methods. In an attempt to obtain conclusive answers, the authors identified three main types of inquiry-oriented approaches:

1. Problem-Solving Approach; engaging the students in fun activities
2. Research Approach; making the students investigate
3. Dialogic-Discourse Approach; causing the students to reflect

The factors which were found to lead the instructors' thinking were the algebra concept, the task at hand, inquiry and peer interactions. However, the limitation in this study is that it was carried out at a high school level with the principal focus being on the teaching of algebra only.

A previous research that is more closely related to my study is [3]. The authors have tried to provide a definition for inquiry-based teaching while taking into consideration the three main usage of inquiry; scientific inquiry, inquiry learning and inquiry teaching. According to the results obtained, both the means and the ends are essentials to determining the success of inquiry-based teaching. They also remarked that the instructors making use of inquiry-based teaching approaches should concentrate on the student's response and involvement as a measure of success. Another finding that has been teachers should collaborate with each other in order to create the right environment for inquiry-based teaching to be effective, while respecting each other's values and beliefs. However, it is important to note again that this study was conducted based on science teaching, not engineering.

A research that was more focused on undergraduate students is [4]. In this particular study, the challenges faced by instructors applying inquiry-based teaching at college level were explored. It was found that an extensive instructional preparation and support are required for the success of inquiry-based teaching. Students' and instructors' characteristics that may hinder inquiry-based teaching were found to be background, abilities, attitudes, habits, behaviour, beliefs and conceptions of science and nature of inquiry. Contextual barriers included logistics and lack of institutional support and incentives.

In [4] itself, a few reasons have been explained as to why lecturers at universities find it difficult to implement inquiry-based teaching.

1. Lecturers at universities and colleges are more concerned about using their time and resources for conducting research instead of investing that time in learning new teaching approaches.

2. Some lecturers apprehend that they may be less prone to get a promotion if they are categorized as good teachers instead of good researchers.

3. Many lecturers are unaware of inquiry-based teaching approaches and the effects these may have on the learning process for students.

4. Generally, college and university lecturers undergo little teaching training and do not have a well-defined framework for the design and implementation of their subject areas.

5. Instructors also mention a few contextual features for the non-adoption of inquiry-based teaching such as; time consuming, large class sizes, non-conducive class environment, not enough support from peers; not enough recognition from the institutions for their efforts to implement inquiry-based teaching.

My research questions and questionnaire questions are largely based on findings from the studies mentioned in this literature review. Although the chosen groups in these studies are different from the target group in my investigation, the same principles and research methods are applicable.

Methodology

Questionnaires were handed out to a total of 69 students, 23 students from each of the three engineering departments selected, namely electrical engineering, mechanical engineering and civil engineering.

Question 1:
Students were asked whether they are familiar with the term 'inquiry-based teaching' or not.

Question 2: A brief definition of inquiry-based teaching was given as:
"Inquiry-based teaching basically implies that students are made to actively participate in class".
Students were then asked to identify the inquiry-based teaching approaches their lecturers might be implementing in class from three approaches which were provided; they had the choice to select one or more.

      (i)   Experienced-centered lessons

      (ii)   Problem-centered lessons

      (iii)   Question-centered lessons

Question 3:

The following statement was given:

"Engineering is a highly practical field which is often taught in a more theoretical manner."

The students were then asked if they would be more interested and more engaged in class if their lecturer would carry out group discussions, ask them to investigate the concepts instead of merely reciting it to them and raise points for them to reflect on.

Question 4:

Three approaches to inquiry-based teaching were listed and the students were asked to identify of the approaches would sustain their interest more if implemented in their classes. A brief description of each approach was given as:

> (i)   Problem-solving approach: It engages the students in group discussions
>
> (ii) Research approach: It prompts the students to investigate a concept
>
> (iii) Dialogic-Discourse approach: It causes the students to reflect on a concept

Question 5:

Students were asked whether they would be more likely to attend a lecture if they knew it will not be the usual "speech being delivered" kind of class, but instead be an interactive and lively class.

Results

Table 1 to Table 5 show the results obtained from each question.

EE represents the number of electrical engineering students.

CE represents the number of civil engineering students.

ME represents the number of mechanical engineering students.

Table 1: Data collected for Question 1.

	EE	CE	ME
Yes	0	0	3
No	20	18	16
Maybe	2	5	4
Total respondents	22	23	23

Table 2: Data collected for Question 2.

	EE	CE	ME
Experienced-centered lessons	8	4	1
Problem-centered lessons	17	23	11
Question-centered lessons	15	10	13
None of the above	0	1	1
Total respondents	23	23	23

www.ijergs.org

Table 3: Data collected for Question 3.

	EE	CE	ME
Yes	19	16	15
No	4	7	8
Total respondents	23	23	23

Table 4: Data collected for Question 4.

	EE	CE	ME
Problem-solving approach	12	14	16
Research approach	6	5	4
Dialogic-discourse approach	5	4	3
Total Respondents	23	23	23

Table 5: Data collected for Question 5.

	EE	CE	ME
Yes	20	16	19
No	3	7	4
Total Respondents	23	23	23

Discussion
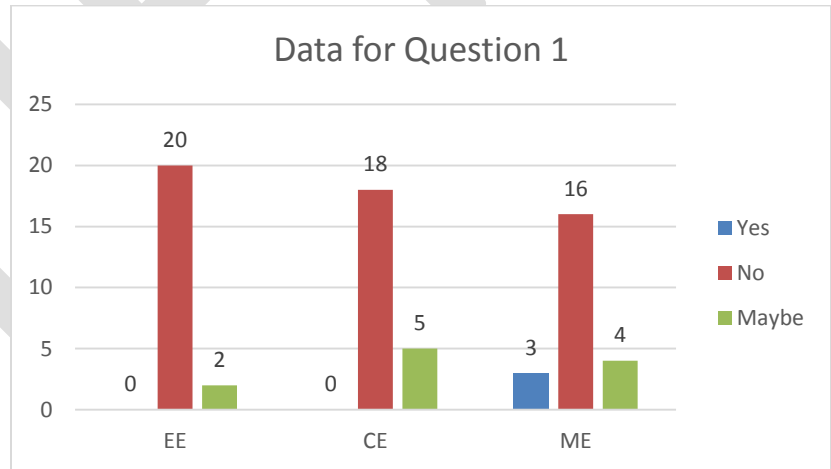
Fig. 1. Graphical representation of data collected for Question 1.

The objective of this question is to have an accurate idea about the extent of familiarity of engineering students with the term 'inquiry-based teaching'. From the results collected, it can be said that the majority of students, from any of the three groups, is unfamiliar with the term. It is worth noting that the largest proportion of students who is not familiar with the term comes from the electrical

121   www.ijergs.org

engineering group, accounting for 90.01% from this group. The percentages of students from civil engineering group and mechanical engineering group who are unfamiliar with the term are 78.26% and 69.57% respectively. Interestingly, only 3 students from the mechanical engineering group acknowledged being familiar with the term, compared to none from the other two groups. Finally, the number of students who responded by 'maybe' are fairly low for all three groups although a slightly higher number was expected.
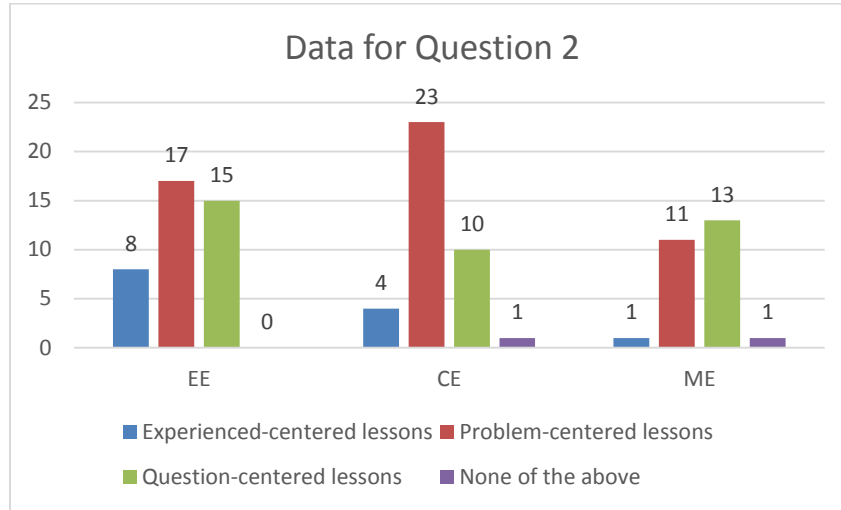
Fig. 2. Graphical representation of data collected for Question 2.

The objective of this question is to learn about the types of inquiry-based teaching approaches students can identify that are being implemented in their current engineering classes. The majority of students in the electrical engineering and civil engineering groups identified 'problem-centered lessons through solution and method approaches' as the most common inquiry-based teaching approach and 'question-centered lessons through topic and chapter-wise inquiries' as the second most common approach being implemented by their lecturers. However, it is vice-versa when it comes to the mechanical engineering group. Also, the least common inquiry-based teaching approach identified to be implemented in classes by students from all three groups is 'experienced-centered lessons through free and illustrated approaches'. The number of students who could not identify any of the approaches is almost insignificant.
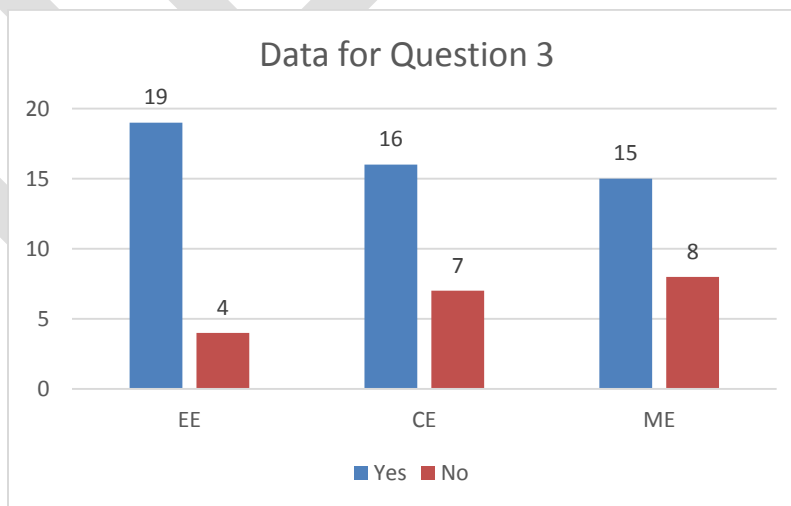
Fig. 3. Graphical representation of data collected for Question 3.

The aim of this question is to determine whether inquiry-based teaching can indeed raise student interest and engagement in class. The results prove that this hypothesis is correct since the vast majority of students; that is 82.61% from electrical engineering group, 69.57% from civil engineering group and 65.22% from mechanical engineering group, agreed that they would indeed be more interested and engaged in class if inquiry-based teaching were implemented. It is interesting to note that only 4 students from the electrical engineering group acknowledge that they would not be interested compared to twice that number for the mechanical engineering group.
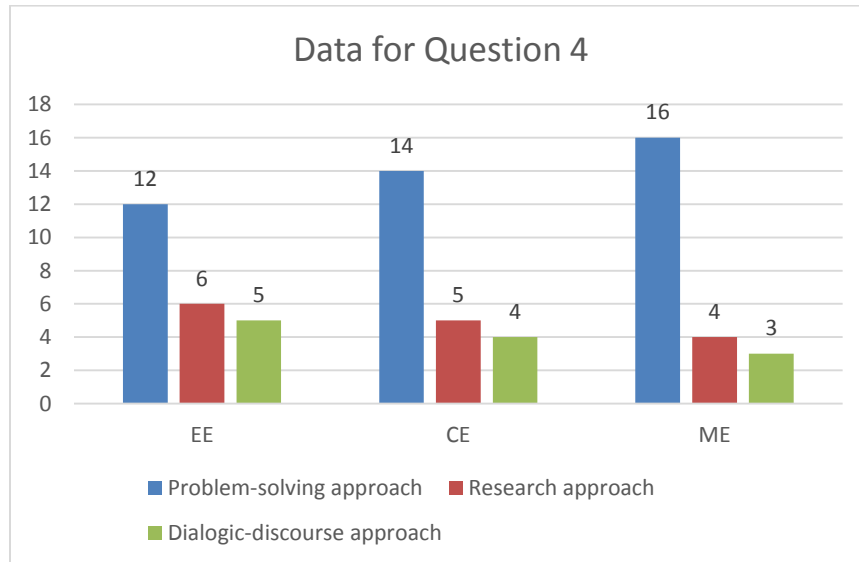
Fig. 4. Graphical representation of data collected for Question 4.

The objective of this question is to identify which inquiry-based approach can be used to make students express more interest and engagement in a class. Surprisingly, the majority of students in all three groups opted for the problem-solving approach. The highest proportion of 69.57% is from the mechanical engineering group, followed by 60.87% from the civil engineering group and 52.17% from the electrical engineering group. The second most popular option, again in all three groups, has been the research approach and the least desirable option has been the dialogic-discourse approach.
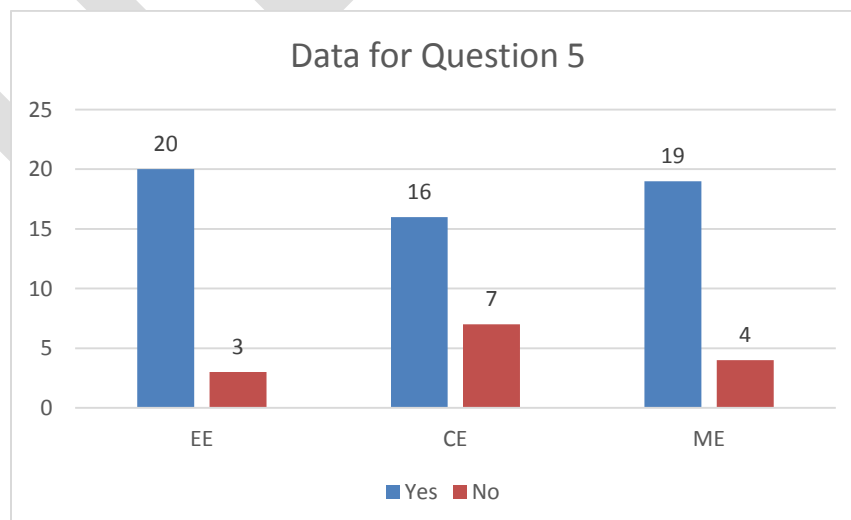
Fig. 5. Graphical representation of data collected for Question 5.

The objective of this question is to mainly determine whether the implementation of inquiry-based teaching in classes can be a factor for the raise in the attendance level of engineering students. At the same, it also allows us to have an idea about their interest and engagement level in classes if inquiry-based teaching were adopted. From the results obtained, it can be seen that over 69.57% of students from the civil engineering group, 82.61% from the mechanical engineering group and 86.96% from the electrical engineering group positively responded to the question, thus accepting that inquiry-based teaching implementation would make them more likely to attend a class. Although 7 students from the civil engineering group stated otherwise, the number is rather insignificant when it comes to the electrical and the mechanical group. It cannot, however, be denied that there is an anomaly due to the 7 students who responded negatively from the civil engineering group.

Conclusion and Recommendations

From the findings of this study, it can said that inquiry-based teaching approaches, if carefully selected and implemented, can cause student interest and engagement levels to rise significantly. The academic background of the students also prove to be a factor in this study. As far as this particular research is concerned, the main conclusions are:

1. Most engineering students are not familiar with the term 'inquiry-based teaching', although a rather insignificant number express some doubts as to whether they are familiar with the term or not.

2. Among the types of inquiry-based teaching, problem-centered lessons and question-centered lessons have proven to be mostly widespread and recognized by engineering students. The least known approach has been the research-centered lessons.

3. A vast majority of engineering students has stated that the implementation of inquiry-based teaching in their classes would indeed cause them to show more interest and become more engaged in the class.

4. When asked to choose which approach to inquiry-based teaching would sustain their interest more in a class, the problem-solving approach which causes students to engage in discussions, was the most desirable one. The second choice was the research approach which prompts students to investigate a concept. The last choice of approach was the dialogic-discourse approach which causes students to reflect on a concept.

5. Finally, it was found that engineering students are much more likely to attend a lecture when they know that the class will be interactive and lively due to the implementation of inquiry-based teaching methods.

It should, however, be noted that this particular study has been conducted on engineering students from three different engineering departments only. Although the trends suggest that the same results would apply to any other student group, further research would be necessary to confirm this hypothesis fully. Also, the same study, if conducted on students other than those from engineering background, might produce different results.

REFERENCES:

[1] Approaches to Inquiry Teaching: Elementary teacher's perspectives, Joseph Irelanda, James J. Wattersb, J. Lunn Brownleed and Mandy Luptonc, International Journal of Science Education, 2014, Vol. 36, No. 10, 1733–1750.

[2] Instructors' Decisions That Integrate Inquiry Teaching Into Undergraduate Courses: How Do I Make This Fit, Iris Alkaher Hakibbutzim and Erin Dolan Virginia Tech., International Journal for the Scholarship of Teaching and Learning, Volume 5, Number 2, Article 9, 7-11.

[3] Practice-based Perspectives of Inquiry Teaching of High School- Algebra, Olive Chapman, National Council of Teachers of Mathematics Research Conference, Boston, April, 2015.

[4] Reforming Science Teaching: What Research says about Inquiry, Ronald D. Anderson, Journal of Science Teacher Education, 13(1): 1-12, 2002.

GREENHOUSE CONTROLLING SYSTEM USING GSM

Yash Soni & Kalgi Trivedi

Guided by- Asst. Prof. Bhagirathi Dodiya

Electronics & Communication Engineering, Sal College of Engineering, Gujarat Technological University, Gujarat, India

Email- soniyash6989@gmail.com

Abstract - The system proposed in this project is "Green House" which is a smart technology to provide plants and trees the required nourishment from the sunlight and to prevent the same from the harmful effects. Therefore this project focuses on developing a system that can automatically monitor and predict changes of temperature, light, humidity and soil moisture in the greenhouse. The objective of the research is to develop an automatic control and monitoring system using sensors and Short Message Service (SMS) technology. This proposed system also has a mechanism to alert farmers regarding the parameter changes in the greenhouse so that early precaution steps can be taken. System components used are Humidity sensor, Temperature sensor, soil moisture sensor, light sensor, Transistor switches, relay nodes for automatic control, Microcontroller to control greenhouse information. To make this more efficient a GSM has been linked with the system.

Keywords - Greenhouse controlling, automatic Greenhouse, Embedded Greenhouse, Greenhouse controlling using sensors, GSM operated Greenhouse

I. INTRODUCTION

We live in the world where everything can be controlled and operated automatically, but there are still a few important sectors in our country where automation has not been adopted or not been put to a full-fledged use, perhaps because of several reasons one such reason is cost. One such field is agriculture. Agriculture has been one of the primary occupations of man since early civilizations and even today manual interventions in farming are inevitable. [12]Greenhouses form an important part of the agriculture and horticulture sectors in our country as they can be used to grow plants under controlled climate conditions for optimum produce. Automating a greenhouse envisages monitoring and controlling of the climatic parameters which directly or indirectly govern the plant growth and hence their produce. Automation is process control of industrial machinery and processes, thereby replacing human operations.

II. LITERATURE REVIEW

The concern with a lot consumer needs and demand for the agriculture products has stimulated awareness among the farmer that increases their products in the market by implementing advance technologies in the industry. The products that are important that may come to farmers' interest that controls the use of natural sources and natural environment which controls agriculture with various aspects. Therefore, this problem makes farmers' interest to implement agro-conditions sending alert notification messages to farmers using GSM and SMS technology. The proposed system is aimed to be a reliable and cost.

The agro-environmental remote monitoring system can be implemented in various conditions such as in monitoring temperature, soil and water levels. By utilizing existing technology, the natural environment and resource which we get naturally, the temperature is very important criteria for the plants to be monitored efficiently.

Previously, human labor plays major role in the monitoring farm and plants in the agriculture field. For some crucial plants such as vegetarian and flower plants, which need 24 hours attention from human so that the plant quantities and qualities are controlled with proper management by the collected data and information from the field. This will provide enormous foundation for future growth and future development of their plants in the green house. However, with the increasing size in farming areas, this type of manual practice is increases time consuming the cost of the labor.[2]

III. IMPLEMENTATION
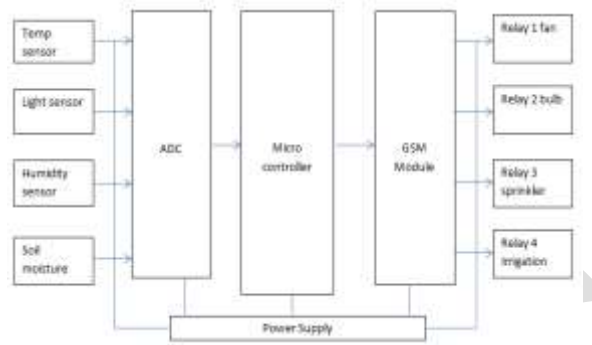
Sensors: -

We are going to use temperature sensor, Light sensor, Humidity sensor and Soil moisture sensor to sense temperature, light intensity, humidity in plants and soil moisture respectively. These sensors sense the parameters and gives corresponding voltage output.

ADC: -

Sensors can senses the variation in environmental parameter such as temperature, humidity, light and soil moisture and gives the reading in variation with voltage. So using the analog signal we can't directly send to the GSM modem. So, we have to use analog to digital converter.[1]

Microcontroller: -

We are going to use microcontroller of 8051 family. The microcontroller is the heart of the proposed embedded system. It constantly monitors the digitized parameters of the various sensors and verifies them with the predefined threshold values and checks if any corrective action is to be taken for the condition at that instant of time.[8]

GSM Module: -

A GSM modem is a wireless modem that works with a GSM wireless network. A wireless modem behaves like a dial-up modem. The main difference between them is that a dial-up modem sends and receives data through a fixed telephone line while a wireless modem sends and receives data through radio waves. Like a GSM mobile phone, a GSM modem requires a SIM card from a wireless carrier in order to operate.[3] [4] [5] [10]

IV. WORKING & TESTING

The system above consists of four input (temperature, humidity, Light and soil moisture sensor) are four outputs (Fan, water pump, Lamp and sprinkler). Microcontroller is the main brain for this system because it controls the overall system in the Green house. Temperature sensor used to detect the temperature in the greenhouse. When temperature sensor detects the high temperature, microcontroller will send the signal to the fan to stable the greenhouse condition. Then, when light sensor detects no light, microcontroller will send the signal to lamp and lamp will be ON automatically. Water pump is used to supply water to the sprinkler and make sure the sprinkler watered the plants in the greenhouse.

As we see in figure, the microcontroller controls circuit that will be connected to the soil sensor, humidity sensor, temperature sensor and light sensor. The microcontroller receives the value from sensors and analysis and then compares it with the threshold value stored in the microcontroller memory, based on this value the microcontroller takes the appropriate procedures and also controls the output device based on these values; the microcontroller sends the report by the GSM modem to the farmer's phone.

As soon as the change of temperature or humidity absence of air for instance has been detected, GSM modem sends SMS on a number provided in the GSM code. Through this section user can manage greenhouse hardware or manage the SMS service.

Initially a temperature point is set. The temperature sensor senses the change in input temperature. After signal conditioning, this analog signal is given to the microcontroller. The microcontroller converts it to digital format using on chip value, the controller unit will start the heater. Once it reaches to the set limit, it will start the blower to bring the temperature down. Once it reaches below a set point, it will switch of the blower. In this way, temperature is controlled. Similarly, an intensity of light can be controlled.[11] Initially, intensity point is set. Light dependent resistor senses the change in input intensity of light. If the intensity of light sensed below the low limit set, the controller unit will switch on bulb. Once it reaches the set limit it will switch off the bulb. In this way, intensity of light is controlled[7]. Humidity can be control by using humidity sensor. Initially humidity sensor is set. Humidity sensor senses the change in humidity. If the humidity sensed below the low limit set, the controller unit will turn on the dehumidifier. Once it reaches the set limit it will switch on the humidifier. In this way, humidity is controlled. After it senses intensity of temperature, light, humidity and soil moisture it gives digital display at the output on LCD.[6]

V. SOFTWARE DESIGN
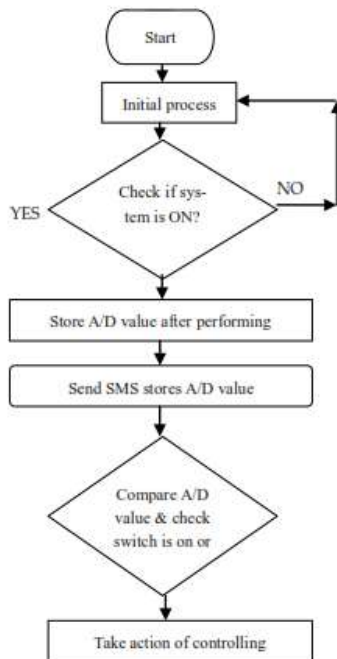
VI. CONCLUSION & FUTURE WORK

The system could be developed by different ways such as sending emails when an alarm happens, or using different devices such as PLCs, in addition to measure the conditions that have been mentioned, other conditions may be included like shade and fire detection.

This project offers a design of fully automated greenhouse management system. From the experiment it could be seen that it is fulfilling all requirements related greenhouse monitoring. The automatic greenhouse sensor design could help in increasing the productivity of plants.

As it has been mentioned earlier, we are not only providing automatic control over the devices like light, motor pump but also we have a mechanism to alert farmers regarding the parameter changes in the greenhouse so that early precaution steps can be taken. Thus this construction, productivity of cropping can be continuously increased so it can handle famine problem around the world. Thus we can say that the greenhouse monitoring system using GSM is far better than the same system using the different technologies.

REFERENCES:

[1]ADC, Intersil, www.intersil.com

[2]Advantages & Disadvantages of Greenhouse, retrieved from the EHOW online website: http://www.ehow.com

[3]GSM tutorial. Retrieved from the website: http://ecee.colorado.edu/~ecen4242/gsm/index.htm

[4]GSM characteristics. Retrieved from the GSM server online website: http://gsmserver.com/articles/gsmcharact.php

[5]GSM technical Specification (1995) GSM 11.11.V 5.0.0, p.1-91

[6]Humidity sensor, MaxDetect Technology Co. LTD, http://www.humiditycn.com

[7]Light sensor, Texas Instruments, www.ti.com

[8]Microcontroller AT89C51 datasheet www.atmel.com

[9]Soil Moisture sensor, Vernier software & technology, www.vernier.com

[10]SIM 300 module, SIMCOM Ltd,.

[11]Temperature sensor LM35, National Semiconductor Corporation, Dec 1994

[12]Top Greenhouses LTD. Retrieved from online website: http://www.top.pro

EXPERMENTAL STUDY OF MODULUS OF ELASTICITY DUE TO CHANGE IN STEEL FIBER REINFORCED CONCRETE AND SIZE OF AGGREGATES

T.PRATHAP, L.SIVA REDDY

Department of structural engineering, Annamacharya institute of technology,kadapa.

Email:thiruveedhula.pratap@gmail.com,sivareddy.lingala@gmail.com

Abstract— This paper presents a experimental study considers the effect of aggregate size &steel fibers on the modulus of elasticity of concrete. The modulus of elasticity of concrete is a very important parameter reflecting the ability of concrete to deform elastically. Modulus of elasticity of high strength concrete is very important in avoiding excessive deformation, providing satisfactory serviceability, and avoiding the most cost-effective designs. The present experimental study considers the effect of aggregate size and steel fibers on the modulus of elasticity of concrete. Crimped steel fibers at volume fraction of 0%.0.5%, 1.0% and 1.5% were used. Study on effect of volume fraction of fibers and change of aggregate size on the modulus of elasticity of concrete was also deemed as an important part of present experimental investigation. This work aims in studying the mechanical behavior of concrete in terms of modulus of elasticity with the change of aggregate size reinforced with steel fibers of different series for M30 and M50 grade concretes.

Index Terms— steel fibers, different size of aggregates, compressive test, split tensile test, cement, water, vibrator, weighing machine

1.Introduction

The usage of fibers from the past few years was increasing drastically. Due to its flexibility in usage and accuracy in attaining required properties fiber RCC usage is increasing day by day. [6] To make its usage more feasible engineering properties like Compressive &tensile strength, flexible strength, durability, flexural toughness and resistance to impact, various changes are to be adopted [2]. There by the mechanical properties depend on type, size, shape, surface texture of aggregates and the amount of fiber added[1]. SFRC is being increasingly used to improve static and dynamic tensile strength, energy absorbing capacity and better fatigue strength.To avoid miscellaneous properties like wise honey combing, bleeding& segregation to fresh concrete and spiking, cracking to horded concrete, the change in the workability properties should be implemented [5].This paper suggests a new volume fraction of fibers to be used in producing SFRC with in 0.5% to 1.5%.the addition of fibers [3] may reduce the workability of the mix & will cause balling which will be extremely difficult to separate by vibration [8]. The experimental observations indicated that with an increase in volume of fibers strength and toughness and peak stress increases with a slight reduction in young's modulus. The main advantages of these fibers fast& perfect mixable fibers & high performance and crack resistance, optimization costs with lower fiber dosages, steel fibers reduces the permeability & water migration in concrete[5]. From this work it is observed that with increase in % volume of fibers the young's modulus decreases with an increase in strain fraction [7].

2. Existing techniques:

The influence of the fiber distribution and orientation on the post-cracking behavior of steel fiber reinforced self-compacting concrete. A result data obtained has been analyzed and compared with a control specimen (0% fiber). However higher percentage of fiber can be used with special fiber adding techniques and also placement procedures. According to ACI 544, 3R-08, aspect ratio is referred to the ratio of fiber length over the diameter. The normal range of aspect ratio for steel fiber is from 20 to 100. Aspect ratio of steel fiber greater than 100 is not recommended, as it will cause inadequate workability, formation of mat in the mix and also non uniform distribution of fiber in the mix.

It is found that the splitting tensile test overestimates the post-cracking parameters. Specimens with notched plane parallel to the concrete flow direction show considerable higher post-cracking strength than specimens with notched plane perpendicular to the flow direction.

3. Contribution: This is an experimental set up of casting SFRC cylindrical specimens standard size with change of aggregate sizes such as 20mm,16mm,10mm and with varying percentages of fibers such as 0%,0.5%,1% &1.5% to study the stress-strain relationship in tension & compression aspect ratios of steel fibers used in concrete mix are varied between 50 and 100.

The experimental program was designed to determine the modulus of elasticity of M30 & M50 grade concrete standard cylinders for M30/20 mix proportion 0.46:1:1.26:3.12 and M50/20 mix proportion 0.39:1:0.74:3.08 under the compression and split tensile tests.

3.1 Test procedure: This experimental program consists of twenty four cylinders for each grade namely M30/20mm/0 % ,M30/20mm/0.5 %
,M30/20mm/1%,M30/20mm/1.5%,M30/16mm/0%M30/16mm/0.5%,M30/16mm/1%,M30/16mm/1.5%,M30/10mm/0%,M30/10mm/0.5%,M30/10mm/1%,M30/10mm/1.5%forM30gradeandM50/20mm/0%,M50/20mm/0.5%,M50/20mm/10%,M50/20mm/1.5%,M50/16mm/0%,M50/16mm/0.5%,M50/16mm/1%,M50/16mm/1.5%,and0/10mm/0%,M50/10mm/0.5%,M50/10mm/1% ,M50/10mm/1.5% for M50 grade concrete. The arrangement of the cylindrical specimen subjected to split tensile loading and compressive loading.

3.2 Compression test: Then place the cylinder in test setup and apply the load continuously without any After 28 days curing, the cylindrical specimens were tested in the compression testing machine of capacity of 200 tons. An extensometer of gauge length 200mm and a least count of 0.002mm has been used to note the deformation values. So a cylinder mounted with an extensometer was used to find out the deformation values during loading. The vertical strips of extensometer were removed before placing the cylinder in test setup so as to avoid the damage of extensometer during loading shock to note the deformation values. And stop the applying of the load after the specimen has failed. The compressive strength of the specimen can be calculated by

 Compressive strength (MPa) = Failure load / cross sectional area

3.3 Split tensile test: In Split tensile strength test, cylinder specimens of dimension 150 mm diameter and 300 mm length were cast. The specimens were demoulded after 24 hours of casting and were transferred to curing tank where in they were allowed to cure for

28 days. The strain gauges of 350Ω resistance capacity and a gauge factor of 2.1 have been used to note the strain values. After the strain gauges have been attached to the specimens, they were tested under compression testing machine of Capacity 200 tons. Split Tensile strength was calculated as:

Split Tensile strength (MPa) = $2P / \pi DL$ Where ,P=failureload,

D=diameter of cylinder,

L = length of cylinder.

4. Results:

4.1 Modulus of elasticity in compression: the failure stress values increases with the increase of steel fiber content. And the percentage increase in failure stresses were 51.8%, 45.8% and 57.14% for M30 grade and 38.5%, 40% and 35.71% for M50 grade concrete. The following are the graphs showing the relationship between stress and strain of casted specimens after testing in compression.
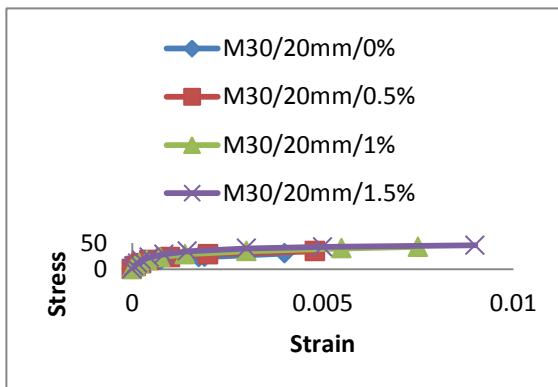
Fig1:Stress Vs strain graph for M30/20mm
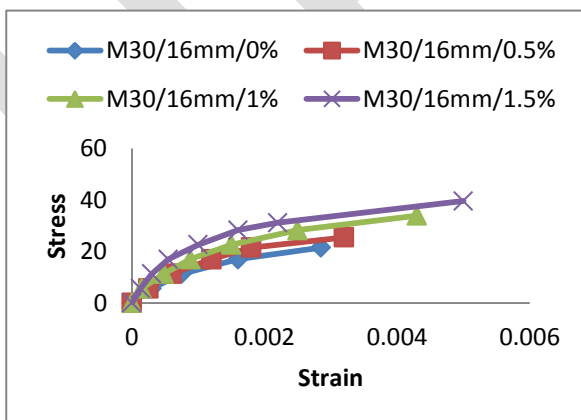
Fig2:Stress Vs strain graph for M30/16mm

Percentage increase in modulus of elasticity of steel fiber based concrete mixes were 118.36%, 117.42% and 326.2% for M30 grade and 140%, 92.76% and 120.6% for M50 grade concrete
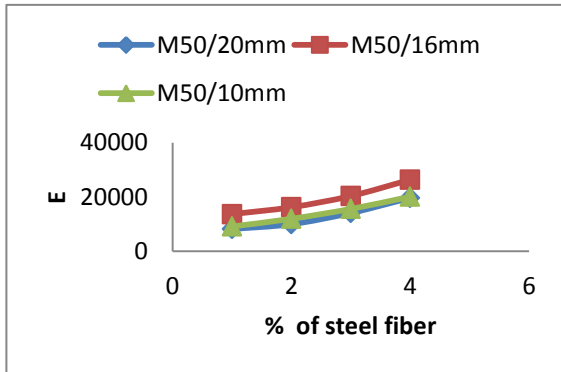
Fig3:E Vs % of fiber for m50
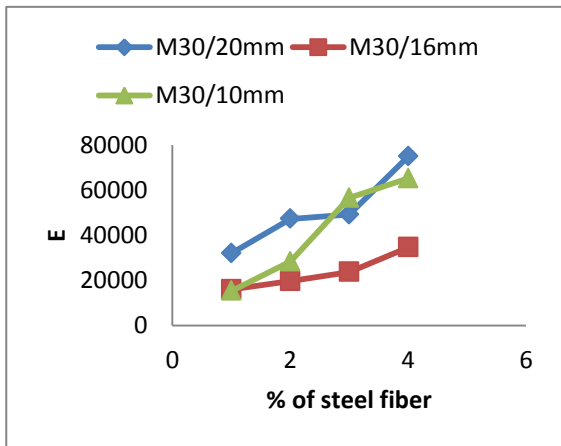
Fig 4: E Vs % of fiber for M30

The percentage increase in modulus of elasticity of steel fiber reinforced concrete at 33% of the maximum stresses were 45.8%,60% and 60% for M30 grade, and 38.83% ,50% and 43.32% for M50 grade concrete. **4.2 Modulus of elasticity in tension:** It is observed that the failure stresses were increased with the increase of steel fiber content. And the percentage increase in failure stresses were 45.8%, 60% and 60% for M30 grade and 38.72%, 50% and 50% for M50 grade concrete. The following are the graphs showing the relationship between stress and strain of casted specimens after testing in tension

The percentage increase in modulus of elasticity of steel fiber reinforced concrete at 33% of the maximum stresses were 45.8%,60% and 60% for M30 grade, and 38.83% ,50% and 43.32% for M50 grade concrete
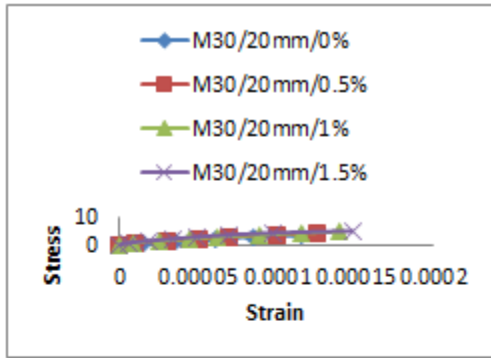
Fig 5:Stress strain graph for M30/20
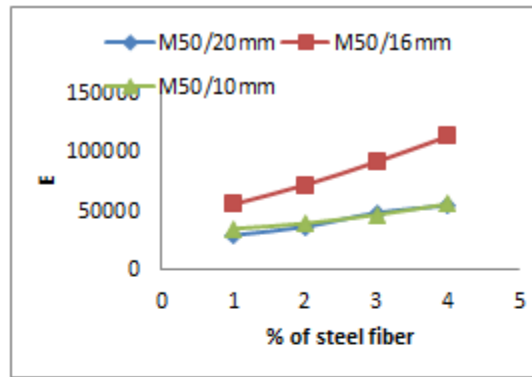
Fig7: EVs%of steel fiberforM50
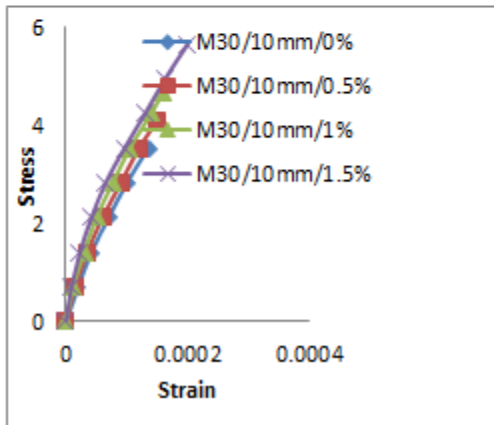
Fig 6:Stress strain graph for M30/10
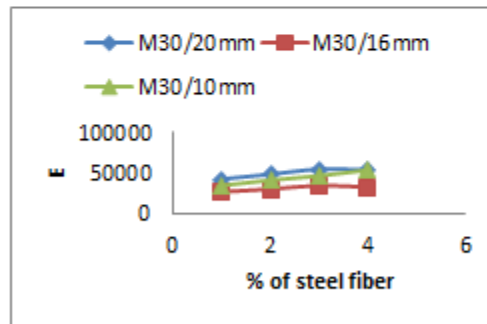
Fig 8:EVs%of steel fiberforM30

The relationship between ultimate stress (σ_U) and % of steel fiber content and the percentage increase in the ultimate stress were 45.8%, 60% and 60% for M30 grade, and 38.72% ,50% and 50% for M50 grade concrete
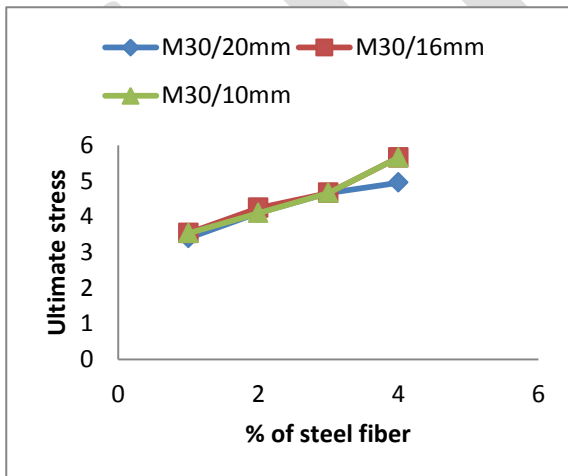
Fig 9:σ_UVs%ofsteelfiberforM30
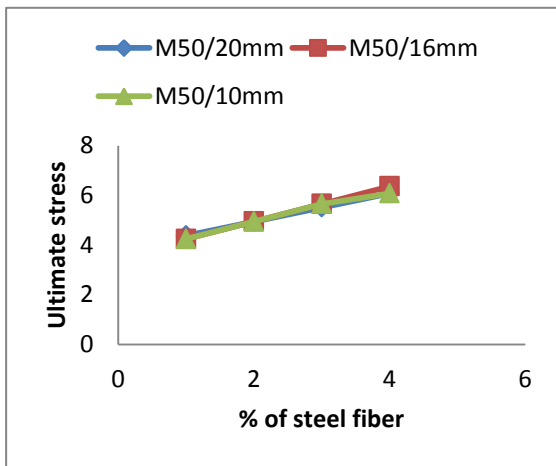
Fig 10:σ_U Vs%ofsteelfiberforM50

Conclusion: It is observed that,the failure stresses increased with the increase of steel fiber content [i.e.0-1.5%] as 51.8%,45.8% and 57.14% for M30 grade and 38.5% ,40% and 35.71% for M50 grade concrete in compression and 45.8%,60% and 60% for M30 grade and 38.72%, 50% and 50% for M50 grade concrete in tension. It is also observed that,the modulus of elasticity (E) value increases with the increase of steel fiber content.It is also observed that,the ultimate stress and modulus of elasticity (E) value were increased with the decrease of aggregate size . From the comparisions of compression and tension reults,it was cleared that the ultimate stress values in tension were higher than those in compression.i.e,5 times for M30 and 14 times for M50 grade concretes.

The modulus of elasticity (E) values in tension were higher than those in compression. i.e,94 times for M30 and 55 times for M50 grade concretes.

REFERENCES:

[1]. A.M Shende et al. "Comparative Study on Steel Fiber Reinforced cum Control Concrete" International Journal of Advanced Engineering Sciences and Technologies Vol. No. 6, Issue No. 1, 116 – 120.

[2]. Banthia, N,Chokri,K, and Trottier,JF,1995. Impact tests on Cement-Based Fiber Reinforced Composites. ACI Publications, Detroit, USA, SP, 155-9, pp.171-188

[3]. BS 1881: Part 121:1983," Testing concrete Method for determination of static modulus of elasticity in compression".

[4]. Elsaigh, WA and Kearsley, EP, 2002."Effect of Steel Fiber Content on Properties of Concrete". Journal of Concrete/Beton, South Africa, No 102, pp. 8-12

[5]. Er Prashant Y.Pawade et al. "Effect of Steel Fibers on Modulus of Elasticity of Concrete" (IJAEST) International Journal of Advanced Engineering Sciences and Technologies Vol No. 7, Issue No. 2, 169 – 177

[6]. Johnston, CD, and Zemp, WR, 1991. "Flexural Fatigue performance of Steel Fiber reinforced concrete- Influence of Fiber Content, Aspect Ratio, and Type". ACI Material Journal, 88, No.4, pp. 374-383.

[7]. J. Mater. "Mechanical Properties of Steel Fiber Reinforced Concrete", Journal of Materials in Civil Engineering, Volume 19, Issue 5, 2007

[8].Saravana Raja Mohan. K, Parthiban. K "Strength and behavior of Fly Ash based Steel Fiber Reinforced Concrete Composite.

[9]. S. Hagihara, S. Nakamura, Y. Masuda, and M. Kono, "Experimental study on mechanical properties and creep behavior

of high-strength concrete in early age," *Concrete Research and Technology*, vol. 11, no. 1, pp. 39–50, 2000 (Japanese).

[10]. S. Swaddiwudhipong, H. R. Lu, and T. H.Wee, "Direct tension test and tensile strain capacity of concrete at early age," *Cement and Concrete Research*, vol. 33, no. 12, pp. 2077–2084, 2003.

[11]. T. J.Hirsh, "Modulus of elasticity of concrete affected by elastic moduli of cement paste matrix and aggregate," *ACI Journal*, vol. 59, no. 3, pp. 427–452,

1962

[12]. U. J. Counto, "The effect of the elastic modulus of the aggregate on the elastic modulus, creep and creep recovery of concrete," *Magazine of Concrete Research*, vol. 16, pp. 129–138,1964

Impact of Wind on the Output of Photovoltaic panel and Solar Illuminance/Intensity

Joseph Amajama[1], Julie C. Ogbulezie[2], Nsed A. Akonjom[3], Victor C. Onuabuchi[4]

[1 & 2]Electronics and Computer Technology Unit, Department of Physics, University of Calabar – Nigeria

[3]Department of Physics/Geology/Geophysics, Federal University Ndufu-Alike Ikwo – Nigeria

[4]Department of Science and Computer Education, Enugu State University of Science and Technology – Nigeria

joeamajama2014@yahoo.com; +234-7036357493

Abstract— The impact of Wind on the output of photovoltaic panel and solar illuminance/intensity has been probed. The collision of the molecular particles of the air with that of the photonic particles of the sun results in a change in the propagation direction of the falling photonic particles towards the opposite direction of the incident air particles. Hence, at near constant air temperature of 87 ± 3 ^{0}F, air pressure of 29.87 ± 0.04 inHg, relative humidity of $72 \pm$ % and solar illuminance/intensity of 18000 ± 6000 Lux; photovoltaic panel outputs (short circuit current and open circuit voltage) and solar illuminance/intensity are favoured by increase in wind speed: that is, when the wind is towards the front of an observer (or panel) with the sun, some distance away in front and when the wind is towards the back of the observer (or panel) and the sun is behind. But, it is unfavourable when the wind's direction is towards the back of an observer (or panel) and the sun is some distance in front of the observer (or panel) or the sun is some distance behind the observer (or panel) and the wind direction is towards the front of the observer (or panel). For short, under same weather conditions, solar illuminance/intensity is favoured when the direction of the propagation of the solar photonic particles are in phase with the molecular particles of the wind and unfavoured when out of phase. Similarly under similar weather conditions, the output of a photovoltaic panel is favoured when the propagation of the solar photonic particles are in phase with the molecular particles of the wind and unfavoured when out of phase.

Keywords— Impact, Wind, Output, Photovoltaic panel, Solar illuminance, Solar intensity, Weather parameters and Particles.

INTRODUCTION

The photovoltaic panel is one of the green power generation technologies. Today, it finds application more than ever before in space crafts, marine navigation aids, telecommunication, cathodic protection, water pumping, remote area power supply (RAPS) systems and many others [1]. There is an ever-growing quest by power generation scientists and engineers to enhance the power efficiency of photovoltaic panels.

Photovoltaic cells are made of semiconductors materials such as Silicon (Si) or Cadmium Telluride (CdTe) [2]. Solar radiation is the energy that drives the photovoltaic cells. Solar radiations consist of high energetic particles [3]. These particles from the sun are observed in the form of light. As the particles rain on photovoltaic panels, electrons (or holes) are extracted and excited and generate current. The design of the semiconductor diode ensures that the released electrons move in a single or uniform direction and produces electricity [4]. Sets of solar cells are combined to make a solar panel. The amount of solar radiation/particles (solar illuminace/intensity) has a marked effect on the output of photovoltaic panel [5].

The amount of solar radiation reaching the earth's surface varies greatly because of changing atmospheric conditions and the changing position of the sun [6]. The atmospheric condition of a place at a particular time defines the weather of that place [7]. Weather parameters: air temperature, air pressure and relative humidity affect the output performance of the photovoltaic panel [8] [9] [10]. Wind is one of the weather parameters. This paper seeks to search the effect of wind on photovoltaic panel.

RESEARCH METHODOLOGY

Measurement of weather parameters: air temperature, air pressure, relative humidity and wind speed and direction were done intermittently in the course of daylight and simultaneously, solar illuminace/intensity and output voltage and current (open circuit voltage and short circuit current) of the photovoltaic panel.

The coordinates of the location in Calabar Metropolis where the experiment was carried out is: 4057'31.7"N, 8020'49.7"E. The measurements of the weather parameters: air temperature, air pressure, relative humidity and solar illuminance/intensity were done only when the direction of the wind was in the (west south west) WSW direction. This is because; the location where the experiment

was carried out was WSW to the rising sun from the east (E). The measurements were done between the hours of 6 am and 2 pm just before the sun starts sailing towards the west (W). This was done to reach a verdict on the wind speed effect on the photovoltaic panel output.

The photovoltaic panel is the mono-crystalline cell type with 1.5 W, 12V rating. The dimension of the photovoltaic plate, excluding the metallic frame of the panel is 45 cm by 14.5 cm. The panel was mounted on a platform of about 105 cm and exposed to direct sunlight. The outputs of the photovoltaic panel (current and voltage) were measured with the aid of a multi-metre and the solar illuminance/intensity was measured with a Digital Illuminance Meter (DT-1309 model).

RESULT AND ANALYSIS

The following figures where deduced from the experiments. Figs 1, 2, 3, 4, 5 and 6 show: Output Current versus Wind's Speed (WSW) without observing constant Air temperature, Air pressure, Relative humidity and Solar illuminance/intensity; Output current versus Wind (WSW) at near constant Air temperature (87 ± 3 ^{0}F), Air pressure (29.87 ± 0.04 inHg), Relative humidity (72 ± 6 %) and Solar illuminance/intensity (18000 ± 6000 Lux); Output Voltage versus Wind's Speed (WSW) without observing constant Air temperature, Air pressure, Relative humidity and Solar illuminance/intensity; Output current versus Wind (WSW) at near constant Air temperature (87 ± 3 ^{0}F), Air pressure (29.87 ± 0.04 inHg), Relative humidity (72 ± 6 %) and Solar illuminance/intensity (18000 ± 6000 Lux); Output Voltage versus Wind' Speed (WSW) without observing constant Air temperature, Air pressure, Relative humidity and Solar illuminance/intensity and Output current versus Wind (WSW) at near constant Air temperature (87 ± 3 ^{0}F), Air pressure (29.87 ± 0.04 inHg), Relative humidity (72 ± 6 %) and Solar illuminance/intensity (18000 ± 6000 Lux).
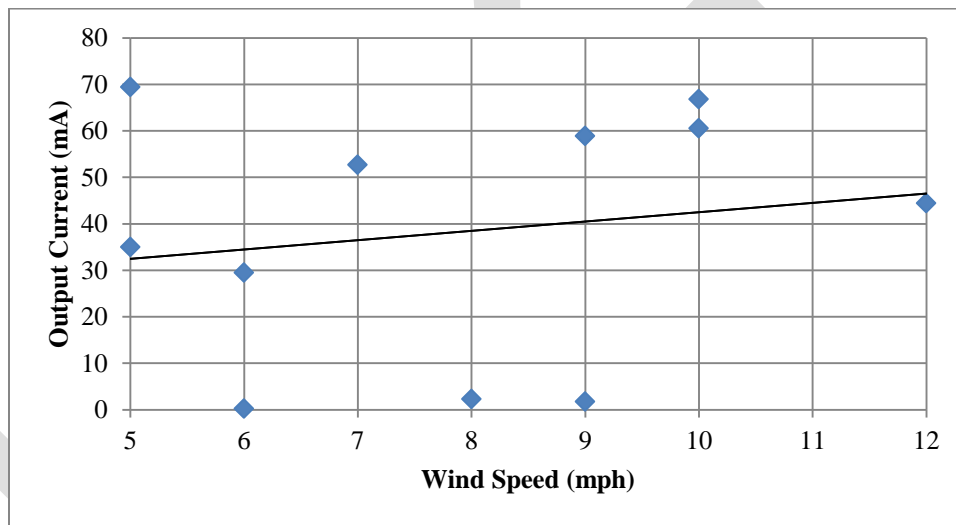
Fig.1: Output Current versus Wind's Speed (WSW) without observing constant Air temperature, Air pressure, Relative humidity and Solar illuminance/intensity
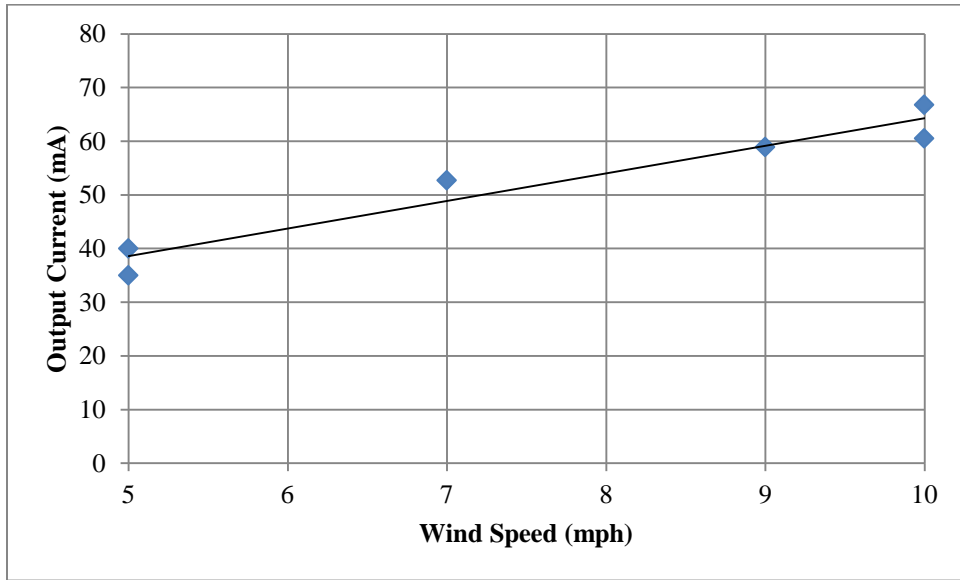
Fig. 2: Output current versus Wind (WSW) at near constant Air temperature (87 $\pm$ 3 ^{0}F), Air pressure (29.87 $\pm$ 0.04 inHg), Relative humidity (72 $\pm$ 6 %) and Solar illuminance/intensity (18000 $\pm$ 6000 Lux)
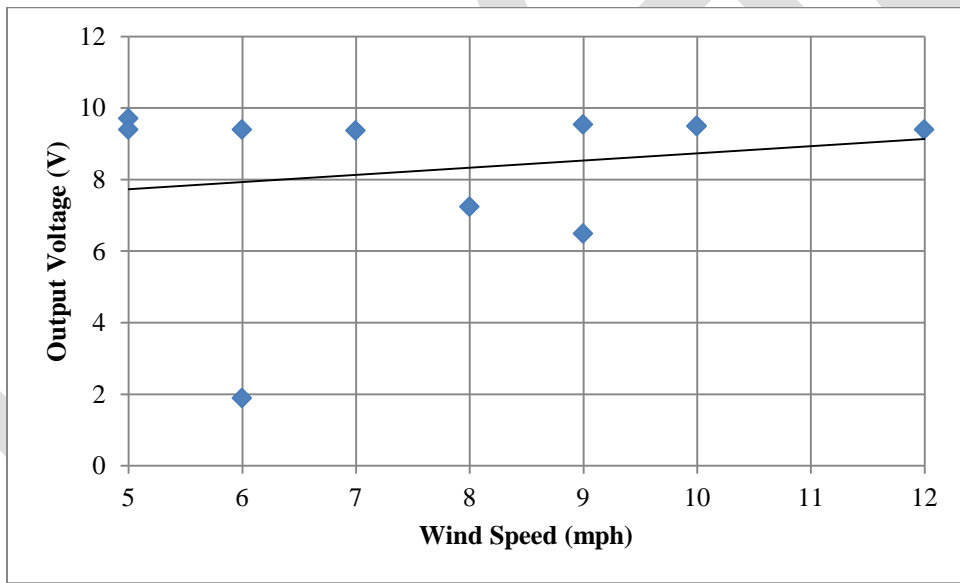
Fig. 3: Output Voltage versus Wind Speed (WSW) without observing constant Air temperature, Air pressure, Relative humidity and Solar illuminance/intensity
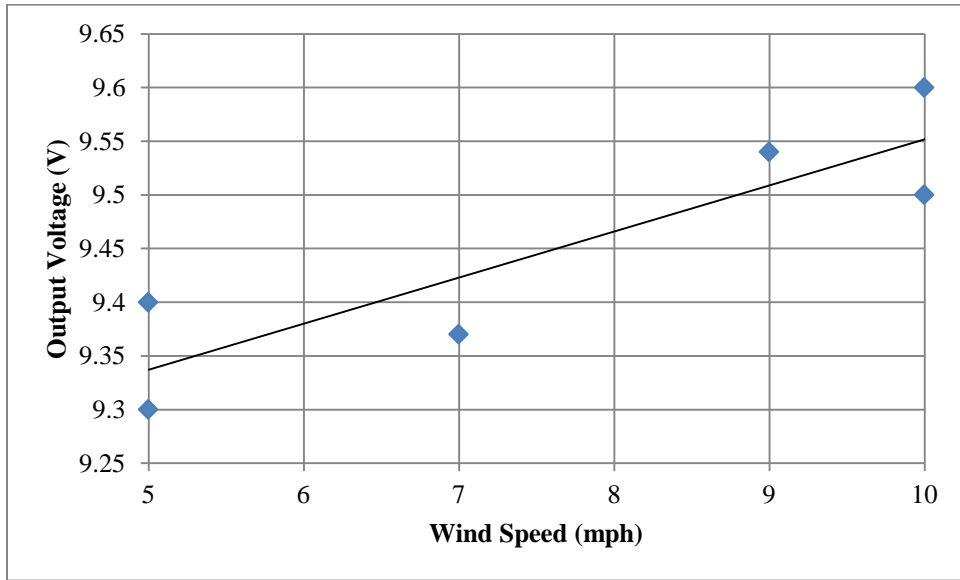
Fig. 4: Output current versus Wind (WSW) at near constant Air temperature (87 $\pm$ 3 ^{0}F), Air pressure (29.87 $\pm$ 0.04 inHg), Relative humidity (72 $\pm$ 6%) and Solar illuminance/intensity (18000 $\pm$ 6000 Lux)
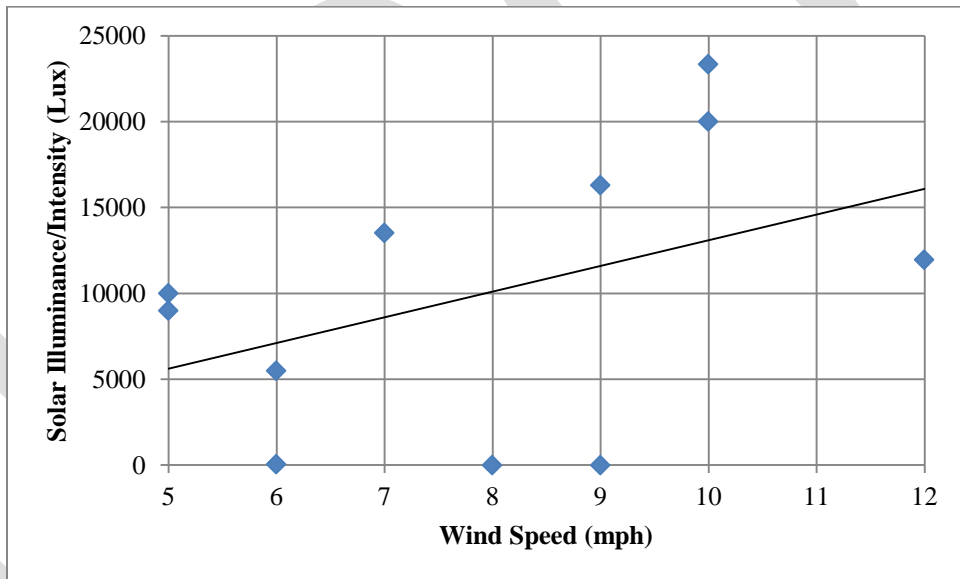
Fig. 5: Wind''s Speed (WSW) and Solar illumination/intensity without observing constant Air temperature, Air pressure, Relative humidity and Solar illuminance/intensity
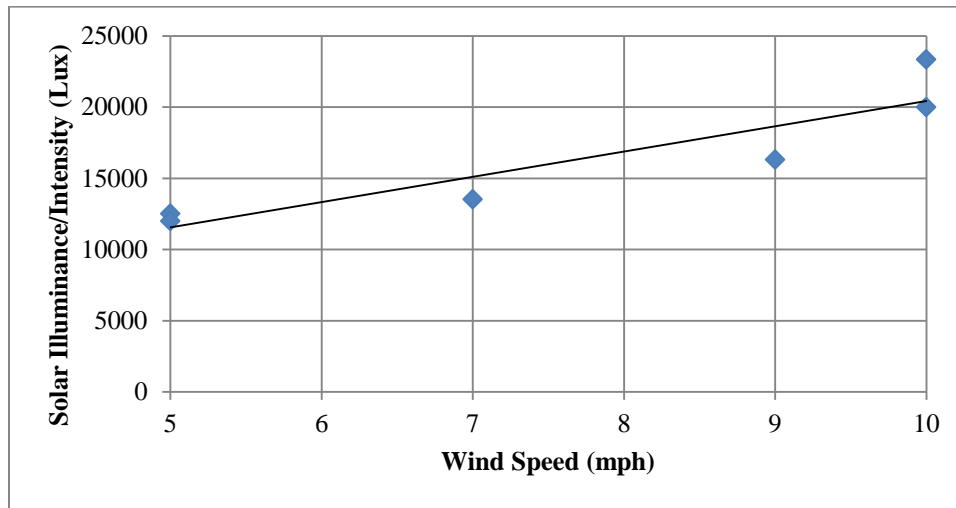
Fig. 6: Output current versus Wind (WSW) at near constant Air temperature ($87 \pm 3\,^0$F), Air pressure (29.87 ± 0.04 inHg), Relative humidity ($72 \pm 6\%$) and Solar illuminance/intensity (18000 ± 6000 Lux)
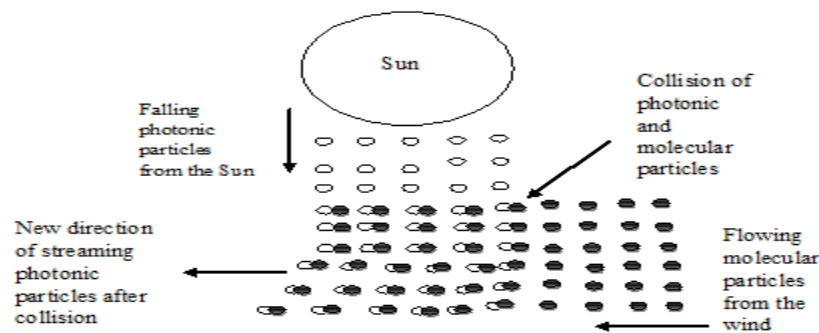
Fig. 7: Reflection of solar particles after collision with air molecular particles

Earlier research has shown that wind has an effect on propagating radio waves [11]. The radio waves transmit better if the wind propagates in a similar path as the wave from the transmitter antenna to the receiver antenna, but worse in the contrary direction [11]. That is, the speed of the wind waves aids the radio waves propagation to some extent if it is coursing parallel to the signal, but becomes detrimental when the wind wave is tangential or anti-parallel. In a mathematical light, the wind wave has a direct proportional relationship with the strength of radio waves if both are travelling in a parallel direction from the transmitter to the receiver antenna, but an inverse proportional relationship when they are at a tangent [11].

Electromagnetic radiations share similar properties [12]. Solar radiations are electromagnetic radiations just like radio waves. They are made up of photonic particles that exhibit waves. Similarly, the wind is a natural motion of air, strong enough to be felt [13]. The air is made of molecular particles that also exhibit waves in the form of a wind. The collision of the molecular particles of the air with that of the photonic particles of the sun results in a change in the propagation direction of the falling photonic particles towards the opposite direction of the incident air particles as captured in Fig. 7.

Hence, in the experiment conducted, the wind's direction was observed steady to deduce the effect of the wind' speed on the output of the photovoltaic panel. The position of the area where the experiment was conducted was in the WSW direction to the rising sun from E and measurements were taken when the wind was in the WSW direction. Figs 1, 2, 3 and 4 show that the output of the photovoltaic panel, that is, short circuit current and open circuit voltage increased slightly with increase in the wind's speed. This led to a conclusion, extracted from the representation in Figs 2 and 4 that: assuming all other weather parameters are observed constant: the wind's speed enhances the photovoltaic panel's output, if the wind's direction is towards the front of the panel and the sun is at some position away in front of the panel or the wind is towards the back of the panel and the sun is some distance behind the panel. The contrary of the output performance will be registered when the wind's direction is towards the back of the panel with the sun some position in front of the panel or the sun is some distance behind the front of the panel and the wind's direction is towards the front of the panel.

Also, Figs 5 and 6 have shown that: solar illuminace/intensity increases when the wind's speed is increased, with the wind's wave towards the front of an observer and the sun is some distance in front of the observer, but it is contrariwise when the wind's direction

is towards the back of the observer with the sun some position away in front of the observer or the wind's wave is towards the front of the observer and the sun is some distance behind the observer. Hence, Fig 5 spells; if other weather parameters are observed constant: solar illuminance/intensity is empowered by wind's speed, if the wind is towards the front of the observer and the sun is in front of the observer or the wind is towards the back of the observer and the sun is some distance behind the observer. And, solar illuminance/intensity is depowered when the wind is towards the front of the observer and the sun is some distance behind the observer or the wind is toward the back of the observer and the sun is some distance in front of the observer.

CONCLUSION

The research has shown that wind speed enhances photovoltaic panel's output when the wind is towards the front of the panel with the sun some distance away in front of the panel or the wind is towards the back of the panel and the sun is some distance behind the panel. The contrary of the performance above is the case when the wind towards the panel's front and the sun is some distance away behind the panel or the wind is towards the back of the panel and the sun is some distance in front and of the panel. Also, solar illuminance/intensity strength is increased with wind's speed, when the wind wave is towards the direction of the front of the observer with the sun some distance in front of the observer or the wind's direction is towards the back of the observer and the sun is behind the panel. But, the output performance is contrariwise when the wind's wave is towards the observer's back with the sun some distance in front of the observer or the wind's wave is towards the front of the observer and the sun is some distance behind the observer.

Hence, photovoltaic panel outputs (short circuit current and open circuit voltage) and solar illuminance/intensity are favoured by increase in wind speed when the wind is towards the position of observer's (or panel's) front with the sun some distance away in front of the observer or when the wind's direction is towards the back of the observer (or panel) with the sun behind the observer (or panel), but unfavourable when the wind is towards the position of the front of the observer (or panel) and the sun is some distance behind the observer (or panel) or the wind's direction is towards the back of the observer (or panel) and the sun is in front of the observer (or panel).

For short, under same weather conditions, solar illuminance/intensity is favoured when the direction of the propagation of the solar photonic particles are in phase with the molecular particles of the wind and unfavoured when out of phase. Similarly under similar weather conditions, the output of a photovoltaic panel is favoured when the propagation of the solar photonic particles are in phase with the molecular particles of the wind and unfavoured when out of phase

REFERENCES:

[1] Mekhilef S., Saidur R. & Kamalisarvestani M. (2012). Effect of dust, humidity and air velocity on efficiency of photovoltaic cells. Renewable and Sustainable Energy Reviews: 12, 2920-2925.

[2] Abiola-Ogedengbe A. (2013). Experimental investigation of wind effect on solar panels. Electronic Thesis and Dissertation Repository. Paper 1177.

[3] Droge W. (n.d.). Acceleration and Propagation of Solar Energetic Particles. Bartol Research Institute, University of Delaware, Newark, USA. Retrieved 30 August, 2016 from, http://www.lpl.arizona.edu/~guofan/literature/EnergeticParticles/SEP/acceleration%20and%20propagation%20of%20solar%20energy%20particles.pdf.

[4] Gray J. L. (2003). The physics of the solar cell. Chichester: John Wiley & Sons Ltd, 61-112.

[5] Amajama J. (2016). Effect of Solar ILLuminance (or Intensity) on Solar (Photovoltaic) cell's output and the use of Converging lenses and X or Gamma rays to enhance output performance. International Journal of Engineering Research and General science: 4 (4), 284-289.

[6] What influences the amount of solar radiation? - NREL (2016). In Shining on. Retrieved 30 August, 2016 from http://rredc.nrel.gov/solar/pubs/shining/chap3.html.

[7] Amajama, J. (2016). Impact of Weather Components on (UHF) Radio Signal. International Journal of Enginearing Research and General Science, 4 (3), 481-494.

[8] Amajama J. & S. E. Mopta (2016). Effect of Air temperature on the Output of photovoltaic panels and its relationship with Solar illuminance/intensity. International Journal of Scientific Engineering and Applied Science (IJSEAS): 2 (8), 161-166.

[9] Amajama J. (2016). Effect of Air Pressure on the Output of Photovoltaic Panel and Solar Illuminance (or Intensity). International Journal of Scientific Engineering and Applied Science (IJSEAS): 2 (8), 139-144.

[10] Amajama J. (2016). Effect of Relative humidity on Photovoltaic panels' Output and Solar Illuminance/Intensity. Journal of Scientific and Engineering Research (IJSEAS): 3 (4), 1-5.

[11] Amajama, J., & Oku, D. E (2016). Wind versus UHF Radio signal. International Journal of Science, Engineering and Technology Research (IJSETR); 5 (2), 583-585.

[12] Characteristics of electromagnetic waves (2016). In Daenotes. Retrieved 30 August, 2016 from http://www.daenotes.com/electronics/microwave-radar/characteristics-of-electromagnetic-waves.

[13] Wind (2016). Cambridge Advanced Learner's Dictionary and Thesaurus. Cambridge: Cambridge University Press.

Application of Wavelet Transform on Images: A Review

Garima Singh[1], Pushpa Koranga[2], DikendraVerma[3]

[1]M.Tech Scholar, GEHU, Bhimtal, singh.garima993@gmail.com

Abstract- Due to rise in the digital technology the use of digital images have also been increased. There are various techniques used for transformation of image being image compression, image denoising, image fragmentation etc. the compression technique is basically used so that the storage space used by the images can be minimized in this regard the wavelet plays a very important role. This paper focuses on the work that has been done in the field of image transformation using wavelets.

Keywords- Fourier Transform, Haar, PSNR, MSE, DWT, DCT, ROI

INTRODUCTION

Wavelet transform is basically an improved version of the Fourier transform where Fourier transform is a powerful tool that is used for analyzing the components of a stationary signal. Wavelet analysis is basically introduced to improve seismic signal analysis by switching from short time Fourier analysis to new better algorithm to detect and analyze abrupt changes in Daubechies[2,3], Mallet[4]. The major drawback encountered with Fourier transform is that it does not contain any local information.

'Wavelet' is a term introduced by Jean Morlet in the year 1982 which means small wave. The detailed mathematical study and applications of wavelet transform is given by Morlet & Grossman [5]. Wavelet analysis is basically used to solve difficult problems in the fields like mathematics, signal processing, pattern recognition, image processing, and computer graphics and in medical imaging.

WAVELET TRANSFORM

The word wavelet corresponds to a small wave (the sinusoids used in Fourier analysis are big waves) and in brief, a wavelet can be expressed as an oscillation that decays quickly.

The mathematical conditions for wavelets are:

$$\int_{-\infty}^{\infty} |\varphi(t)|^2 \, dt < \infty \tag{1}$$

$$\int_{-\infty}^{\infty} |\varphi(t)| \, dt = 0 \tag{2}$$

$$\int_{-\infty}^{\infty} \frac{|\varphi(w)|}{|w|} \, dw < \infty \tag{3}$$

The equation (3) is known as the admissibility condition.

The condition of the mother wavelet introduced by Morlet is given by:

$$\varphi_{a,b}(t) = \frac{1}{\sqrt{|a|}} \, \varphi\left(\frac{t-b}{a}\right), \, a, b \in R, a \neq 0 \tag{4}$$

Parameter a here is the scaling parameter or scale, which measures the degree of compression. The parameter b is the translation parameter which determines the time location of the wavelet. If $|a| < 1$, then the wavelet in equation (4) is the compressed version (smaller support in time-domain) of the mother wavelet and it corresponds mainly to the higher frequencies. On the other hand, when $|a| > 1$, then $\psi_{a,b}(t)$ has a larger time-width than $\psi(t)$ and corresponds to lower frequencies. Thus, wavelets have time-widths adapted to their frequencies. This is the main reason for the success of the Morlet wavelets in signal processing and time-frequency signal analysis.

The main advantage of using the wavelets is that they offer a simultaneous localization in time and frequency domain. The second main advantage of wavelets is that, using fast wavelet transform, it is computationally very fast. Wavelets even have the great advantage of being able to separate the fine details in a signal. Very small wavelets can be used to isolate very fine details in a signal, while very large wavelets can identify coarse details. Wavelet theory is capable of revealing aspects of data that other signal analysis

techniques miss the aspects like trends, breakdown points, and discontinuities in higher derivatives and self-similarity. It can often compress or de-noise a signal without appreciable degradation [18].

APPLICATIONS

K. Grochenig and W.R. Madych on their paper proposed the notion of multiresolution analysis and formulated a very interesting relation between the theory of compactly supported wavelet basis and the theory of similar tiling for construction [1].

Francois G. Meyer, Amir Averbuch and Jan- Olov Stromberg developed a new fast 2-D convolution- decimation algorithm with factorized non- separable 2-D filters to demonstrate that an advantage can be gained by constructing a basis adapted to target image. The algorithm proposed by them is four times faster than the standard convolution- decimation and produces great textures when applied on Barbara and fingerprint images. The block diagram for the wavelet packet compression algo is shown in fig.2 where the compression consists of three parts(a)selection of the best basis, and calculation of the coefficients of the image, (b)quantization of the coefficients, and (c) entropy coding [6].
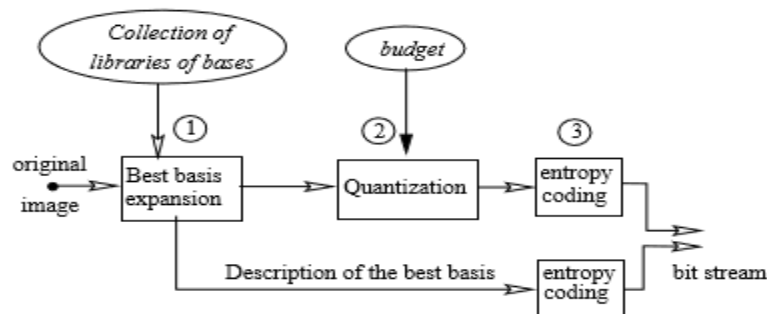
Fig. 2 Block diagram of wavelet packet compression algorithm [6]

Adrian Munteanu, Jan Cornelis, Geert Van Der Auwera, & Paul Cristea introduced a new wavelet based embedded compression technique that efficiently exploits the intraband dependencies and make use of the quad-tree approach to encode he significance maps [7].

Tim Flaherty, Yang Wang in their paper generated the result of Grochenig and W.R. Madych where they showed that a Haar- type wavelet basis of $L^2(R^n)$ can be constructed from the characteristic function X_Ω of a compact set Ω, if and only if Ω is an integral affine tile of Lebresgne measure[1] one to the multi-wavelet settings[8].

Edmud Y. Lam & Joseph W. Goodman offered a comprehensive mathematical analysis of the DCT coefficient distribution of natural images to show that by using a doubly stochastic model, the Laplacian distribution of the coefficients can be determined [9].

Charilaos Christopouloss, Athanassios Skodras & Touradj Ebrahimi proposed that JPEG 2000 is a superior technique to all the existing still image compression standards on the basis of their comparative study. The reconstructed images compared at 1 bpp by means of JPEG and JPEG 2000 is shown in fig.2 [10].
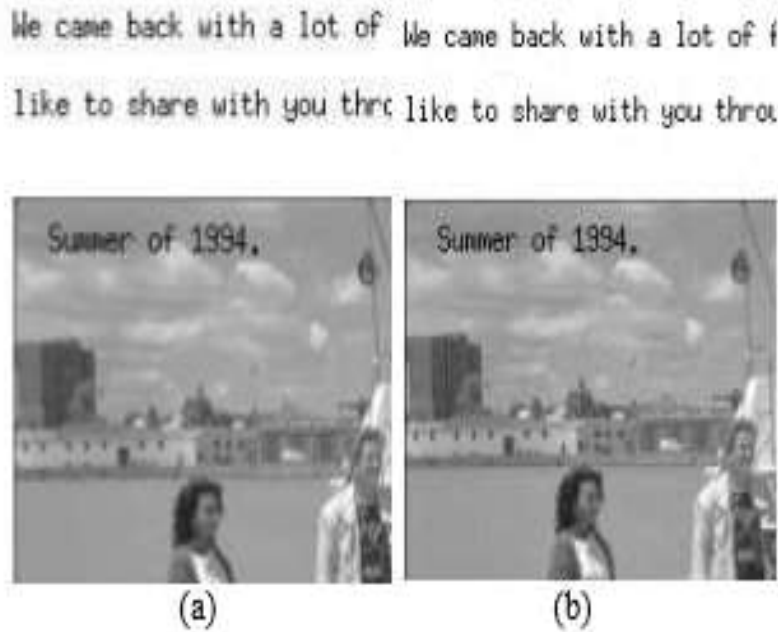
Fig. 2 Reconstructed images compressed at 1 bpp by means of: (a) JPEG (b) JPEG 2000 [10]

Albert Cohen & Basarab Matei introduced new multiscale representations for images which incorporates the L^2 error approach method in which the BW method gave the best results while the EA method provides the best results in case of visuality [11].

Sonja Grgic, Mislav Grgic and Zovko- Cihlar presented comparative study of different wavelet-based image compression system by examining wavelets on the basis of different wavelet functions, filter orders, no. of decompositions, compression ratio and image contents for implementation in a still image compression system [12].

Pitor Porwik, Agnieszka Lisowska presented graphic dependencies between the parts of Haar and wavelet spectra and also compared the wavelets in the 2-D space. The work show the graphical way of presentation of decomposition levels for both the Haar matrix based methods & wavelets [13].

R. Sudhakar, Ms R Karthiga, S. Jayaraman, proposed that the latest techniques such as EBCOT, ASWDR perform better than its predecessors such as EZW, WDR. They also produced some of the lowest errors per compression rate & highest perceptual quality by using wavelet coding techniques such as EZW, SPIHT, SPECK, WDR algorithm and ASWDR algorithm [14].

Uli Grasemann, Risto Mikkulainen, proposed a method based on the coevolutionary genetic algorithm used in [15] to evolve specialized wavelets for fingerprint images to show how the evolved wavelets outperform the hand-designed wavelet techniques. The progress of evolution during a typical run is shown at generations 1, 10, 20 and 50 in the figure 3. The top row in the figure shows the winner wavelets, and the bottom rows show the resulting compressed test image at 16:1. From the experiment it is concluded that the first generation produces a more or less random wavelet that performs poorly whereas, over the next generations, both image quality and the smoothness of the wavelets increase sharply and the performance keeps increasing after generation 50, although the differences are less obvious [16].
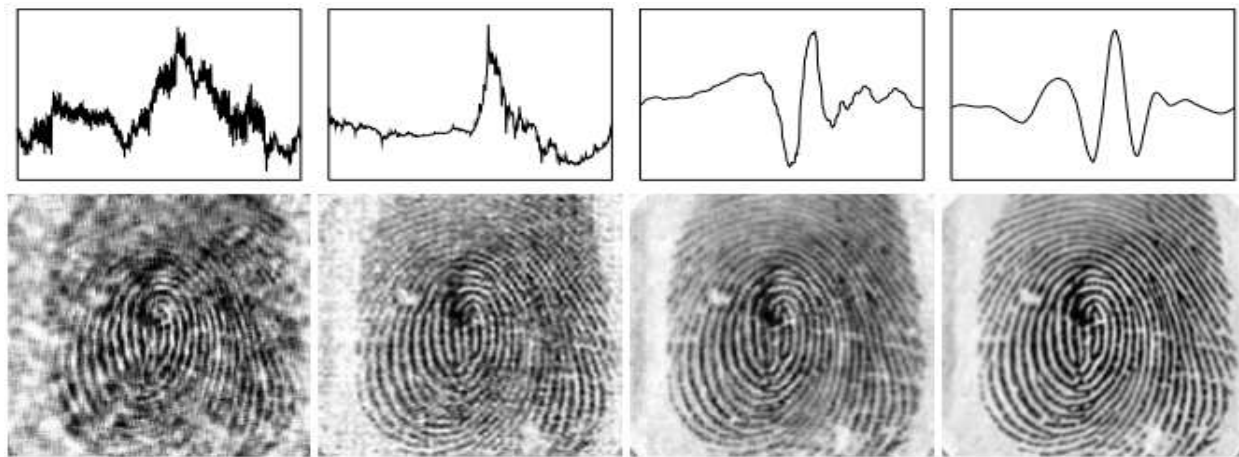
Generation 1   Generation 10   Generation 20   Generation 50

Fig.3 The progress of evolution during a typical run is shown at generations 1, 10, 20 and 50 [16]

Agnieszka Lisowska introduced theory of geometrical wavelets called wedgelets to code images with edges in a very efficient way. The theory of extended wedgelets was also presented to represent images in an efficient & sparse way then in case of known wedgelets and it produce a better visual effects along with higher compression ratio [17].

M. Sifuzzaman, M.R. Islam and M.Z. Ali presented the advantages of using wavelet transform compared to Fourier transform. The examination of the fingerprint performed by them is shown in fig 4 [18].

Original Image   Compressed Image

Fig .4 The fingerprint compressed image using wavelet transform reconstructed by the mathematician using software [18]

Anuj Bhardwaj and Rashid Ali used MFHWT algorithm for image compression to show that this algorithm produce better results than those obtained by any other methods on an average [19]. The result obtained by this method is shown in Fig.5

Lena Original Image   Applying 1 level MFHWT   Reconstructed Image
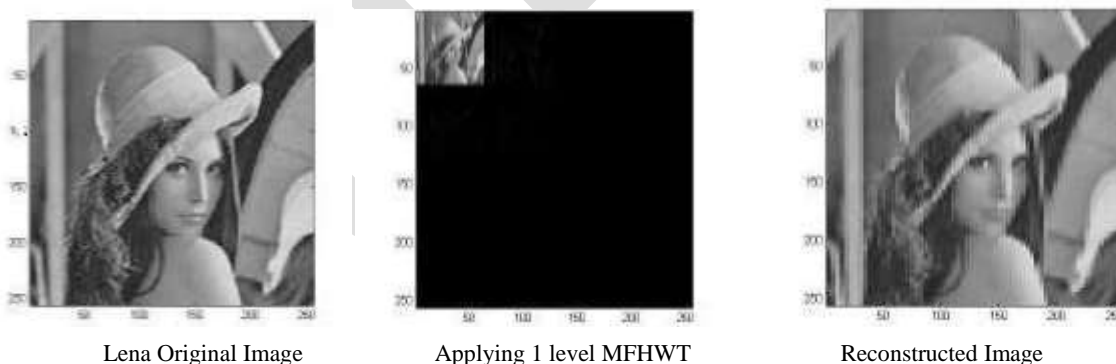
Fig.5 Operations performed on Lena.jpg Image [19]

Kamrul Hasan Talukder & Koichi Harada applied DWT to estimate the detail matrices from the information matrix to synthesize the reconstructed image using the estimated detail matrices and information matrix provided by the wavelet transform [20].

P. Raviraj & M.Y. Sanavullah developed computationally efficient & effective algorithm using Haar wavelet transform for compression of lossy images to minimize the computational requirements by applying various thresholding techniques to improve the quality of the reconstructed image. The experimental results for the cameraman image are shown in fig.6 [21].
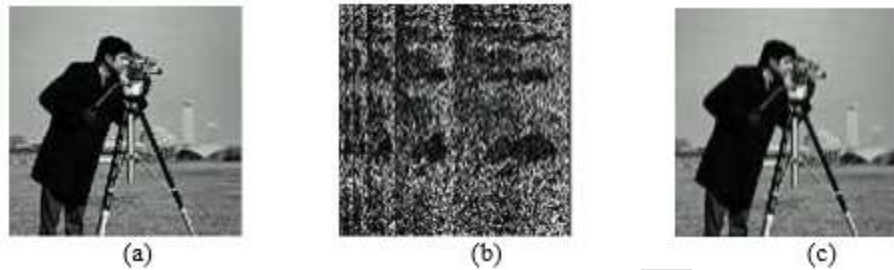
Fig.6. (a) Original, (b) Decomposed, (c) Reconstructed Images using Haar wavelet transform [21]

D. Vijendra Babu, Dr. N.R. Alamelu presented an enhanced image compression method using partial EZW algorithm. The proposed partial EZW algorithm on comparison with the EZW algo comes out to be more superior as it was capable of encoding each arbitrary shape ROI regions independently. This algorithm was also compared with other techniques such as SPIHT, modifies SPIHT and embedded Zero Wavelet [22].

Anitha S presented the overview of various compression techniques based on DCT, DWT, and ROI & Neural Networks for the 2-D images [23].

CONCLUSION

In this paper we have reviewed how we can process the images using wavelet transform and found that the result obtained from wavelet transform using various wavelets and thresholding techniques are much more effective as compared to the Fourier transform. New advancements are being rapidly done in this area & the number of thresholding and denoising techniques are increasing day by day to improve the mean square error and the peak signal to noise ratio of the images without sacrificing the quality of the image. Therefore, wavelet analysis has proven to be a major area of research.

REFERENCES:

[1] K.Grochenig, R.Madych, "Multiresolution Analysis, Haar Bases and Self-similar Tilings of R^n", IEEE TRANSACTIONS ON INFORMATION THEORY, VOL. 38, NO.2, MARCH 1992.

[2] Daubechies. I, "The wavelet transform, time-frequency localization and signal analysis", IEEE Transformation and Information Theory,36; 961- 1005, 1990.

[3] Daubechics. I, "Ten Lectures on Wavelets", SIAM, Philadelphia, PA, 1992

[4] Mallat.S, "A wavelet Tour of Signal Processing", Academi Press, New York, 1999.

[5] Grossmann. A, Morlet. J, "Decomposition of Hardy functions into square integrable wavelets of constant shape", SIAM Journal of Analysis, 15: 723-736, 1984.

[6] Francois G. Meyer, Amir Averbuch and Jan- Olov Stromberg, "Fast Adaptive Wavelet Packet Image Compression", IEEE Transactions on Image Processing, April1998.

[7] Adrian Munteanu, Jan Cornelis, Geert Van der Auwera, and Paul Cristea, ''Wavelet Image Compression— The Quadtree Coding Approach'', IEEE TRANSACTIONS ON INFORMATION TECHNOLOGY IN BIOMEDICINE, VOL. 3, NO. 3, SEPTEMBER 1999

[8] Tim Flaherty, Yang Wang, ''HAAR TYPE MULTI-WAVELET BASES AND SELFAFFINE MULTITILES", ASIAN J. MATH Vol. 3, No.2, pp. 387400, June 1999.

[9] Edmund Y. Lam, Joseph W. Goodman, "A Mathematical Analysis of the DCT Coefficient Distributions for Images", IEEE TRANSACTIONS ON IMAGE PROCESSING, VOL. 9, NO. 10, OCTOBER 2000.

[10] Charilaos Christopouloss, Athanassios Skodras, Touradj Ebrahimi,'' THE JPEG2000 STILL IMAGE CODING SYSTEM: AN OVERVIEW",IEEE Transactions on Consumer Electronics, Vol. 46, No. 4, pp. 1103-1127, November 2000.

[11] Albert Cohen, Basarab Matei, "COMPACT REPRESENTATION OF IMAGES BY EDGE ADAPTED MULTISCALE TRANSFORM", IEEE 2001.

[12] Sonja Grgic, Mislav Grgic, Zovko- Cihlar, ''Performance Analysis of Image Compression Using Wavelets", IEEE TRANSACTIONS ON INDUSTRIAL ELECTRONICS, VOL. 48, NO. 3, JUNE 2001.

[13] Pitor Porwik, Agnieszka Lisowska,'' The Haar–Wavelet Transform in Digital Image Processing: Its Status and Achievements", Machine Graphics & Vision, Vol. 13, n o. 1/2, 2004, pp .79-98.

[14] R. Sudhakar, Ms R Karthiga, S. Jayaraman," Image Compression using Coding of Wavelet Coefficients – A Survey", ICGST-GVIP Journal, Volume (5), Issue (6), June 2005.

[15] U. Grasemann and R. Miikkulainen,"Evolving wavelets using a coevolutionary genetic algorithm and lifting", Genetic and Evolutionary Computation Conference, volume II, pages 969–980, New York, NY, 2004, Springer.

[16] Uli Grasemann, Risto Mikkulainen, "Effective Image Compression using Evolved Wavelet", GECCO'05, June 25–29, 2005, Washington, DC, USA.

[17] Agnieszka Lisowska, "Extended Wedgelets — Geometrical Wavelets in Efficient Image Coding", Machine GRAPHICS & VISION, Vol.0, no.0, 0000, pp.

[18] M. Sifuzzaman, M.R. Islam, M.Z. Ali, "Application of Wavelet Transform and its Advantages Compared to Fourier Transform", Journal of Physical Sciences, Vol. 13, 2009.

[19] Anuj Bhardwaj, Rashid Ali, "Image Compression Using Modified Fast Haar Wavelet Transform", World Applied Sciences Journal 7 (5): 647-653, 2009.

[20] Kamrul Hasan Talukder & Koichi Harada, '' Haar Wavelet Based Approach for Image Compression and Quality Assessment of Compressed Image", IAENG International Journal of Applied Mathematics, 36:1, IJAM_36_1_9.

[21] P. Raviraj, M.Y. Sanavullah," The Modified 2D-Haar Wavelet Transformation in Image Compression", Middle-East Journal of Scientific Research 2 (2): 73-78, 2007.

[22] D. Vijendra Babu, Dr. N.R. Alamelu," Wavelet Based Medical Image Compression Using ROI EZW", Int. J. of Recent Trends in Engineering and Technology, Vol. 1, No. 3, Nov 2009.

[23] Anitha S,''2D image compression technique-A survey", International Journal of Scientific & Engineering Research ,Volume 2, Issue 7, July-2011.

Response of Structures Composed of Random Visco-elastic Material Properties

Neethu Balakrishnan[1], Anima P [2]

[1]PG Scholar, Dept of Civil Engineering, Universal Engineering College, Vallivattom, Thrissur, Kerala, India

[2]Associate professor, Dept of Civil Engineering, Universal Engineering College, Vallivattom, Thrissur, Kerala, India

[1]neethubalakrishnan69@gmail.com

Abstract— Visco-elasticity is the property of materials that exhibit both viscous and elastic characteristics when undergoing deformation due to applied external load. Visco-elastic materials (VEM) properties depend both on temperature and time. To mathematically characterize the properties of visco-elastic materials, Prony series and Laplace Transform are utilized. In general, these materials exhibit certain amount of scatter in their properties due to the dispersion in the values of material properties and applied external load. For design purposes, it is essential to know the potential variations in the structural response due to the system or external randomness. In the present work, the static and dynamic response of structures, where certain components are composed of visco-elastic materials are considered. Two cases are studied. The first consists of studying the response of solid rocket propellant grain and the second study is on vibration isolators for a PCB with aerospace application. The study considers the random response due to presence of inherent scatter in the values of applied loads and material properties. For sensitive applications where design margins are narrow, it is important to consider the dispersions in design parameters for optimal and safe design based on rational decisions than arbitrary safety factors.

Keywords— Visco-elastic Materials, Finite element method, Prony series, Equivalent modulus

NOMENCLATURE

D	Displacement
E	Young's modulus
P	Load
C_X	Coefficient of variation in the random variable X
δ	Deflection
E_e, ρ_i, E_i, D_g, τ_j, D_j,	Degrees of freedom of the Prony series
E_g, D_g	Independent terms of the Prony series
E_i, D_j	Dependent terms of the Prony series
$E(t)$	Relaxation modulus
G	Shear
$g(t)$	Shear relaxation modulus as a function of time
G	Acceleration due to gravity
G_∞	Long term modulus or Equilibrium modulus

INTRODUCTION

The mechanical properties of crystalline materials, at constant temperature, can be described in terms of stress and strain, the mathematical description of visco-elastic materials involves the introduction of a new variable time. Visco-elasticity and related phenomena are of great importance in the study of biological materials. Just as strain can be measured in more than one way, so the related rate of strain (i.e., the amount of strain per unit time) can be measured in a number of different ways [1]. A visco-elastic material will return to its original shape after any deforming force has been removed (i.e., it will show an elastic response) even though it will take time to do so (i.e., it will have a viscous component to the response). Visco-elasticity is the property of materials that exhibit both viscous (dashpot-like) and elastic (spring-like) characteristics when undergoing deformation. Food, synthetic polymers, wood, soil and biological soft tissue as well as metals at high temperature display significant visco-elastic effects. The term

elasticity refers to solid materials, and in these cases the stress is a linear function of the strain. Visco-elastic material (VEM) properties depending on both temperature and time. When unloaded, it eventually returns to the original, undeformed state. [1].

Arvin. H [1] studied comparing molecular theories that describe VEMs behavior and models based on fractional derivatives. Their work demonstrated that, from a reduced number of parameters, it is possible to predict with some precision the dynamic behavior of those materials. A methodology was established to perform the modeling in finite beam elements and rectangular plates with a VEM layer, in order to attenuate the effect of vibration on structures. Ayatac Arikoglu [2] studied the vibration and thermal buckling behaviour of sandwich beams with composite facings and visco-elastic core in comparison with sandwich plate. They examined the effects of fiber angle, aspect ratio and the core thickness on the performance of the beam and plate elements. They concluded that there is a considerable difference between the predictions of mentioned elements for some fiber angles. Prony series is used in an attempt to apply an efficient numerical method in the time domain to relate relaxation and creep functions of VEMs, which were tested using experimental data from a few polymeric materials. Carlos Alberto Bavastri [4] discussed about the method for determining the Prony Series coefficients of a visco-elastic relaxation modulus using load versus time data for different sequences of load ratio adjusted to the convolution integrals of tested materials. For lightweight and flexible structures, the sandwich with a visco-elastic core is very effective in controlling and reducing vibration responses. Jayakumar. K et.al, [5] discussed about the Multivariate method to examine the response statistics to account scatter in the material properties.

In the present work, to generate the equivalent modulus of visco-elastic materials relaxation modulus versus time curve is used. This is utilized to carry out frequency and transient response analysis of structures composed of visco-elastic materials. The material randomness is considered i.e., material properties are not deterministic. Finite element method based software PreWin/ FEAST^{SMT} is used for analysis. PreWin/ FEAST^{SMT} is indigenous software continuously being developed at Vikram Sarabhai Space Centre/Indian Space Research Organization.

PRONY SERIES

For visco-elastic materials it is necessary to consider the time-dependent response. The time-dependent uniaxial stress $\sigma(t)$ and strain $\varepsilon(t)$ can be obtained by equation (1a and 1b) considering this material under isothermal, nonaging linear conditions [4].

$$\sigma(t) = \int_{\tau=0}^{\tau=t} E(t-\tau)\frac{\partial \varepsilon(t)}{\partial \tau}\,d\tau \qquad (1a) \; , \qquad \varepsilon(t) = \int_{\tau=0}^{\tau=t} D(t-\tau)\frac{\partial \sigma(t)}{\partial \tau}\,d\tau \qquad (1b)$$

where t is the time-like integration variable and $E(t)$ and $D(t)$ are experimentally obtained relaxation modulus and creep compliance, respectively.

Even though these material functions are obtained from experimental observation, it is necessary to represent them by mathematical functions in order to perform stress analysis on visco-elastic materials and to inter convert these visco-elastic functions. Among all analytical representations available, the Prony Series is one of the most used due to computational efficiency associated with its exponential basis function. The analytical description of relaxation modulus $E(t)$ and creep compliance $D(t)$ by Prony series is expressed in equation (2a and 2b)

$$E(t) = E_e + \sum_{i=1}^{M} E_i e^{-\frac{t}{\tau_i}} \qquad (2a), \qquad D(t) = D_g + \sum_{i=1}^{N} D_j \left(1 - e^{-\frac{t}{\tau_j}}\right) \qquad (2b)$$

where, E_e, ρ_i, E_i, and D_g, τ_j, D_j, are degrees of freedom of the Prony series. Equations (2a and 2b) are obtained representing the viscoelastic material by a mechanical model consisting of linear springs and dashpots. The terms E_e and D_g are called independent terms. The exponential terms ρ_i and τ_j are known as time constants because they appear in association with the time variable t. The set of terms E_i and D_j are the dependent terms of the Prony series and the number of terms used (M and N, respectively) is determined accordingly to the experimental data. Usually around 8 to 16 terms must be used in Prony series equation (2a and 2b) to have a satisfactory mathematical model to be fitted from experimental data [3]. The Prony series for the shear relaxation is

$$g(t) = G_\infty + \sum_{i=1}^{N} G_i e^{-\frac{t}{\tau_i}} \qquad (3)$$

where, $g(t)$ is the shear relaxation modulus, G_∞ is the long term modulus or equilibrium modulus, G_i is the constants, t is the time, τ_i is the relaxation times. The advantage of the Prony series is that its Laplace transform can be easily obtained.

PRONY SERIES IN LAPLACE TRANSFORM

Using the equation (3) for shear relaxation, when t = 0, shear relaxation modulus will be

$$g(t = 0) = G_0 = G_\infty + \sum_{i=1}^{N} G_i \qquad (4)$$

From eq. (4) we can find G_∞, and substituting this in equation (3), we get

$$g(t) = G_0 - \sum_{i=1}^{N} G_i \left(1 - e^{-\frac{t}{\tau_i}}\right) \qquad (5)$$

Applying Laplace transform to eq. (5)

$$G(S) = \frac{G_0 - \sum_{i=1}^{N} G_i}{S} + \sum_{i=1}^{N} \frac{G_i}{S + \frac{1}{\tau_i}} \qquad (6)$$

Substituting the values of G_i, τ_i and $S = \frac{1}{2t}$, to determine, G_0

$$G_0 = \frac{E}{2(1 + \nu)} \qquad (7)$$

where, E = Young's modulus (1594.11), ν = Poisson's ratio (0.4924). From this we can find the value of $g(t)$ and $G(S)$ for each time.

PROBABILISTIC ANALYSIS

Probabilistic composite mechanics and probabilistic composite structural analysis are formal methods, which are used to quantify the scatter that is observed in composite material properties and structural response [6]. Probabilistic structural response estimate for different random input parameters the following methods have widely been applied: Monte-Carlo simulation, Convex method, Multi-variate method.

In this present work, Multi- variate method is used for determining the statistical measures, mean and standard deviation. The sensitivity of the responses due to scatter in the values of system parameters are expressed using their respective (non-dimensional) coefficient of variation.

The dependent variable ψ and displacement δ is functionally related to the basic random variables E, μ, t, l and ρ. For mathematical simplicity these variables are denoted by X_1, X_2,...,X_5, respectively. It is assumed that these basic variables have small dispersion about their mean values X_1^*, X_2^*,..., X_5^*, respectively. This implies a good quality control during the manufacturing process, which is true for the most aerospace applications. Under this assumption, ψ lends itself to Taylor series expansion about the mean values [5]. Keeping only up to second power of small quantities, ψ can be expressed as:

$$\psi(X_1, X_2, \ldots\ldots, X_3)$$
$$= \psi(X_1^*, X_{2,\ldots\ldots}^* X_5^*) + \sum_{i=0}^{5} \frac{\partial \psi}{\partial X_i}(X_i - X_i^*) + \frac{1}{2}\sum_{i=1}^{5}\sum_{j=1}^{5} \frac{\partial^2 \psi}{\partial X_i \partial X_j}(X_i - X_i^*)(X_j - X_j^*) \quad (8)$$

All derivatives of ψ are evaluated at the mean values of the basic random variables [5]. The mean and the variance of the independent variable ψ are obtained from equation (8).

$$Var(\Psi) = E\big[(\Psi - \mu_X)^2\big]$$

$$\cong \frac{1}{2}\sum_{i=0}^{5} Var(X_i)\left(\frac{\partial \Psi}{\partial X_i}\right)^2 + \frac{1}{4}\sum_{i=1}^{5}\sum_{j=1}^{5} \frac{\partial^2 \Psi}{\partial X_i^2}\frac{\partial^2 \Psi}{\partial X_j^2} Var(X_i)Var(X_j) \qquad (9)$$

The positive square root of variance is the standard deviation.

A. MEAN

The mean value μ_x is simply the average value. It is also known as the expected value. If X is continuous, probability density function of X is $f_X(x)$: Therefore, the mean is

$$E[X] = \mu_x = \int_{-\infty}^{+\infty} x\, f_X(x)dx \qquad (10)$$

B. VARIANCE

The variance of σ^2_x is the second moment of the PDF about the mean, expressed as $Var(X)$:

$$Var(X) = \int_{-\infty}^{+\infty} (\eta - \mu_x)^2 \cdot f_X(\eta)d\eta \qquad (11)$$

C. STANDARD DEVIATION

The positive square root of the variance is known as the standard deviation σ_X :

$$\sigma_X = \sqrt{Var(X)} \qquad (12)$$

D. COEFFICIENT OF VARIATION

Coefficient of variation C_X a non-dimensional term expressed in %, is the ratio of the standard deviation and the mean:

$$C_X = \frac{\sigma_x}{\mu_x} \times 100 \qquad (13)$$

ANALYSIS

A. STATIC ANALYSIS FOR SOLID PROPELLANT ROCKET

A solid propellant rocket is the simplest form of chemical propulsion. The fuel and the oxidizer are both incorporated in a single solid called the propellant grain, located inside a container called the motor casing. A solid propellant is combustive matter, stable at room temperature, which once ignited, releases gas continuously at elevated temperature. A grain must hold its shape over an extended temperature range, and must withstand the stresses and strains imposed on it during handling, ignition, and firing in a rocket. A schematic illustration of the typical solid propellant rocket motor is shown in Figure 1.
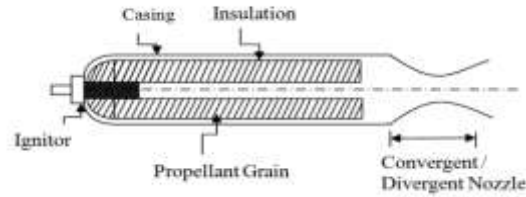
Figure 1: Typical Solid Propellant Motor

An axisymmetric cylindrical shaped solid propellant grain is modeled for structural analysis. Insulation as well as steel casing is provided around propellant grain. The typical material properties are considered.

The Young's modulus, pressure, Poisson's ratio are considered to have scatter about their mean, which are the random independent variables. The deflections are obtained for a range of dispersion in the random variables and are expressed as coefficient of variation.
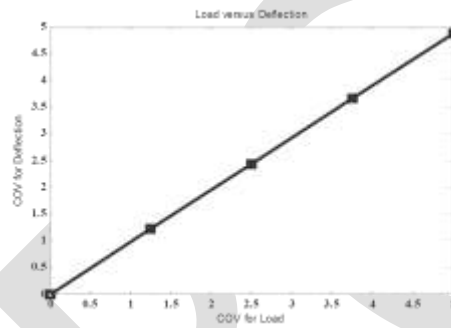
Figure 2: Scatter in deflection due to dispersion in pressure P
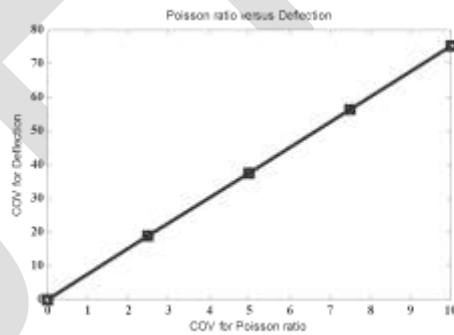
Figure 3: Scatter in deflection due to dispersion in Poisson's Ratio μ
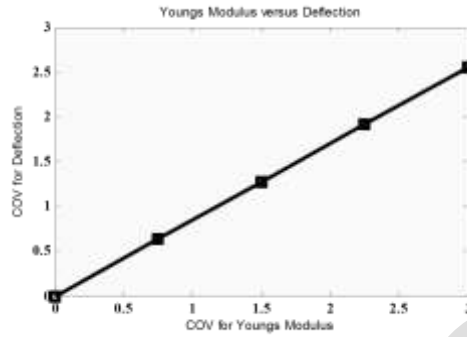
Figure 4: Scatter in deflection due to dispersion in Young's Modulus E

From the analysis it is found that the deformation of solid propellant is more sensitive to change in the values of pressure and Poisson's ratio than Young's modulus shown in Figure 2, 3, 4.

B. TRANSIENT RESPONSE ANALYSIS FOR PCB BOX

A Printed Circuit Board (PCB) mechanically supports and electrically connects electronic components using conductive tracks, pads and other features etched from copper sheets laminated onto a non-conductive substrate. Advanced PCBs may contain components - capacitors, resistors or active devices - embedded in the substrate.

A PCB box to applied base excitation is the modeled for structural analysis. This PCB box is mounted on visco-elastic pads for vibration isolation. The Young's modulus is considered to have scatter about their mean, which are the random independent variable. The displacement, velocity and acceleration are obtained for different base excitation for a range of dispersion in the random variable.
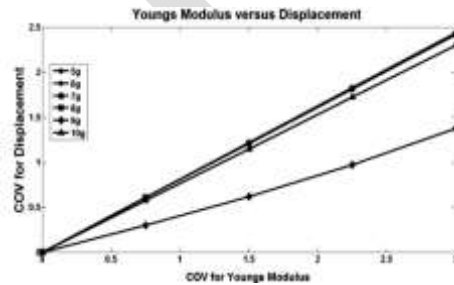
Figure 5: Scatter in displacement due to dispersion in Young's Modulus
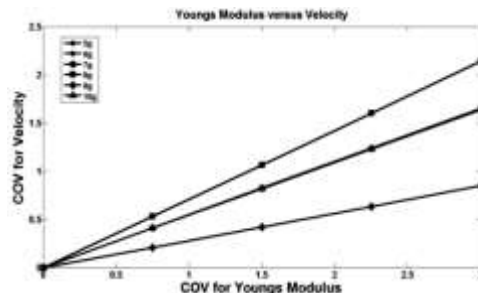
Figure 6: Scatter in velocity due to dispersion   in Young's Modulus
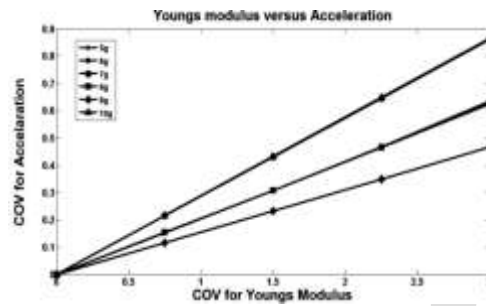
Figure 7: Scatter in acceleration due to Dispersion in Young's Modulus

The frequency response of PCB to applied base excitation is examined for the given configuration. Generally, aerospace structures are designed for high natural frequencies. This is to ensure that the excitation frequencies do not cause resonance in the system.

The PCB box mentioned in section B is considered for transient response analysis.
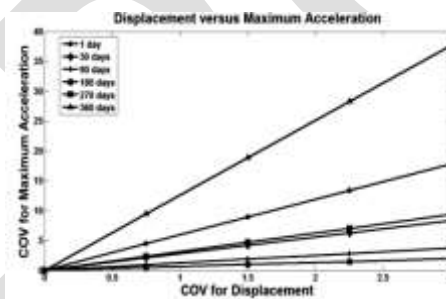
Figure 8: Scatter in maximum acceleration due to dispersion in the initial displacement

From the analysis, it is inferred that the maximum acceleration response increases due to poor vibration isolation by the visco-elastic pads shown in Figure 8.

CONCLUSION

In this paper, structures composed of VEM are examined, for static load and base excitation case. The response statistics due to dispersions in the applied load and system properties are evaluated. This aids in identifying the most sensitive parameter or load which influence its behavior.

The static response of the structure is sensitive to the Young's modulus and applied load. The Young's modulus dispersion does not cause large dispersions in the acceleration response, but the initial displacement does. For low margin design, such studies are useful for optimal and safe design.

ACKNOWLEDGEMENT

REFERENCES:

[1] Arvin.H, Sadighi.M, (2010) "A numerical study of free and forced vibration of composite sandwich beam with viscoelastic core" Journal of Composites Structures., pp.996-1008

[2] Aytac Arikoglu, Ibrahim Ozkol., (2010) "Vibration analysis of composite sandwich beams with viscoelastic core" Journal of Composites Structures., pp.3031-3039

[3] Bennigof.K., Jefferey, "Frequency Response Analysis Of Complex Structures: Issues,Trends and Recent Developments"47thAIAA/ASME/AHS/ASC Structures Structural Dynamics and Materials

[4] Carlos Alberto Bavastri, Juliana E. Lopes Pacheco (2015) **"**Visco-elastic Relaxation Modulus Characterization Using Prony Series", Journal of Solids and Structures 12. pp. 420-445

[5] Jayakumar K, D.Yadav, B. Nageswara Rao., (2009) "Nonlinear free vibration analysis of simply supported piezo-laminated plates with random actuation electric potential difference and material properties" Communications in Nonlinear Science and Numerical Simulation 14.,pp.1646-1663

[6] Justin Kaiser., Jayakumar. K., (2010) "Free vibration response of anistropic composite plates with random material properties.

[7] J.L.White "Finite element in linear viscoelasticity" The Boeing Company Kent, Washington

[8] Meirovitch.,Leonard "Fundamental of Vibrations" Mc.Graw-Hill International Edition

[9] Mohamed Lamjed Bouazizi, Noureddine Bouhaddi.,(2015) " Model reduction methods for viscoelastic sandwich structures in frequency and time domains" Journal Of Composites Structures.,pp.12-29

[10] N. T. Asnani (1984) "Vibration and damping analysis of multilayered rectangular plates with constrained viscoelastic layers"., Journal of Sound and Vibration., 597-614

[11] Rade, D.A, Faria,A.W., (2010) " Sensitivity analysis of frequency response functions of composite sandwich plates containing viscoelastic layers" Journal Of Composites Structures.,pp.364-374

[12] T.A. Stock, P.X. Bellini and P.L.N. Murthy, A Probabilistic Approach to Composite Micromechanics, NASA Technical Memorandum 101366, Virginia, 1988

[13] Tzikang Chen, "Determining a Prony Series for a viscoelastic material from time varying strain data": NASA/TM-2000-210123

[14] Zak,A.R.,(1967) "Structural Analysis of Realistic Solid-Propellant Materials."Journal of Spacecraft and Rockets5, pp, 270

BAYESIAN FILTER TECHNIQUE FOR SPAM E-MAIL DETECTION: AN OVERVIEW

Sayali Wavhal

B.Tech Electrical, Veermata Jijabai Technological Institute, Matunga, Mumbai

Email: sayali.wavhal@gmail.com

Abstract— As web is expanding day by day and people generally rely on web for communication, e-mails are the fastest way to send information from one place to another. E-mail is an effective tool for communication as it saves a lot of time and cost. Spam, also known as Unsolicited Commercial E-mail, is an unfortunate problem on the Internet. Spam increases the load on the servers and the bandwidth of the Internet Service Providers and the added cost to handle this load must be compensated by the users. Mailbox management has become a big task because these unwanted emails clog the inbox. In this paper, we review one of the most popular Machine Learning methods using text categorization, Bayesian filter for Spam E-mail Detection

Keywords— Spam, unsolicited, text categorization, machine learning, spam e-mail detection, Bayesian filter.

INTRODUCTION

The e-mailboxes of millions of people are cluttered with unsolicited bulk email known as 'spam'. Many email spam messages may also contain disguised links that appear to be for familiar websites but in fact lead to phishing web sites or sites that are hosting malware. Being incredibly cheap to send, spam causes a lot of trouble to the Internet community: large amounts of spam-traffic between servers cause delays in delivery of legitimate email, people with dialup Internet access have to spend bandwidth downloading junk email. Sorting out the unwanted messages takes time and introduces a risk of deleting legitimate mail by mistake. According to a Cyberoam report in 2014, there are an average of 54 billion spam messages sent every day. Although, it is commonly believed that a change in Internet protocols can be the only effective solution to the spam problem, it is acknowledged that this cannot be achieved in a short time. In recent years, anti-spam filters have become necessary tools to face up the continuously growing spam phenomenon.

SPAM FILTERS

There are two general approaches to mail filtering: knowledge engineering and machine learning.

- ➢ Knowledge Engineering (KE): A set of rules is created according to which messages are categorized as spam or legitimate mail. Some of the methods following this approach are as follows:
  1. Domain filter: They allow mails from specific domain only. Keeping track of domains that are valid for the user is cumbersome.
  2. Blacklisting filters: They use the database of known abusers and filter unknown addresses as well. This requires constant updating of the database.
  3. Whitelist filters: Mailer programs learns all the contacts of a user and let mail from those contacts through. This means everyone should first communicate his/her e-mail ID to the user and only then send email.

  The major drawback of this method is that the set of rules must be constantly updated, and maintaining it is not convenient for most users.
- ➢ Machine Learning (ML): The machine learning approach does not require specifying any rules explicitly. Instead, a set of pre-classified documents is needed. A specific algorithm is then used to "learn" the classification rules from this data.

Use of text categorization techniques based on machine learning and pattern recognition approaches for email semantic content analysis is an effective way of spam detection compared to the knowledge engineering approach. In this work, we focus on Bayesian spam filters based on textual content analysis. The advantages of these techniques are the automatic construction of classification rules and their potentially higher generalisation capability with respect to manually encoded rules.

TEXT MINING

With regard to the analysis of the semantic content of e-mails, several researchers in recent years have investigated text categorisation techniques based on the machine learning and pattern recognition approaches due to their potentially higher generalization capability.

The first step, named tokenization, consists of extracting a plain text representation of document content. Prepare a corpus, which is a collection of all documents. Inspect the corpus and identify the real words. Different text may contain "Hello!", "Hello," "hello…" etc. for example. We would consider all of these the same. Clean the corpus by translating all letters to lower case, remove numbers, punctuation and non-content words like "I", "me", "you" etc. and finally remove the excess white space. In the end, tokenize the corpus. A token is a single element in a text string, in most cases a word. From here, Naïve Bayes classifier is used to build a spam filter based on the words in the message.

NAÏVE BAYES CLASSIFIER

Bayesian filters, considered the most advanced form of content-based filtering, employ the laws of mathematical probability to determine which messages are legitimate and which are spam. Naive Bayes classifiers work by correlating the use of tokens, with spam and non-spam e-mails and then using Bayes' theorem to calculate a probability that an email is or is not spam.

Particular words have particular probabilities of occurring in spam email and in legitimate email. The filter does not know these probabilities in advance, and must first be trained so it can build them up. To train the filter, the user must manually indicate whether a new email is spam or not. For all words in each training email, the filter will adjust the probabilities that each word will appear in spam or legitimate email in its database. After training, the word probabilities (also known as likelihood functions) are used to compute the probability that an email with a particular set of words in it belongs to either category. Each word in the email contributes to the email's spam probability, or only the most interesting words. This contribution is called the posterior probability and is computed using Bayes' theorem. Then, the email's spam probability is computed over all words in the email, and if the total exceeds a certain threshold (say 95%), the filter will mark the email as a spam. Bayesian email filters utilize Bayes' theorem. Bayes' theorem is used several times in the context of spam.

➢ **Computing the probability that a message containing a given word is spam:**
   Let's suppose the suspected message contains the word "X" is likely to be a spam.
   The formula used by the software to determine that is derived from Bayes' theorem,

$$\Pr(S|W) = \frac{\Pr(W|S) \cdot \Pr(S)}{\Pr(W|S) \cdot \Pr(S) + \Pr(W|H) \cdot \Pr(H)}$$

   Where :
   Pr(S|W) is the probability that a message is a spam, knowing that the word "X" is in it;
   Pr(S) is the overall probability that any given message is spam;
   Pr(W|S) is the probability that the word "X" appears in spam messages;
   Pr(H) is the overall probability that any given message is not spam(is ham);
   Pr(W|H) is the probability that the word "X" appears in ham messages.

Of course, determining whether a message is spam or ham based only on the presence of the word "X" is error-prone, which is why Bayesian spam software tries to consider several words and combine their spamicities to determine a message's overall probability of being spam. Most reports have shown that Bayesian filters works correctly over 99 percent for one user.

SHORTCOMINGS OF BAYESIAN SPAM FILTERING

Depending on the implementation, Bayesian spam filtering may be susceptible to Bayesian poisoning, a technique used by spammers in an attempt to degrade the effectiveness of spam filters that rely on Bayesian filtering. A spammer practicing Bayesian poisoning will send out emails with large amounts of legitimate text (gathered from legitimate news or literary sources). Spammer tactics include insertion of random innocuous words that are not normally associated with spam, thereby decreasing the email's spam score, making it more likely to slip past a Bayesian spam filter. Another technique used to try to defeat Bayesian spam filters is to replace text with pictures, either directly included or linked. The whole text of the message, or some part of it, is replaced with a picture where the same text is "drawn". The spam filter is usually unable to analyze this picture. It is worth pointing out that this trick is often used in phishing e-mails, which are one of the most harmful kinds of spam.

SPAM FILTERING FOR TEXT EMBEDDED WITH IMAGES

Although the effectiveness of text categorisation techniques could be affected by tricks used by spammers for content obscuring, spam e-mails containing such kinds of tricks can be identified by other modules of spam filter, for instance by performing lexicographic analysis or analysis of syntactic anomalies. Carrying out semantic analysis of text embedded into images attached to e-mails first requires text extraction by Optical Character Recognition (OCR) techniques.
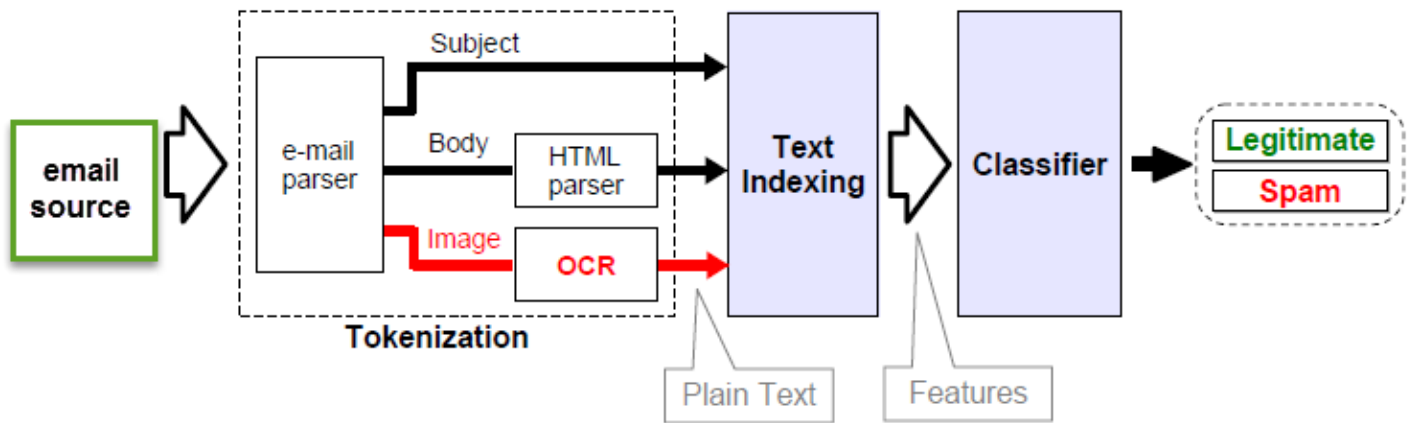
Figure: Block diagram for spam filter with text information embedded into images

The text contained in the body of the e-mail and that embedded into images can be viewed simply as a different "coding" of the message carried by an e-mail. Accordingly, semantic analysis of text embedded into images using text categorization techniques is similar to the ones applied to the body of the e-mail. The basic idea is to extend the phase of tokenization in the document processing steps by including plain text extraction from attached images, as well as from the subject and body fields.

However, it should be taken into account that a vocabulary in which clean digital text is mixed with noisy text (due to OCR) could affect the generalization capability of a text classifier. To avoid including spurious terms generated by OCR noise in the vocabulary, only the terms coming from the subject and body fields could be used to create it. Terms extracted from images can instead be used only at the indexing phase, when the feature vector representation of e-mails is constructed. Consider now the indexing phase. For e-mails containing text embedded into images, a possible choice is to use both the terms belonging to such text and the ones belonging to the subject and body fields to compute the feature vector. However, if terms belonging to images attached to training emails are not included in the vocabulary, it could be better not to use them even for indexing training e-mails. The rationale is again to avoid that OCR noise affects the generalization capability of the text classifier. In this case, the whole training phase of the text classifier would be carried out without taking into account text extracted from images. Such text would be used only for indexing testing e-mails at the classification phase.

Indexing of testing e-mails can also be performed in different ways, to take into account that in spam e-mails with attached images the whole spam message is often embedded into images, while the body field contains only bogus text or random words. One possibility is the following: if an e-mail does not contain attached images, its feature vector is computed as usual from the text in the subject and body fields; otherwise it is computed using only text extracted from attached images. In other words, text in the subject and body is disregarded at classification phase, if the e-mail has text embedded into an attached image. A more complex strategy can also be used: both the above feature vectors can be computed, namely one taking into account only terms in the subject and body fields, and the other one taking into account only terms in the text extracted from images. These two feature vectors are then independently classified, and the two classification outcomes (either at the score or at the decision level) are then combined either within the considered module of the spam filter to yield a single decision for that module, or at a higher level outside that module. This strategy could be effective if the spam message is often (but not always) carried only by text embedded into images. For instance, the maximum of the two scores could be taken, assuming that the text classifier is trained to give higher scores to spam e-mails.

CONCLUSION

Whatever new filtering capabilities arise, it is just a matter of time before spammers find ways to evade them. Because of this text distortion and image spam, spam filtering are not just simple text classification and information retrieval problems anymore. This paper represents a critical analysis of spam e-mail filtering and how Bayesian filter can adapt to new distortion patterns to develop new techniques for spam filtering is addressed.

REFERENCES:

[1] Konstantin Tretyakov, "Machine Learning techniques in Spam Filtering", Data Mining Problem-oriented Seminar, MTAT.03.177, May 2004, pp. 60-79.
[2] Giorgio Fumera, Ignazio Pillai, Fabio Roli, "Spam Filtering Based On The Analysis Of Text Information Embedded Into Images", Journal of Machine Learning Research 7 (2006) 2699-2720.

[3] Eric Chen, "Data Mining Applied to Email SPAM Detection and Filtering", CS445 Hw1

[4] https://en.wikipedia.org/wiki/Naive_Bayes_spam_filtering

[4] https://en.wikipedia.org/wiki/Naive_Bayes_spam_filtering

Cavitation detection of centrifugal pump using Time – Domain method

Maamar Ali Saud AL Tobi[1],Mahmood Hamid Juma Al Sabari[2]

[1]Caledonian College of Engineering, Oman. Email: altubi555@gmail.com

[2]Caledonian college of Engineering, Oman. Email: mahmood11039@cceoman.net

Abstract— This paper studies cavitation detection of centrifugal pump using Time –Domain method. Centrifugal pump is the most popular pump which is widely used in the world. The centrifugal pump may face many problems, one of these is cavitation. Cavitation is formation of bubbles or cavities in liquid that is developed when there is low pressure around the impeller. Cavitation can lead to failure of pump housing, impeller damage and decreased flow and pressure. So, this project is to detect the cavitation fault using time domain method and particularly using parameters such as; Kurtosis, RMS, Mean and Peak. The vibration signals were collected from different positions, namely, vertical, horizontal and axial, and all results were compared for healthy and cavitation conditions. The results were plotted as graphs using MATLAB and tables were also provided.

Keywords— Centrifugal pump, Cavitation, Time domain, Root Mean Square, peak, Mean and kurtosis.

INTRODUCTION

The most popular pumps used in the world are centrifugal pumps. There are various applications for the centrifugal pumps in industries such like; water pumping from lower level to higher one, and to transfer different liquids . The important two parts of this type of pumps are the impeller and the volute. The impeller part can be either open, semi-open or closed, and its purpose to imparting kinetic energy by rotation to the incoming fluid. The second part is volute which is used to redirect the fluid from the impeller and channels to be in a single direction. The main purpose of the pump is to increase the pressure of the incoming fluid and channel and make it in the desired direction [1].

Cavitation is the formation and collapse of vapor bubbles inside the pump. Cavitation occurs when the absolute pressure on the liquid is less than the liquid vapor pressure. The sound can be heard when the vapor bubbles collapse occur, this sound like some rocks are moving inside the pump. If the energy of the vapor bubbles collapse is enough, they can affect on the internal casing and remove metal from it. If the cavitation occurs, the efficiency of the pump will reduce. Also the pressure and flow may have a sudden change at the output discharge.

The cavitation produces vibration and noise. When the pump works under cavitation condition for a period of time (enough time) may leading to such following problems:

- Pitting on the casing wall and impeller.
- Failure early.
- Break the shaft.
- Mechanical seal failure early.

There are five types of cavitation which are vaporization cavitation, internal re-circulation cavitation, vane passing syndrome cavitation, air aspiration cavitation and turbulence cavitation.

There are many methods which have been used for cavitation fault detection. Al Hashmi, 2013 [2], used a method that called statistical analysis of acoustic signal for cavitation detection and Mckee et al, 2012 [1], applied a method based on statistical parameters for a centrifugal pump to indicate cavitation signal. Kristoffer et al, 2015 [3], used method based on the spectral and statistical of cavitation vibration and Chudina,2002., [4] studies the noise as an indicator of cavitation in a centrifugal pump.

There are two methods to display the dynamic signal; one is called time domain method and another known as frequency domain method. Figure 1 shows the time domain, the *y* axis represents the amplitude of the signal and the *x* axis represents the time. Time domain representation is known as amplitude over time trend and is shown in Figure 1 [5].
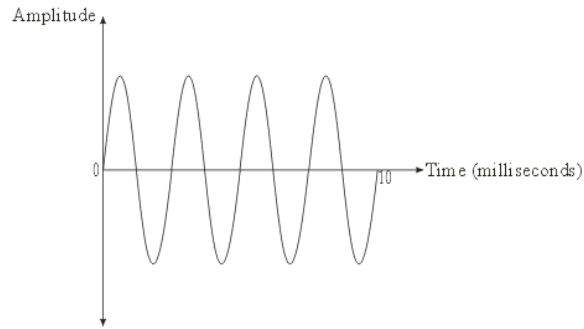
Figure 1: Time Domain [5]

There are different parameters in the time domain that can be used to describe the signal like Peak, Peak to Peak and RMS. By looking at the graph which represents the change of the signal with respect to time can easily understand the peak and peak to peak.

The vibration signal contains power, to measure this power use RMS. To calculate RMS use [6]:

$$\text{RMS} = \sqrt{\frac{1}{N}\sum_{i=1}^{N}(x_i - \bar{x})^2} \qquad (1)$$

Where N is Signal length, Xi is signal values and xi is Mean

$$\bar{x} = \frac{1}{N}\sum_{i=1}^{N} x_i \qquad (2)$$

Kurtosis Factor 'KF' is the measurement of distribution flatness. It is used as an indicator of major peaks in a set of data [6].

$$K = \frac{1}{N}\sum_{i=1}^{N}\frac{(x_i - \bar{x})^2}{RMS^4} \qquad (3)$$

This paper is divided into four parts including introduction. Part 2 presents experimental work and methodology. Part 3 illustrates results and discussion. Finally, a conclusion with remarks is given in part 4.

EXPERIMENTAL WORK AND METHODOLOGY

The tests were carried out on the dynamic laboratory at the Caledonian college of engineering. The experimental setup is a test rig as shown in Figure 2 which contains a centrifugal pump with specifications as; 2HP (1.5kW), 3000 RPM, discharge 1"*1" and the capacity 9.5 m3/h. Also it has a tank with volume 0.0716391m3 (19 Gallon), and two pressure gauges, one with range from -1 to 4 bar (-15 to 60 psi), and other with range from 0 to 7 bar (0 to 100 psi). The diameters of the Pipeline delivery is 1" and this pipeline contains two valves.
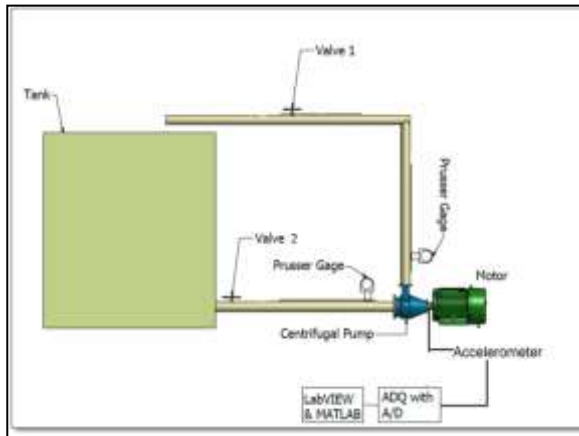
Figure 2: Experimental setupTest Rig

This study is based on collecting and analyzing of vibration data. The vibration signals obtained from a test rig by an accelerometer sensor located on the suction eye. The DAQ (Data Acquisition system) used to amplify and filer the signals at a proper sampling rate with the A/D card (analog to digital converter) to convert the analog signals which are obtained by the accelerometer sensor to the digital signal. LABVIEW software was used to capturing the signals, and MATLAB used for the further processing and analysis of the data.

The vibration data was collected and analyzed in two conditions; with cavitation condition and then with healthy condition. Centrifugal pump was running under healthy condition and cavitation condition by adjusting suction valve. MATLAB was utilized for the analysis of the obtained signals using time domain method with parameters such as mean, peak, root mean square and kurtosis.

RESULTS AND DISCUSSION

This study has investigated the application of time domain as an indicator for the centrifugal pump condition and particularly to distinguish between healthy and cavitation conditions. The time domain signal was plotted using MATLAB software and some parameters like RMS, Peak, Mean, and Kurtosis are calculated for each signal at both conditions. A histogram was also measured and plotted using MATLAB. Frequency domain was used to confirm the presence of each condition.

Figure 3 shows the time domain, histogram and frequency domain for axial position in healthy condition.
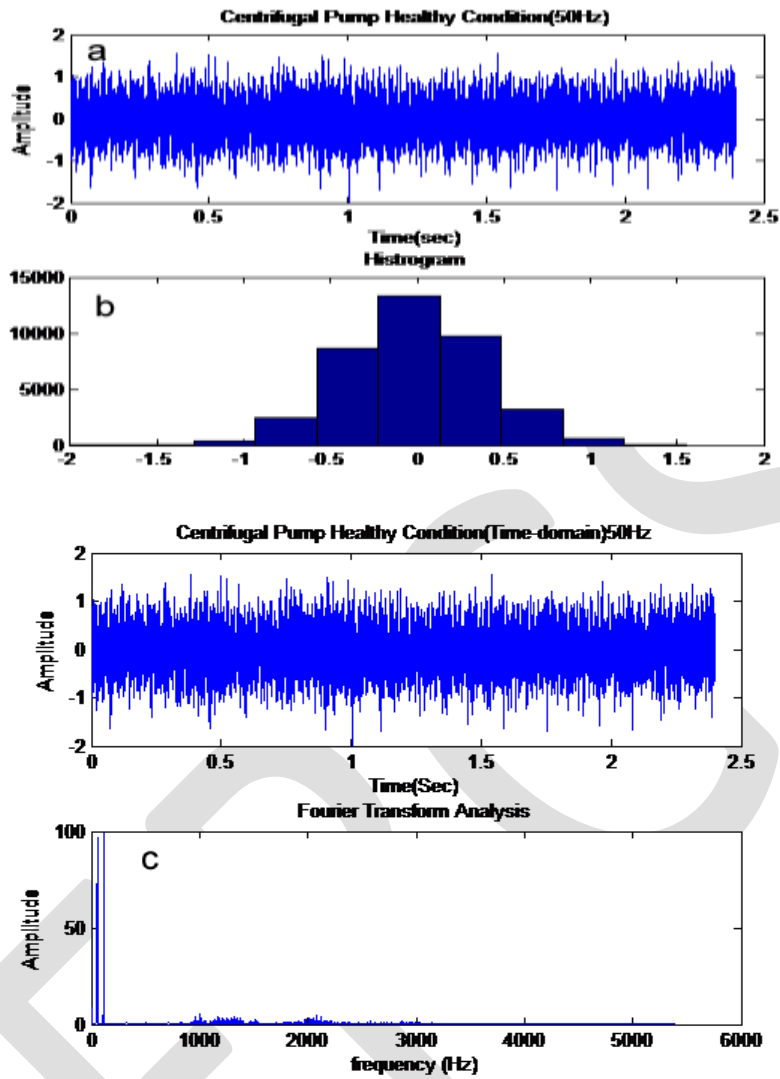
Figure 3: (a) Time domain, (b) histogram and (c) frequency domain of pump at healthy axial reading.

The graph shows the time domain, histogram and frequency domain for axial position in cavitation condition.
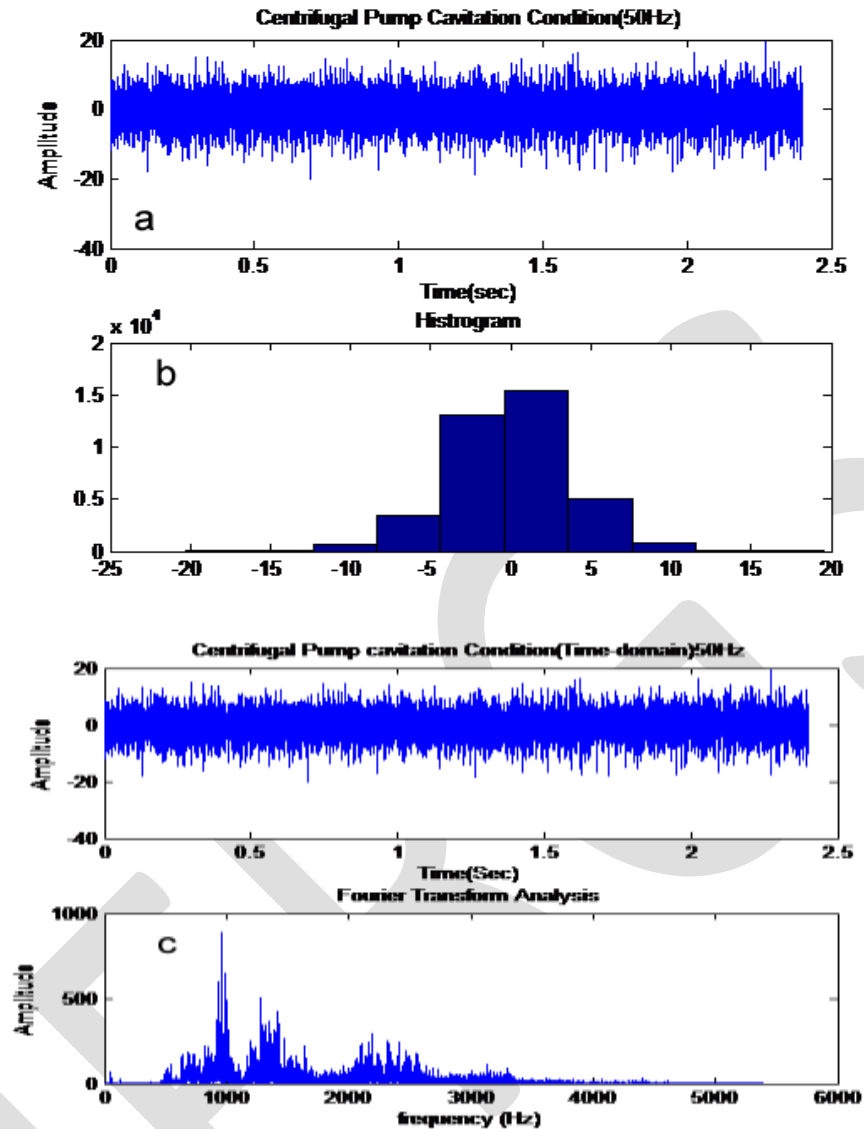
Figure 4: (a) Time domain, (b) histogram and (c) frequency domain of pump cavitation axial reading

By comparing between a healthy condition and cavitation condition, can observe there is different in the distribution of histogram and by looking to the frequency domain, at the healthy condition the amplitude is very low after 1000Hz but at the cavitation condition the amplitude after 1000Hz is high and it remains irregular high up 3000Hz. Vibration and frequency at cavitation condition were found as random and at broadband or higher frequencies. Also by comparing the parameters for both condition, found there are different in peak and RMS value. The value of RMS and peak at cavitation condition value is greater than of healthy condition.

Time domain can be used as an indicator for the centrifugal pump condition and particularly as for this work, it was obviously observed that parameters like RMS and Peak can easily show higher values with cavitation condition compared the values of healthy condition. Kurtosis parameter is also a good indicator but not effective compared the parameters of RMS and Peak. Comparative graph in Figure 4 and 5 shows the values difference between healthy and cavitation conditions for the RMS and Peak parameters respectively.
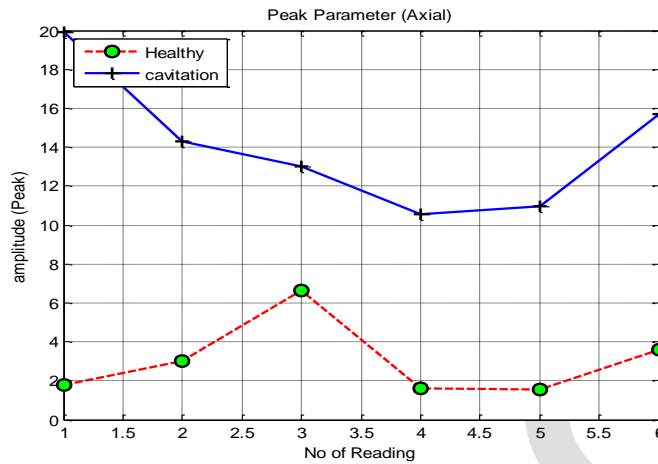
Figure 5: Comparatives Peak parameters for Healthy and cavitation condition.
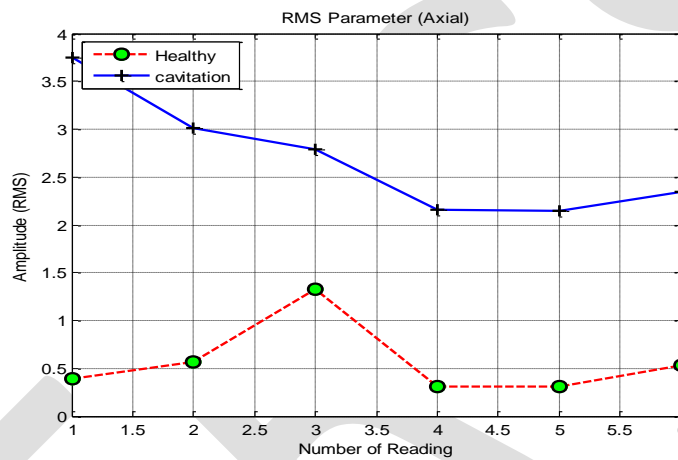
Figure 6 : Comparatives RMS parameters for Healthy and cavitation condition

CONCLUSION

The paper has been done successfully throughout collection of the reading (vibration signals) from centrifugal pump test rig and use time domain as an indicator for the centrifugal pump condition and particularly to distinguish between healthy and cavitation conditions. Moreover, the results were plotted as graphs using MATLAB and parameters were given in tables. The results have shown that the time domain can be used as an indicator for the centrifugal pump condition and particularly RMS and Peak values were found to be the best parameters of time domain to detect the cavitation. Moreover, the best position of accelerometer sensor is axial from suction location. Finally, it is clearly has been observed that cavitation has random vibration in which its detection is required more attention.

REFERENCES:

[1] Mckee, KK, Forbes, G, Mazhar, I, Entwistle, R, Hodkiewicz, M & Howard, I 2012, 'A single cavitation indicator based on statistical parameters for a centrifugal pump'. inWCEAM World Congress of Engineering Asset Management. vol. 8, South Korea, pp. 6pp, A single cavitation indicator based on statistical parameters for a centrifugal pump, 1 January.

[2]Al-Hashmi, S., 2013. Statistical Analysis of Acoustic Signal for Cavitation Detection. International Journal of Emerging Technology and Advanced Engineering, 3(4), pp.55-66.

[3]Kristoffer , M., Forbes, G., Mazhar, I., Entwistle, R., Hodkiewicz, M. and Howard, I., 2015. A vibration cavitation sensitivity parameter based on spectral and statistical methods. Expert Systems with Applications, 42 , pp.67-78.

[4]Chudina, M., 2002. Noise as an Indicator of Cavitation in a Centrifugal. *ACOUSTICAL PHYSICS*, 49(4), pp.463-74.

[5]Mitchell, J.,1993. Introduction to Machinery analysis and Monitoring. second edition edition. Tulsa: PennWell Publishing Company.

[6]Al-Tubi, M. & Al-Raheem, K., 2010. Rooling Element Bearing Faults Detection. Caledonian journal of Engineering, 6(1), pp.44-48.

Swarm Robotics: Nature Inspired Systems

Smriti Prasad[1],Soukhya Rawool[2]

[1]Department of Electrical Engineering, Sardar Patel College of Engineering, Mumbai, Maharashtra, India
smriti.prasad2095@gmail.com, +91 9969275863

[2]Department of Electrical Engineering, Sardar Patel College of Engineering, Mumbai, Maharashtra, India
soukhya.sr8@gmail.com, +91 9820643377

Abstract— Swarm robotics is a developing field offering vast scope for research and formulating specialized applications. Modeled on the behavior of natural swarms in the environment, swarm robotics aims to capitalize on the great potential that decentralized swarm systems consisting of a large number of relatively simple units offer. This paper introduces major aspects of swarm robotics with majority focus on analyzing coordinated actions of natural colonies to help define and understand the characteristics, principles of operation and modeling techniques used to configure and operate swarm robotic systems. The distinctive benefits of swarm systems, which heavily rely on effective localized information exchange and coordination has been discussed along with the immense potential that the field of swarm robotics offers, if properly exploited.

Keywords— Information exchange, stigmergy, coordinated behavior, self-organization, decentralized operation, natural colonies, cooperative control, autonomy.

1. INTRODUCTION

Swarm robotics deals with the coordination and integration of large groups of simplistic robots that are controlled using local means. The swarm bot comprises of many small robots, which are autonomous and portable. These robots can either be independent or self-assemble into a swarm formation. With the help of these small robots, the costs are lowered and the system is much more stable and robust as the interaction is local and the probability of error for individual robots is minimized. The individual robots aren't sentient enough to carry out heavy tasks on their own but can do so, when they are in a swarm by distributing the labor and coordinating within themselves. These swarms are self-adaptable, self-organized and decentralized. The inspiration behind swarm robotics came from nature itself. Large societies of insects could carry out insurmountable tasks, which couldn't have been possible if they worked alone. The potential applications of swarm robotics are tasks that can be miniaturized, require cheap designs or tasks that are executed on a large scale and are dangerous to humans and robots such as disaster relief, search operations or military applications.

2. INSPIRATION FROM NATURE SWARMS

Nature based swarms have been the inspiration behind most of the foundational research on swarm robotics. The behavior of social anthropoids, birds or fishes, as a collective functioning unit and their intra-organizational interactions have demonstrated noteworthy features such as effective division of labor, great flexibility, path planning, robustness and so on. Although the individual members of these swarms, which may largely vary in size from a group of ten to millions, may not possess great intelligence or capabilities, the group as a whole demonstrates superlative degrees of performance, accomplishing complex tasks such as large distance migration, foraging for food, nest building etc. This is achieved by effective information exchange and coordination among the individuals. Some of the most recent examples found in nature are discussed below:

2.1. ANT AND BEE COLONIES

Ants use pheromone, tactile sensations and sound as means of information exchange. They leave behind pheromone trails along a route towards food resources, in the environment. The best path is identified when other ants successively pick up these trails along the shortest routes thereby strengthening the decision to follow these better routes.

2.2. BIRD CROWDS

It observed that birds arrange themselves into unique formations during migration. This pattern formation is not merely coincidental but indeed a deliberate action, which helps birds to accurately navigate across hundreds of miles to their desired location. They

employ inputs from a variety of factors such as magnetic fields, sun compass, time estimation, and visual landmarks, to aid in the above process.

2.3. BACTERIA COLONIES

Bacteria operate as biofilms that are simply multi-cellular clusters with individual cells communicating via inter-cell signals. Such cooperative functioning allows for a division of labor at cellular level, improving resource access abilities, increasing resistance to deterrents, thus benefitting at a global level and vastly increasing survival chances of the aggregate bacteria communities.

2.4 FISH SCHOOLS

Fish usually live in a group known as fish schools that continuously organize themselves in a specific shape that facilitates rapid and smooth, upstream-downstream locomotion, by effectively avoiding collisions with neighboring fish schools with the help of "schooling marks" on their shoulders. This helps them in efficient movement, safeguarding against predators and also in foraging.

Above mechanisms are not just impressive on their own but offer immense potential if properly implemented in robotic systems.

3. CHARACTERISTICS OF SWARM ROBOTICS

3.1. PARALLEL

A swarm can have a large population size, which helps in dealing with multiple targets at once. These targets can be spread over a wide range in the environment hence the search time for swarm is reduced significantly.

3.2. SCALABLE

The swarm is localized, which enables the individuals to join or quit at whim without disrupting the whole swarm. The swarm is adaptable to change in size because of the task reallocation strategies. They are adaptable to different sizes of the population without modifying the software or hardware, which renders them very useful in real-time applications.

3.3. STABLE

The swarm is not affected majorly even if a part of the swarm quits due to exigent circumstances. The swarm remains functional but the performance might get affected due to fewer robots. In dangerous environments, this is an important asset.

3.4. ECONOMICAL

Cost of swarm is significantly low in terms of designing, manufacturing and maintenance. Individual units can be massively manufactured while a single robot needs precise manufacturing.

3.5. ENERGY EFFICIENT

Individual units are smaller and simpler as compared to a single robot, which reduces the energy cost and consumption. This helps in improving the lifetime of swarm.

3.6. AUTONOMY

Individual units are autonomous and capable of exercising control by interacting and motioning in environment. They don't need to be given commands externally.

3.7. DECENTRALIZATION

With help of predetermined rules, individuals can complete tasks without centralized controls. This guarantees scalability and flexibility of swarm.

3.8. HOMOGENOUS

Division of roles amongst individuals must be small and the number of robots for each role must be large. These roles indicate physical structure of robots and shouldn't be changed during tasks.

3.9. FLEXIBILITY

If swarm has high flexibility, it can deal with different tasks using the same hardware and implementing minor changes to the software. This is helpful in foraging techniques, searching or flocking. With help of machine learning, robots can learn from past behavior and modify their strategy accordingly.

4. PRINCIPLES OF OPERATION

Swarm robotics is primarily based on the principles of swarm intelligence which are heavily borrowed and in fact derived from the collective behavior of social insects such as ants, honey bees, wasps, termites and so on. Scientific studies have shown that, a social insect colony consists of autonomous units distributed in the environment and functioning in a decentralized manner. These insects or units are not equipped to assess a global scheme or to centralize information about the state of its entire colony but in fact interact with each other and the environment based on local information that is without knowledge of the global work pattern. Each insect or unit simply follows a small set of behavioral rules. This behavior can be broken down into following two primary principles of swarm intelligence:

4.1. STIGMERGY

It entails a mechanism of indirect co-ordination between the colony units or their actions through the environment. The local environment serves as a work state memory by storing traces left by an agent's actions, which provide a stimulus for subsequent actions thereby eliciting a behavioral response from itself or other units of the swarm or colony. This principle can be best understood by studying nest building in social wasps. Building activities are governed by the local configuration of cells detected by the wasps on the nest. They sense the local configurations of cells on the outer periphery of the comb with their antennae and use this information to decide where to build a new cell. Indeed, the architecture by itself provides enough data and constraints to ensure the coordination of the wasp building activity. Potential building sites on the comb differ in probability to be chosen by wasps when they start to build a new cell. Wasps have a higher probability to add new cells to a corner area with three existing adjacent walls as against starting a new row, by expanding on the side of an existing row. Such behavior helps the individual agents to make decisions, simply by relying on localized information from their immediate work area or environment.

4.2. SELF ORGANIZATION

Self-organization is a set of dynamical mechanisms, which produce intelligent structures at the global level of a system from interactions among its lower level, autonomously functioning units that are not explicitly programmed at the individual level. It is based on four essential components:

4.2.1. POSITIVE FEEDBACK RESULTING IN ACTIVITY AMPLIFICATION

This can be understood by understanding how a decision is made by a colony of ants in choosing between a short path and a long path leading to a food source. Using the trail, the shortest branch is selected in most cases. Initially both paths are given equal preference by the first ants to reach the food source. The ones that take the shortest path reach the nest first and thus in accordance with the trail-laying trail-following behavior the shorter route gets more prominently marked with pheromone thereby attracting the ants that wish to traverse from the nest to the food source. Thus here, the positive feedback amplifies an initial difference induced by the path geometry making it easy to make a choice between the two without the need of complex decision making algorithms or programming, eventually establishing a trail network at the global level.

4.2.2. NEGATIVE FEEDBACK FOR ACTIVITY BALANCING OR STABILIZATION BY COMPENSATING FOR THE POSITIVE FEEDBACK

Continuing with the above example of food foraging among ants we can categorize the following factors as contributors of a negative feedback. Insufficient number of available foraging agents, exhaustion of food source, and the disappearance of pheromone trail on account of evaporation or a competition between alternative paths to attract foragers.

4.2.3. AMPLIFICATION OF RANDOM FLUCTUATIONS BY POSITIVE FEEDBACKS

Amplifying random fluctuations is essential to the growth of swarm colonies as these random behaviors followed by various insect groups, which are often described as stochastic behavior or actions, often help to engender new global structures. Moreover the importance of randomness can be gauged by the fact that it helps to engage the colony in finding newer or maybe better solutions to existing tasks and problems. Consider an instance where misguided or lost foragers can discover unexploited food sources, and then recruit nest mates to these food sources.

4.2.4. MULTIPLE INTERACTIONS

Irrespective of being direct or stigmergic in nature, multiple interactions among independent units of a swarm are essential to generate deterministic outcomes and for producing large and sustainable structures. The whole foundation of a swarm colony ceases to exist if the individual units do not interact and hence exchange information among themselves and the environment.

5. MODELING SWARM ROBOTS

5.1. GENERAL MODELING

The swarm robotics model is essential for executing the coordination algorithms for monitoring the behavior and communication patterns of individual units. These robots have rudimentary functions like sensing, interacting and motioning. The model is divided into 3 modules depending on the functions they wish to accomplish: information exchange, basic and advanced behavior.

5.1.1. INFORMATION EXCHANGE MODULE

This is the crux of swarm robotics as it enables cooperation between robots and helps control the swarm. It has two main functions: limited sensing and local communication. Information exchange can occur in 2 ways: interaction with robots or the environment. In nature, we can have examples of direct interaction via tentacles, voice or gesture. Indirect interaction, though, is much more subtle. In this, the individuals sense the message in the environment, react to it and send back the message in the environment. Pheromones are one example of this. There are three ways of sharing information:

5.1.1.1. Direct communication: similar to wireless networks.

5.1.1.2. Communication through environment: the environment acts as the medium for interaction and is also known as stigmergy.

5.1.1.3. Sensing: Individuals can sense the robots and the environment with help of sensors. It can be helpful in obstacle avoidance, target search, etc.

5.1.2. BASIC BEHAVIOR MODULE

Its individuals have functions such as motioning and local planning. These set swarm robotics apart from multi agent systems and sensor networks systems. It is based on input from communicating and sensing that help the robots to compute their desired movements.

5.1.3. ADVANCED BEHAVIOR MODULE

Robots in complex swarms have additional functions such as task decomposition, allocation and adaptive learning. Task decomposition and allocation help in improving the efficiency of swarm and adaptive learning enhances adaptability of the swarm in different environments.

5.2. MODELING METHODS FOR SWARM ROBOTICS

Modeling helps to conform the swarm robotic algorithm to be scalable for hundreds of thousands of robots.

5.2.1. SENSOR-BASED MODELING

The sensors and actuators form the main components of the system along with the other objects in the environment.

5.2.2. MICROSCOPIC MODELING

Robots and interactions are modeled as finite state systems. Behavior of each unit is defined as many states and transfer condition is based on input from communication and sensing.

5.2.3. MACROSCOPIC MODELING

It is opposite of microscopic modeling. System behaves as a differential equation and the system state is the average number of robots for a particular state at some time step.

5.2.4. MODELING FROM SWARM INTELLIGENCE ALGORITHMS

These are cooperative schemes from swarm intelligence algorithms that are implemented by swarm robotics. Most common example is the particle swarm optimization (PSO). PSO imitates the flocking of birds. Another example is that of ant colonies. These inspirations provide efficient heuristics for searching and routing in a dynamic environment.

6. COOPERATION SCHEMES BETWEEN ROBOTS

Cooperation is an essential element of a swarm robotics model since the system primarily functions due to coordinated or synchronized interactions between the lower-level autonomous units. In fact coordination is considered as an advanced behavior in the swarm robotics modeling. Cooperation occurs at two levels: individual level and swarm level in swarm robotics. Individual level coordination correlates and synchronizes the responses of the swarm agents and their learning and adaptive behaviors with stimuli from environment and is imperative to yield useful actions out of individual agents. Swarm level coordination integrates the former cooperation, to yield the typical collective tasks such as gather, disperse or formation.

Following are few schemes describing coordination that focus on the physical layer of the robots.

6.1. SWARM ARCHITECTURE

The architecture of the swarm forms a basis or skeleton for robotic activities and interactions between agents. Most importantly it helps define the topology for communication and local exchange of information among robots. The architecture of swarm thus largely affects the co-ordination based swarm performance. Hence it is imperative to select the architecture with careful consideration of several factors such as the scale of operation, frequency and complexity of interactions and cooperation among the robots.

6.2. DETERMINING LOCATIONS

Individual swarm units function without a centralized governing system and hence are entirely self-reliant in identifying, differentiating and locating neighboring robots in their domain of function. The absence of a global coordinating system needs to be countered by making available a method for locating other robots within stipulated time. This is realized using on board sensors and filters, which can sense and distinguish between different sound and light waves across the spectrum. While absolute positioning can be applied in some cases it is more important to establish a relative positioning mechanism since robots have limited abilities and localized functioning without a central supervised control. Thus employing a relative positioning algorithm can only ensure coordination.

6.3. PHYSICAL LINKS

Physical connections need to be used in certain situations, which cannot be dealt with by a single robotic agent. These may include coordinated transportation or crossing over large gaps. In these cases, the robots should interact, exchange relevant information and dock before they continue to execute their actions. Several types of physical associations using sensors and actuators for surpassing gaps and difficult terrains have been developed along with infrared ray based localizing and docking methods.

6.4. SELF-ORGANIZATION AND SELF-ASSEMBLY

Self-organization involves local interactions of the lower level units to result in a global structure. The actions of basic units or robots are not supervised or controlled by a centralized monitoring program. A robot establishes communication with the other robots through the already built structures i.e. the interactions and responses of robots are mentored by the process of building. One can study such schemes by simply observing colony insects like ant or bees building their nests. Either discrete or continuous interaction is employed by ants to communicate with environment during the nest building process. While discrete interaction responds to the type of stimulation, the continuous interaction gives a response corresponding to the size of stimulation. Self-assembly describes the ability of few swarm system's to organize themselves from individual units into intended configurations without human aid.

7. FUTURE SCOPE

The swarms as a whole can carry out jobs that can provide new avenues to humans for harnessing power of machines. Ability of controlling swarms can have wide applications from medicine to military. They can be used in military, search and rescue operations, or in areas that can be dangerous for humans. They can also be used in industrial applications for improving manufacturing processes and ensuring workplace safety. The upcoming technologies in this are the bionic aero vehicles, which are inspired by swarm intelligence, machine bees or cockroaches with surveillance equipment, which can be used in future defense operations.

8. CONCLUSION

Swarm robotics is an upcoming research field that draws inspiration from swarm intelligence and robotics. Along with cooperation algorithms that enable control for swarm, manufacturing is imperative for developing swarm robotic systems. With the advent of Micro Electro Mechanical technology in terms of the actuators, sensors and electronic components; size and cost of robots has reduced substantially. Further progress in hardware technology and cooperative algorithms in swarm intelligence and nature will go a long way in boosting the development of swarm robotic systems.

REFERENCES:

[1] Roderich Gross, Michael Bonani, Francesco Mondada, and Marco Dorigo "Autonomous Self-Assembly in Swarm-Bots", IEEE TRANSACTIONS ON ROBOTICS, VOL. 22, NO. 6, DECEMBER 2006.

[2] Ying TAN, Zhong-yang ZHENG "Research Advance in Swarm Robotics", Defence Technology 9 (2013) 18-39.

[3] O.Holland and C.Melhuish, "Stigmergy, self-organization, and sorting in collective robotics", Artificial Life, VOL.5, NO. 2, pages 173–202, 1999.

[4] Elio Tuci, Roderich Gross, Vito Trianni, Francesco Mondada, Michael Bonani and Marco Dorigo, "Cooperation Through Self-Assembly in Multi-Robot Systems", ACM Transactions on Autonomous and Adaptive Systems, Vol. 1, No. 2, December 2006, Pages 115–150.

[5] Shervin Nouyan and Marco Dorigo, "Chain Based Path Formation in Swarms of Robots", IRIDIA – Technical Report Series, Technical Report No. TR/IRIDIA/2006-020, August 2006.

[6] E. Bonabeau, Marco Dorigo, and G. Theraulaz, "Swarm Intelligence: From Natural to Artificial systems, Oxford University Press, New York, USA, 1999.

[7] E. Şahin, "Swarm robotics: from sources of inspiration to domains of application", Swarm Robotics Workshop: State- of-the-Art Survey, E. Şahin and W. Spears, Eds., Lecture Notes in Computer Science, NO. 3342, pp. 10–20, Berlin, Germany, 2005.

[8] Frederick Ducatelle, Gianni A. Di Caro, Carlo Pinciroli and Luca M. Gambardella, "Self-organized Cooperation between Robotic Swarms", Swarm Intelligence, 5(2):73–96.

[9] Simon Garnier, Jacques Gautrais and Guy Theraulaz, "The biological principles of swarm intelligence", Swarm Intelligence (June 2007) Vol.1, Issue 1, pp 3-31.

[10] Nicole El Zoghby, Valeria Loscri, Enrico Natalizio, V´eronique Cherfaoui, "Robot Cooperation and Swarm Intelligence"

Wireless Sensor and Robot Networks: From Topology Control to Communication Aspects, World Scientific Publishing Company,

pp.168-201, 2014

PLC BASED WASTE WATER TREATMENT AND FIRE ALARM SYSTEM

Shruthi M N, Suresh D S, Rajendra C J, R Sekar

M tech, Department of Electronics and Communication, Channabasaveshvara Institute of Technology, Tumkur-572103, Karnataka,

shrumn.426@gmail.com

Abstract— Water is basic necessity of life used for many purposes one of which is industrial use. Industries generally take water from rivers or lakes but they have to pay heavy taxes for that. So it's necessary for them to recycle that to reduce cost and also conserve it. Main function of this project is to clean industry effluent and recycle it for further use. Many manufacturing industries produce their products with using water. With their products industries produce wastewater, which can be removed with the help of waste water treatment process along with water recycling can help us to sustainably manage our vital water resources. In this system, propose a few automated processes for a partial automation of the apartment which can be mostly used in residential areas and industries. It is developed using PLC. The main intent is treated water which can be in turn used for many other purposes and can be cost effective as well. In this paper, our major focus is about industrial automation. Thus by the use of PLCs all the input and output field devices can be controlled automatically with the proper programming. PLC automates the sequence of operation to avoid human interference so accuracy is improved and speed of process has been increased. This will reduce the manual manpower too. Everything seems to be more efficient due to the PLCs. The main aim is industrial and small enterprises sewage treatment to realize the good sewage treatment of automatic control system with high accurate, reliability, convenient and flexible control and scalability.

Keywords— PLC (Programmable Logic Controller), Smoke Sensor, Solenoid Valve, DC Motor, Automation, Water Pump, Waste Water treatment.

INTRODUCTION

Many nations and regions all over the world are facing threats of severe water scarcities or deprivation of the water environment resulting from issues such as hot-headed population growth, rising living standards carried about by economic progress and growing use of industrial water. Almost all industrial processes produce some form of pollute water. Throughout the years the solicitation for high calibre, greater effectiveness and computerized machines has enhanced in the mechanical part of water treatment plants. However, with growing urban population, altering lifestyles and industrialization the quality of contaminated water has worsened over the years and hence requires action before it can be reprocessed for any purpose.

Water treatment plants require consistent observing and audit at incessant interims. There are possibilities of blunders at ascertaining and various stages required with human works furthermore the absence of few structures of microcontrollers. The standard PLC micro830 is utilized to switch the exertion of the subsystems at the passageway of the plant. PLC small scale 830 applications are generally utilized as a part of industry to control and simplicity dull procedure. This contains mechanization of water treatment plant utilizing PLC miniaturized scale 830. Programmable Logic Controller is interfaced with debased water treatment for working the valves. Programmable Logic Controller is utilized to control the part of machine consequently. It is automated modern microchip made controller that executes discrete or consecutive rationale in mechanical environment. It was built up to swap mechanical hand-off, clock and counter subsequently it is likewise called modern Programmable Logic Controller. Controlling high Pressure is unsafe employment, so here robotization assumes enthusiastic part. There are various fields where weight and water level control fundamental to be done momentarily. Consequently it creates dreary exchange to handle the item naturally furthermore preparing time may shift because of human supervision botches. This may not give unsurprising results. Along these lines computerization has critical influence in this procedure. Robotization revises the human errors, rise the repeatability and precision of the framework and decrease the time ingesting.

The point of this framework portrays operation of Programmable Logic Controller to current real-time model of the sullied water treatment plant. Utilizing Programmable Logic Controller the position of the parameters can't just be perpetually checked additionally the procedure of the crucial parameters can be controlled.

This kind of operation has numerous advantages. It includes: improved wellbeing level and saving of time, money and time redeemable by the time conservation, actual procedures checking, life and dependability of plant has to be upgraded, suppleness using the structure can be change, simplicity of stacking report of the plans. By utilizing Programmable Logic Controller made mechanization around commercial enterprises, lofts can prompt an enhanced, loose life by diminishing expenses and edifying the magnificence of life.

BLOCK DIAGRAM

Figure 1 depicts the simple outline of the system hardware. The proposed work includes inputs, outputs, hardware and PLC. The input consists of reservoir tanks, power supply, smoke sensor and master switch ON/OFF. The output consists of DC motors, control valves, water pumps and buzzer. The reservoir tank consisting of the waste water to be treated. The water pump controlled by PLC, pumps the water through a mesh to filter macro particle like sand, stones etc. the next stage consists of the filter membrane which filter minute or dissolved particle present in the water. At last chlorination process will takes place. The solenoid valves open and close according to the controlling action of PLC to allow the water treatment in different stages. send back the treated water to the small scale industries, apartment and also can be recycled for horticultural. This treated water is delivered to the small scale industries or apartments one after the other for some predefined length of time and so embedded timer functions in this system to do the process. Whole process for waste water treatment is keep on repeat.
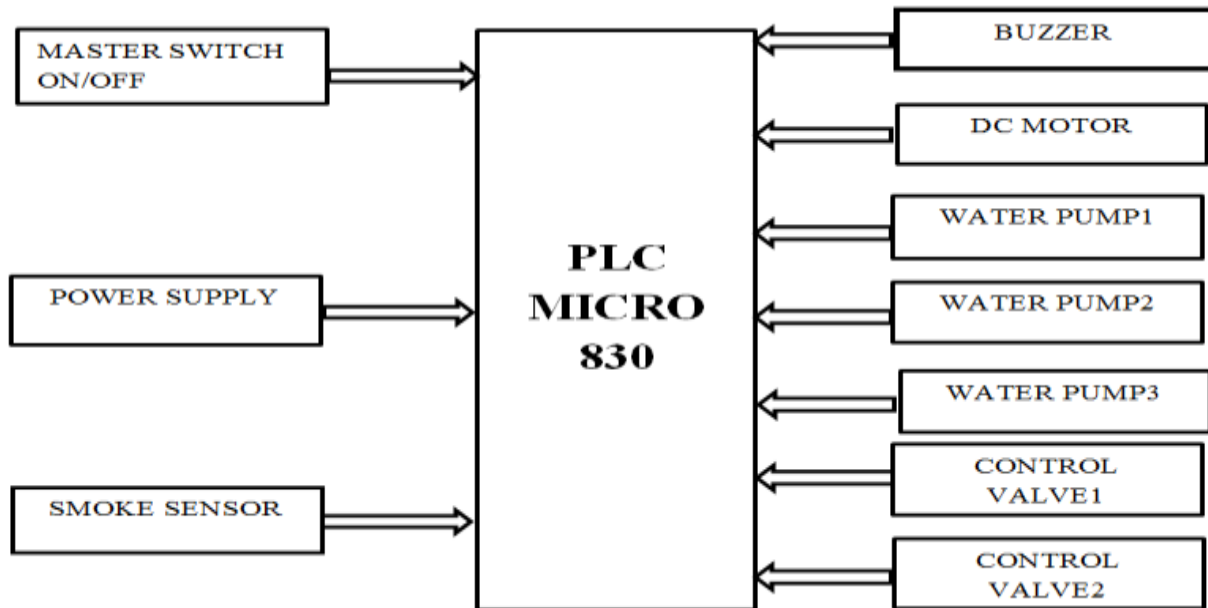
Figure1. Block diagram of Programmable Logic Controller based waste water treatment

Smoke Sensor: Smoke sensor MQ7 identifies the nearness of carbon monoxide within air and its reads the output of the analogue voltage at fixations from 10 to 10,000 ppm. Only one analogue input pin from PLC micro 830 required sensor's simple analogue voltage for the purpose of interface. The smoke sensor used here is MQ7. This MQ7 sensor is suitable for an wide range of applications and very reasonable.

Control valve: In this system 12V solenoid valve using as a control valve. A solenoid control valve working as a electromechanically. This 12V solenoid valve is controlled by an electric current through a solenoid valve. These are utilized to stop, discharge, measurements and circulate liquids. These valves give minimized configuration, safe and quick operating, great medium similarity of the materials utilized, long administration life, low control power and high unwavering quality.

DC Motor: A DC motor has being controlled by PLC micro 830. In this system using 5V DC motor. It will operate the stirrer. A DC motor's any class of electrical machines that proselytes direct current electrical force into mechanical force. A DC engine's velocity can be controlled over a wide range, utilizing either a changing the quality of current in its field windings or by variable supply voltage.

Water Pump: In this system using a 6V DC water pump for pumping water into the tank when water level in the tank reduces to low level and turn off on filling of water to maximum level.

Programmable Logic Controller: The programmable logic controller is characterized as a computerized electronic gadget to execute capacities and to store direction, for example, sequencing, rationale, timing, math words to control machines, procedures and numbering. PLC is utilized to control the succession of operation. In this framework PLC is controlling the info parameters like sensors, power supply and output parameters like water pump, solenoid valves, DC motors. Programmable logic controller i.e. the input or output character is like that of an electromagnetic pneumatic valve controller or relay. In the electronic memory the program

will be stored. In any case, the undertaking of a PLC have quickly increased, Timer and counter capacities, which can be executed for all intents and purposes by any of today's PLCs. The PLC utilized as a part of this framework is micro830. Everything is by all accounts more exact, solid and more proficient because of PLCs. The Programmable logic controller depicted in the figure 2.
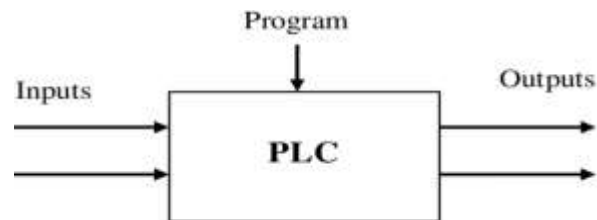
Figure 2 Programmable logic controller

SOFTWARE REQUIREMENTS

RS Logix-500: The ladder logic programming group which helps customer to amplify execution, spare endeavour progression time and upgrade effectiveness. This application is designed to work in windows operating system. RS Logix helps the program with DOS based programming packages for the SLC 500 and Micrologix group of processors, making code maintenance on equipment essentials convenient and straightforward.

Ladder Logic: Ladder logic is one of the programming language which exhibits in graphical form it is widely used to design software for programming logic controllers. After connecting our hardware parts to the programming logic controllers it is essential that to write a program for PLC controller operations. The most widely used language to program a PLC is ladder logic. The software engineer builds up the system and unites their PC to PLC's through a system or Ethernet link and after that download the project to PLC.

Each line in the programming code of ladder logic is represented as "Rung". The Programmable Logic Controller actualizes the code first rung at once beginning with the primary rung and a working down. Fundamentally ladder logic functions are IF-THEN proclamations. each rung is actualized from the left to right. The outputs at the right part of every rung are set to a condition that mirrors the status of the lenient contacts in a specific rung. The below figure 3 shows the sample programming on ladder logic.
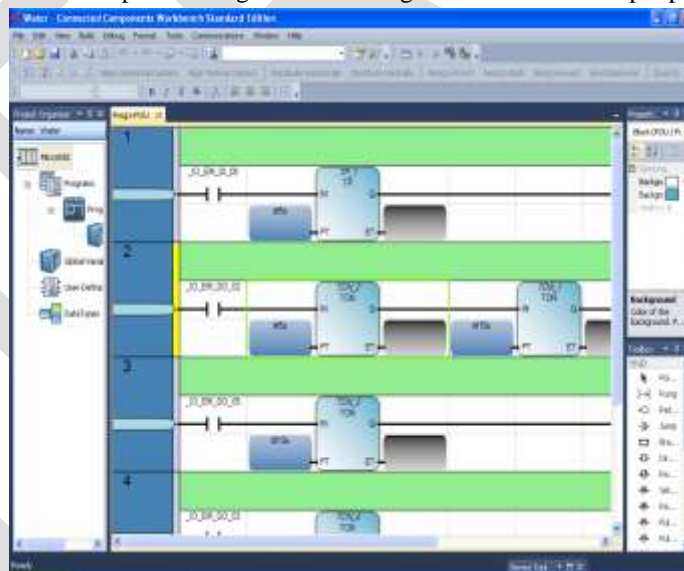
Figure 3 Sample programming on ladder logic.

RS Linx: RS Linx is utilized to interface the Rockwell and and project automation. RS Linx acts as a communication server for the RS Logix 500 application. Likewise, different open interfaces are accommodated outsider HMI, accumulation of information and examination bundles or custom customer application programming. RS Linx gives an OPC client interface to C/C++ customers and an OPC computerization interface for VB/VBA customers. A complete arrangement of correspondence drivers is accommodated the systems administration needs from more established legacy Allen Bradley system bolstered by remote steering through 1785-KA, 1785-KA5, 5130-KA, and 5820-EI to the more up to date more fit controller logic gates. Communication hardware for example PC-based network card or serial port, PCMCIA is bolstered.

RS Emulator: When hardware part is not connected to PLC even then can check the results of the system by using software called RS Emulator. It exercises series give backing to the S88 hardware stage state model for cluster and machine control applications through the stage director discretionary component. It incorporates test the application code and HMI screens at the work area without requiring the genuine equipment, Reduce equipment damage and related expenses coming about because of utilization programming mistakes; Get the items to market speedier by diminishing the advancement and reconciliation time.

Flow Chart
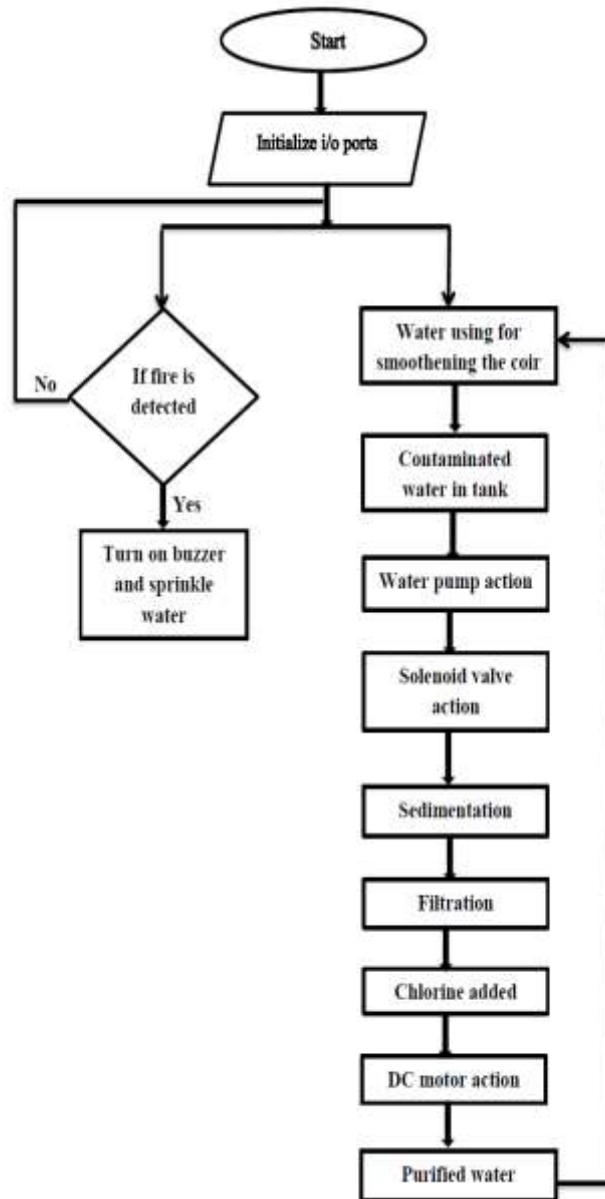
RESULTS

The Snapshot of the prototype designed for this project is shown in the figure 4

Figure 4 Snapshot of the prototype designed.

The designed model demonstrates the automated wastewater treatment process and fire alarm system around the small scale industry by utilizing Programmable logic controller micro 830 and 24V power supply. The designed system mainly includes the reservoir container and storage container, pumps, solenoid valve, DC motor in which sedimentation, filtration and chlorination process happen. The PLC set up depends on which device utilizing as a part of the procedure. At the end of procedure purified water passed to the industry.
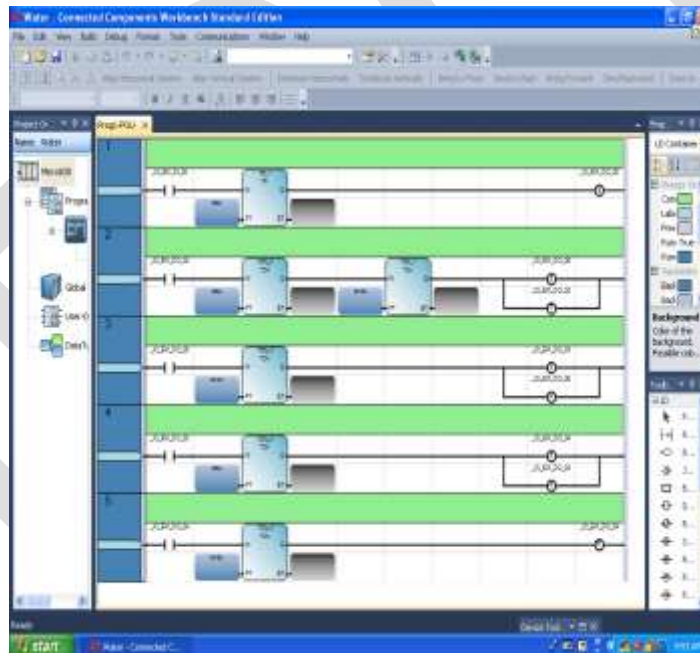
Figure 5 snap shot of ladder logic program of waste water treatment process.

The ladder logic program has and continues to show the traditional way of electrical orders of working. The ladder program represents the interconnection of field devices in a manner that the turning ON or activation, off one device will switch ON another device rendering to a prearranged order of events.

The instruction by instruction Programmable logic controller here executes the program. The prior step and proper action is made Based on the program and the status of the input achieved. The activity may be enactment of specific output and the outcomes can be put off and stored in memory.

The based on the programming instructions, a Programmable logic controller takes input from sensors and real-world device and controls the real-world output devices. To write programming instructions the ladder logic programs are used in Programmable logic controllers
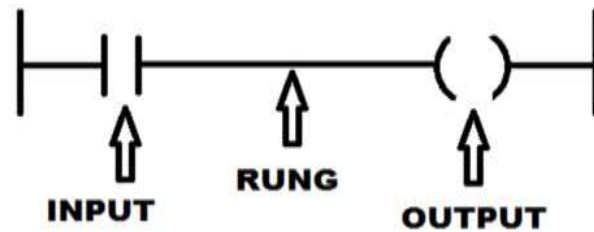
Figure 6 Simple ladder logic

A ladder logic program mainly includes the following elements.

- Rung
- Input and
- Output

A ladder logic program includes one or more horizontal lines known as rungs. The rungs include elements of the input and output. In a ladder logic program, the output element is known as coil and the input element is known as contact.

ACKNOWLEDGMENT

CONCLUSION

The treatment of contaminated water can be done with this proposed work, this waste water treatment plant clean up the small scale industry effluents. So, treated water can be recycled for further use. Thus, purified water is recycled and stored. It has great importance in small and large scale industries as well as in society. Water is one of the very important natural resource and one of the basic necessities in human life. Waste water treatment processes are very precise and good controlled. It is technically proven that any kind of pollutant water can be removed from proposed system. The waste water treatment of this system is treated depending on the type of industries. The PLC micro830 based this proposed work has a great role to play in discharging the contaminated and polluted water before releasing it back to the environment. By using PLC micro830 achieved automated treated water process and defeat the constraints of manual power. By utilizing Programmable Logic Controller micro830 the less cost automation system for small scale industries can be designed and it is easier to understand for the user. Use of treated water and recycling process in our daily life is one of the great contributions in saving limited reservoir of water.

FUTURE SCOPE

By knowing the methodology of PLC micro830 controller used in the proposed system, it can be further develop for large scale industries, residencies or apartment and also for drinking purpose. Without these waste water treatment, not able to get purified water for domestic uses. The control engineer can investigate the procedure if any blunders happens furthermore be monitored what is going on during the process of system. For real time monitoring and controlling purpose can be use SCADA system. This PLC micro830 based automation prompts a superior, agreeable life by diminishing expense and enhance the nature of human's life.

REFERENCES:

[1] G.Venkateswarlu, Jayashree Sahu, Y.Sriya, Sruti Pappala, PLC and SCADA Based Secured and Sustainable Living, IJSER, Volume 4, Issue 4, April 2015.

[2] Rhowel Dellosa, Jon Edward Hernandez, Richard Mangay, Rockie Rob, Microcontroller Based Wastewater Management System, IJSTR, Volume 3, Issue10, October 2014.

[3]   Gengenbach, Michael F, Incentives in the Water Chain: Wastewater Treatment   and Reuse in Developing Countries, Thesis, Wageningen University, Netherlands, 2010.

[4]   Abudi, ZaidunNaji, The Effect of Sand Filter Characteristics on Removal Efficiency of Organic Matter from Grey Water, Al-Qadisiya Journal for   engineering sciences, Vol. 04, No. 02, 2011.

[5]   Er. Ravinder Kumar, Sahil Jungral, Tavleen Singh, Ankit Gupta, Tanveer Hussain Khan, Effluent Treatment Plant Using PLC, IJERG, Volume 4, Issue 2, March-April 2016.

[6]   Raj Shah, Aditya Vadalkar, Omkar Bengrut, Prof.Mrs.M.P.Sardey, Automation of Water Treatment Plant, IJTRE, Volume 1, Issue 8, April-2014.

[7]   S.T.Sanamdikar, K.R.Harne, Advanced Method For Sewage Water Treatment, IJATC, Volume 1, Issue 2, 2012.

[8]   M.Aarthi, L.DhivyaBharathi, S.Giridharan, E.Jayasri, P.Brindha, PLC Based Water Recycling In Steel Plant, IJARMATE, 2016.

[9]   Omar Asif, Md. Belayat Hossain, Mamun Hasan, Mir Toufikur Rahman,Muhammad, E. H. Chowdhury, Fire-Detectors Review and Design of an Automated, Quick Responsive Fire-Alarm System Based on SMS, IJCNS; September 2014

[10]   Frank D.Petruzella, Programmable Logic Controller, 3rd edition, Mc Graw Hill, pages:20-32, 2010.

[11]   S.W.Cheon, J.S.Lee, K.C.Kwon, D.H.Kim, and H.Kim, The Software Verification and Validation Process for a PLC-based Engineered Safety Features-Component Control System in Nuclear Power Plants, The 30th Annual Conference of the IEEE Industrial Electronics Society, pp.827-831, 2004

[12]   B. Mulman, T. Devinder, and W. Gi-Nam., "Generation of PLC Ladder Diagram Using Modular Structure", International Conference on Computational Intelligence for Modelling, Vienna, pp. 1194-1198, Oct 2008.

OPTIMIZATION OF RAW WATER INTAKE LEVEL IN A DAM RESERVOIR

Mohammed MACHKOR [1, 2], Lahcen MESSAOUDI [2]

1 Provincial laboratory of the Mixed Agency TAZA-Guercif, National Office of Electricity and Water potable-water branch.
machkor.mohammed@gmail.com.

2 Moulay Ismail University, Faculty of Sciences, Department of Chemistry, Materials Membranes and Processes of Separation Team, PO Box 11201, Zitoune, Meknes, Morocco.amnaylah@yahoo.fr.

Abstract— Generally surface water is increasingly threatened by the change in the physic-chemical and biological quality. Indeed, since they are always exposed to frequent climate change on the one hand and influenced by the management of the other hand, some processes can be saved especially in Dam retained water such as: thermal stratification and eutrophication which contributes to the decrease of the content of dissolved oxygen or to anoxia and to release iron and manganese.

Thermal stratification result when there is the warming of the surface layers leading to the temperature difference by creating three distinct layers: epilimnion metalimnion and Hypolimnion.

This work aims to study the whole mass of water from the dam holding Bab Louta to optimize the best level of intake that should supply the treatment plant.

The Bab Louta dam, which supplies TAZA city of drinking water, is not immune to these two phenomena. A study was conducted during 2014 on the various layers of the water retained in order to determine the best level of raw water outlet to power the treatment plant.

Keywords— Dam Reservoir, eutrophication, thermal stratification, level of intake, physical and chemical parameters, epilimnion metalimnion and hypolimnion.

INTRODUCTION

Year after year, the lakes and dams are aging, transform and deteriorate. Operators in the field of water are increasingly concerned about the water quality of their lakes and wonder about how it could be changed. Indeed, it's carried out biological and chemical transformations which cause an inhomogeneous mass of water in terms of temperature and dissolved oxygen. These changes are the main causes of the appearance of thermal stratification and eutrophication.

According to the European Commission Nitrates Directive, eutrophication is defined as 'the enrichment of water by nitrogen compounds causing an accelerated growth of algae and higher forms of plant life to produce an undesirable disturbance to the balance of organisms present in the water and to the quality of water concerned [1].

Nixon [2] defines eutrophication succinctly: It's an increase in the rate of supply of organic matter to an ecosystem.

Arguably eutrophication has been in the hearts of several studies and that's what deducted by Jorgensen and Richardson [3] .

A second phenomenon compounds the effects of eutrophication; it's about the thermal stratification of the water masses of the reservoir lakes due to the difference density of water bodies in connection with the temperature, which causes zoning in water: epilimnion, metalimnion and Hypolimnion [4].

The negative effects caused by eutrophication on water treatment process are numerous:

> ➢ Increased chlorine demand thus increased risk of THM formation.
> ➢ The increase in pH making difficult the coagulation-flocculation process.
> ➢ Algae, that manage to resist treatment, cause clogging of rapid sand filters.
> ➢ The appearance of bad tastes and odors in water is surely because of the eutrophication.

To overcome these two phenomena, the optimization level of the raw water intake in the dam remains one of the solutions by National Office of Electricity and Water potable.

Many researches have carried out by applying systems analysis techniques to control water quality through reservoir operations.

S. Richard and al [5] has made a follow-up of physic-chemical water quality characteristics at Petit Saut hydroelectric dam.

F. Donald and al [6] has conducted a study about enhancing water quality in hydropower system operations. Mc Cully [7] and Baghel and al [8] have given a lot of interest in the development of water resources dams.

 A.Gartet and al [9] has conducted a study on the treatment and management of the risks of pollution on the waters of the Sahla dam in

order to find solutions to the problem of the degradation of the quality of these waters.

In this study, we conducted two sampling companies to determine the best level of raw water at Bab louta dam which supplies a water treatment plant.

1. MATERIALS AND METHODS

1.1. LOCATION OF BAB LOUTA DAM

Considered as the main resource supplying drinking water the city of Taza and its regions, the DAM Bab louta was built on Wadi Bou Sbâa, (upstream of Oued Bou Hellou) is located approximately 40 km as the crow flies south west the city of Taza. Its coordinates are:
Latitude: 34° 00' 36" N   ;   Longitude: 42° 21' 00" W

Figure 1.Location of Bab louta dam [10].

1.2 METHODOLOGY

The two sampling companies were conducted during the month of February 2014 and during the month of November 2014. All the physic-chemical parameters have been analyzed in situ according to the method described in table 1:

Table 1.Method of Analysis of physic-chemical parameters

Parameter to analyze	Method of Analysis	reference
Temperature	Thermometer of 0.5 °C of Uncertainty	----------------
Dissolved oxygen	Portable oximeter	(NF EN ISO 5814, October 2012) [11].
pH	pH meter	(NF EN ISO 10523, May 2012) [12].
Turbidity	Turbidity meter	(NF EN ISO 7027, August 2016) [13].
Manganese	Analysis kit of manganese 0.03-0.5 mg/l -Mn	(VISOCOLOR HE, 2012) [14].
Penetration of the light	Secchi disk	(NF EN ISO 7027, August 2016) [13].

2. RESULTS AND DISCUSSION

2.1. STUDY OF STRATIFICATION ON FEBRUARY 2014

During the company of sampling on February 2014, in order to carry out a study of stratification of the dam, we have obtained the following results:

The values of the temperature are expressed in (°C) as a function of the depth in (m) (table 2), and then they are transformed into a vertical temperature profile (figure 2).

Table 2: The values of the temperature in (°C) as a function of the depth (m)

Depth (m)	Temperature (°C)
0.2	12.1
1	11.8
2	11.4
3	11.4
5	11.2
6	11.1
7	10.9
8	10.7
9	10.7
10	10.7
11	10.7
12	10.6
13	10.6
15	10.5
16	10.5
20	10.4
22	10.4
25	10.4
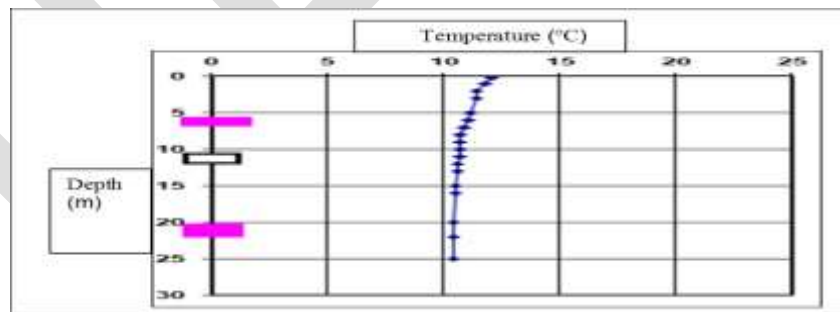
Figure 2. Vertical temperature profile

▭ : Represents the level n° II of the water intake.
▬ : Represents the current level n° I and III of the water intake.

The values of dissolved oxygen are expressed in (°C) as a function of the depth (m) (table 3), and then they are transformed into a vertical dissolved oxygen profile (figure 3).

Table3. The values dissolved oxygen (mg/l) as a function of the depth (m)

Depth (m)	dissolved oxygen (mg/l)
0.2	7.73
1	7.55
2	7.52
5	7.25
6	7.59
7	7.91
8	7.77
9	7.22
10	1.8
11	0.4
12	0.13
13	0.04
15	0
16	0
17	0
20	0
23	0
24	0
25	0
26	0

Figure 3.Vertical dissolved oxygen profile

The values of pH are obtained as a function of the depth in m (table 4), and then they are transformed into a vertical pH profile (figure 4).

Table4. The values of pH as a function of the depth (m)

Depth (m)	pH
0.2	8.28
5	8.26
8	8.22
10	8.20

13	8.20
15	8.16
20	8.16
22	8.11
25	8.10
26	8.09
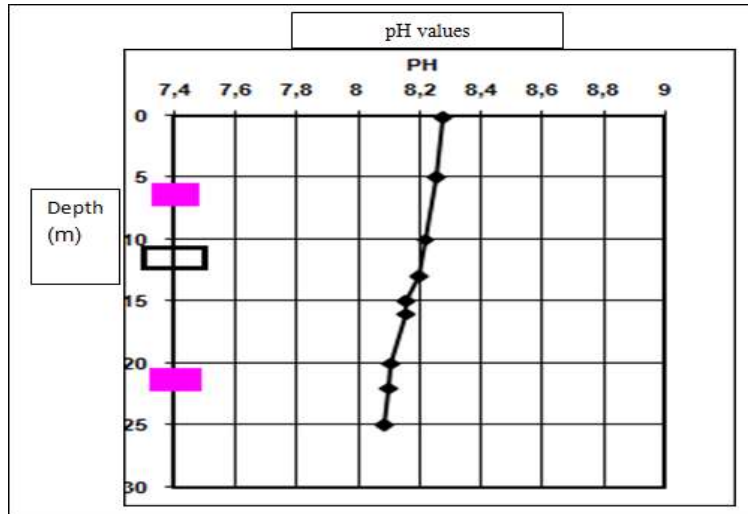
Figure4.Vertical pH profile

The values of turbidity are expressed in (NTU) as a function of the depth (m) (table 5), and then they are transformed into a vertical turbidity profile (figure 5).

Table 5**.**The values of turbidity as a function of the depth in m

Depth (m)	Turbidity (NTU)
0.2	32.4
5	47.3
10	61.3
13	105
15	120
20	125
22	131
25	140
26	164
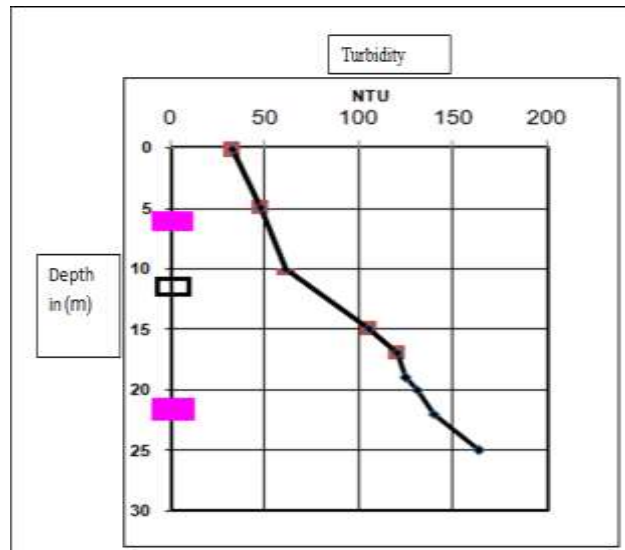
Figure 5.Vertical turbidity profile

2.2. INTERPRETATION 1 OF RESULTS

The study of stratification for the month of February gave the following results:
- ✓ The temperature difference between the surface and the bottom of the retainer is 1.7°C; so the total mass of water is almost de-stratified because of its brewing thus contributing to the cancellation of the thermocline (figure2).
- ✓ Dissolved oxygen levels fluctuate between 9.45 mg/L in surface waters and 7.8 mg/L in the waters of the bottom of the retainer. In effect, the atmosphere being the largest reservoir of oxygen, its dissemination to the water column to the air/water interface is carried out by a slow process and the effectiveness of these gaseous exchanges depends on the degree of oxygen saturation of the surface water. [15].
- ✓ The pH values measured in the range between 8.28 units in surface waters and 8.09 pH units at the bottom of the retainer. In effect, the surface waters are warmer compared to those of the bottom, and since the pH and temperature vary in the same direction, this explains the values of pH. In addition, the assimilation of carbon dioxide by plants is directly linked to the increase in photosynthesis which gives high values of pH at the layer epilimnion [16].
- ✓ Turbidity values obtained vary between 32.4 NTU in surface waters and 164 NTU in the waters of the bottom of the retainer. In effect, in the hypolimnion layer that is where are concentrated the materials in suspension that settle by gravity.
- ✓ The penetration of the light is evaluated at 40 cm. This penetration depends on the degree of the clarity and transparency of the surface waters. In this case, this low value of penetration of light due to the high values of turbidity.

2.3. STUDY OF STRATIFICATION ON NOVEMBER 2014

Concerning the company of sampling of November 2014, we have obtained the following results:

The values of the temperature are expressed in (°C) as a function of the depth (m) (table 6), and then they are transformed into a vertical temperature profile (figure 6).

Table6.The values of the temperature in (°C) as a function of the depth (m)

Depth in m	Temperature in °C
0.2	18.3
1	18.7
2	18.8
3	18.8
5	18.8
6	18.8
7	18.8
8	18.8

9	18.7
10	16.5
11	15.2
12	14.2
13	13.6
15	13.2
16	13.2
20	13.0
22	13.0
25	13.0
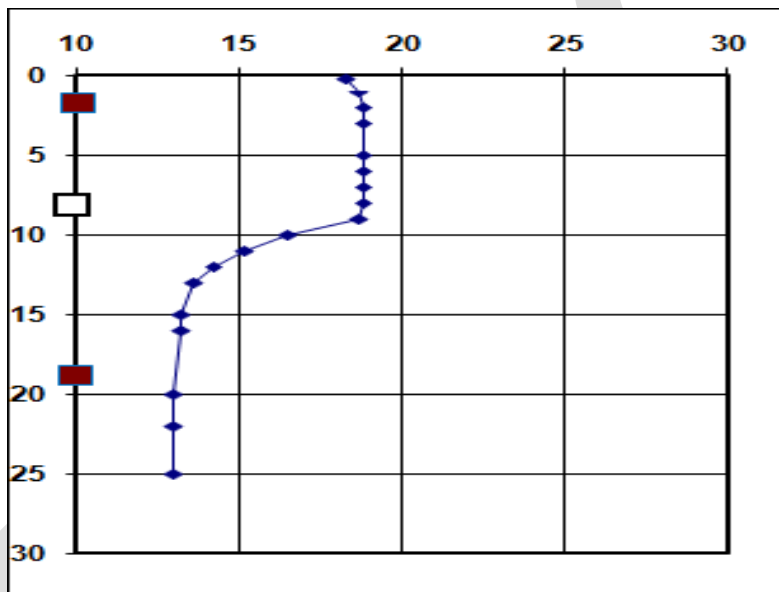
Figure 6.Vertical temperature profile

The values of dissolved oxygen are expressed in (mg/l) as a function of the depth (m) (table 7), and then they are transformed into a vertical dissolved oxygen profile (figure 7).

Table7.The values dissolved oxygen (mg/l) as a function of the depth (m)

Depth in m	dissolved oxygen in mg/l
0.2	7.73
1	7.55
2	7.52
5	7.25
6	7.59
7	7.91
8	7.77
9	7.22
10	1.8
11	0.4
12	0.13

13	0.04
15	0
16	0
17	0
20	0
23	0
24	0
25	0
26	0
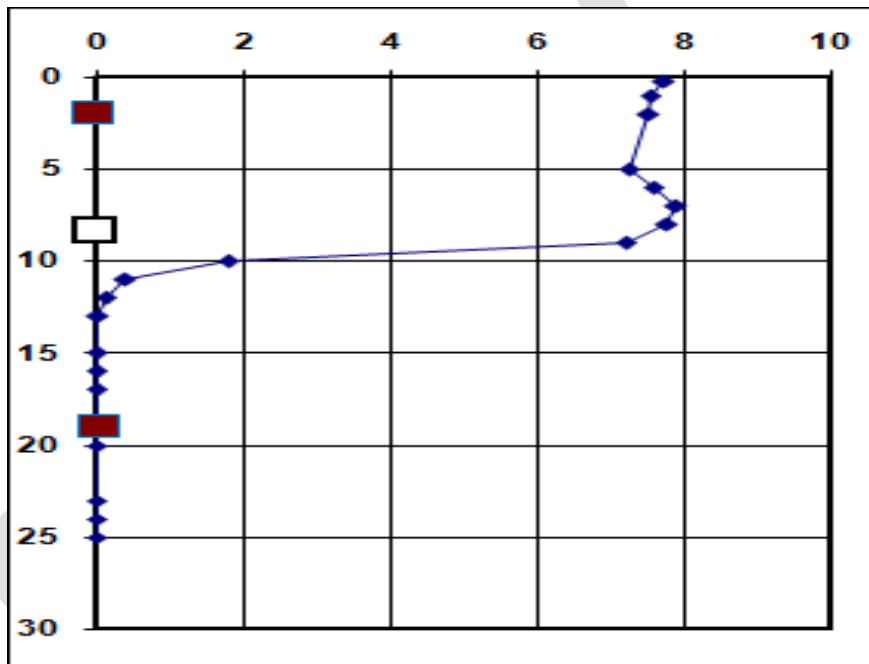
Figure 7.Vertical dissolved oxygen profile

The values of pH are obtained as a function of the depth (m) (table 8), and then they are transformed into a vertical pH profile (figure 8).

Table8. The values of pH as a function of the depth (m)

Depth in m	pH
0.2	8.48
5	8.68
8	8.27
10	8.27
13	8.20
15	8.04
20	7.95
22	7.90
25	7.90
26	7.89
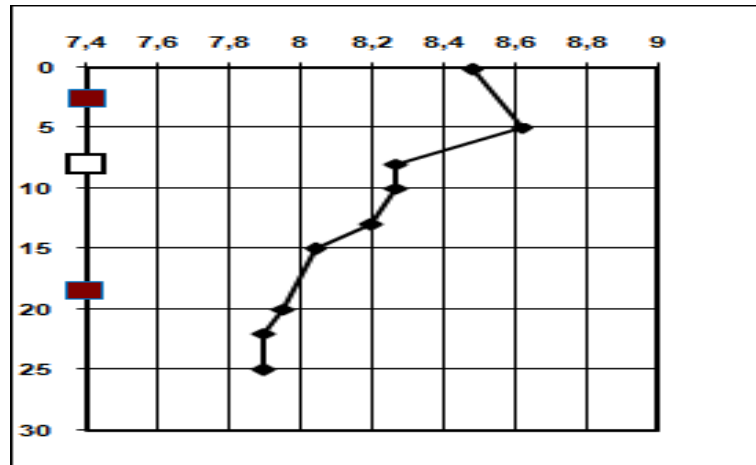
Figure8. Vertical pH profile

The values of manganese are expressed in (mg/l) as a function of the depth (m) (table 9), and then they are transformed into a vertical dissolved oxygen profile (figure 9).

Table 9.The values of manganese as a function of the depth (m)

Depth in m	Manganese content in mg/l
0.2	0
5	0
10	0.2
12	0.5
15	0.6
17	0.7
20	0.7
22	0.7
25	0.8
26	0.8
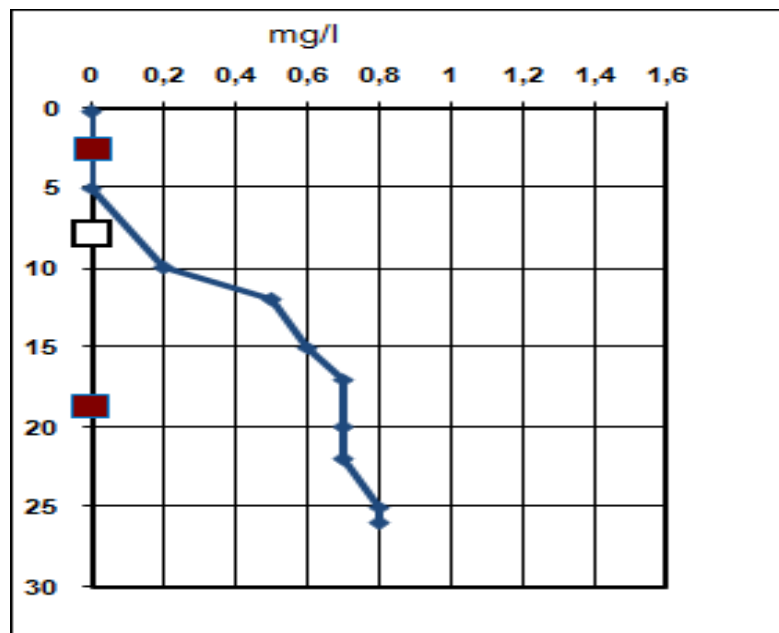
Figure 9.Vertical manganese content profile

2.4. INTERPRETATION 2 OF RESULTS

The results of analyzes of stratification relating to the sample of November 2014 show what follows:

➢ The temperature difference between the surface and the bottom of the retainer is 5.3°C so that the total mass of water is stratified. This stratification, which is manifested by the training of different layers are quite distinct, is due essentially to the heating of the mass of water; and by difference in densities, we have obtained this temperature difference.

➢ An anoxia of waters of the retainer from 14 m depth. It is from this level where it begins to have high manganese content (0.55 mg/l) and this as a result of the depletion of dissolved oxygen resulting in algal activity and the release of the organic matter.

➢ The pH values measured vary between 8.48 units in surface waters and 7.89 pH units at the bottom of the retainer.

➢ Concentrations of manganese obtained vary between 0.2 mg/L at 10 m depth and 0.8 mg/L in the bottom of the retainer. This explains well the existing correlation between anoxia and concentrations of manganese.

➢ The penetration of the light is evaluated at 180 cm. During this period, the low values of turbidity involve a penetration of important light compared to the winter period.

CONCLUSION

The current study of stratification conducted on the mass of water of Bab louta dam has shown that the intake level n° II remains the most recommended from which the raw water must be drawn to feed the water treatment plant and ,therefore, to save the reagents which are used in the treatment process. This choice is based on criteria which must meet the quality of the raw water.

This solution is not considered unique but it remains necessary by adopting other solutions such as the biological solution by putting the silver carp in the retainer of dam.

REFERENCES:

[1] Anonymous.''Council Directive of 21 May 1991 concerning urban waste water treatment (91/271/EEC)''. Official Journal L , 175,1991.

[2] Nixon, S. W. ''Coastal marine eutrophication: a definition, social causes, and future concerns''. Ophelia, 41 , 199–219,1995.

[3] Jørgensen, B. B. and Richardson, K. (eds).'' Eutrophication in Coastal Marine Ecosystems''. American Geophysical Union, Coastal and Estuarine Studies 52 (p. 273). Washington, D.C,1996.

[4] A. Foutlane, A. Bouloud & K. Ghedda.'' Restoration of the quality of the waters in dams retainers''. IAHS Publ. no. 243, pp. 287-297,1997.

[5] S. Richard,A. Arnoux and P. Cerdan . ''Evolution in physico-chemical water quality in the reservoirand downstream following the filling of Petit-Saut dam''. Hydroécologie appliquée,9. , 57-83,1997.

 [6] Donald F. Hayes, Jackson K. Brown,John W. Labadie and Thomas G. Sanders .'' Enhancing water quality in hydropower system operations''. WATER RESOURCES RESEARCH, VOL. 34, NO. 3, , 471-483,1998.

[7] McCully, P. ''Silenced rivers: the ecology and politics of large dams.Enlarged and updated''. London and New York.: Zed Books,2001.

[8] Baghel R., Nüsser M. ''Discussing Large Dams in Asia after the World Commission on Dams: Is a Political Ecology Approach the Way Forward?'' water alternatives,3 (2) , 231-248,2010.

[9] Abdelghani Gartet, Mohammed El Fengour, Jaouad Gartet & Carmelo Conesa García. ''Degradation of the quality of the waters of the SAHLA DAM: treatment and management of the risks of pollution-province of Taounate, GIR - Northern Morocco''. Papeles de Geografía , 41-54,2009.

[10] ''National Parc Tazeka''. (s.d.). taken from www.voyagesmaroc.ch.

[11] NF EN ISO 5814. ''Water Quality - Determination of the dissolved oxygen - electrochemical method to the Probe'' -. AFNOR, October, 2012.

[12] NF EN ISO 10523. ''Water Quality - Determination of the pH''. AFNOR, May ,2012.

[13] NF EN ISO 7027.''Water Quality - Determination of Turbidity - Part 1: Quantitative Methods''. AFNOR, August ,2016.

[14] VISOCOLOR HE. ''Test Kits for the analysis of water'',2012.

[15] Milaine Richer-Bond and Martin Genest. ''Studies of eutrophication 2009-2011, in the framework of the implementation of the Program lakes protection''. Service of the town planning and the environment, March, 2013.

[16] BENSAFIA D. and REMINI B. ''the role of the vase in the acceleration of eutrophication of waters of dams. experimental study''. Larhyss Journal , 161-181, September ,2014.

REVIEW OF STABILITY ANALYSIS OF NON-LINEAR CONTROL SYSTEMS

Banajit Boro

City University of London, London, Email: Banajit.Boro.1@city.ac.uk

Abstract- The importance of control system in mechanical, electrical and electronics has been enhanced to a great extent in the recent years. This paper provides an evaluation of several stability analysis strategies to the non-linear control systems. Nonlinear control systems pertain with nonlinear systems that are time-variant. As control system design in general aims to satisfy certain performance objectives, such as stability, accurate input tracking, disturbance rejection, and robustness or insensitivity to parameter uncertainty, the dissimilar nature of nonlinear systems essentially demands for a diversity of design methods of different nature. The major considerations of this study are transfer functions along with stability and steady state error. To improve the stability of the nonlinear systems, numerous researches have been proposed.

Keywords – Control systems, Non-linear control systems, Stability analysis, Lyapunov, Popov criterion, fuzzy controller, Takagi-Sugeno.

INTRODUCTION

A Control system is a device, or set of devices, that manages, commands, directs or regulates the behavior of other devices or systems. Industrial control systems are used in industrial production for controlling equipment or machines. The main feature of control system is, there should be a clear mathematical relation between input and output of the system. When the relation between input and output of the system can be represented by a linear proportionality, the system is called linear control system. Again when the relation between input and output cannot be represented by single linear proportionality, rather the input and output are related by some non-linear relation, the system is referred as non-linear control system.

There are two common classes of control systems, open loop control systems and closed loop control systems. In open loop control systems output is generated based on inputs. In closed loop control systems current output is taken into consideration and corrections are made based on feedback. A closed loop system is also called a feedback control system. The controlling mechanism is classified into linear control system and non-linear control system. Most of the theories and practices focus on feedback control. A typical layout of a feedback control system is shown in Figure 1 [1].
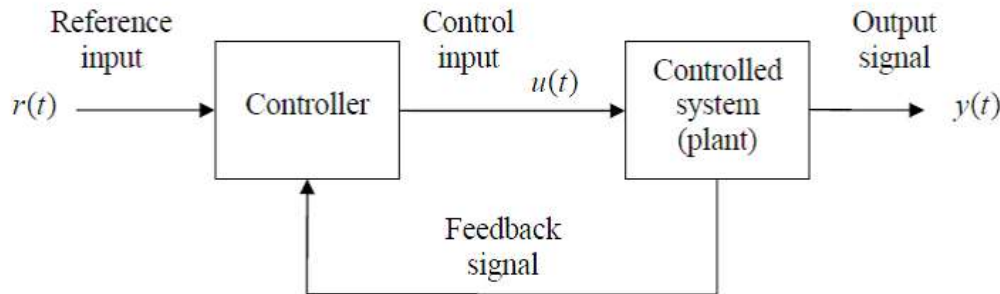
Figure 1: Basic Feedback control system

Nonlinear control systems are the systems that are nonlinear, time-variant, or both. Control theory is an interdisciplinary branch of engineering and mathematics that is concerned with the behavior of dynamical systems with inputs, and how to modify the output by changes in the input using feedback. The system to be controlled is called the "plant". In order to make the output of a system follow a desired reference signal a controller is designed which compares the output of the plant to the desired output, and provides feedback to the plant to modify the output to bring it closer to the desired output.
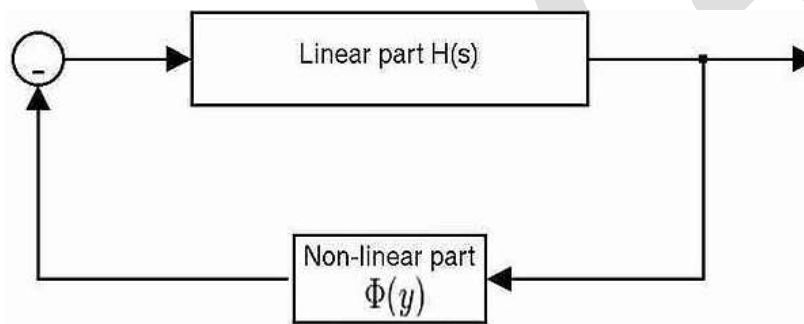
Figure 2: Nonlinear Control System

Nonlinear control systems are control systems in which nonlinearity plays a substantial role, either in the controlled process (plant) or in the controller itself. Nonlinear plants ascend definitely in numerous engineering and natural systems, including mechanical and biological systems, aerospace and automotive control, industrial process control, and many others.

The control system which contains at least one nonlinear factor is called as nonlinear control system. The nonlinear factor is the static characteristic between the input and output that cannot satisfy the linear relationship. The subject of nonlinear control system includes all of the mathematical relationship except the linear relationship. Thus there is no common design method for nonlinear systems.

Properties of nonlinear control systems are:

- They do not follow the principle of superposition (linearity and homogeneity).
- They may have multiple isolated equilibrium points.
- They may exhibit properties such as limit cycle, bifurcation, chaos.
- Finite escape time: Solutions of nonlinear systems may not exist for all times.

Nonlinear control systems are classified into two types: Smooth nonlinearities and non-smooth nonlinearities. Smooth nonlinearities are theoretically easier to deal with than non-smooth nonlinearities. The nonlinearities are, in a sense, invertible. Indeed, there exists a class of smooth nonlinear problems which are "close to" linear in the sense that they can be converted, via feedback, into linear problems. The associated design strategy is known as "feedback linearization".

Non-smooth nonlinearities are typically more challenging as they lack a globally definable inverse. One of the most common forms of non-smooth nonlinearity is that of actuator amplitude and/or slew rate limits. Approaches to this problem can be classified as being unexpected, cautious, evolutionary, and tactical. In the serendipitous approach, one allows occasional violation of the constraints but no particular precautions are taken to mitigate the consequences of the constraints [2].

Stability analysis plays a major role in control systems. Several techniques and methodologies exist for the analysis and design of nonlinear control systems. A brief and generic explanation of some prominent ones is presented in the literature review.

LITERATURE REVIEW

Stability of a system covers a wider class of systems that do not obey the superposition principle, and applies to more real-world systems, because all real control systems are nonlinear. These systems are often governed by nonlinear differential equations. Advanced mathematical concepts like limit cycle theory, Poincaré maps, Lyapunov stability theorem, and describing functions are described in this section.

The problem of absolute stability of an indirect control system with one non-linearity was analysed by Popov [3] by using a special method which differs from the second method of Liapounoff. In the obtained criteria of absolute stability, main condition is expressed by means of the transfer function of the linear part of the system. It is proved that by plotting Liapounoff function of the general type, a quadratic form plus an integral from non-linearity, it is impossible to obtain stability area for the analysed problem (in the parameter space) wider than the area resulting from application of the suggested criteria.

Billings [4] proposed a study dealing with the identification of block-oriented and bilinear systems, selection of input signals; structure detection, parameter estimation and results from catastrophe theory were included. The limitations, relationships and applicability of the methods were discussed throughout. Although the identification time using these inputs was reduced by a factor of 70, compared with a Gaussian white input, anomalies appeared in the fourth-order autocorrelation functions.

Qu [5] presented the definitive treatment of stability analysis and robust control design for nonlinear uncertain systems. This was the first work to tackle robust control design for nonlinear entities as power systems, robotics, and more. It shows how to build high performance and better control into systems that are too complex to be modelled accurately. A unique feature of this research is that, Lyapunov-based approach to control design is employed, which is the only universal approach for nonlinear systems.

Cao and Lin [6] have described Takagi-Sugeno (TS) fuzzy models as an effective representation of complex nonlinear systems in terms of fuzzy sets and fuzzy reasoning applied to a set of linear input-output sub-models. In this study, the TS fuzzy modeling approach is utilized to carry out the stability analysis and control design for nonlinear systems with actuator saturation. The TS fuzzy representation of a nonlinear system subject to actuator saturation is obtained and the modeling error is also captured by norm-bounded uncertainties. A set invariance condition for the system in the TS fuzzy representation is first established. Based on this set invariance condition, the problem of estimating the domain of attraction of a TS fuzzy system under a constant state feedback law is formulated and solved as a linear matrix inequality (LMI) optimization problem. By viewing the state feedback gain as an extra free parameter in the LMI optimization problem, we arrive at a method for designing state feedback gain that maximizes the domain of

attraction. A fuzzy scheduling control design method is also presented to further broaden the domain of attraction. An inverted pendulum is used to show the effectiveness of the proposed fuzzy controller.

Tomescu [7] presented a stability analysis method for nonlinear processes with Takagi-Sugeno (T-S) fuzzy logic controllers (FLCs). The design of the FLCs was established on heuristic fuzzy rules. The stability analysis of the fuzzy control systems were executed using LaSalle's invariant set principle with non-quadratic Lyapunov candidate function. This study explained that if the derivative of Lyapunov function is negative semi-definite in the active region of each fuzzy rule, then the overall system will be asymptotically stable in the sense of Lyapunov (ISL). The stability theorem suggested in the paper ensures sufficient stability conditions for fuzzy control systems controlling a class of nonlinear processes. Here the controller implements an (often heuristic) set of logical (or discrete) rules for synthesizing the control signal based on the observed outputs. Defuzzification and fuzzification procedures are used to obtain a smooth control law from discrete rules. The stability analysis algorithm ensuring the stability of the class of fuzzy logic control systems considered is based on their theorem.

Another research considers the delay-dependent stability analysis and controller design for uncertain T–S fuzzy system with time-varying delay. A new method is provided by introducing some free-weighting matrices and employing the lower bound of time-varying delay. Based on the Lyapunov–Krasovskii functional method, sufficient condition for the asymptotical stability of the system is obtained. By constructing the Lyapunov–Krasovskii functional appropriately, the researchers could avoid the supplementary requirement that the time-derivative of time-varying delay must be smaller than one. The fuzzy state feedback gain was derived through the numerical solution of a set of linear matrix inequalities (LMIs). The upper bound of time-delay was obtained by using convex optimization such that the system could be stabilized for all time-delays [8].

Marinosson [9] proposed a system where the stability properties of equilibrium points of general continuous autonomous nonlinear systems were analyzed via linear programming. The novel methods presented did not require the nonlinear system to be of any specific type, like piecewise affine, and show that it is possible to extract a lot of non-trivial information regarding stability by using linear constraints. The Linear Program LP1 gives explicit linear programs for dynamical systems such that if there is no feasible solution of the program, then the equilibrium of the system under consideration cannot be a constant. The bounds of the derivatives of the Lyapunov function are equally good and it hardly seems possible to improve them, without making major restrictions concerning the system in question. Linear Program LP2 gives explicit linear programs for dynamical systems too. Such a linear program, generated for a particular system, has the property that a feasible solution of it defines a continuous piecewise affine (CPWA) Lyapunov function for the system. In both cases a lower bound of the region of attraction is provided by the preimages of the Lyapunov or Lyapunov-like function.

Cho and Lee [10] present an adaptive control approach using a model matching technique for 3-DOF nonlinear crane systems. The proposed control is linearly composed of two control frameworks: nominal PD control and corrective control. A nonlinear crane model is approximated by means of feedback linearization to design nominal PD control avoiding perturbation. A corrective control to compensate system error feasibly occurring due to perturbation, which is derived by using Lyapunov stability theory with bound of perturbation, is proposed. Additionally, stability analysis is achieved for the proposed crane control system and they analytically derived sufficient stability condition with respect to its perturbation.

Sahu, Gupta and Subudhi [11] explained a new method to analyze the condition and region of stability of nonlinear time-varying systems by introducing the notions of dynamic poles and dynamic-Routh's stability method. The stability analysis is carried out in a special type of complex plane called g(t)-plane which is similar to the traditional s-plane where both real and imaginary axis have time

dependent parameters. The theorem is established and numerical examples from literature are solved with simulation results to show the efficacy and accuracy of the proposed method. The phase plane curve is presented for showing the stability condition of the nonlinear time varying systems. Their theorem comprises of the following steps:

(i) The necessary condition for the nonlinear system to be stable is; all the elements of the first column of dynamic-Routh's array must have positive values.

(ii) If a zero is present on the first column of dynamic Routh's array, then the corresponding dynamic pole will oscillate on the imaginary axis.

(iii) The number of times of sign change of the elements of first column of dynamic-Routh's array is the number of dynamic poles on the right hand side of g-plane which force the nonlinear system to be unstable.

Yadav, Choudhary and Thirunavukarasu [12] discussed a new class of PID controller where the system to be controlled is assumed to be modeled or approximated by second-order transfer functions. The design is done by using sigmoidal function, which is represented as a nonlinear function. The controller design by nonlinear method presented consists of a nonlinear gain in cascade with a linear constant gain PID controller. The sigmoidal function represents nonlinear gain k as the function of the error e, as shown below.

$$k = k_0 + k_1 \left\{ \frac{2}{1 + \exp(-k_2 e)} - 1 \right\}$$

Where k_0, k_1 and k_2 are user-defined positive constants, the gain k is lower-bounded by $k_{min}=k_0-k_1$ when e=-∞, that is upper-bounded by $k_{max}=k_0+k_1$ when e=+∞, that is $k_{min}<k<k_{max}$, and furthermore $k=k_0$ when e = 0. Thus k defines the central value of k, k1. Linear PID controller for magnetic levitation gives better response, quick setting time with high precision and high stability. But the system response is up to certain limit. In real world applications process won't be stable. Definite uncertainties will be affecting the system throughout the process. So for such kind of uncertainties classical PID doesn't hold good.

Jankovic [13] illustrated a particular application where the disturbance decoupling paradigm is used to design a controller that coordinates the electronic throttle and variable cam timing actuators to achieve a desired transient engine performance. The problem of coordinating the electronically controlled throttle (ETC) and variable cam timing (VCT) actuators in controlling the torque of gasoline (spark-ignited) engines has been considered. The main challenge is due to the multivariable and nonlinear nature of the plant under control. To illustrate this, the steady state air intake in VCT engines where both actuators (the throttle and the VCT) control the amount of air and, in turn, engine torque are reflected.

Forbes [14] describes the input-output stability theory as in how inputs map to outputs through an operator that represents a system to be controlled or the controller itself. Within this framework, the Small Gain, Passivity, and Conic Sector Stability theorems have been used to assess the stability of a negative feedback interconnection involving two systems that each have specific input-output properties. Firstly, characterization of the input-output properties of Linear Time-Varying (LTV) systems are taken into consideration for which various theorems are presented, that ensure that a LTV system has finite gain, is passive, or is conic. Next, the stability of various negative feedback interconnections is examined. Motivated by the robust nature of passivity-based control, we consider how to overcome passivity violations. This investigation leads to the hybrid conic systems framework whereby systems are described in terms of multiple conic bounds over different operating ranges. A special case relevant to systems that experience a passivity violation

is the hybrid passive/finite gain framework. Sufficient conditions are derived that ensure the negative feedback interconnection of two hybrid conic systems is stable.

Svarc [15] described the Popov criterion for the stability of nonlinear control systems. The Popov criterion gives sufficient conditions for stability of nonlinear systems in the frequency domain. It has a direct graphical interpretation and is convenient for both design and analysis. In the article presented, a table of transfer functions of linear parts of nonlinear systems is constructed. The tables include frequency response functions and offers solutions to the stability of the given systems. The table makes a direct stability analysis of selected nonlinear systems possible. The stability analysis is solved analytically and graphically. Then it is easy to find out if the nonlinear system is or is not stable.

A framework for real-time, full-state feedback, unconstrained, nonlinear model predictive control that combines trajectory optimization and tracking control in a single, unified approach has been examined. The proposed method uses an iterative optimal control algorithm, namely Sequential Linear Quadratic (SLQ), in a Model Predictive Control (MPC) setting to solve the underlying nonlinear control stability problem and simultaneously derive the optimal feedforward and feedback terms. The customized solver can generate trajectories of multiple seconds within only a few milliseconds. The performance of the approach is validated on two different hardware platforms, an AscTec Firefly hexacopter and the ball balancing robot Rezero [16].

Jake Bouvrie and Boumediene Hamzi explained briefly about the balanced reduction of the load in Nonlinear control systems that behaves linearly when lifted into a high (or infinite) dimensional feature space where balanced truncation may be carried out implicitly. A system expressed in the coordinates where each state is equally controllable and observable is called its balanced realization. This method uses samples of the impulse response of a linear system to construct empirical controllability and observability [17].

CONCLUSION

Control system design has reached a degree of significant development and there exists extensive understanding of "standard" stability problems of the nonlinear systems. The aim of this review is to briefly assess recent developments in nonlinear control and look past the various solutions to innovate a novel technique to stabilize the nonlinear control systems. The literature review describes several stability analysis techniques for the nonlinear control systems. We assume a general perspective in the solutions studied and propose an alternate solution for this work that could be established by reducing the nonlinear system into a linear system using trajectory optimization techniques.

REFERENCES:

[1] Nahum Shimkin, "Nonlinear Control Systems", Technion – Israel Institute of Technology, Israel, 2009.

[2] Graham C. Goodwin, "A Brief Overview of Nonlinear Control", Centre for Integrated Dynamics and Control, University of Newcastle, Australia, 2001.

[3] V. M. Popov, "Absolute Stability of Non-linear Automatic Control Systems", Avtomat. i Telemekh, Volume 22, Issue 8, 961–979., 1961.

[4] S.A. Billings, "Identification of Nonlinear Systems - A Survey", IEE Proc. Part D127, Page 272, 1980.

[5] Zhihua Qu, Robust Control of Nonlinear Uncertain Systems, 1st edition, John Wiley & Sons, Inc. New York, USA, 1998.

[6] Yong-Yan Cao, Zongli Lin, Robust stability analysis and fuzzy-scheduling control for nonlinear systems subject to actuator saturation, IEEE Transactions on Fuzzy Systems, Volume: 11, Issue: 1, 10.1109/TFUZZ.2002.806317, Feb 2003.

[7] Marius-Lucian Tomescu, Stability Analysis Method for Fuzzy Control Systems Dedicated Controlling Nonlinear Processes, Acta Polytechnica Hungarica, Vol. 4, No. 3, 2007.

[8] Engang Tian, Chen Peng, Delay-dependent stability analysis and synthesis of uncertain T–S fuzzy systems with time-varying delay, Volume 157, Issue 4, 16 February 2006.

[9] Marinosson, S., Stability Analysis of Nonlinear Systems with Linear Programming: A Lyapunov Functions Based Approach. Gerhard-Mercator-University, Duisburg, 2002.

[10] Hyun Cheol Cho and Kwon Soon Lee, Adaptive control and stability analysis of nonlinear crane systems with perturbation, Journal of Mechanical Science and Technology 22, 2008.

[11] Basant Kumar Sahu, Madan M. Gupta, Bidyadhar Subudhi, Stability Analysis of Nonlinear Systems using Dynamic-Routh's Stability Criterion: A New Approach, 2013 International Conference on Advances in Computing, Communications and Informatics (ICACCI), 2013.

[12] Eadala Sarath Yadav, Santosh Kumar Choudhary, I Thirunavukarasu, Design and Simulation of Nonlinear Control System for Magnetic Levitation of Steel Ball, International Research Journal of Engineering and Technology, Volume: 02, Issue: 08, November, 2015.

[13] Mrdjan Jankovic, Nonlinear Control in Automotive Engine Applications, Ford Research Laboratory, June 2002.

[14] James Richard Forbes, Extensions of Input-Output Stability Theory and the Control of Aerospace Systems Graduate Department of Aerospace Science and Engineering, University of Toronto, 2011.

[15] Ivan Svarc, A New Approach to Popov Criterion for Stability Analysis of Nonlinear Control Systems, Advanced Materials Research, Vols. 463-464, pp. 1549-1552, 2012.

[16] Michael Neunert, Cedric de Crousaz, Fadri Furrer, Mina Kamel, Farbod Farshidian, Roland Siegwart, Jonas Buchli, Fast Nonlinear Model Predictive Control for Unified Trajectory Optimization and Tracking, Proceedings of the 2016 IEEE/RSJ International Conference on Robotics and Automation (ICRA 2016) - (c) IEEE, 2016.

[17] Jake Bouvrie, Boumediene Hamzi, Empirical estimators for stochastically forced nonlinear systems: Observability, controllability and the invariant measure, American Control Conference (ACC), IEEE, 2012.

CHANGE IN STRENGTH PARAMETERS BY ADDITION OF Tio$_2$ & Sio$_2$ NANO-PARTICLES IN CONCRETE

First Author[1] TUMU BHARGAVI , PG STUDENT, AMARA INSTITUTE OF ENGINEERING AND TECHNOLOGY ,GUNTUR,t.bhargavi3@gmail.com

Second Author[2] M.NAGESWAR RAO, ASSISTANT PROFESSOR, AMARA INSTITUTE OF ENGINEERING AND TECHNOLOGY ,GUNTUR, t.bhargavi3@gmail.com

ABSTRACT: The recent researches on Nano materials and nano technologies have highlighted the potential use of these materials in various fields such as medicine, construction, automobile industry, etc., this is due to special characteristics of materials at the nano scale. Building materials domain can be one of the main beneficiaries of the researches, with applications that will improve the characteristics of concrete and steel, glass and insulating materials. Improving the material resistance and increasing of their durability will reduce environmental pollution by reducing the carbon footprint of the building. Based on the previous study we have conducted the following tests on concrete consisting of Nano particles i.e., Compressive strength of cubes and cylinders, Split tensile strength of cylinders and Flexural strength of beams. In this study by using nano particles (silica dioxide and titanium dioxide) which leads to densifying of the micro and nanostructure resulting in improved mechanical properties. In this study we have added 0.1, 0.125, 0.25, 0.5, 0.75 and 1.0 percentage of Sio$_2$ and Tio$_2$. The addition of Sio$_2$ and Tio$_2$ in different percentages, improves strength properties of concrete.

Keywords: Nano materials , Nano particles , pozzolana, Duro concrete Mix Design

INTRODUCTION:

This standard lays down the recommended procedure for designing concrete mixes for general types of construction using the concreting materials normally available. The design is carried out for a desired compressive strength and workability of concrete, using continuously graded aggregates. This standard does not include the design of concrete mixes for flexural strength or when gap-graded aggregates or various admixtures and pozzolana are to be used. All requirements of IS : 456-1978 and IS : 1343-1980 in so far as they apply, shall be deemed to form part of this standard except where otherwise laid down in this standard.

Water to cement ratio (W/C ratio) is the single most important factor governing the strength and durability of concrete. Strength of concrete depends upon W/C ratio rather than the cement content. Abram's law states that higher the water/cement ratio, lower is the strength of concrete. As a thumb rule every 1% increase in quantity of water added, reduces the strength of concrete by 5%. A water/cement ratio of only 0.38 is required for complete hydration of cement. (Although this is the theoretical limit, water cement ratio lower than 0.38 will also increase the strength, since all the cement that is added, does not hydrate) Water added for workability over and above this water/cement ratio of 0.38, evaporates leaving cavities in the concrete. These cavities are in the form of thin capillaries. They reduce the strength and durability of concrete. Hence, it is very important to control the water/cement ratio on site. Every extra lit of water will approx. reduce the strength of concrete by 2 to 3 N/mm^2 and increase the workability by 25 mm. As stated earlier, the water/cement ratio strongly influences the permeability of concrete and durability of concrete. Revised IS 456-2000 has restricted the maximum water/cement ratios for durability considerations by clause 8.2.4.1, table 5.

Trail No	Empty Weight of Bottle (W1)	Weight of Bottle + Dry aggregates (W2)	Weight of bottle + aggregates + water (W3)	Weight of bottle + water	Specific gravity
1	660	1080	1738	1442	3
2	660	1090	1738	1442	3.2
3	660	1095	1730	1442	3.4
				Avg.	3.2

Cement is the core material in concrete, which acts as a binding agent and imparts strength to the concrete. From durability considerations cement content should not be reduced below $300Kg/m^3$ for RCC. IS 456 –2000 (Refer annexure VI page 78 of Duro concrete Mix Design Manual) recommends higher cement contents for more severe conditions of exposure of weathering agents to the concrete. It is not necessary that higher cement content would result in higher strength. In fact latest findings show that for the same water/cement ratio, a leaner mix will give better strength. However, this does not mean that we can achieve higher grades of concrete by just lowering the water/cement ratio. This is because lower water/cement ratios will mean lower water contents and result in lower workability. In fact for achieving a given workability, a certain quantity of water will be required. If lower water/cement ratio is to be achieved without disturbing the workability, cement content will have to be increased. Higher cement content helps us in getting the desired workability at a lower water/cement ratio. In most of the mix design methods, the water contents to achieve different workability levels are given in form of empirical relations. Water/cement ratios required to achieve target mean strengths are interpolated from graphs given in IS 10262 Clause 3.1 and 3.2 of Duro concrete.

Observations:

Record of Observations of Coarse Aggregates

Table:1

S.No	% of T0.io2	Split Tensile Strength (Mpa)			
		7days	Average	28days	
1	0	0.86	0.91	1.74	1.79
		0.98		1.78	
		0.90		1.86	
2	0.1	0.99	1.02	1.87	1.89
		1.16		1.82	

		0.92		1.98	
3	0.5	1.20	1.12	2.05	2.05
		1.16		2.16	
		1.02		1.95	
4	1.0	1.13	1.21	2.16	2.18

Table: 2

Results and discussions:

S.NO	% of Chemical added SiO$_2$ (%)	Workability		
		Slump Cone (mm)	Compaction Factor	Vee-bee Consistometer (Sec)
1	0	70	0.9	4
2	0.1	75	0.9	4
3	0.125	75	0.92	4
4	0.25	80	0.93	5
5	0.5	80	0.93	5
6	0.75	80	0.94	5
7	1.00	85	0.94	5

Table: 3

S.No	MIX PROPORTION	W/C	NANO SiO$_2$ (%)	NANO TiO$_2$ (%)	NO.OF CUBES
1	M20	0.48	0.10	0.10	9
2	M20	0.48	0.125	0.125	9
3	M20	0.48	0.25	0.25	9
4	M20	0.48	0.50	0.50	9

| 5 | M20 | 0.48 | 0.75 | 0.75 | 9 |
| 6 | M20 | 0.48 | 1 | 1 | 9 |

- Studied the variation of compressive Strength of concrete with Nano-particles Tio2 & Sio2.

- Studied the variation of Flexural and Split Tensile Strength of concrete with Nano-particles Tio2 & Sio2.

Table: 4

S.NO	% of Chemical added TiO$_2$ (%)	Workability		
		Slump Cone (mm)	Compaction Factor	Vee-bee Consistometer (Sec)
1	0	72	0.9	4
2	0.1	74	0.91	4
3	0.125	74	0.91	4
4	0.25	78	0.92	5
5	0.5	80	0.92	5
6	0.75	80	0.93	5
7	1.00	85	0.93	5

Table: 5

S.No	% of Sio2	Compressive Strength (Mpa)					
		3days	Average	7days	Average	28days	Average
1	0	O9.33	9.18	18.4	18.23	28	27.93
		8.66		18.8		27.1	
		9.55		17.5		28.7	
2	0.1	11.5	11.55	23.33	23.03	35.0	34.72
		11.77		22.72		34.66	
		11.4		23.04		34.50	
3	0.125	10.75	11.20	22.01	21.45	33.0	33.06
		11.62		20.98		33.25	
		11.24		21.37		32.94	
4	0.25	10.69	10.49	21.4	21.18	32.09	32.34
		10.24		21.0		32.37	
		10.54		21.16		32.58	

5	0.5	10.43	10.40	21.97	20.99	31.30	31.47
		10.11		20.58		31.57	
		10.67		20.43		30.81	
6	0.75	11.08	10.23	20.35	20.21	31.29	31.22
		10.80		20.03		31.66	
		10.39		20.26		31.47	
7	1.0	9.93	9.76	19.86	19.51	29.82	29.86
		9.79		19.48		29.4	
		9.58		19.21		30.37	

Table: 6

| S.No | % of Sio2 | Flexural Strength (Mpa) | | | |
		7days	Average	28days	
1	0	0.42	0.34	1.28	1.29
		0.28		1.36	
		0.32		1.24	
2	0.1	0.40	0.40	1.25	1.30
		0.35		1.35	
		0.45		1.30	
3	0.5	0.45	0.46	1.40	1.40
		0.45		1.45	
		0.46		1.35	
4	1.0	0.60	0.48	1.45	1.41
		0.45		1.45	
		0.40		1.35	

Table: 7

| S.No | % of Sio2 | Flexural Strength (Mpa) | | | |
		7days	Average	28days	
1	0	0.42	0.34	1.28	1.29
		0.28		1.36	
		0.32		1.24	
2	0.1	0.40	0.40	1.25	1.30
		0.35		1.35	
		0.45		1.30	
3	0.5	0.45	0.46	1.40	1.40
		0.45		1.45	

		0.46		1.35	
4	1.0	0.60	0.48	1.45	1.41
		0.45		1.45	
		0.40		1.35	

Table: 8

S.No	% of Sio2	Split Tensile Strength (Mpa)			
		7days	Average	28days	
1	0	0.86	0.91	1.74	1.79
		0.98		1.78	
		0.90		1.86	
2	0.1	1.11	1.21	2.01	2.07
		1.20		1.95	
		1.33		2.25	
3	0.5	1.27	1.24	2.29	2.33
		1.34		2.53	
		1.11		2.07	
4	1.0	1.39	1.29	2.45	2.55
		1.22		2.67	
		1.26		2.53	

Table: 9

S.No	% of Tio2	Compressive Strength (Mpa)			
		7days	Average	28days	
1	0	20.32	20.84	32.18	31.82
		21.4		31.5	
		20.8		31.8	
2	0.1	21.62	21.48	33.86	33.09
		22.18		33.05	
		20.66		32.38	
3	0.5	21.65	21.82	36.33	36.07
		22.35		35.76	
		21.95		36.12	
4	1.0	21.86	22.06	38.07	37.86
		22.20		37.82	

		22.14			37.70	

Table:10

S.No	% of Tio2	Compressive Strength (Mpa)					
		3days	Average	7days	Average	28days	Average
1	0	9.33	9.18	18.4	18.23	28	27.93
		8.66		18.8		27.1	
		9.55		17.5		28.7	
2	0.1	11.09	10.66	20.82	20.51	30.20	31.17
		10.6		20.49		31.82	
		10.31		20.24		31.5	
3	0.125	10.42	10.71	22.2	21.72	33.27	32.23
		10.15		21.56		31.62	
		9.87		21.42		30.90	
4	0.25	11.49	10.85	22.0	21.84	34.49	34.12
		10.76		21.48		34.02	
		10.58		21.72		33.87	
5	0.5	12.06	11.72	20.33	22.73	36.20	36.12
		11.64		20.58		36.53	
		11.48		20.82		35.65	
6	0.75	12.27	11.8	23.46	22.92	36.82	36.73
		11.63		22.71		36.45	
		11.50		22.59		36.93	
7	1.0	12.6	12.24	23.47	23.27	37.80	37.63
		12.14		23.07		37.41	
		12.0		23.29		37.7	

Table:11

Conclusion:

By making the water cement ratio as 0.48, the 28 days compressive strength of concrete at different% of nano silica and nano titanium has been achieved as 3 – 5 times of conventional concrete. The present generations of cement based materials provides an economical option to add several alternative materials currently in use although several projects have been carried out to demonstrate the usefulness of these materials, research is still needed to update current code requirements, quality assurance procedures and design process to safely utilize these new materials to their ultimate potential.

We are making a point and that the setting time should be increased for concrete than that for ordinary concrete to have a healthy look and more strength.

- Use of IS: 10262 – 1982 code specifications helped in designing concrete mix.
- Addition of cement with nano silica &nano Titanium increase the cement.
- Cement quantity used and helped improving the ultimate compressive strength of concrete.
- Failure due to excess cement content is avoided by addition of nano materials.
- By the final mix obtained the increase in compressive strength is observed and tensile strength is not obtained.

By making the water cement ratio as 0.48, the 28 days compressive strength of concrete at different% of nano silica and nano titanium has been achieved as 3 – 5 times of conventional concrete. The present generations of cement based materials provides an economical option to add several alternative materials currently in use although several projects have been carried out to demonstrate the usefulness of these materials, research is still needed to update current code requirements, quality assurance procedures and design process to safely utilize these new materials to their ultimate potential.

We are making a point and that the setting time should be increased for concrete than that for ordinary concrete to have a healthy look and more strength.

- Use of IS: 10262 – 1982 code specifications helped in designing concrete mix.
- Addition of cement with nano silica & nano Titanium increase the cement the
- Cement quantity used and helped improving the ultimate compressive strength of concrete.
- Failure due to excess cement content is avoided by addition of nano materials.
- By the final mix obtained the increase in compressive strength is observed and tensile strength is not obtained.

REFERENCES:

1. A.A. Maghsoudi and F. Arabpour Dahooei (2009)**,** application of nanotechnology in self compacting concrete design, *Archive of SID Vol. 22, No. 3, October 2009 – 229.*

2. Ali Akbar Firoozi, Mohd Raihan Taha and Ali Asghar Firoozi (2014), Nanotechnology in Civil Engineering, *EJGE, Vol. 19 [2014], Bund. T*

3. Amit Srivastava and Kirti Singh (2011), nano technology in civil engineering and construction: a review on state of the art and future prospects, *Proceedings of Indian Geotechnical Conference,December 15-17, 2011, Kochi (Paper No.R-024)*

4. B. Bhuvaneshwari, Saptarshi sasmal, Nagesh r.iyer (2011) Nano science to Nanotechnology for Civil Engineering – Proof of Concepts, *Recent Researches in Geography, Geology, Energy, Environment and Biomedicine.*

5. Kasthurirangan Gopalakrishnan (2011) Nanotechnology in Civil Infrastructure, *springer.*

6. Patel Abhiyan S., Rathod Hiren A.,Neeraj SharmaD. (2013), an overview on Application of Nanotechnology in Construction Industry, *International Journal of Innovative Research in Science, Engineering and Technology*, Vol. 2, Issue 11, November 2013.

7. Radu olar (2011) Nano materials and nanotechnologies for civil engineering, *Buletinul Institutului Politehnic Din Iaşi, 4, 2011.*

8. Saurav (2012) Application of nanotechnology in building materials, *International Journal of Engineering Research and Applications , Vol. 2, Issue5, September- October 2012, pp.1077-1082.*

9. V.Kartik Ganesh (2012) Innovations in the Methodology of Usage of Nanomaterials in Civil Engineering Works, *International Journal of Software and Web Sciences.*

10. Zhi Ge and Zhili Gao (2008) Applications of Nanotechnology and Nano materials in Construction, "*First   International Conference on Construction in Developing Countries",* August 4-5, 2008.

Extension of Fourier-Stieltjes Transform

V. D. Sharma, P. D. Dolas

HOD, Department of Mathematics, Arts, Commerce and Science College, Kiran Nagar, Amravati, India, 444606

Email: vdsharma@gmail.com

Abstract— A linear phase shift introduced in time domain signals results in a frequency domain is a Modulation theorem of integral transform and the Parseval's theorem is the sum (or integral) of the square of a function is equal to the sum (or integral) of the square of its transform. The properties of the Fourier transform provided valuable insight into how signal operations in the time-domain are described in the frequency-domain.

In the present work, Fourier-Stieltjes Transform is extended in distributional generalized sense. Adjoint operators for the distributional Fourier-Stieltjes Transform is obtained. Also,Modulation and Parseval's Theorem for the Fourier-Stieltjes Transform are proved.

Keywords— Fourier Transform, Steiltjes Transform, Inversion Formula of Fourier-Stieltjes Transform, Fourier-Steiltjes Transform, Generalized function.

INTRODUCTION

Mathematically, the sum (or integral) of the square of a function is equal to the sum (or integral) of the square of its transform is a Parseval's Identity(Parseval's Theorem). This theorem originates from series by Marc-Antoine Parseval's in 1799, which was later applied to the Fourier series. Although the term "Parseval's theorem" is often used to describe the unitarily of any Fourier transform, especially in Physics and Engineering, the most general form of this property is more properly called the Plancherel theorem.

Modulation is an important property for Transform that $F[\cos(2\pi k_0 x)f(x)](k)$ can be expressed in terms of $F[f(x)] = F(k)$ as follows [5]-

$$F[\cos(2\pi k_0 x)f(x)](k) = \frac{1}{2}[F(k - k_0) + F(k + k_0)].$$

In the same manner we have, $F[\sin(2\pi k_0 x)f(x)](k) = \frac{1}{2i}[F(k - k_0) - F(k + k_0)].$

We live in the time-domain. The integral transform converts a signal or system representation to the frequency-domain, which provides another way to visualize a signal or system convenient for analysis and design. The properties of the transform provided valuable insight into how signal operations in the time-domain are described in the frequency-domain.

Fourier transform is a technique employed to solve ODE's, PDE's, Initial value problems, boundary value problems, Integral equations, Signal processing, in computers, image processing and so on[7].

Similarly, The Stieltjes transform is also used in many areas such as continued fraction, probability and signal processing. It was first introduced by T.S. Stieltjes in connection to the moment problems for semi-infinite interval [6]. In the present work of this paper, we also defined the adjoint operators of Fourier- Stieltjes Transform.

We had already define the Conventional Fourier-Stieltjes Transform of a complex valued smooth function $f(t, x)$ is defined by convergent integral [3] as -

$$FS\{f(t,x)\} = F(s,p) = \int_0^\infty \int_0^\infty f(t,x)\ e^{-ist}\ (x+y)^{-p}\ dt\ dx\ .$$

In the same manner, we had defined the Distributional Fourier- Stieltjes Transform in [3] as-

$$FS\{f(t,x)\} = F(s,p) = \langle f(t,x), e^{-ist}(x+y)^{-p}\rangle$$

Where, FS_α^* is dual space consist of continuous linear function on FS_α and $f(t,x) \in FS_\alpha$, for some $s > 0$ and $k > Re\ p$.

From our previous work, Inversion formula for the Distributional Fourier-Stieltjes Transform is defined as follows-

$$f(t,x) = \lim_{r,q\to\infty} \frac{1}{4\pi^2} \int_{-r}^{r} \int_0^q F(s,p)\ e^{ist}(x+y)^{(p+1)}\ dp\ ds$$

Outline of this paper-

In section 1, we developed the Modulation theorem for Fourier-Stieltjes Transform. Section 2, gives the Parseval's theorem for the Fourier-Stieltjes Transform. Section 3, defines the adjoint operators for Distributional Fourier-Stieltjes Transform. The notation and terminology is given by A.H. Zemanian[2].

1. Modulation Property

i] Prove that-

$FS\{f(t,x)\cos(at+bx)\}(s,p)$

$$= \frac{1}{2}\{FS[e^{ibx}f(t,x)](s-a,p) + FS[e^{-ibx}f(t,x)](s+a,p)\}$$

Proof:- We have

$FS\{f(t,x)\cos(at+bx)\}(s,p)$

$$= \int_0^\infty \int_0^\infty f(t,x)\cos(at+bx)\,e^{-ist}(x+y)^{-p}\,dt\,dx$$

$$= \int_0^\infty \int_0^\infty f(t,x)\left[\frac{e^{i(at+bx)}+e^{-i(at+bx)}}{2}\right]e^{-ist}(x+y)^{-p}\,dt\,dx$$

$$= \frac{1}{2}\int_0^\infty \int_0^\infty [f(t,x)e^{i(at+bx)}e^{-ist}(x+y)^{-p} + f(t,x)\,e^{-i(at+bx)}e^{-ist}(x+y)^{-p}]\,dt\,dx$$

$$= \frac{1}{2}\int_0^\infty \int_0^\infty f(t,x)e^{i(at+bx)}e^{-ist}(x+y)^{-p}\,dt\,dx$$

$$+ \frac{1}{2}\int_0^\infty \int_0^\infty f(t,x)\,e^{-i(at+bx)}e^{-ist}(x+y)^{-p}\,dt\,dx$$

$$= \frac{1}{2}\{\int_0^\infty \int_0^\infty e^{ibx}f(t,x)e^{-i(s-a)t}(x+y)^{-p}\,dt\,dx$$

$$+ \int_0^\infty \int_0^\infty e^{-ibx}f(t,x)\,e^{-i(s+a)t}(x+y)^{-p}\,dt\,dx\}$$

$FS\{f(t,x)\cos(at+bx)\}(s,p)$

$$= \frac{1}{2}\{FS[e^{ibx}f(t,x)](s-a,p) + FS[e^{-ibx}f(t,x)](s+a,p)\}$$

ii] Prove that-

$$FS\{f(t,x)\sin(at+bx)\}(s,p) = \frac{1}{2i}\{FS[e^{ibx}f(t,x)](s-a,p) - FS[e^{-ibx}f(t,x)](s+a,p)\}$$

Proof: - We have

$$FS\{f(t,x)\sin(at+bx)\}(s,p) = \int_0^\infty \int_0^\infty f(t,x)\sin(at+bx)\,e^{-ist}(x+y)^{-p}\,dt\,dx$$

$$= \int_0^\infty \int_0^\infty f(t,x)\left[\frac{e^{i(at+bx)}-e^{-i(at+bx)}}{2i}\right]e^{-ist}(x+y)^{-p}\,dt\,dx$$

$$= \frac{1}{2i}\int_0^\infty \int_0^\infty [f(t,x)e^{i(at+bx)}e^{-ist}(x+y)^{-p} - f(t,x)\,e^{-i(at+bx)}e^{-ist}(x+y)^{-p}]\,dt\,dx$$

$$= \frac{1}{2i}\int_0^\infty \int_0^\infty f(t,x)e^{i(at+bx)}e^{-ist}(x+y)^{-p}\,dt\,dx$$

$$- \frac{1}{2i}\int_0^\infty \int_0^\infty f(t,x)\,e^{-i(at+bx)}e^{-ist}(x+y)^{-p}\,dt\,dx$$

$$= \frac{1}{2i}\{\int_0^\infty \int_0^\infty e^{ibx}f(t,x)e^{-i(s-a)t}(x+y)^{-p}\,dt\,dx$$

$$-\int_0^\infty \int_0^\infty e^{-ibx} f(t,x) \, e^{-i(s+a)t} \, (x+y)^{-p} \, dt \, dx\}$$

$FS\{f(t,x)\sin(at+bx)\}(s,p)$

$$= \frac{1}{2i}\{FS[e^{ibx}f(t,x)](s-a\,,p) - FS[e^{-ibx}f(t,x)](s+a\,,p)\}$$

2. Parseval's Identity for the distributional Fourier- Steiltjes Transform:

Theorem: If $FS\{f(t,x)\}(s,p) = F(s,p)$ and $FS\{g(t,x)\}(s,p) = G(s,p)$ then

i] $\int_0^\infty \int_0^\infty f(t,x) \, \overline{g(t,x)} \, dt \, dx$

$$= \frac{1}{2\pi^2}\int_0^\infty \int_0^\infty FS\{(x+y)f(t,x)\}(s,p) \, \overline{G(s,p)} \, dp \, ds$$

ii] $\int_0^\infty \int_0^\infty |f(t,x)|^2 \, dt \, dx$

$$= \frac{1}{2\pi^2}\int_0^\infty \int_0^\infty |F(s,p)|^2 \, dp \, ds$$

Proof:-We have

$FS\{f(t,x)\}(s,p) = F(s,p) = \int_0^\infty \int_0^\infty f(t,x)e^{-ist} \, (x+y)^{-p} \, dt \, dx$

By using Inversion formula for Fourier-Stieltjes Transform, We have-

$g(t,x) = \frac{1}{4\pi^2}\int_{-\infty}^\infty \int_0^\infty G(s,p) \, e^{ist}(x+y)^{p+1} \, dp \, ds$

$g(t,x) = \frac{1}{2\pi^2}\int_0^\infty \int_0^\infty G(s,p) \, e^{ist}(x+y)^p(x+y) dp ds$

Now it's conjugate is-

$\overline{g(t,x)} = \frac{1}{2\pi^2}\int_0^\infty \int_0^\infty \overline{G(s,p)} \, e^{-ist}(x+y)^p(x+y) dp ds$

Consider,

$\int_0^\infty \int_0^\infty f(t,x) \, \overline{g(t,x)} \, dt \, dx$

$$= \int_0^\infty \int_0^\infty f(t,x) \, dt \, dx \left\{\frac{1}{2\pi^2}\int_0^\infty \int_0^\infty \overline{G(s,p)} \, e^{-ist}(x+y)^p(x+y) dp ds\right\}$$

$$= \frac{1}{2\pi^2}\left[\int_0^\infty \int_0^\infty f(t,x) \, dt \, dx\{\int_0^\infty \int_0^\infty \overline{G(s,p)} \, e^{-ist}(x+y)^p(x+y) dp ds\}\right]$$

$$= \frac{1}{2\pi^2}\left[\int_0^\infty \int_0^\infty \int_0^\infty \int_0^\infty \overline{G(s,p)} \, f(t,x) \, e^{-ist}(x+y)^p(x+y) dp ds \, dt \, dx\right]$$

$$= \frac{1}{2\pi^2}\left[\int_0^\infty \int_0^\infty \overline{G(s,p)} \, dp ds \left\{\int_0^\infty \int_0^\infty f(t,x) \, e^{-ist}(x+y)^p \frac{(x+y)^{-p}}{(x+y)^{-p}}(x+y) dt \, dx\right\}\right]$$

$$= \frac{1}{2\pi^2}\left[\int_0^\infty \int_0^\infty \overline{G(s,p)} \, dp ds\{\int_0^\infty \int_0^\infty (x+y)^{2p+1} f(t,x) \, e^{-ist}(x+y)^{-p} \, dt \, dx\}\right]$$

$\int_0^\infty \int_0^\infty f(t,x) \, \overline{g(t,x)} \, dt \, dx$

$$= \frac{1}{2\pi^2}\int_0^\infty \int_0^\infty FS\{(x+y)^{2p+1}f(t,x)\}(s,p) \, \overline{G(s,p)} dp ds$$

$$= \frac{1}{2\pi^2} \int_0^\infty \int_0^\infty (x+y)^{2p+1} F(s,p) \overline{G(s,p)} \, dp \, ds$$

Putting-

$$f(t,x) = g(t,x) \,,$$

$$F(s,p) = G(s,p) \,,$$

$$\overline{F(s,p)} = \overline{G(s,p)}$$

By using the above result we have-

$$\int_0^\infty \int_0^\infty f(t,x) \, \overline{f(t,x)} \, dt \, dx$$

$$= \frac{1}{2\pi^2} \int_0^\infty \int_0^\infty F(s,p) \, \overline{F(s,p)} \, ds \, dp$$

$$\int_0^\infty \int_0^\infty |f(t,x)|^2 \ dt \, dx$$

$$= \frac{1}{2\pi^2} \int_0^\infty \int_0^\infty |F(s,p)|^2 \, ds \, dp$$

Hence Proved.

3. Adjoint Operators on Distributional Fourier-Stieltjes Transform

3.1 Proposition

The Adjoint shifting operator is a continuous function from FS_α^* to FS_α^* . The adjoint operator is $f(t,x) \rightarrow f(t-\tau,x)$ leads to the operation transform formula-

$$FS\{f(t-\tau,x) = e^{-is\tau} FS\{f(t,x)\}$$

Proof:- Consider

$$FS\{f(t-\tau,x) = \langle f(t-\tau,x), e^{-ist}(x+y)^{-p} \rangle$$

$$= \langle f(t-\tau,x), e^{-is(t+\tau)}(x+y)^{-p} \rangle$$

$$= \langle f(t,x), e^{-is\tau} e^{-ist}(x+y)^{-p} \rangle$$

$$= e^{-is\tau}\langle f(t,x), e^{-ist}(x+y)^{-p} \rangle$$

$$FS\{f(t-\tau,x) = e^{-is\tau} FS\{f(t,x)$$

3.2 Proposition

The adjoint differential operator $f \rightarrow D_t f$ is continuous linear mapping from the dual space FS_α^* into itself. Corresponding transform formula is

$$FS\{D_t f(t,x)\} = (is)FS\{f(t,x)\}$$

Proof:- Consider,

$$FS\{D_t f(t,x)\} = \langle D_t f(t,x), e^{-ist}(x+y)^{-p}\rangle$$

$$= \langle f(t,x), -D_t e^{-ist}(x+y)^{-p}\rangle$$

$$= \langle f(t,x), -(-is)e^{-ist}(x+y)^{-p}\rangle$$

$$= is\langle f(t,x), e^{-ist}(x+y)^{-p}\rangle$$

$$FS\{D_t f(t,x)\} = (is)FS\{f(t,x)\}$$

3.3 Proposition

The adjoint differential operator $f \to D_x f$ is continuous linear mapping from the dual space FS_α^* into itself. Corresponding transform formula is

$$FS\{D_x f(t,x)\} = (p)FS\{f(t,x)\}$$

Proof:- Consider,

$$FS\{D_t f(t,x)\} = \langle D_x f(t,x), e^{-ist}(x+y)^{-p}\rangle$$

$$= \langle f(t,x), -D_x e^{-ist}(x+y)^{-p}\rangle$$
$$= \langle f(t,x), -(-p)e^{-ist}(x+y)^{-p-1}\rangle$$
$$= p\langle f(t,x), e^{-ist}(x+y)^{-(p+1)}\rangle$$

$$FS\{D_t f(t,x)\} = (p)F(s, p+1)$$

3.4 Proposition

The adjoint operator $f \to \theta f$ is a continuous linear mapping of FS_α^* into itself. The adjoint operator is $f(t,x) \to e^{-i\tau t}(x+y)^{-\alpha}f(t,x)$. Corresponding operator transform formula is

$$FS\{e^{-i\tau t}(x+y)^{-\alpha}f(t,x)\} = F(s+\tau, p+1)$$

Proof: Consider,

$$FS\{e^{-i\tau t}(x+y)^{-\alpha}f(t,x)\} = \langle e^{-i\tau t}(x+y)^{-\alpha}f(t,x), e^{-ist}(x+y)^{-p}\rangle$$

$$= \langle f(t,x), e^{-i\tau t}(x+y)^{-\alpha}e^{-ist}(x+y)^{-p}\rangle$$

$$= \langle f(t,x), e^{-it(s+\tau)}(x+y)^{-(p+\alpha)}\rangle$$

$$= F(s+\tau, p+\alpha)$$

$$FS\{e^{-i\tau t}(x+y)^{-\alpha}f(t,x)\} = F(s+\tau, p+1)$$

3.5 Proposition

Noting above proposition the another adjoint operator is $f(t,x) \to (-it)^{k_1}[-\log(x+y)]^{k_2} f(t,x)$. Corresponding operator transform formula is $FS\{(-it)^{k_1}[-\log(x+y)]^{k_2} f(t,x)\} = D_s^{k_1} D_p^{k_2} F(s,p)$

Proof: Consider,

$$FS\{(-it)^{k_1}[-\log(x+y)]^{k_2} f(t,x)\} = \langle (-it)^{k_1}[-\log(x+y)]^{k_2} f(t,x), e^{-ist}(x+y)^{-p} \rangle$$

$$= \langle f(t,x), (-it)^{k_1}[-\log(x+y)]^{k_2} e^{-ist}(x+y)^{-p} \rangle$$

$$= \langle f(t,x), D_s^{k_1} D_p^{k_2} e^{-ist}(x+y)^{-p} \rangle$$

$$= D_s^{k_1} D_p^{k_2} \langle f(t,x), e^{-ist}(x+y)^{-p} \rangle$$

$$FS\{(-it)^{k_1}[-\log(x+y)]^{k_2} f(t,x)\} = D_s^{k_1} D_p^{k_2} F(s,p)$$

CONCLUSION

In the present work, Fourier-Stieltjes Transform is extended in distributional generalized sense. Adjoint operators for the distributional Fourier-Stieltjes Transform is obtained. Also,Modulation and Parseval's Theorem for the Fourier-Stieltjes Transform are proved.

REFERENCES:

[1] Sharma V.D. and Dolas P.D.: Generalization of Fourier-Stieltjes transform, American Jr. of Mathematics and Sciences, Vol.2, No.1, January 13, ISSN No. 2250-3102.

[2] Zemanian A.H.:- Generalized integral transformation, Inter science publisher, New York, 1965.

[3] Sharma V.D. and Dolas P.D.:- Analyticity of Distribution Generalized FS transform, Int. Jr. of Math. Analysis,Vol. 6, 2012, No. 9, 447-451.

[4] Sharma V.D.:- Modulation and Parseval's Theorem for Generalized Two Dimensional Fractional Fourier Transform, Int. Jr. of Mathematical Archiev, 2014, vol.5, No. 9, 247-251.

[5] Bracewell, R.: Modulation Theorem, The Fourier Transform and its application, 3rd edition, New York: McGraw-Hill, p. 108, 1999.

[6] Dennis Nemzer: Extending The Stieltjes Transform, Sarajevo Journal Of Mathematics, Vol.10 (23) (2014), 197-208.

[7] Debnath Loknath : Integral Transform and their application, Second edition, London, New York, 2007.

[8] Xiaotong Wang, Guanlei Xu, Yue Ma, Lijia Zhou, Longtao Wang: Generalized Parseval's Theorem on Fractional Fourier Transform for Discrete Signals and Filtering of LFM Signals, Journal of Signal and Information Processing, 2013, 4, 274-281.

[9] A.H. Zemanian: Distribution theory and Transform Analysis, Mcgraw Hill, New york, 1965.

[10] Sharma V.D. and Dolas P.D.: Some S-Type spaces of Fourier-Stieltjes Transform, Int. Jr. of Engineering and Innovation Technology, Vol. 3, Issue 3, Sept. 2013, 361-363.

Analysis Of Gearbox Casing Using FEA

Neeta T. Chavan , Student, M.E. Design, Mechanical Department, Pillai Hoc, Maharashtra, India

Assistant Prof. Gunchita Kaur-Wadhwa , Mechanical Department Pillai Hoc, Maharashtra, India

Associate Prof. Basavaraj S.Talikoti Mechanical Department, PIIT Panvel, Maharashtra, India

chavan.neeta@gmail.com

Abstract— Gearbox casing is the main component in automobile world which is used to protect components inside the gearbox. It consists of gears, shafts, bearings and oil. It is fluid containing casing which gives support to the moving parts. Gearbox failure occurs mainly due to the design issues, manufacturing defects, oil deficiency, excessive time at stoppage and high loading. In this project loading case is considered. Major challenge for such problems are whether to consider static analysis, dynamic analysis, or perturbation analysis and conditional circumstances for it to be performed. In this work static dynamic as well as perturbation analysis have been performed on gearbox casing. Model is to be developed in Abaqus/CAE and then same model is used for Finite Element Analysis by using Abaqus/Standard 6.10.1 for static analysis and dynamic analysis. Harmonic analysis is also performed by Abaqus software called as perturbation analysis for strain and frequency. Stress and frequency graph in both the cases that is in static and dynamic analysis is performed and results from static and dynamic are compared. Frequency effect on strain levels are linear and no surplus strain linearity is produced due to dynamic effect as compared to the static case. By using Abaqus/ standard it is found that results boost for dynamic case as compared to static case.

Keywords— Abaqus/CAE, Gearbox casing, Static stress analysis, Maximum principle stress, Minimum principle stress,

INTRODUCTION

Gearbox casing is the shell in which assembly of gears are sealed. The components of gearbox casing are gears, bearings, shafts and oil. The gearbox casing act as house the transmission components. The movement of the gear produces vibration in the gearbox casing. Any automobile vehicle requires high torque when they are climbing an elevated surface like a mountain and also at the initial idling, as its speeds is very low. But when vehicle is running with high speeds on plane road high torque is not required due to momentum. Therefore, the device which is required for two reasons, torque speed combination range and to maintain engine speed according to road condition as per drivers need. This device is known as gearbox or transmission box.

Lower gears have high torque and low power. Higher gears have high power but low torque. Due to the engine power stroke, the input shaft rotates once. Hence, the output shaft rotates. Then two such power strokes are required for one full rotation of output shaft which means that all power is transferred into one rotation. Hence, it has high torque. In case of high gear, the input shaft rotates only once means one power stroke, and the output shaft rotates several times. One power stroke rotates the output shaft several times. Hence the high speed, high power but low torque. Therefore, torque, speed and power are important factors in gearbox.

LITERATURE REVIEW

This chapter provides Review of Literature on topics related to gearbox casing. More work has been done for analysis of gearbox casing by using vibrational analysis by condition monitoring techniques, FFT analyzer, time frequency domain analysis also FEA analysis by using ANSYS.
Mirunalini Thirugnanasambandam, [1] determined the design and static analysis, natural frequency of casing and torsional, lateral critical speed of two stage gearbox casing. Amit Aherwar, [2] Studied vibration based techniques for condition monitoring in transmission system, in time frequency domain removes noise. Vijaykumar, Mr. Shivaraju, [3] Presented vibration based technique for condition monitoring in gearbox system also determined vibration analysis of gearbox casing using Finite Element Analysis (FEA), ANSYS software for natural vibrational modes and harmonic frequency response for casing to prevent resonance. M. S. Patil, [4] Studied vibrational analysis for gearbox casing using finite element analysis (FEA) by applying ANSYS software to determine the natural frequency of gearbox casing. Ashwani Kumar, [5] Studied gearbox casing of heavy vehicles and effect of mechanical properties of material on natural frequency and mode shapes. Vijay N.A., [6] have studied the gear box casing for permanent magnet dc motors. According to author, it is essential to analyze gearbox casing to decide dimensions and predict its behavior under operating

conditions, also it support to shaft and bearings. Ramamurti V. [7] presented design methodology for two stage gearbox, it involves comparison of design stresses obtained from classical methodology and FEM model, also raised due to stress.

PROBLEM DEFINATION

The main aim of this project is static analysis of casing in presence of generalized modes and critically studying the things for future improvements, in vibration characteristics raised due to stress. Also providing dynamic analysis of casing in presence of generalized modes and critically studying the things for future improvements from stress perspective.

SCOPE

To complete this project successfully, following scope has been defined

- Development of new methods for analysis
- Development of analytical technique and finite element implementation

OBJECTIVES

- To achieve the above stated aim the following objectives are implemented in the project.
- To determine casing response to fluctuations in terms of vibration level
- To carry out static stress analysis by applying load effect in the gearbox casing
- To simulate the observed facts in Abaqus

METHODOLOGY

The following are incorporated the research and further to utilize the information gained by the above stated literature review the under defined are used.

- Motivation and literature survey
- Casing problems and evaluation measures
- Modeling and analysis tools
- Harmonic response and interpretations
- Comparison within themselves

FINITE ELEMENT ANALYSIS BY ABAQUS

- In this analysis dimensions are taken from one of the literature [1]. Dimensions of the housing provided are of 700*450*200. Material used is gray cast iron because it has excellent vibration damping capacity. It has high compressive strength, low tensile strength, self-damping, does not vibrate, high resistance to wear. It contains 2.5-3.8% C, 1.1-2.8% Si, 0.4-1 % Mn, 0.15 % P and 0.10 % S. [8]. Also, density- 7200kg/m³, Elastic- Young's modulus- 2 e11 N/m², Poisson's ratio- 0.28 [9]. Due to higher complexity and nonlinearity, Aabaqus has been used. First solid model is to be developed in Abaqus /CEA 6.10.1 and then that can be used for further analysis.[10]
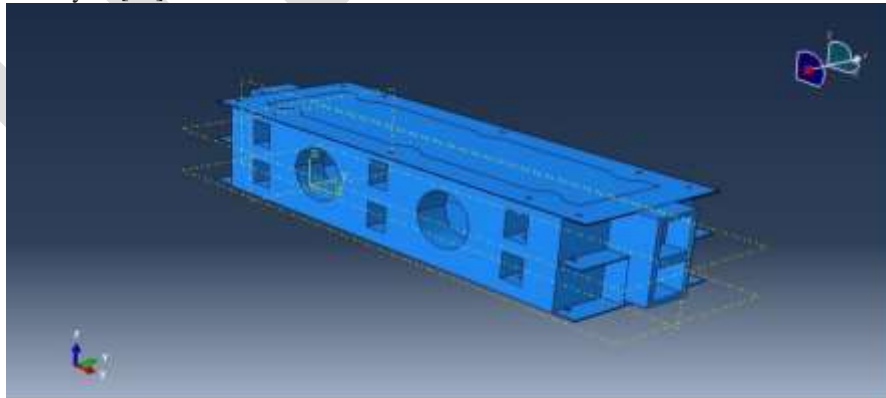
Fig -1: Model of gearbox casing
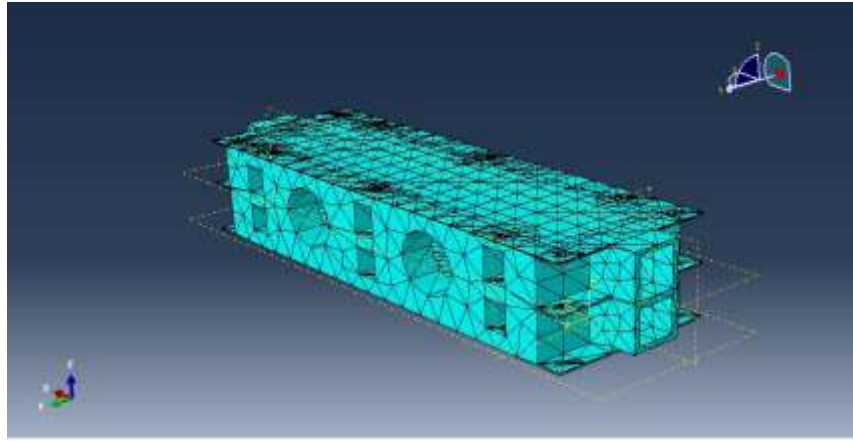
Fig -2: Meshing of gearbox casing

A. Static Analysis
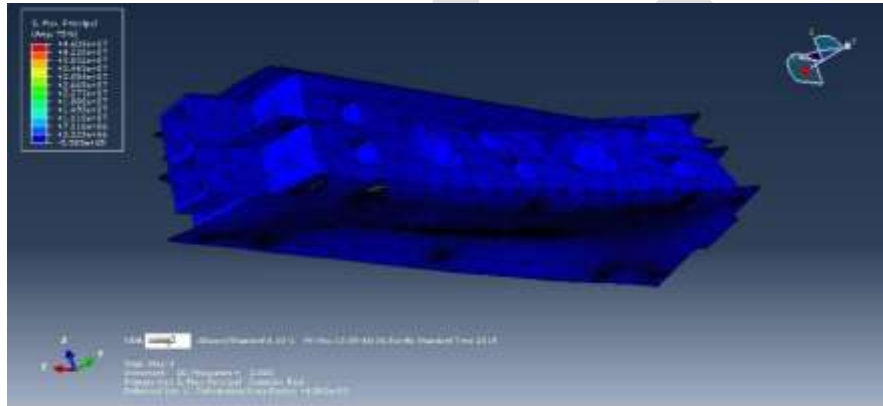
Fig 3: Static Stress by Maximum Principal Stress
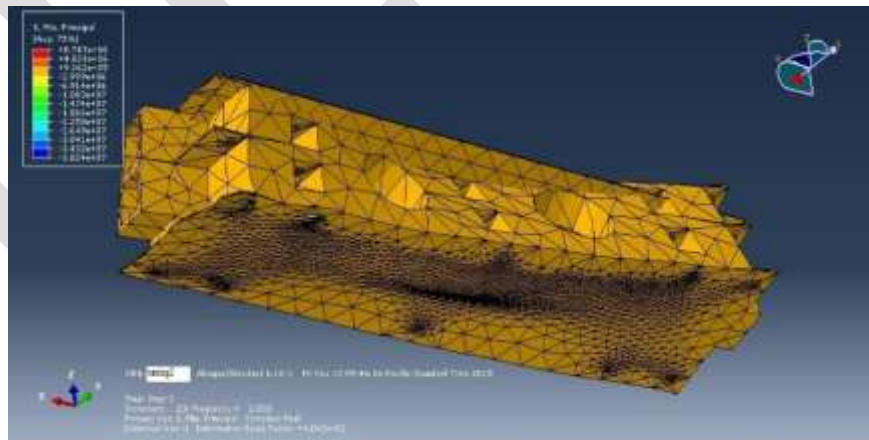
Fig -4: Static Stresses by Minimum Principal Stress

B. Dynamic Results

Step- Steady state dynamic
Load applied- 60000N
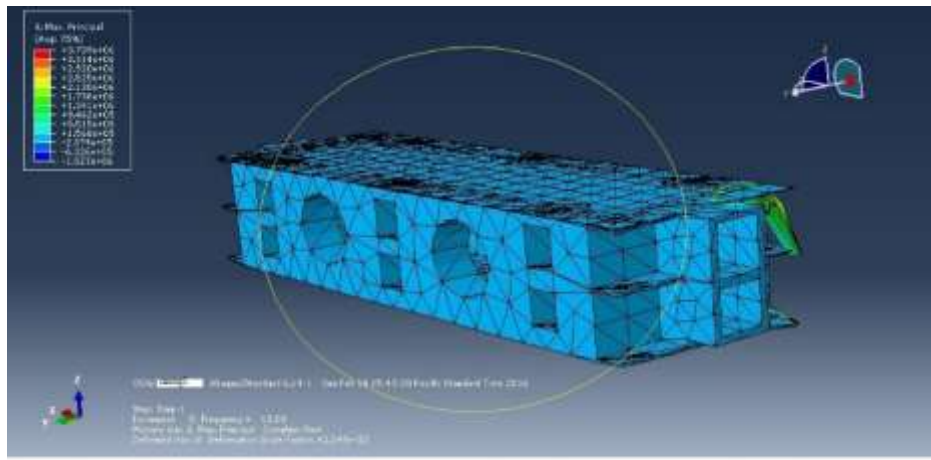
Fig -5 : Dynamic-Stress by Maximum Principal Stress
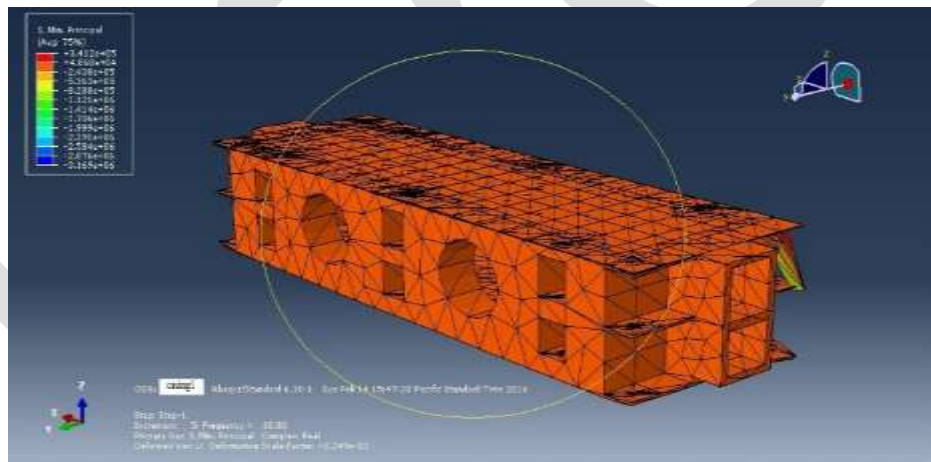
Fig -6: Dynamic stress by Minimum Principle Stress

CONCLUSION

Static analysis and dynamic analysis is to be done with Abaqus/Standard 6.10.1 results shows that dynamic stress boost than static stress. Von Mises stress are significant as against earlier predictions of maximum principle stress & deformations are less significant.

Harmonic analysis is performed for static and dynamic case shows that Frequency effect on strain levels is linear and no surplus strain linearity is produced due to dynamic effect as against static case. All modes are equally responsive to nearly all frequencies. But response boost up lot when forcing frequency matches with corresponding casing frequency.

REFERENCES:

Mirunalini Thirugnanasambandam, "Design of Transmission Housing," Proc Indian Natn Sci Acad 75, pp. 137-143, 2009.

M. S. K. Amit Aherwar, "Vibration Analysis Techniques For Gearbox Diagnostic: A Review," International Journal of Advanced Engineering Technology E-ISSN 0976-3945, vol. Vol.III, no. Issue II, pp. 04-12, April-June, 2012.

A. P. M. M. Mr.vijaykumar, "Vibration Analysis for Gearbox Casing Using Finite Element Analysis," The International Journal Of Engineering And Science (IJES), vol. III, no. 2, pp. 18-36, 2014.

J. M.S. PATIL, "Vibration Analysis of Gearbox Casing using Software tool ANSYS and FFT Analyze," International Journal Of Research In Aeronautical And Mechanical Engineering International Journal Of Research In Aeronautical And Mechanical Engineering , vol. III, no. 12, pp. 12-19, December 2015.

Ashwani Kumar, "Free Vibration and Material Mechanical Properties Influence Based Frequency and Mode Shape Analysis of Transmission Gearbox Casing," Elsevier Science Direct,Procedia Engineering, pp. 1096-1106, 2014.

R. K. A. Vijay N.A., "FE Analysis of Gear Box Casing used for Permanent Magnet D.C. Motors," International Journal of Engineering Research and General Science, vol. III, no. 4, pp. 92-99, July-August, 2015.

G. P. ,. Ramamurti V, "A Computer-aided design of a two-stage gearbox, Advances in Engineering Software," Elsevier science direct, vol. 28, no. 1, pp. 73-82, January 1997.

O. Khanna, Material Science and Metallurgy, New Delhi: Dhanpat Rai Publications, 2010.

Metal handbook, Tata McGrow Hill, 2008 Fourth Edition.

Abaqus reference manual

DEVELOPMENT OF SLAB THICKNESS DESIGN GUIDE

Pratyush Singh, P. C. Diwan

Civil Engineering Department, Swami Vivekanand University, Sagar, India, pratyushsingh1605@gmail.com

Abstract—Sustainability of concrete pavements depends on the rate of pavements deterioration. Cracks, as the main reason behind the deteriorations of concrete pavements, are initiated at the top or the bottom surface layer of concrete slab and then, propagated into depth of concrete slab due to fatigue of concrete. The load transfer efficiency across joints and cracks depends on the shear transfer capability of aggregate interlock and cement paste. The shear transfer capability of aggregate interlock and cement paste is an important factor. Using Miner's rule, equations for calculating the fatigue damage of concrete slab were developed.

Keywords— Concrete, pavement, slab, subbase, fatigue.

INTRODUCTION

The use of concrete pavement without an asphalt top layer dates back to Scotland in 1865 (Croney and Croney, 1998). With the growing worldwide interest in this field during the 20th century, concrete pavement technology has been embraced in Australia since the 1970s (Cruickshank, 1981). Concrete pavements were traditionally designed based on theoretical equations developed by Westergaard (1926, 1933, and 1947). Using finite element techniques, mechanistic approaches for designing of concrete pavements were developed. The mid-edge bottom-up transverse fatigue cracking was the only failure mode of the concrete pavements considered in the mechanistic design guides. Initiation and propagation of other fatigue related cracks in concrete pavements, designed based on the mechanistic approach, led to the development of mechanistic-empirical approaches in concrete pavement design guides.

While the mechanistic part of design guides provides required information on calculation of the critical stresses and deflections in pavements, the empirical part specifies possible failure modes of pavements under the applied loads. The applied loads can be vehicular and/or environmentally related. Vehicular loads have been considered as static loads in concrete pavement design guides but in reality, they are dynamic in nature as their locations upon pavement change with time.

Magnitude and configuration of vehicular loads together with environmental effects have a significant effect on induced tensile stresses within concrete pavements (Yu et al. 1998 and Hiller and Roesler 2002). Since a variety of axle group configurations is employed in heavy vehicle industries and across countries, further study is required to determine the interrelationship between concrete pavement distresses and pavement responses to the applied loads. Furthermore, the fact that structural responses of concrete pavements may be affected by the frequency and speed of vehicular loads (Izquierdo et al., 1997) has not been yet considered in concrete pavement design guides.

The most serious problem in concrete pavements is crack generation and propagation (Hossain et al., 2003). Cracking occurs in the first days after placement due to plastic shrinkage and the reaction between cement and aggregates in the setting time (Nawy, 2001). It then spreads over the pavement surface and propagates deeper in the concrete due to external factors such as drying shrinkage and fatigue. Although the use of appropriate curing methods could reduce the development of early edge cracking in pavement, current concrete pavement guides normally require the provision of reinforcement and / or concrete joints to minimise the development of secondary cracks in the pavement surfaces.

The fatigue life of concrete is traditionally estimated based on laboratory fatigue tests of concrete prism beams under one-directional cyclic loading using third point loading configuration. Since concrete pavements curl upward or downward during nighttime or daytime temperature gradients, results of the traditional fatigue test may be insufficient as the pavement curvature is not considered during the test. This also is a shortcoming which needs to be addressed.

CONCRETE PAVEMENT

Concrete as a versatile construction material has been used in many civil applications such as pavement. Since performance and deterioration of concrete pavements can be related to concrete properties, it is necessary to know how to achieve a better quality of

www.ijergs.org

concrete. Regarding the possible fatigue failure modes of concrete pavements, the most important concrete properties are concrete strength, modulus of elasticity, coefficient of thermal expansion, shrinkage and concrete fatigue life.

Concrete strength

The applied loads on concrete pavements are usually transferred to sublayers by bending actions which subsequently induce a tensile stress at the top or the bottom surface layer of the concrete slab. If the magnitude of induced tensile stress is equal or more than the flexural strength of the concrete, cracks as the main reason behind concrete pavement deteriorations are initiated at the surface layers and then propagated into the depth of the concrete slab. As a result, and in contrast with other structures where concrete compressive strength is used to design the concrete members, concrete flexural strength or modulus of rupture becomes an important concrete property used in concrete pavement design guides.

Factors affecting concrete strength are:

-       Cement characteristics and content

-       Water/cement, liquid/ cement, and/or water/cementitious ratios

-       Aggregate quality and interaction with cement paste

-       Type and percentage of chemical and mineral admixtures

-       Procedure and mixing time of constituents

-       Degree of compaction

-       Degree of hydration which is related to curing methods

-       Quality control and assurance.

Since a relationship between compressive and flexural strengths of conventional concrete is known to exist, the former is normally used to estimate the latter for practical reasons. Note that the performance of a concrete pavement under loads depends on several factors and consequently monitoring the concrete strength alone is not sufficient to produce a sustainable pavement.

Concrete Pavement

Structural responses of concrete pavements are affected by a number of factors including distance between joints, thickness of concrete slab, concrete properties, load transfer devices, joint width, boundary condition between concrete slab and subbase, subbase type, thickness and properties of subbase, subgrade characteristics, environmental effects and configuration, magnitude and location of vehicular loads upon pavement.

Concrete pavement contains a number of relatively thin concrete bases, known internationally as concrete slabs, finite in length and width, over a subbase resting on a foundation soil known also as subgrade (Fig.1). The width of concrete slab is equal to the width of traffic lane, normally 3600 mm. However, the length of concrete slab varies depending on concrete pavement types. Concrete slabs are connected to each other or shoulder in the longitudinal and transverse directions through transverse and longitudinal joints respectively. Joints allow them to expand / shrink with temperature fluctuations. A debonding layer is placed between the concrete slab and the subbase to reduce early age cracking.
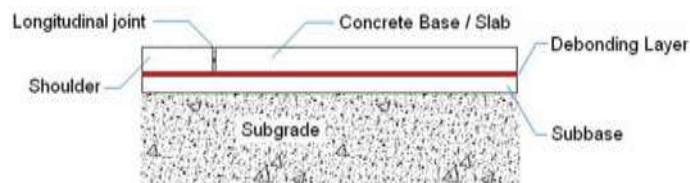

Figure 1. Cross section of a typical concrete pavement

Concrete pavement cross section

Subgrade

Subgrade is the foundation soil which is compacted to achieve an appropriate strength. While soils also exhibit some nonlinear behaviour and other interesting characteristics, a full investigation of this layer is beyond the scope of this research. Because of its strong effect on concrete pavement responses, however, a brief background of soil modelling idealization as pavement foundation is illustrated in this section.

A variety of subgrade model idealizations including Winkler, Dense Liquid (DL), Elastic Solid (ES), Two Parametric (TP), Zhemochkin-Sinitsyn Staerman (ZSS), and Kerr-Vlasok (KV) have been developed during the past centuries. Only, those employed widely in relevant research are subsequently discussed here.

Debonding layer

In terms of the classical friction model, the magnitude of interface frictional force between two layers depends on the smoothness of the contact surface presented as coefficient of friction and the normal force applied to the sliding plane. However, classical friction model can not be used in concrete pavement systems as friction force between concrete slab and subbase depends on different components including adhesion, shear and bearing (Wimsatt et al. 1987 and Wesevich et al. 1987). This results in a greater friction between the concrete slab and the subbase than that calculated based on the classical friction model.

Note that different boundary conditions including bonded, unbonded and partially bonded may be created between the concrete slab and the subbase depending on the magnitude of friction force. While the bonded boundary condition keeps the concrete slab and subbase together with no vertical separation, a fully unbonded boundary condition allows them to be separated under tensile force without inducing any frictional force between these layers. A partially bonded boundary condition, on the other hand, keeps the concrete slab and the subbase together for a certain frictional force. Beyond this frictional force, a vertical separation will occur between these layers.

Concrete slab (base)

The concrete slab is the top layer in the pavement section (see Fig. 3-1). It contains a concrete with a compressive strength more than 32 MPa to ensure the durability of the wearing surface and to provide sufficient flexural strength to avoid unpredictable deteriorations in pavements. Although the concrete slab thickness was traditionally considered to be between 200 mm and 250 mm, it is now designed based on damage processes considered in concrete pavement design guides.

Thickness of concrete slab is affected by the fatigue flexural strength of the concrete, type of joints, the value of load transfer efficiency (LTE), availability of the shoulder, strength of foundation soil and subbase, erosion of the subbase and subgrade materials, environmental effects and expected traffic load. In accordance with the provision of transverse joint and the availability of reinforcement, concrete pavements are classified as Jointed Plain Concrete Pavement (JPCP), Jointed Reinforced Concrete Pavement (JRCP) and Continuously Reinforced Concrete Pavement (CRCP).

Jointed Plain Concrete Pavement (JPCP)

JPCP has a natural configuration compared with other concrete pavements. In this configuration, the joint's pattern closely resembles natural cracks in an unreinforced concrete pavement. Distance between longitudinal joints depends on traffic lane configuration and vary from 3.6 m to 4.6 m. Transverse joints, on the other hand, are located 4.2 m or 4.5 m apart from each other in undowelled skewed joints or in dowelled square joints respectively. Distance between transverse joints is affected by joint and concrete slab integrities. Since slab length is much more affected by joint integrity than slab integrity, transverse joints of concrete pavement with more than 4.2 m length are modified with dowel.

Surface roughness

Surface roughness is a longitudinal profile of pavement surface elevations in 305 mm intervals (Huang, 2004). In accordance with ASTM E867, pavement roughness is "the deviation of a surface from a true planar surface with characteristic dimensions that affect vehicle dynamics and ride quality". Pavement roughness is normally measured based on International Roughness index (IRI) to provide a more realistic, practical and comparable approach. The IRI is a longitudinal surface profile along the wheel path of the pavement. It is calculated based on surface elevation data collected from either mechanical profilometer or a topographical survey. The method for calculation of the IRI can be found elsewhere (Sayers et al., 1986). It is presented in units of m/km.

Concrete pavement has a smooth surface when it is relatively new but its surface becomes rougher during its performance under the traffic loads. As a result, a rough surface can be observed at the end of pavement service life (Bhatti and Stoner, 1998).

Shoulder

The positive effects of shoulders in structural response and performance of concrete pavements have been accepted worldwide. Bituminous shoulders when placed next to a concrete pavement will experience further compaction from the traffic after road opening. Consequently, a vertical gap between the top surfaces of concrete slab and shoulder is produced which results in a loss of restrain at the longitudinal edge of the concrete slab. This ultimately results in deteriorations of concrete slab. As a result, concrete shoulders have been widely used in concrete pavements to prolong the pavement life.

Joints

Joints are usually utilised to reduce effects of climatic forces on the concrete slab. The climatic forces are due to shrinkage-loss of moisture contents and temperature gradients through depth of the concrete slab. Load transfer devices and sealant are the main components of joints. In terms of the economical point of view, the distance between joints should be long enough to minimise the number of load transfer devices but short enough to eliminate transverse cracking (Kelleher and Larson, 1989).

A variety of joints namely, isolation joints, contraction joints, construction joints and expansion joints is used in pavement constructions (CCAA, 1999). Byrum and Hansen (1994) indicated that joint opening is the key factor in stress distribution around the joint.

Load Transfer Efficiency (LTE)

LTE is an important factor in performance of transverse joints and cracks. It is measured to evaluate joint operation under the applied load. It can be calculated by the following equation:

$$LTE\% = \delta\_U / \delta\_L * 100 \qquad (1)$$

Where δU is deflection of the unloaded slab and δL is deflection of the loaded slab. LTE is affected by dowel size, aggregate interlock, width of joints, and subbase or subgrade strength.

Based on results of Harvey et al. (2003), the LTE did not change by changing the traffic volume on the sections reinforced with DBR. Furthermore, the LTE was less sensitive to temperature changes. In addition to the use of suitable dowels, the improvement of subgrade strength can improve the LTE as reported by Hossain and Wojakowski (1996).

Differential Deflection

Differential deflection is another important factor, which provides further information on joint performance. It is the value of difference between the edges of adjacent slabs and presents the vertical distance between the loaded and unloaded slabs on the opposite sides of the joint. It is computed by using Equation (2).

$$DD = \delta L - \delta U \qquad (2)$$

It is noteworthy that LTE does not correlate with the amount of differential deflection. In other words, different values of the LTE can result in the same value of the DD. The differential deflection defines the sensitivity of the pavement to impact loads, applied at the edge of transverse joints of unloaded slab. The impact load results in further deterioration or joint faulting. Hence, the DD becomes an important factor when dynamic behaviour of rigid pavement is investigated (Popehn et al., 2003).**ACKNOWLEDGMENT**

If acknowledgement is there wishing thanks to the people who helped in work than it must come before the conclusion and must be same as other section like introduction and other sub section.

CONCRETE PAVEMENT ANALYSIS

A.   Analytical Solution

Westergaard (1926, 1927, 1933, 1939, 1943 and 1947) developed comprehensive analytical solutions for analysing concrete pavements under centre, edge and corner loadings using the classical thin-plate theory. In Westergaard study, concrete pavement was modelled as a homogenous, isotropic, elastic thin slab resting on a Winkler foundation. To simplify the analysis procedure, Westergaard assumed that:

-         The foundation soil acts like a bed of springs (the use of dense liquid foundation)

- A fully bonded boundary condition exists between concrete slab and foundation soil
- Shear and frictional forces are negligible
- The semi-infinite foundation is not restricted by a rigid layer
- Concrete slab has a uniform thickness
- Neutral axis is at mid-depth of the concrete slab
- Vehicular loads are uniformly distributed at tyre-pavement contact area having a circular (for centre and corner loadings) or semi circular (for edge loadings) shape.
- The load is applied normal to the surface of concrete slab
- Pavement acts as a single semi-infinitely large, homogenous, isotropic elastic slab with no discontinuities.

The above mentioned simplifications imply some limitations as follows:
- stresses and deflections can be only calculated for centre, edge and corner loadings
- Shear and frictional forces acting on concrete slab surfaces are ignored
- Availability of voids under concrete slab and discontinuities in concrete slab due to crack generation or provision of joints is not considered
- The method was developed for single wheel load and consequently real axle group configurations cannot be taken into consideration.
- Since no discontinuities were considered in the Westergaard method, effects of the LTE at joints or cracks on pavement performance were not addressed. Despite limitations associated with Westergaard analytical solution, his equations are still used. Ioannides et al. (1985) revised the original Westergaard equations for edge loading. Since all Westergaard's equations are based on single tyre with a circular tyre pavement contact area, Huang (1993) developed an equation to convert effects of dual tyres to single tyre with circular tyre pavement contact shape. Further information on Westergaard method can be found in the work of Westergaard (1926, 1927, 1933, 1939, 1943 and 1947).

B.   Numerical Solution

The expensive cost of experimental studies associated with progressive development in numerical computation together with a rapid growth in software and hardware technologies leads to the use of numerical analysis for investigation of those problems with a complex geometry, boundary conditions, and material properties.

C.   Discrete Element Method (DEM)

Hudson and Matlock (1966) were the first to apply the DEM in concrete pavement analysis using Winkler foundation. In their contribution, the original bending stiffness of the concrete slab at joints was reduced to simulate joint effects in concrete pavement behaviour. This model was then modified by Vora and Matlock (1970) to take into consideration different element sizing and anisotropic skew slabs. Furthermore, foundation soil was idealized using semi-infinite elastic solid elements.

This method does not allow incorporating elements with different sizes into the analysis easily. Furthermore, stress estimations at free edges are not converged to unique values.

D.   Finite Element Method (FEM)

The initial idea of dividing a given domain into discrete parts goes back to ancient mathematicians. The concept of finite element technics was firstly used by Hrenikoff (1941) for aircraft analysis using truss and beam elements. To efficiently analyse the torsion problem, the use of triangular elements was then incorporated into the method (Courant, 1943). Seven years later in 1950, the Boeing Company used triangula elements for wing analysis. Further research on finite element technics by Argyris and Kelsey (1960) and Turner et al. in 1956 represented the new form of this method. The term "finite element" was used by Clough in 1960. It is important to note that the accuracy of a finite element analysis depends on several factors such as meshing size and element types.

Nowadays, finite element techniques are extensively used to treat complex engineering problems in several areas such as structural, mechanical, electrical, geological and thermal (Reddy, 1993). In general, finite element analysis packages can be divided into two categories, general purpose finite element programs such as ABAQUS and ANSYS, which are very powerful for nonlinear dynamic analysis, and specific finite element programs developed for concrete pavement analysis using the classical thin plate theory or 3D solid elements.

DEVELOPMENT OF SLAB THICKNESS DESIGN GUIDE

As mentioned earlier, concrete pavements were traditionally designed based on theoretical solutions such as Westergaard method (1926, 1933, and 1947). Contribution of finite element analysis for determining stress distribution within concrete slabs later led to a mechanistic approach which was extensively adopted in the PCA (1985) and Austroads (2004) slab thickness design guides. The bottom-up mid-edge transverse cracking due to mid-edge loading was the only fatigue damage mode of concrete pavements considered in the mechanistic approach.

A.   Cross section of the concrete pavement

Based on the concrete pavement technology in Australia, the cross section of the pavement considered in this guide contains concrete slabs, debonding layer, subbase and subgrade. This guide was developed to design JPCP and JRCP. Since Austroads recommendations for selection of concrete slab dimensions were used in this research, distances between transverse joints and longitudinal joints (length and width of the concrete slab) are in accordance with Austroads (2004).

B.   Concrete Characteristics

The concrete pavements are subjected to environmental effects simultaneously of construction. If the pavement is subjected to an environmentally induced stress before having adequate strength to resist the stress, a crack is initiated in the pavement. As a result, a

minimum concrete flexural strength is considered in the design guides.

C.   Subbase

The longevity of concrete pavements is affected by the provision of subbase layer. A LMC subbase of 150 mm thick and compressive strength of 5 MPa is constantly considered in the finite element analyses performed in this research. Hence, further study is required to determine the optimum characteristics of subbase for different types of concrete pavements and variety of subgrade soil. While this guide is used, a LMC subbase with the aforementioned characteristics shall be constructed over the subgrade and under the concrete slab.

D.   Prediction of the maximum induced tensile stress

A comparison between results of vehicular induced tensile stress in finite element analysis with corresponding stresses predicted by using Austroads stress prediction model shows that the Austroads is not able to accurately predict the induced tensile stresses in the pavement subjected to TADT and QADT loadings. Furthermore, the prediction of induced tensile stress in the Austroads method is based on this assumption that only 6 per cent of the traffic passes along the edge area of the traffic lane (Packard and Tayabji, 1985). The edge area is along the longitudinal edge of the concrete slab and in a transverse distance of 600 mm from longitudinal joints or edges. As a result, the Austroads equation cannot be used for other values of edge loading. The work of Lennie and Bunker (2005) showed that the volume of the traffic passing along edge area in the Queensland State is much higher than the above mentioned assumption.

For a bonded traffic lane of JPCP confined at one of its longitudinal edges by a shoulder, the maximum vehicular induced tensile stress is predicted using the following equations:

SAST: $\sigma V = Pi \times (0.0153 — 2.208 \times 10^{-5} \times (Pf — 53))$ (3)
SADT: $\sigma V = Pi \times (0.0124 — 1.1 \times 10^{-5} \times (Pf — 80))$ (4)
TAST: $\sigma V = Pi \times (0.00708 — 3.0 \times 10^{-6} \times (Pf. — 90))$ (5)
TADT: $\sigma V = Pi \times (0.00607 — 1.87 \times 10^{-6} \times (Pi — 135))$ (6)
TRDT: $\sigma V = Pi \times (0.00456 — 1.623 \times 10^{-6} \times (Pi — 180))$ (7)
QADT: $\sigma V = Pi \times (0.00348 — 7.33 \times 10^{-7} \times (Pi — 220))$ (8)

Where Cr, (MPa) is maximum vehicular induced tensile stress in a bonded confined lane due to mid-edge loading at free edge, and Pi (kN) is the ultimate axle group load and is equal to axle group load multiplied by load safety factor (LSF). This table is represented in this chapter as Table 1.

Table 1. Load safety factor for concrete pavement design Project Design

Project Design Reliability	85%	90%	95%	97.50
Load Safety	1.05	1.1	1.2	1.25

RESULTS

Results show the accuracy of the aforementioned equations for stress prediction in both bonded and unbonded pavements.

Results of finite element analyses were also used to contribute effects of different loading conditions and adjacent traffic lanes (provision of shoulders at both longitudinal edges of the traffic lane) into Equations 3 to 8 for prediction of maximum vehicular induced tensile stresses within the concrete pavement. Consequently, the following equation was developed:

   $\sigma Vi = C1 \ XC2 \ XC3 \ XCLS \ X \ \sigma Vi - V 1$ (9)

Table 2. Variations of coefficient C2

Type of Axle Group	Unbonded Pavement		Bonded Pavement	
	Centre Loading	Corner Loading	Centre Loading	Corner Loading
SAST	0.535	0.547	0.546	0.644
SADT	0.617	0.468	0.61	0.565
TAST	0.55	0.84	0.585	1.13
TADT	0.654	0.725	1.45	0.842
TRDT	0.656	0.791	0.656	0.992

QADT	0.738	1.045	0.485	1.025

Table 3. Variations of coefficient C3

Type of Axle Group	Centre Loading		Mid-Edge Loading		Corner Loading	
	Bonded Pavement	Unbonded Pavement	Bonded Pavement	Unbonded Pavement	Bonded Pavement	Unbonded Pavement
SAST	0.892	0.932	0.496	0.757	0.866	0.903
SADT	0.896	0.937	0.611	0.764	1.063	1.118
TAST	0.936	0.965	0.526	0.669	0.671	0.849
TADT	0.891	0.937	0.578	0.658	0.913	1.013
TRDT	0.866	0.953	0.639	0.693	0.827	0.857
QADT	1.08	1.04	0.554	0.725	0.757	0.795

CONCLUSION

Dynamic amplifications and the concept of stress repetition described in this work were factored into the design procedure of concrete pavements. Using Miner's rule and taking into the consideration of results, prediction model of slab thickness for concrete pavements, mid-edge, edge and longitudinal cracks were developed. Finally, the design procedure was developed.

It is recommended that the use of debonding layer between concrete slab and subbase in regions with harsh environmental conditions be restricted.

REFERENCES:

[1] AASHTO Implementation Manual for Quality Assurance. AASHTO Highway Subcommittee on Construction. American Association of State Highway and Transportation Officials, Washington, D.C., February 1996a.

[2] AASHTO Quality Assurance Guide Specification. AASHTO Highway Subcommittee on Construction. American Association of State Highway and Transportation Officials, Washington, D.C., February 1996b.

[3] AASHTO Guide Specifications for Highway Construction. AASHTO Highway Subcommittee on Construction, American Association of State Highway and Transportation Officials, Washington, D.C., 1993.

[4] American Concrete Pavement Association (ACPA). Concrete Types.2005.http://www.pavement.com/PavTech/Tech/ Fundamentals/fundtypes.html. Accessed on September 2005.

[5] American Concrete Pavement Association. Technical Tips and Techniques. Concrete Pavement Progress. Volume 40. Number 2. September 6, 2004a. http://www.pavement.com/CPP/2004/CPP-090604.pdf. Accessed on October 20, 2005.

[6] American Concrete Pavement Association. Improving Smoothness Measurements. Better Roads (For the Government/Contractor Project Team). August 2004b. http://www.betterroads.com/articles/aug04b.htm. Accessed on September 2005.

[7] American Concrete Pavement Association (ACPA), Database of State DOT Concrete Pavement Practices. 1999. http://www.pavement.com/PavTech/Tech/StPract/Query.asp. Accessed on March 2004.

[8] American Concrete Pavement Association. Constructing Smooth Concrete Pavements. Technical Bulletin-006.0-C. Concrete Pavement Technology.1990.

[9] Atkins, Harold N. Highway Materials, Soils, and Concretes. Fourth Edition. Prentice Hall. Pearson Education, Inc., Upper Saddle River, New Jersey. 2003.

[10] Chamberlin, P. Synthesis of Highway Practice 212 - Performance-Related Specifications for Highway Construction and Rehabilitation. National Cooperative Highway Research Program. National Academy Press. Washington, D.C., 1995.

[11] Chang, Luh-Maan, and Machine Hsie. Developing Acceptance-Sampling Methods for Quality Construction. Journal of Construction Engineering and Management. pp. 246-253. June 1995.

[12] Chiang, C.L. Statistical Methods of Analysis.World Scientific Publishing Co. Pte. Ltd.,Singapore, 2003.

[13] Correa, Angel L., and Bing Wong. Concrete Pavement Rehabilitation: Guide forDiamond Grinding. Federal Highway Administration. Washington, D.C., June 2001.

[14] Darter, Michael I., M. Abderlrahaman, T. Hoerner, M. Phillips, K.D. Smith, and P.A. Okamoto. Performance-Related Specifications for Concrete Pavements. Volume II No. FHWA-RD-93-043. Federal Highway Administration, Washington, D.C., November 2003.

[15] Darter, Michael I.; Hoerner, Todd E.; Okamoto, Paul A. Guide to Developing Performance-Related Specifications for PCC Pavements. Volume III: Appendices C through F. Publication No. FHWA-RD-98-171. Federal Highway Administration. U.S. Department of Transportation. 1999.

Induction of sensitive skin and sensitive scalp by hair dyeing

Audrey Bernard[1]; Anne-Sophie Ficheux[1]; Anne-Sophie Nedelec[2]; Pauline Bourgeois[2]; Nicolas Hornez[2]; Alexandre Batardière[2];

Laurent Misery[3]; Alain-Claude Roudot[1]

1: Laboratoire d'Evaluation du Risque Chimique pour le Consommateur (LERCCo), Université de Bretagne Occidentale, UFR

Sciences et Techniques, Brest, France, 6 Av. Victor Le Gorgeu, CS93837, 29200 Brest, France

2: Farcoderm, 56 Rue Yves Collet, 29200 Brest, France

3: Centre Hospitalier et Universitaire de Brest, Service de Dermatologie, 2 Avenue Maréchal Foch, 29200 Brest, France

Corresponding Author contact:

Audrey Bernard,

E-mail address: audrey.bernard@univ-brest.fr

Abstract: Hair dyes are more and more used and the role of the exposure to these products in the development of skin reactions in the exposed region is suspected.

The aim of this study is to assess the effects of hair dyes on facial skin and scalp sensitivity by performing a Computer Assisted Web Interview on 1257 women older than 15 years old.

Differences were observed in the scores evaluating facial skin and scalp sensitivity according to different parameters. Women aged between 15 and 24 years old suffered more from skin and scalp sensitivity both for hair dye users and for non-users. The results obtained according to hair dye usage patterns indicated the highest sensitivity of the scalp and facial skin when the hair dyeing process was performed at home with professional products, or when the type of product used was bleach alone or bleach followed by another dyeing product.

The severity of facial skin and scalp sensitivity depends on different factors and seems to be potentially exacerbated by the hair dyeing process.

Keywords: Hair dye; Skin sensitivity, Scalp sensitivity; French women; Web survey; Dermatology; Sensitivity scores

[16]   Introduction:

Sensitive (or reactive/hyper-reactive) skin is defined as skin that exhibits erythema and/or subjective symptoms of irritation (stinging, tingling sensation, prickling, burning, pain…) [1–3] caused by various factors, which may be physical, chemical, psychological or hormonal. Sensitive skin symptoms occur over a wide range of intensities [4] and may be an adverse reaction occurring in response to topically applied agents such as cosmetics [5–7] with a usually rapid onset (within minutes) [7]. Most of the time, sensitive skin is located on the face but other localizations such as the scalp, hands, feet or neck are possible [2,8]. Thus, a sensitive scalp condition can exist even if the symptoms are different from those observed for facial skin sensitivity.

Only few of sensitive skin symptoms are objective clinical signs thereby giving to sensitive skin a subjective nature [9]. Thus, one of the best ways to study these symptoms is to conduct an epidemiological study [1], integrating questions about skin and scalp sensitivity symptoms and their intensity, the answers to which will be used to calculate the Sensitive Scalp Severity Score (3S score) [1] and the Sensitive Scale-10 (SS-10) for facial skin [8].

Some cosmetic product users may develop a burning, stinging or itching reaction after application of the product, without visible lesions [10,11]. Yet, in the case of a mild reaction, users will seldom seek medical care, resulting in an unreported reaction. It therefore remains difficult to assess the incidence of skin reactions due to the use of cosmetic products [10].

Hair dyes belong to the hair care branch of cosmetics. According to Draelos, approximately 70 % of women in developed countries use hair dye [12]. In France, the percentage of hair dye users in the general population of French women (15-70 years old) was assessed at 64 % [13]. Some adverse skin reactions are attributed to hair dyes, especially allergic contact dermatitis which may be severe and require a physician consultation. Mild skin reactions to hair dyes are usually identified by the users themselves due to the relative short timeframe between exposure and the development of skin reactions in the exposed region [14]. Corbett indicated that some colorants contained in hair dye give rise to skin problems including sensitization or irritation [15]. Hence, hair dye components such as ammonia or hydrogen peroxide are also liable to induce sensitization and irritation especially on users with a sensitive scalp [15]. Seo [16] indicated that more complaints are reported about side-effects of hair dyes on the scalp in relation to the increased use of hair dyes. In 2005, Søsted published the results of his study on contact dermatitis due to hair dye and determined, for the lifetime prevalence of skin symptoms, that 4.9 % of a sample of Danish adults who dyed their hair experienced redness, scaling and itching after the use of hair dye [17]. The results of Alghamdi's survey in 2012 indicated that 15.1% of the participants reported redness, 14.4% scaling, and 31.3% itchiness caused by the use of hair dyes. Among the participants who reported side effects, 85 % did not seek medical attention [18].

The purpose of this study was to analyse the effects of hair dyes on facial skin sensitivity and on scalp sensitivity by performing a survey on hair dye consumption among French women including an evaluation of the severity of skin sensitivity based on the Sensitive Scale-10 and of Sensitive Scalp Severity by the 3S score.

[17]   Materials and Methods:

[18] Survey:

A web survey was carried out in April 2015 in collaboration with a private survey company: Consumer Science and Analytics (CSA). The questionnaire was designed by the authors and executed by the CSA. This survey was developed to provide information on French women's hair dye usage patterns and on the presence and intensity of dermatological symptoms on the scalp or face. To obtain a representative sample of the French female population, quotas were applied taking into account age, socio-professional category, geographical area and degree of urbanization. However, in order to obtain sufficient data to study the possible link between hair dye use and modification of sensitivity, a quota of 75 % of hair colouring users was required. Thereby, the study was conducted on 1257 women older than 15 years old (939 users and 318 non-users).

Only women were involved in this survey because a previous study indicated that the percentage of hair dye users among the French male population was only 6 % [19].

[19] Ethical considerations:

This study was carried out in accordance with the principles outlined in the Declaration of Helsinki of 1973 as revised in 2000 [20] and in compliance with the "Protection of Human Subjects and Animals in Research" as described in the recommendations of the International Committee of Medical Journal Editor [21]. The questionnaire designed by the authors and used in this survey was totally anonymous, i.e. no identifying information were asked to the respondents. The execution of the survey was subcontracted to the CSA, a specialized company member of ESOMAR (European Society for Opinion and Marketing Research). The CSA performs its survey in the respect of the ICC/ESOMAR International Code on Market and Social Research [22].

[20] Questionnaire:

The following questions about hair dye use were put to the interviewees:

[1] Have you dyed your hair during the last 12 months?

[2] Where did you have your hair dyed? At the hairdresser, at home using a professional product or at home using a supermarket product?

[3] Which type of hair dye product did you use? Hair bleach alone, lightener, permanent dye, semi-permanent dye, temporary dye, vegetal dye or hair bleach plus another dye?

Dermatological evaluations were performed according to various parameters thanks to the 10-item Sensitive Scale named Sensitive Scale-10 (SS-10) for facial skin [8] and the 3S score (Sensitive Scalp Score) [1] for the scalp.

The following questions about sensitive scalp and sensitive skin severity were put to the participants:

Fig. 1.   Which symptoms did you have on your scalp? Tightness, burning, prickling, itching and/or pain?

Fig. 2.   Which grade would you give to each symptom?

    Fig. 3.   0= absent

    Fig. 4.   1= not troublesome

    Fig. 5.   2= somewhat troublesome

    Fig. 6.   3= very troublesome

Fig. 7.   Which symptoms did you have on your facial skin? Irritability, Stinging, Burning, Heat sensation, Tautness, Itching,

    Pain, General discomfort, Flushes, Redness?

Fig. 8.   What was the symptoms' intensity on a scale from 0 to 10?

Women were also asked to report the pre-existence of skin disease such as eczema, psoriasis, ringworm, folliculitis, seborrheic

dermatitis, acne, urticaria; and if they performed a skin patch test prior to hair dyeing.

[21] Statistical analysis:

The global 3S score was calculated for each participant by adding together the grades of the 5 symptoms on the scalp (maximum

possible score = 15) and the global SS-10 score by adding the intensity of the 10 symptoms on the skin (maximum possible score =

100). The global scores were then compared using the Kruskal-Wallis test and Dunn multiple pairwise comparisons. The statistical

analyses were run with the XLSTAT 2015 software (Addinsoft). Groups that were not significantly different from each other are

represented in the results' tables with the same letter (A, B, C, D or E) and contrariwise the groups represented by a given letter were

statistically different from groups with other letters.

As there were more or less substantial differences between sample sizes in the groups compared, random resampling was performed to

obtain groups of the same size before statistical analysis.

[22]   Results:

Mean and standard deviation values are presented in the various tables of results.

[23] Sensitive Scalp Score:

I.   3S score results by age group according to hair dye use:

The Sensitive Scalp Scores were calculated for hair dye users and non-users of each age group (Table 1). When considering the entire

population, i.e. women older than 15 years old, there were no statistical differences between scores obtained for users and non-users.

However, by looking at age sub-populations, statistical differences appeared between the scores of users and non-users for two age

classes (15-24 and 50-64 years old). In these cases, the highest mean scores were found among hair dye users with values of 3.34 and

1.70 respectively for the 15-24 and 50-64 year-old users, while 3S score means of 2.31 and 1.62 were obtained respectively for 15-24

and 50-64 year-old non-users. No statistical difference was observed between users and non-users of the other age classes.

Table 1: Women 3S Score results according to age and hair dye use

Age and hair dye use	Minimal 3S Score	Maximal 3S Score	3S Score mean	3S Score SD	p-value
Non users ≥ 15 years old (n=318) $(n_R=939)$	0.00	15.00	2.08	2.91	0.93
Users ≥ 15 years old (n=939)	0.00	15.00	2.02	2.77	
Non users 15-24 years old (n=66) $(n_R=107)$	0.00	15.00	2.31	2.83	0.03
Users 15-24 years old (n=107)	0.00	14.00	3.34	3.48	
Non users 25-34 years old (n=64) $(n_R=131)$	0.00	8.00	1.84	2.06	0.40
Users 25-34 years old (n=131)	0.00	15.00	2.33	2.93	
Non users 35-49 years old (n=77) $(n_R=242)$	0.00	15.00	2.35	2.63	0.20
Users 35-49 years old (n=242)	0.00	15.00	2.16	2.89	
Non users 50-64 years old (n=46) $(n_R=260)$	0.00	15.00	1.62	3.57	0.00
Users 50-64 years olds (n=260)	0.00	15.00	1.70	2.52	
Non users ≥ 65 years old (n=65) $(n_R=199)$	0.00	8.00	1.67	2.21	0.43
Users ≥ 65 years old (n=199)	0.00	14.00	1.38	2.05	

$(n_R=000)$ = Sample size after resampling

II.   3S score results by age group among hair dye users:

 Sensitive Scalp Scores were calculated for hair dye users at hairdressers (Table 2) and at home with supermarket products (Table 3)

according to their age. The highest 3S score means of 3.15 (hairdresser) and 3.45 (supermarket products) were obtained for women

aged between 15 and 24 years old with a marked statistical difference, i.e. p-value <0.0001, with the other age groups (≥ 25 years old).

The lowest 3S score means were obtained for women older than 65 years old with means of 1.24 (hairdresser) and 1.50 (supermarket

products).

Table 2: Women hair dye users at the hairdresser 3S Score results according to their age

Age	Minimal 3S Score	Maximal 3S Score	3S Score mean	3S Score SD	p-value	Statistical group
15-24 years old (n=53) *(n$_R$=133)*	0.00	14.00	3.15	3.37		B
25-34 years old (n=66) *(n$_R$=133)*	0.00	10.00	1.44	1.91		A
35-49 years old (n=112) *(n$_R$=133)*	0.00	11.00	1.58	2.39	< 0.0001	A
50-64 years old (n=123) *(n$_R$=133)*	0.00	14.00	1.60	2.45		A
≥ 65 years old (n=133)	0.00	8.00	1.24	1.72		A

(n$_R$=000) = Sample size after resampling
Groups that were not significantly different from each other are represented with the same letter (A or B) and contrariwise were statistically different from groups with other letters.

Table 3: Women hair dye users, at home with supermarket products, 3S Score results according to their age

Age	Minimal 3S Score	Maximal 3S Score	3S Score mean	3S Score SD	p-value	Statistical group
15-24 years old (n=32) *(n$_R$=112)*	0.00	11.00	3.45	3.05		C
25-34 years old (n=52) *(n$_R$=112)*	0.00	15.00	2.85	3.30		B
35-49 years old (n=112)	0.00	15.00	2.40	2.93	< 0.0001	B
50-64 years old (n=104) *(n$_R$=112)*	0.00	12.00	2.19	2.66		B
≥ 65 years old (n=51) *(n$_R$=112)*	0.00	11.00	1.50	2.21		A

(n$_R$=000) = Sample size after resampling
Groups that were not significantly different from each other are represented with the same letter (A, B or C) and contrariwise were statistically different from groups with other letters.

III.   3S score results for users according to the place of use:

The Sensitive Scalp Score was calculated for hair dye users by considering the place of use (Table 4). The lowest 3S score mean of

1.65 was obtained for women who had their hair dyed at the hairdresser with a clear statistical difference with mean scores obtained

for women dyeing their hair at home with supermarket (2.20) or professional products (2.78).

Table 4: Women hair dye users 3S Score results according to the place of use

Place of use	Minimal 3S Score	Maximal 3S Score	3S Score mean	3S Score SD	p-value	Statistical group
At the hairdresser (n=487)	0.00	14.00	1.65	2.37		A
At home using supermarket products (n=351) *(n_R=487)*	0.00	15.00	2.20	2.76	< 0.0001	B
At home using professional products (n=101) *(n_R=487)*	0.00	15.00	2.78	3.62		B

(n_r=000) = Sample size after resampling
Groups that were not significantly different from each other are represented with the same letter (A or B) and contrariwise were statistically different from groups with other letters.

IV. 3S score results for users with differentiation according to the type of hair dye used:

The Sensitive Scalp Score was calculated for hair dye users depending on the type of product used (Table 5). The highest 3S score mean of 3.39 was obtained for women who applied bleach followed by another hair dye with no statistical difference with scores obtained for women who applied bleach alone. The lowest mean scores were found in the cases of use of semi-permanent (1.62) and temporary (1.62) hair dyes.

Table 5: Women hair dye users 3S Score results according to the type of hair dye used

Type of hair dye	Minimal 3S Score	Maximal 3S Score	3S Score mean	3S Score SD	p-value	Statistical group
Bleach + other dye (n=28) *(nr=503)*	0.00	14.00	3.39	3.93		D
Bleach solely (n=27) *(nr=503)*	0.00	11.00	2.88	3.32		CD
Lightener (n=88) *(nr=503)*	0.00	15.00	2.40	2.99		BC
Permanent (n=503)	0.00	15.00	2.01	2.77	< 0.0001	A
Semi-permanent (n=104) *(nr=503)*	0.00	14.00	1.62	2.21		A
Temporary (n=36) *(nr=503)*	0.00	7.00	1.62	1.70		A
Vegetal (n=37) *(nr=503)*	0.00	10.00	2.07	2.36		B

(nr=000) = Sample size after resampling
Groups that were not significantly different from each other are represented with the same letter (A, B, C or D) and contrariwise were statistically different from groups with other letters.

V.   3S score results for users according to their skin disease:

The Sensitive Scalp Score was calculated for hair dye users by taking into consideration their known skin disease (Table 6). The

lowest 3S score mean of 1.48 was obtained for women with no skin disease with a marked statistical difference compared to scores

obtained for women with skin disease, reaching a mean of 3.67 for users suffering from dermatitis.

Table 6: Women hair dye users 3S Score results according to their skin disease

Skin diseases	Minimal 3S Score	Maximal 3S Score	3S Score mean	3S Score SD	p-value	Statistical group
None (n=674)	0.00	15.00	1.48	2.31	< 0.0001	A
Eczema (n=87) *(nr=674)*	0.00	14.00	3.39	3.36		B
Psoriasis (n=53) *(nr=674)*	0.00	15.00	3.42	3.45		B
Dermatitis (n=32) *(nr=674)*	0.00	15.00	3.67	3.82		BC
Acne (n=82) *(nr=674)*	0.00	15.00	3.61	3.21		C

(nr=000) = Sample size after resampling
Groups that were not significantly different from each other are represented with the same letter (A, B or C) and contrariwise were
statistically different from groups with other letters.

[24] Facial skin Sensitive Scale-10 results:

VI.   SS-10 score results by age group among hair dye users:

The Sensitive Scale-10 score was assessed by age classes among the women hair dye users (Table 7). There were no statistical

differences between scores obtained for age groups from 25 to 64 years old. Women older than 65 years old presented the lowest

mean score of 3.39 with clear statistical differences with the other groups. The highest scores were found for 15-24 year-olds, i.e. a

mean of 18.93, with marked statistical differences with the scores of women older than 25 years old.

Table 7: Women hair dye users with SS-10 Score results according to their age

Age	Minimal SS-10 Score	Maximal SS-10 Score	SS-10 Score mean	SS-10 Score SD	p-value	Statistical group
15-24 years old (n=107) *(nr=260)*	0.00	82.00	18.93	24.85	< 0.0001	C
25-34 years old (n=131) *(nr=260)*	0.00	88.00	11.33	19.13		B
35-49 years old (n=242) *(nr=260)*	0.00	93.00	10.04	16.73		B
50-64 years old (n=260)	0.00	94.00	8.26	15.39		B
≥ 65 years old (n=199) *(nr=260)*	0.00	51.00	3.39	6.48		A

(nr=000) = Sample size after resampling
Groups that were not significantly different from each other are represented with the same letter (A, B or C) and contrariwise were statistically different from groups with other letters.

VII.   SS-10 score results for users according to the place of use:

Sensitive Scale-10 scores were assessed among the women hair dye users depending on the place they dyed their hair (Table 8). Women dyeing their hair at the hairdresser obtained the lowest mean score (7.43) with statistical differences with groups of women who dyed their hair at home. The highest score was found for women using professional products at home, with a mean score of 12.96.

Table 8: Women hair dye users SS-10 Score results according to the place of use

Place of use	Minimal SS-10 Score	Maximal SS-10 Score	SS-10 Score mean	SS-10 Score SD	p-value	Statistical group
At the hairdresser (n=487)	0.00	89.00	7.43	14.67		A
At home using supermarket products (n=351) *(nr=487)*	0.00	77.00	9.14	15.92	< 0.0001	B
At home using professional products (n=101) *(nr=487)*	0.00	93.00	12.96	20.47		C

(nr=000) = Sample size after resampling
Groups that were not significantly different from each other are represented with the same letter (A, B or C) and contrariwise were statistically different from groups with other letters.

VIII.   SS-10 score results for users according to the type of hair dye used:

Sensitive Scale-10 scores were assessed among the women hair dye users depending on the type of hair dye used (Table 9). Women applying bleach followed by another hair dye obtained the highest mean score value (24.34) with statistical differences with the other groups. The group of women with the lowest mean score, i.e. 7.75, is the group of permanent dye users.

Table 9: Women hair dye users SS-10 Score results according to the type of hair dye used

Type of hair dye	Minimal SS-10 Score	Maximal SS-10 Score	SS-10 Score mean	SS-10 Score SD	p-value	Statistical group
Bleach + other dye (n=28) *(nr=503)*	0.00	79.00	24.34	28.79		E
Bleach solely (n=27) *(nr=503)*	0.00	79.00	17.54	24.25		D
Lightener (n=88) *(nr=503)*	0.00	94.00	14.75	23.33	< 0.0001	CD
Permanent (n=503)	0.00	93.00	7.75	15.13		A
Semi-permanent (n=104) *(nr=503)*	0.00	89.00	10.21	15.83		BC

Temporary (n=36) *(nr=503)*	0.00	51.00	8.88	13.18		B
Vegetal (n=37) *(nr=503)*	0.00	43.00	7.85	12.23		B

(nr=000) = Sample size after resampling
Groups that were not significantly different from each other are represented with the same letter (A, B, C, D or E) and contrariwise were statistically different from groups with other letters.

IX.   SS-10 score results for users according to their skin disease:

Sensitive Scale-10 scores were assessed among the women hair dye users according to whether or not they had a known skin disease (Table 10). Women with no skin disease obtained the lowest mean score of 6.66 with statistical differences with groups of women with a skin disease. Women suffering from eczema had the highest mean score (21.02) with statistical differences with all the other groups.

Table 10: Women hair dye users SS-10 Score results according to their skin disease

Skin disease	Minimal SS-10 Score	Maximal SS-10 Score	SS-10 Score mean	SS-10 Score SD	p-value	Statistical group
None (n=674)	0.00	77.00	6.66	13.13	< 0.0001	A
Eczema (n=87) *(nr=674)*	0.00	94.00	21.02	25.59		D
Psoriasis (n=53) *(nr=674)*	0.00	79.00	15.62	22.31		C
Dermatitis (n=32) *(nr=674)*	0.00	70.00	10.68	16.88		B
Acne (n=82) *(nr=674)*	0.00	93.00	16.83	24.69		C

(nr=000) = Sample size after resampling
Groups that were not significantly different from each other are represented with the same letter (A, B, C or D) and contrariwise were statistically different from groups with other letters.

[25]   Discussion:

To our knowledge, this is the first study that assesses local side effects of hair dye use on facial skin and scalp sensitivity by an epidemiological approach using sensitivity scores. It allows us to highlight that some types of hair dye as well as the place of use influence sensitivity to a varying degree. Owing to the fact that reactions to hair dye are identified by the users due to their rapid onset [14], and that mainly of the symptoms are subjective, the implementation of an epidemiological study is appropriate to assess facial skin and scalp sensitivity [1]. Furthermore, this kind of study based on subjects' declarations by means of self-questionnaires on web is relevant because the subjects can easily identify sensitive skin symptoms and thus do not necessary require a dermatological consultation [23].

The scores obtained in the present study suggest that women between 15 and 24 years old are more likely than older women to exhibit skin and scalp sensitivity and appear to be more reactive to hair dyes as regards the differences in scores between users and non-users of this age class. This observation goes against previous results [1], which suggested that the prevalence of scalp sensitivity increases with the age. However, higher reactivity to hair dye obtained for 15-24 year-old is consistent with other studies stating that the skin of younger adults has been demonstrated to be more sensitive than the skin of elderly subjects [24] and that skin irritant reactivity declines with advanced age [3,25]. Women experiencing reactivity to hair dye in their youth, could stop the use of such products, thus leading to an older population of users composed predominantly of women non or less reactive to hair dyes but the frequencies of hair dye use found for the 15-24 year-old group were clearly lower than those found for women older than 65 years old, independently of the place or type of product used, in our hair dye consumption study [13]. The assumption of a possible link between the frequency of use and sensitivity scores was investigated but no link was highlighted between sensitivity changes and the frequency of use.

Some authors' conclusions emphasize that there could be a relationship between sensitive skin and other dermatological conditions [26]. Especially, skin reactivity could be exacerbated by eczema [2,3,27,28]. Fairly logically, the scores obtained for users with a dermatological disease were higher than the healthy users' scores both for scalp and facial skin sensitivity. Users exhibiting the highest sensitive scalp severity suffered from dermatitis or acne, and those with the highest facial skin sensitivity suffered from acne or eczema.

The place of hair dyeing and the type of product used seem to affect the results of sensitivity. Indeed, women who had their hair dyed at the hairdresser presented the lowest scalp and facial skin sensitivity, and the highest scores were obtained in the case of women dyeing their hair at home with professional products. This ascertainment is probably linked to the fact that women using professional products were found to be the most exposed to hair dye [13]. The scores assessed for women using professional products at home seem not to be related to excessive processing time because the vast majority reported that they respected the recommended time or decreased it. Rather, these scores could probably be explained by the complexity of the mixture preparation of professional products, and by the availability on the market of products with high concentrations of oxidants which may lead to improper use of professional products. Moreover, the results of facial skin and scalp sensitivity varied significantly depending on the type of hair dye used. The highest scores, both for scalp and facial skin, were obtained for women using bleach followed by another dye or bleach alone. A possible explanation is that bleach may be composed of hydrogen peroxide, ammonium persulfate and/or potassium persulfate. Persulfates are used in order to increase the action of bleaching agents and can cause irritant contact dermatitis as well as allergic contact dermatitis [11]. Brown reported on the fact that hydrogen peroxide can cause skin irritation, and ammonium and potassium persulfate have been found to cause a variety of reactions which vary in severity depending on the amount of these components in the

bleach [29]. For Fujita, hydrogen peroxide can cause sensory irritation on the skin surface, such as a stinging, prickling or burning sensation [30].

[26]   Conclusion:

In this study, the effects of hair dyes on facial skin sensitivity and on scalp sensitivity was analyse by performing a survey on hair dye consumption among French women and an evaluation of the severity of skin sensitivity based on the Sensitive Scale-10 and of Sensitive Scalp Severity by the 3S score. The severity of facial skin and scalp sensitivity depends on different factors such as age and dermatological disease. It also seems to be potentially exacerbated by the hair dyeing process, especially when women use professional hair dyeing products at home or when the type of product used is bleach, whether alone or followed by another dye.

Aknowledgments:

REFERENCES:

[1]   Misery L, Rahhali N, Ambonati M, et al. Evaluation of sensitive scalp severity and symptomatology by using a new score: Sensitive scalp. J. Eur. Acad. Dermatol. Venereol. 2011;25:1295–1298.

[2]   Misery L, Boussetta S, Nocera T, et al. Sensitive skin in Europe. J. Eur. Acad. Dermatol. Venereol. 2009;23:376–381.

[3]   Primavera G, Berardesca E. Sensitive skin: mechanisms and diagnosis. Int. J. Cosmet. Sci. 2005;27:1–10.

[4]   Coyerly J, Peters L, Whittle E, et al. Susceptibility to skin stinging, non-immunologic contact urticaria and acute skin irritation; is there a relationship? Contact Dermatitis. 1998;38:90–95.

[5]   Berardesca E, Farage M, Maibach H. Sensitive skin: an overview. Int. J. Cosmet. Sci. 2013;35:2–8.

[6]   Guinot C, Malvy D, Mauger E, et al. Self-reported skin sensitivity in a general adult population in France: data of the SU.VI.MAX cohort. J. Eur. Acad. Dermatol. Venereol. 2006;20:380–390.

[7]   Pons-Guiraud A. Sensitive skin: a complex and multifactorial syndrome. J. Cosmet. Dermatol. 2004;3:145–148.

[8]   Misery L, Jean-Decoster C, Mery S, et al. A New Ten-Item Questionnaire For Assessing Sensitive Skin: The Sensitive Scale-10. Acta Derm. Venereol. 2014;94:635–639.

[9]   Diogo L, Papoila AL. Is it possible to characterize objectively sensitive skin? Skin Res. Technol. 2010;16:30–37.

[10]   Ortiz KJ, Yiannias JA. Contact dermatitis to cosmetics, fragrances, and botanicals. Dermatol. Ther. 2004;17:264–271.

[11]   Scheman A. ADVERSE REACTIONS TO COSMETIC INGREDIENTS. Dermatol. Clin. 2000;18:685–698.

[12]   Draelos ZK, editor. Cosmetic dermatology: products and procedures. Chichester, West Sussex ; Hoboken, NJ: Wiley-Blackwell Pub; 2010.

[13]   Bernard A, Houssin A, Ficheux AS, et al. Consumption of hair dye products by the French women population: Usage pattern and exposure assessment. Food Chem. Toxicol. 2016;88:123–132.

[14]   Sosted H, Agner T, Andersen KE, et al. 55 cases of allergic reactions to hair dye: a descriptive, consumer complaint-based study. Contact Dermatitis. 2002;47:299–303.

[15]   Corbett JF. Hair coloring. Clin. Dermatol. 1988;6:93–101.

[16]   Seo J-A, Bae I-H, Jang W-H, et al. Hydrogen peroxide and monoethanolamine are the key causative ingredients for hair dye-induced dermatitis and hair loss. J. Dermatol. Sci. 2012;66:12–19.

[17]   Sosted H, Hesse U, Menne T, et al. Contact dermatitis to hair dyes in a Danish adult population: an interview-based study. Br. J. Dermatol. 2005;153:132–135.

[18]   AlGhamdi KM, Moussa NA, Bolduc C, et al. Local Side Effects Caused by Hair Dye Use in Females: Cross-sectional Survey. J. Cutan. Med. Surg. 2012;16:39.

[19]   Ficheux AS, Wesolek N, Chevillotte G, et al. Consumption of cosmetic products by the French population. First part: Frequency data. Food Chem. Toxicol. 2015;78:159–169.

[20]   World Medical Association. Declaration of Helsinki. Recommendations guiding physicians in biomedical research involving human subjects. 52nd General Assembly, Edinburgh, Scotland, October 2000. 2000;

[21]   International Committee of Medical Journal Editors (ICMJE). International Committee of Medical Journal Editors (ICMJE): Uniform Requirements for Manuscripts Submitted to Biomedical Journals: writing and editing for biomedical publication. Haematologica. 2004;89:264.

[22]   ICC/ESOMAR. ICC/ESOMAR International Code on Market and Social Research [Internet]. 2008. Available from: http://www.iccwbo.org/Advocacy-Codes-and-Rules/Document-centre/2008/ICC/ESOMAR-INTERNATIONAL-CODE-ON-MARKET-AND-SOCIAL-RESEARCH/.

[23]   Misery L, Sibaud V, Merial-Kieny C, et al. Sensitive skin in the American population: prevalence, clinical data, and role of the dermatologist. Int. J. Dermatol. 2011;50:961–967.

[24]   Cua AB, Wilhelm K-P, Maibach HI. Cutaneous sodium lauryl sulphate irritation potential: age and regional variability. Br. J. Dermatol. 1990;123:607–613.

[25]   Robinson MK. Population differences in acute skin irritation responses. Race, sex, age, sensitive skin and repeat subject comparisons. Contact Dermatitis. 2002;46:86–93.

[26]   Farage MA, Katsarou A, Maibach HI. Sensory, clinical and physiological factors in sensitive skin: a review. Contact Dermatitis. 2006;55:1–14.

[27]   Bettley FR. NON-SPECIFIC IRRITANT REACTIONS IN ECZEMATOUS SUBJECTS. Br. J. Dermatol. 1964;76:116–119.

[28]   Misery L, Sibaud V, Ambronati M, et al. Sensitive scalp: does this condition exist? An epidemiological study. Contact Dermatitis. 2008;58:234–238.

[29]   Brown N. Health Hazard Manual for Cosmetologists, Hairdressers, Beauticians and Barbers. Man. User Guid. [Internet]. 1987; Available from: http://digitalcommons.ilr.cornell.edu/manuals/6.

[30]   Fujita F, Azuma T, Tajiri M, et al. Significance of hair-dye base-induced sensory irritation: Sensory irritation of hair dyes. Int. J. Cosmet. Sci. 2010;32:217–224.

International Journal of Engineering Research and general science is an open access peer review publication which is established for publishing the latest trends in engineering and give priority to quality papers which emphasis on basic and important concept through which there would be remarkable contribution to the research arena and also publish the genuine research work in the field of science, engineering and technologies